

**CHARACTERIZATION OF THE
AUTOLYTIC SYSTEMS IN SELECTED
STREPTOCOCCAL SPECIES**

By

KERSHNEY NAIDOO

**Submitted in fulfilment of the academic
requirements for the degree of**

MASTER OF SCIENCE

**In the School of Biochemistry, Genetics,
Microbiology and Plant Pathology,
University of KwaZulu-Natal
Pietermaritzburg**

2005

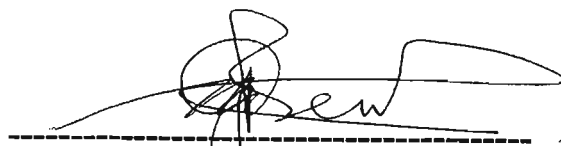
PREFACE

The experimental work described in this thesis for MSc was carried out in the Department of Genetics, School of Biochemistry, Genetics, Microbiology and Plant Pathology, University of KwaZulu-Natal, Pietermaritzburg from January 2004 to December 2005, under the supervision of Doctor Mervyn Beukes. The Biacore analysis was conducted at the Pasteur Institute, Strasbourg, France and the University of Western Cape, South Africa.

These studies represent the original work by the author and have not otherwise been submitted in any form for any degree or diploma to any University. Where use has been made of the work of others, it is dually acknowledged in the text.



Kershney Naidoo (Miss)



Dr. Mervyn Beukes (Supervisor)

ACKNOWLEDGMENTS

I would like to express my appreciation and gratitude to the following persons and organizations for their contributions to this thesis:

A special Thank You to my supervisor, Dr. Mervyn Beukes, for your endless guidance, supervision and advice during my research study. Your faith and intellectual belief in me has been an inspiration for me to always excel. You are more than just a mentor to me and your opinions will always be valued. The friendship and memories we've shared will last a lifetime.

To my parents, Mum and Dad, I am truly thankful for having such caring and understanding parents. Daddy, you were always there for me and encouraged me to go the extra mile. Mummy, your love has inspired me in more ways than one, to never give up but always have faith in myself. Thank you for proof-reading my thesis and enduring the science that went with it. I love you both endlessly. To my sister Shivani, you always kept me young at heart. I love you Angel.

Thank you to the genetics technical staff (Mrs. P. Wallis, Mr. D. Lakay, Mrs. M. Brunkhorst and Mr. G. Zondi) for the pleasant working environment and the many laughs we shared.

To the academic members of the Biochemistry Department, thank you for always supporting my endeavours.

To the collaborators in Strasbourg and Bonn, thank you for your hospitality and for welcoming me into your laboratories. My international visits were most memorable and will always be cherished.

To my special friends – Natalie van Zuydam for her intellectual chats and the many fun times we enjoyed, Kavitha & Logan for the great memories we shared and always encouraging me!

To my fellow postgraduate students, Rizwana Desai for her faith and support in my research, Chandani Sewpersad for the special times we shared, Kovashni Pillay for her friendship, Clint Sliedrecht for the inspiring chats we shared, Veron Ramsuran and the crew for the fun Friday afternoons shared under the “tree”!

Also to the many Honours and Postgraduate students in ‘Lab B23B’, every member of the Molecular Genetics Research Group (MGRG), and my many friends in all the other departments. Each of you guys made the scientific journey so much more enjoyable!

To the staff, colleagues and my many friends at Edgars, Pietermaritzburg – my weekends will always be treasured for having shared them with you guys. A very special note of appreciation to Vellie Chetty for her love and encouragement during my studies.

Finally, to the National Research Foundation (Thuthuka Grant) and the University of KwaZulu-Natal and Dr. Albert Modi for employing me as a Research assistant and having faith in my molecular skills. Thank you for the financial support.

ABSTRACT

Autolysins are endogenous enzymes responsible for the cleavage of specific bonds in the bacterial sacculus resulting in damage to the integrity and protective properties of the cell wall. The true biological functions of these enzymes are largely unknown. However, they have been implicated in various important biological synthesis processes making their characterization important. Antibiotic susceptibility testing showed these streptococcal strains to have broad spectrum inhibitory concentrations. The major autolysins of selected streptococcal strains were detected and partially characterized by renaturing sodium dodecyl sulfate (SDS)-polyacrylamide gel electrophoresis with substrate-containing gels (zymograms). The autolysins were isolated from the specific culture supernatants using 4% SDS precipitation and were shown to have apparent molecular masses ranging from 60kDa to 20kDa. Four major autolysins named A, B, C, and D from the *Streptococcus milleri* 77 strain were characterized. Lytic enzymes were blotted onto polyvinylidene difluoride (PVDF) membrane and N-terminally sequenced. Sequences showed between 100% and 80% similarity to that of a muramidase, glucosaminidase and a peptidase from *S. mutans*, *S. pyogenes* and *S. pneumonia* respectively. Biochemical characterization confirmed autolysin A to exhibit muramidase activity with both autolysin B and C exhibiting endopeptidase activity. Autolysin D showed an 80% N-terminal sequence similarity to Millericin B, a peptidoglycan hydrolase that is known to exhibit peptidase activity. Autolysis was determined using different buffers at two optimal pHs. Assaying for autolytic activity at different growth stages showed autolysis to be moderate during the lag and early exponential phases of the growth cycle. The activities of autolysins were the highest in the late exponential phase and the stationary phase of growth. Zymogram analysis showed that the *Streptococcal milleri* strains had moderate autolytic expression during the early and late exponential phases of the growth cycle. Control regulatory mechanisms of autolysins were determined in the presence or absence of specific charged groups, such as teichoic acids. In each case the absence of these charged groups inhibited the rate of autolysis, suggesting that the absence of teichoic acids could play a role in the regulation of the autolysins. Two-dimensional-SDS and zymographic-electrophoresis was used to determine total protein profiles for each strain. This is the first report using two-dimensional zymography. Specific proteins which were either up- or down-regulated were identified.

TABLE OF CONTENTS

	PAGE
TITLE	i
PREFACE	ii
ACKNOWLEDGMENTS	iii
ABSTRACT	v
LIST OF FIGURES	xi
LIST OF TABLES	xxv
ABBREVIATIONS	xxvi
CHAPTER ONE: INTRODUCTION AND LITERATURE REVIEW	1
1.1. INTRODUCTION	2
1.2. ENDOGENOUS BACTERIOCIDIAL ENZYMES	3
1.2.1. Cell wall hydrolase specificities	4
1.2.2. Functions of peptidoglycan hydrolases	5
1.2.3. Regulation and control of peptidoglycan hydrolases	6
1.3. PEPTIDOGLYCAN HYDROLASE SYSTEMS	8
1.3.1. <i>Escherichia coli</i> murein hydrolases	8
1.3.1.1. Glycosidases	9
1.3.1.2. Peptidases, Amidases, Endopeptidases and Exopeptidases	10
1.3.2. Peptidoglycan hydrolases of <i>Bacillus subtilis</i>	13
1.3.2.1. Genetic organisation of the <i>Bacillus</i> hydrolases	13
1.3.3. <i>Bacillus licheniformis</i> peptidoglycan hydrolase	14

	PAGE
1.3.4. The peptidoglycan hydrolases of <i>Enterococcus hirae</i> ATCC 9790	15
1.3.5. Peptidoglycan hydrolases from <i>Streptococcus pneumoniae</i>	15
1.3.6. Cell wall hydrolases of <i>Staphylococcus aureus</i>	16
1.3.7. Peptidoglycan hydrolases of other bacterial species	16
 1.4. D – ALANYL – TEICHOIC ACIDS IN GRAM POSITIVE BACTERIA	 17
1.4.1. Teichoic acids as a cell wall constituent	17
1.4.2. Structure of wall teichoic acids and lipoteichoic acids	19
1.4.3. Topography of teichoic acids	22
1.4.4. Teichoic acids and the glycocalyx	23
1.4.5. Functions of teichoic acids	24
1.4.5.1. Role of D – alanyl esters	24
1.4.5.2. Lipoteichoic acid and wall teichoic acid in the content of the envelope	25
1.4.5.3. D-Alanyl esters in autolysin control	26
1.4.6. D-Alanyl esters and pathogenicity	27
1.4.7. Future possibilities using teichoic acids as regulators	29
 1.5. PROGRAMMED CELL DEATH IN BACTERIA DEVELOPMENT	 31
1.5.1. Defining programmed death in bacteria	31
1.5.1.1. Sporulation	32
1.5.1.2. Programmed death and sex	35
1.5.2 Two-component regulatory systems	35
1.5.2.1 Two-component regulatory systems in <i>Staphylococcus aureus</i>	37
1.5.2.2 Two-component signal transduction in <i>Enterococcus faecalis</i>	40

	PAGE
1.5.3 Genes controlling cell death and survival	42
1.5.3.1 <i>Staphylococcus pneumonia</i> lysis by antibiotics and survival of cells	42
1.5.3.2 Genes controlling the survival of <i>Escherichia coli</i>	43
1.6. TWO-DIMENSIONAL GEL ELECTROPHORESIS	45
1.6.1. An introduction to two-dimensional gel electrophoresis	45
1.6.2. Principle of two-dimensional polyacrylamide gel electrophoresis	45
1.6.3. Two-dimensional polyacrylamide technique	47
1.6.3.1. Bacterial protein sample preparation	47
1.6.3.2. Two-dimensional protein electrophoresis	48
1.6.3.3. Staining and detection of 2-Dimensional gels	49
1.7. SURFACE PLASMON RESONANCE (SPR)	50
1.7.1. An introduction to Surface Plasmon Resonance	50
1.7.2. Principle of SPR technology	50
1.7.3. Commercialization of SPR technology	52
1.7.3.1. Biacore's SPR technology	53
1.7.3.1.1. Sensor chip technology	53
1.7.3.1.2. Microfluidics	54
1.7.3.1.3. Surface plasmon resonance detection	55
1.7.3.2. Choice of coupling chemistry	55
1.7.3.3. Advantages of Biacore	55
1.7.4. Applications of Biacore	56
1.8. CONCLUSION	57
1.9. AIMS AND OBJECTIVES	59

	PAGE
CHAPTER TWO: MATERIALS AND METHODS	60
2.1. Bacterial strains, culture and growth conditions	61
2.2. Minimal inhibitory concentration (MIC)	61
2.3. Disk diffusion assay to determine antibiotic susceptibility	61
2.4. Relative Fitness Assay	62
2.5. Gram stain morphology and microscopy	62
2.6. Protein and autolysin extraction	62
2.7. Protein concentrations	63
2.8. Sodium dodecyl sulfate - Polyacrylamide Gel Electrophoresis (SDS-PAGE)	63
2.9. Two Dimensional sodium sulfate - Polyacrylamide Gel Electrophoresis (2-D SDS-PAGE)	64
2.9.1. Sample preparation	64
2.9.2. First-dimension electrophoresis	65
2.9.3. Second-dimension electrophoresis	65
2.9.4. Silver staining	66
2.10. Preparation of cell wall material	67
2.11. Renaturing SDS-PAGE (Zymogram)	67
2.12. Two Dimensional Zymographic analysis	67
2.12.1. First-dimension electrophoresis	68
2.12.2. Second-dimension electrophoresis	68
2.12.3. Staining and visualization of Two-dimensional Zymographic profile	69
2.13. Elution of lytic proteins from zymograms	69
2.14. N-terminal sequencing	69
2.15. Appearance of N-acetyl amino sugars and free amino groups in soluble fragments during lysis of bacterial cell walls	70
2.16. Autolytic assays with whole cells	70
2.17. Autolytic assay on cell wall fractions	70
2.18. Preparation of peptidoglycan fractions	71
2.19. Molecular interaction measurements	71

	PAGE
2.20. Preparation of Auto-inducing peptide (AIP) containing supernatants	72
2.21. <i>Agr</i> auto-induction assay	73
2.22. Molecular manipulations	73
2.23. Construction and design of primers for Polymerase Chain Reaction (PCR)	74
CHAPTER THREE: RESULTS AND DISCUSSION	77
3.1. Minimal inhibitory concentrations (MIC)	78
3.2. Relative fitness assay	85
3.3. Autolytic protein and Zymographic profiles	90
3.4. Two Dimensional sodium sulfate - Polyacrylamide Gel Electrophoresis (2D SDS-PAGE)	97
3.4.1. 2D SDS-PAGE	97
3.4.2. Two Dimensional SDS - Zymographic analysis	105
3.5. Gram stain morphology and microscopy	107
3.6. Autolytic Assays	109
3.7. Autolysin identification	112
3.8. N-terminal Sequencing	113
3.9. Colorimetric Assays	118
3.9.1. Morgan-Elson Assay	118
3.9.2. N-dinitrophenyl Assay	121
3.10. Peptidoglycan Assays	123
3.11. Molecular interaction analysis (Biacore)	128
3.12. Auto Inducing Peptide (AIP) Assays	143
3.13. Molecular manipulations	148
CHAPTER FOUR: CONCLUSION AND FUTURE STUDIES	150
CHAPTER FIVE: REFERENCES	153

LIST OF FIGURES

- Figure 1.1.** Structure of the murein sacculus of *Escherichia coli*. *N*-acetylglucosamine (GlcNAc) and *N*-acetylmuramic acid (MurNAc) are interlinked in an alternating sequence by β -1,4-glycosidic bonds forming polysaccharide chains which are cross linked by peptides of L- and D-alanine, D-glutamic acid and meso-diminopimelic acid (m-A₂pm). [Holtje, 1995].
Page 9
- Figure 1.2.** Cleavage properties of peptidases showing the reduction of proteins into single amino acids.
Page 10
- Figure 1.3.** Protonated D-alanyl ester substituents linked to the 2' hydroxyl of a Gro-P unit (*sn*-glycerol 1-phosphate). Ion pairing of the phosphodiester with the protonated group occurs on rotation of the phosphodiester linkage [Neuhaus and Baddiley, 2003].
Page 18
- Figure 1.4.** Wall teichoic acid. (A) Linkage unit. (B) Poly(Gro-P)(*sn*-glycerol 3-P) moiety from *Bacillus subtilis* 168 and poly(Rbo-P) from *Staphylococcus aureus* H. (C) Substituents on poly(Rbo-P) and poly(Gro-P) are characteristic of these bacteria [Neuhaus and Baddiley, 2003].
Page 20
- Figure 1.5.** Type I lipoteichoic acid. (A) Glycolipid anchor. (B) Poly(Gro-P) (*sn*-glycerol 1-P). (C) Substituents (X) [Neuhaus and Baddiley, 2003].
Page 21
- Figure 1.6.** Topography of wall teichoic acid and lipoteichoic acid in *Staphylococcus aureus*. Peptidoglycan is shown as black lines whilst the wall teichoic acids are the green symbols. Topology of the lipoteichoic acids is depicted as red symbols [Neuhaus and Baddiley, 2003].
Page 21

Figure 1.7. Continuum of ionic charge. A high-magnification, freeze-substituted image of the septal region of an exponentially growing *Bacillus subtilis* 168 cell is shown. The tripartite structure of the walls shows the fibrous nature of the outer layer. The electron photomicrograph is a reprint where A^+ represents the D-alanyl esters of teichoic acids, \oplus represents mobile cations and other fixed cationic functions in peptidoglycan, and \ominus represents the phosphodiester anionic linkages of teichoic acids and anionic groups of peptidoglycan [Neuhaus and Baddiley, 2003]. **Page 30**

Figure 1.8. Programmed death of mother cell in sporulation development of *B. subtilis*. Environmental as well as internal signals are integrated at level of Spo0A, which in turn activates a cascade of sporulation sigma factors. The terminal sigma factor σ^k controls the final stages of sporulation-formation of the spore cortex, coat synthesis and expression of autolysins CwlC and CwlH. Activation of autolysins by an unknown factor causes mother cell lysis and liberation of the spore [Lewis, 2000]. **Page 34**

Figure 1.9. PCD in autolysis of *S. pneumoniae*. At a high cell density of, the concentration of a released pheromone (CSP) increases and activates a two-component signal transduction kinase (ComD) and its response regulator (ComE). Phosphorylated ComE in turn activates transcription of a competence operon containing the genes required for recombination of incoming DNA and the *lytA* gene, responsible for autolysis. Released DNA is picked up by other cells and recombined with the aid of RecA. LytA requires activation, which is controlled by the sensory kinase VncS. Signals originating from cell damage by antibiotics and possibly by other factors converge prior to or at the level of VncS and activate LytA, causing elimination of defective cells [Lewis, 2000]. **Page 36**

Figure 1.10. The *agr* locus showing the various components and their putative actions in the signalling network for *S. aureus* [Gholson *et al.*, 2000]. **Page 39**

Figure 1.11. Diagrammatic representation of the principle of Iso-electric focusing, allowing complex protein mixtures to be separated via their pI values.

Page 46

Figure 1.12. Incorporation of different chemicals to facilitate the disruption of bacterial cells, where each component allows for the solubilization of the protein mixture [Rabilloud, 1996].

Page 48

Figure 1.13. Basic components of an instrument for SPR biosensing: A glass slide with a thin gold coating is mounted on a prism. Light passes through the prism and slide, reflects off the gold and passes back through the prism to a detector. Changes in reflectivity versus angle or wavelength give a signal that is proportional to the volume of biopolymer bound near the surface.

Page 51

Figure 1.14. A typical SPR biosensing experiment showing the optical response versus time. The gold surface with immobilized interactants starts in pure buffer at T₀. At T₁, solution containing the other interactant is introduced to produce an association. At T₂ the flow cell is flushed with pure buffer, after which the dissociation is measured. Lastly the starting surface is regenerated with a sequence of reagents.

Page 52

Figure 1.15. The sensor chip surface.

Page 54

Figure 3.1. Minimal inhibitory concentration determined by the micro titre dilution assay, of Ampicillin and Penicillin against the Streptococcal strains *S. milleri* P35, *S. milleri* 77 and *S. milleri* B200. Antibiotics are represented as follows: (●●●) – Ampicillin and (////) – Penicillin.

Page 81

Figure 3.2. Plot of the radius diameter (mm) of the zone of inhibition versus the concentration of Ampicillin (µg/ml) tested for *S. milleri* 77. MIC was determined on tryptone soy agar plates, where 200µl of starter culture was inoculated into sloppy agar and overlaid. Plots are represented as: Raw data (○) and Fit curve (—).

Page 82

- Figure 3.3.** Disk diffusion assay for *S. milleri* 77 tested against specific antibiotic concentrations ranging from 0 to 30 μ g/ml. **(A)** Disk diffusion assay tested against the antibiotic Ampicillin, establishing the MIC value at 10 μ g/ml. **(B)** Disk diffusion assay tested against the antibiotic Penicillin, establishing the MIC value greater than 30 μ g/ml. **Page 83**
- Figure 3.4.** Minimal inhibitory concentration determined by the disk diffusion assay of Ampicillin and Penicillin against the Streptococcal strains, *S. milleri* P35, *S. milleri* 77 and *S. milleri* B200. Antibiotics are represented as follows: (●) – Ampicillin and (///) – Penicillin. **Page 84**
- Figure 3.5.** Diagrammatic representation of a typical growth cycle during one generation of a bacterial population. The different phases are shown progressively as a sigmoidal curve. **Page 85**
- Figure 3.6.** Relative fitness profiles (raw data) for each Streptococcal strain, in the absence of antibiotic stress. Bacterial growth cycle was monitored as changes in the optical density at 600_{nm} over Time. The plots are represented as follows: *S. milleri* P35 – (●); *S. milleri* 77 – (■); and *S. milleri* B200 – (▲). **Page 86**
- Figure 3.7.** Relative fitness profiles (fit curves) for each Streptococcal strain, in the absence of antibiotic stress. Bacterial growth cycle was monitored as changes in the optical density at 600_{nm} over Time. The plots are represented as follows: *S. milleri* P35 – (—); *S. milleri* 77 – (...); and *S. milleri* B200 – (- · -). **Page 87**
- Figure 3.8.** Relative fitness profiles (raw data) for each Streptococcal strain, presence of Ampicillin at sub minimal inhibitory concentrations. Bacterial growth cycle was monitored as changes in the optical density at 600_{nm} over Time. The plots are represented as follows: *S. milleri* P35 – (●); *S. milleri* 77 – (■); and *S. milleri* B200 – (▲). **Page 88**

Figure 3.9. Relative fitness profiles (fit curves) for each Streptococcal strain, presence of Ampicillin at sub minimal inhibitory concentrations. Bacterial growth cycle was monitored as changes in the optical density at 600_{nm} over Time. The plots are represented as follows: *S. milleri* P35 – (—); *S. milleri* 77 – (...); and *S. milleri* B200 – (— · —). **Page 89**

Figure 3.10. Standard curve. Different concentrations of Bovine serum albumin (0.5 - 200µg/ml) were used as the standard. The plots are represented as follows: Raw data - Black and Fit Curve – Dashed solid line. **Page 90**

Figure 3.11. Polyacrylamide (10%) gel of proteins extracted with 4% SDS from whole cells of *Streptococcus milleri* P35. Lanes 1-5: Represents extractions from stages within the growth cycle. Lanes: 1, mid lag phase; 2, early exponential phase; 3, mid exponential phase; 4, mid stationary phase; and 5, death phase. MWM: BioRad Precision Plus unstained protein standards. **Page 91**

Figure 3.12. Zymogram analysis of proteins extracted with 4% SDS from different stages within the growth cycle of *Streptococcus milleri* P35. The gel contains 0.1% *S. milleri* P35 crude cell wall stained with 0.1% methylene blue in 0.01% KOH. Lanes: 1, mid lag phase; 2, early exponential phase; 3, mid exponential phase; 4, mid stationary phase; and 5, death phase. **Page 92**

Figure 3.13. Polyacrylamide (10%) gel of proteins extracted with 4% SDS from whole cells of *Streptococcus milleri* 77. Lanes 1-5: Represents extractions from stages within the growth cycle. Lanes: 1, mid lag phase; 2, early exponential phase; 3, mid exponential phase; 4, mid stationary phase; and 5, death phase. MWM: BioRad Precision Plus unstained protein standards. **Page 93**

Figure 3.14. Zymogram analysis of proteins extracted with 4% SDS from different stages of the growth cycle of *Streptococcus milleri* 77. The gel contains 0.1% *S. milleri* 77 crude cell wall stained with 0.1% methylene blue in 0.01% KOH. Lanes: 1, mid lag phase; 2, early exponential phase; 3, mid exponential phase; 4, mid stationary phase; and 5, death phase.

Page 94

Figure 3.15. Polyacrylamide (10%) gel of proteins extracted with 4% SDS from whole cells of *Streptococcus milleri* B200. Lanes 1-5: Represents extractions from stages within the growth cycle. Lanes: 1, mid lag phase; 2, early exponential phase; 3, mid exponential phase; 4, mid stationary phase; and 5, death phase. MWM: BioRad Precision Plus unstained protein standards.

Page 95

Figure 3.16. Zymogram analysis of proteins extracted with 4% SDS from different stages of the growth cycle of *Streptococcus milleri* B200. The gel contains 0.1% *S. milleri* B200 crude cell wall stained with 0.1% methylene blue in 0.01% KOH. Lanes: 1, mid lag phase; 2, early exponential phase; 3, mid exponential phase; 4, mid stationary phase; and 5, death phase.

Page 96

Figure 3.17. Polyacrylamide (10%) gel of total protein extracted from whole cells of *Streptococcus milleri* 77. Lanes 1-4: Represents extractions from mid exponential cell cultures, grown in the presence or absence of antibiotic stress. Ampicillin at MIC value of 10 μ g/ml was incorporated into the growing culture. Lanes: 1, 0.5 μ g protein in the absence of antibiotic; 2, 0.5 μ g protein in the presence of 10 μ g/ml ampicillin; 3, 0.5 μ g protein in the absence of antibiotic; and 4, 1 μ g protein in the presence of 10 μ g/ml ampicillin. MWM: BioRad Precision Plus unstained protein standards.

Page 97

Figure 3.18. 2-D PAGE analysis of cellular proteins of *S. milleri* 77 cultured in the absence of antibiotic. Extracted proteins were separated by isoelectric focusing in the pI range of 4 to 7 in the first dimension and a gradient (10%) SDS-PAGE in the second dimension. Resolved proteins were visualized following (A) Coomassie Blue staining and (B) Silver staining. MWM: BioRad Precision Plus unstained protein standards indicated on the extreme left. **Page 98**

Figure 3.19. 2-D PAGE analysis of cellular proteins of *S. milleri* 77 cultured in the presence of antibiotic (Ampicillin - 10µg/ml). Extracted proteins were separated by isoelectric focusing in the pI range of 4 to 7 in the first dimension and a gradient (10%) SDS-PAGE in the second dimension. Resolved proteins were visualized following (A) Coomassie Blue staining and (B) Silver staining. MWM: BioRad Precision Plus unstained protein standards indicated on the extreme left. **Page 99**

Figure 3.20. Comparative analysis of the 2-D PAGE gels of the cellular proteins of *S. milleri* 77. (A) Resolved proteins with cells cultured in the absence of antibiotic stress. (B) Resolved proteins with cells cultured in the presence of antibiotic (Ampicillin - 10µg/ml). **Page 100**

Figure 3.21. (A) Molecular weight standards were based on the BioRad Precision Plus unstained protein standards run in second dimension electrophoresis. (B) Molecular weight and pI grid analysis of the Master gel established using PD QUEST software. **Page 102**

Figure 3.22. Comparative analysis of the 2-D PAGE gels of the cellular proteins of *S. milleri* 77. (A) Resolved proteins with cells cultured in the absence of antibiotic stress. (B) Resolved proteins with cells cultured in the presence of antibiotic (Ampicillin - 10µg/ml). Images obtained using PD Quest Software. Green shows spots matched to the master gel, whilst red depicts unmatched spots. **Page 103**

Figure 3.23. Pop-up margin graphic analysis obtained using PD QUEST software, showing three specific spots at an approximate molecular weight just below 15kDa on the Master Gel (2-D PAGE gel of the cellular proteins of *S. milleri* 77 in the absence of antibiotic stress). Spot number is identified as SSP, the thick black bar (■) in the graph shows these specific spots to be present when cells are cultured in the absence of an antibiotic stress.

Page 104

Figure 3.24. Zymogram analysis of mid exponential phase proteins of *Streptococcus milleri* 77 extracted with 4% SDS. The gel contains 0.2% *S. milleri* 77 crude cell wall material. Extracted proteins were separated by isoelectric focusing in the pI range of 4 to 7 in the first dimension and a gradient (10%) SDS-PAGE in the second dimension. Gels were stained with 0.1% methylene blue in 0.01% KOH.

Page 105

Figure 3.25. *S. milleri* P35 cell morphology from a 48 hour culture. 100X magnification achieved using oil emersion.

Page 107

Figure 3.26. *S. milleri* B200 cell morphology from a 48 hour culture. 100X magnification achieved using oil emersion.

Page 108

Figure 3.27. Autolytic rate shown as a regression plot, with the standard deviation (\mp) plotted above the bar. Different buffers for each assay are shown as follows: Clear bars – 50mM Phosphate buffer (pH 7.2); (●) – 50mM Phosphate buffer in 0.01% Triton X-100 (pH 7.2); (\\) – 50mM Phosphate buffer in 0.01% Deoxycholate (pH 7.2); (=) – 50mM Glycine buffer in 0.01% Triton X-100 (pH 8) and Black bars – Ampicillin induced lysis in 50mM Phosphate buffer (pH 7.2).

Page 109

Figure 3.28. Zymogram analysis of proteins extracted with 4% SDS from different stages within the growth cycle of *Streptococcus milleri* 77. The gel contains 0.1% *S. milleri* 77 crude cell wall stained with 0.1% methylene blue in 0.01% KOH. Lanes: 1, mid lag phase; 2, early exponential phase; 3, mid exponential phase; 4, mid stationary phase; and 5, death phase. A, B, C and D indicate the different putative autolysins selected for further characterization. **Page 112**

Figure 3.29. Illustrative representation demonstrating N-terminal sequencing using Edman chemistry. **Page 114**

Figure 3.30. PVDF blot of protein extracts from *Streptococcus milleri* 77. Blot was stained with Coomassie Blue. Lanes: 1, death phase; 2, mid stationary phase; 3, mid exponential phase; 4, early exponential phase; and 5, mid lag phase. MWM: BioRad Precision Plus unstained protein standards. **Page 115**

Figure 3.31. Morgan-Elson chemistry showing the *N*-acetylglucosamine at the reducing end (A). Proposed structures of the coloured product and chromogens I, II and III in the Morgan-Elson assay reaction (B). Chromogen I depicts the α configuration and chromogen II shows the β configuration described by Takahashi *et al.*, 2003. **Page 119**

Figure 3.32. Liberation of free reducing sugars from the cell walls of *Streptococcus milleri* 77 after digestion with autolysins analyzed by the Morgan-Elson assay. Symbols: \square , cell walls digested with Autolysin A; Δ , cell walls digested with mutanolysin; \diamond , cell walls digested with Autolysin B; and \circ , cell walls digested with Autolysin C; and \blacktriangledown , cell walls digested with Autolysin D. **Page 120**

Figure 3.33. Cleavage properties of peptidases showing the reduction of proteins into single amino acids. **Page 121**

Figure 3.34. Liberation of free amino groups for the digestion of *Streptococcus milleri* cell walls with Autolysins extracted from *Streptococcus milleri* 77 analyzed by the DNP assay. Symbols: □, cell walls digested with Autolysin A; Δ, cell walls digested with mutanolysin; ◇, cell walls digested with Autolysin B; ○, cell walls digested with Autolysin C; and ▼, cell walls digested with Autolysin D. **Page 122**

Figure 3.35. Regression patterns monitoring the presence versus the absence of teichoic acids (a charged group) in the peptidoglycan for each of the Streptococcal strains, with the standard deviation (⊥) plotted above the bar. Peptidoglycan in the presence of teichoic acids is shown as clear bars whilst (⊙) represents the absence of teichoic acids. **Page 124**

Figure 3.36. Regression patterns monitoring the presence versus the absence of teichoic acids (a charged group) in the peptidoglycan for each of the Streptococcal strains, with the standard deviation (⊥) plotted above the bar. Autolytic extract (100μg/ml) of each respective strain was incorporated. Peptidoglycan in the presence of teichoic acids is shown as clear bars whilst (⊙) represents the absence of teichoic acids. The control peptidoglycan, containing no autolytic additives in the presence of teichoic acids is shown as (||). **Page 125**

Figure 3.37. Regression patterns monitoring the presence versus the absence of teichoic acids (a charged group) in the peptidoglycan for each of the Streptococcal strains, with the standard deviation (⊥) plotted above the bar. Antibiotic (Ampicillin) below the MIC value was incorporated. Peptidoglycan in the presence of teichoic acids is shown as clear bars whilst (⊙) represents the absence of teichoic acids. The peptidoglycan containing antibiotic in the presence of teichoic acids are indicated as (\\). The peptidoglycan containing antibiotic in the absence of teichoic acids are shown as (=). **Page 127**

- Figure 3.38.** Enzymatic degradation of the polysaccharide component of the bacterial cell wall by the enzyme Lysozyme [Holtje, 1995]. **Page 128**
- Figure 3.39.** Sensogram showing the immobilization of Lysozyme onto a CM5 sensor chip using amine coupling. **Page 130**
- Figure 3.40.** Sensogram showing the interaction between the Peptidoglycan with intact teichoic acids (shown in Red) and Peptidoglycan without teichoic acids (shown in Green) in the presence of a 10 μ l crude autolytic extract for *Streptococcus milleri* P35. The arrows (\downarrow) 1 and 2 indicate the start and end of the injection of the autolysin sample. The symbol (a) depicts the regeneration of the sensor chip with 5 μ l NaOH. **Page 132**
- Figure 3.41.** Sensogram showing the interaction between the Peptidoglycan with intact teichoic acids (shown in Red) and Peptidoglycan without teichoic acids (shown in Green) in the presence of a 20 μ l crude autolytic extract for *Streptococcus milleri* P35. The arrows (\downarrow) 1 and 2 indicate the start and end of the injection of the autolysin sample. **Page 133**
- Figure 3.42.** Sensogram showing the interaction between the Peptidoglycan with intact teichoic acids (shown in Red) and Peptidoglycan without teichoic acids (shown in Green) in the presence of a 50 μ l crude autolytic extract for *Streptococcus milleri* P35. The arrows (\downarrow) 1 and 2 indicate the start and end of the injection of the autolysin sample. The symbol (a) depicts the regeneration of the sensor chip with 5 μ l NaOH. **Page 134**
- Figure 3.43.** Sensogram showing the interaction between the Peptidoglycan with intact teichoic acids (shown in Red) and Peptidoglycan without teichoic acids (shown in Green) in the presence of a 10 μ l crude autolytic extract for *Streptococcus milleri* 77. The arrows (\downarrow) 1 and 2 indicate the start and end of the injection of the autolysin sample. **Page 136**

Figure 3.44. Sensogram showing the interaction between the Peptidoglycan with intact teichoic acids (shown in Red) and Peptidoglycan without teichoic acids (shown in Green) in the presence of a 20 μ l crude autolytic extract for *Streptococcus milleri* 77. The arrows (\downarrow) **1** and **2** indicate the start and end of the injection of the autolysin sample. The symbol **(a)** depicts the regeneration of the sensor chip with 5 μ l NaOH. **Page 137**

Figure 3.45. Sensogram showing the interaction between the Peptidoglycan with intact teichoic acids (shown in Red) and Peptidoglycan without teichoic acids (shown in Green) in the presence of a 50 μ l crude autolytic extract for *Streptococcus milleri* 77. The arrows (\downarrow) **1** and **2** indicate the start and end of the injection of the autolysin sample. The symbol **(a)** depicts the regeneration of the sensor chip with 5 μ l NaOH. **Page 138**

Figure 3.46. Sensogram showing the interaction between the Peptidoglycan with intact teichoic acids (shown in Red) and Peptidoglycan without teichoic acids (shown in Green) in the presence of a 10 μ l crude autolytic extract for *Streptococcus milleri* B200. The arrows (\downarrow) **1** and **2** indicate the start and end of the injection of the autolysin sample. The symbol **(a)** depicts the regeneration of the sensor chip with 5 μ l NaOH. **Page 140**

Figure 3.47. Sensogram showing the interaction between the Peptidoglycan with intact teichoic acids (shown in Red) and Peptidoglycan without teichoic acids (shown in Green) in the presence of a 20 μ l crude autolytic extract for *Streptococcus milleri* B200. The arrows (\downarrow) **1** and **2** indicate the start and end of the injection of the autolysin sample. The symbol **(a)** depicts the regeneration of the sensor chip with 5 μ l NaOH. **Page 141**

Figure 3.48. Sensogram showing the interaction between the Peptidoglycan with intact teichoic acids (shown in Red) and Peptidoglycan without teichoic acids (shown in Green) in the presence of a 50µl crude autolytic extract for *Streptococcus milleri* B200. The arrows (↓) **1** and **2** indicate the start and end of the injection of the autolysin sample. The symbol **(a)** depicts the regeneration of the sensor chip with 5µl NaOH. **Page 142**

Figure 3.49. Structural diversity of auto-inducing peptides found in Gram positive bacteria. **(A)** Lantibiotic nisin of *Lactococcus lactis*; **(B)** Competence development (ComC) found in *Streptococcus pneumoniae* and **(C)** Cyclic thiolactone- and lactone- peptides, AIP group I of *Staphylococcus aureus* and GBAP (gelatinase biosynthesis-activating pheromone) found in *Enterococcus faecalis*. [Strume *et al.*, 2002] **Page 143**

Figure 3.50. Regression patterns monitoring the rate of autolysis in the presence of differing percentages of Auto-Inducing Peptide additives (% AIP) isolated from a control *Staphylococcus aureus* strain. The standard deviation (\top) is plotted above the bar. The plots are represented as follows: (⊙) – *S. aureus*; (\\) – *S. milleri* P35 and clear bars – *S. milleri* B200. The control plots represent no percentage of AIP added to the assay. This assay was conducted in the absence of antibiotic stress. **Page 145**

Figure 3.51. Regression patterns monitoring the rate of autolysis in the presence of differing percentages of Auto-Inducing Peptide additives (% AIP) isolated from a control *Staphylococcus aureus* strain. The standard deviation (\top) is plotted above the bar. The plots are represented as follows: (⊙) – *S. aureus*; (\\) – *S. milleri* P35 and clear bars – *S. milleri* B200. To each of the reactions ampicillin below the MIC value at 5µg/ml was incorporated. The control plots represent the autolytic rates in the absence of auto-inducing peptide. **Page 147**

Figure 3.52. Isolated DNA from *Streptococcus milleri* and *Staphylococcus aureus* strains. Lanes 1: *S. milleri* P35 DNA; 2: *S. milleri* 77 DNA; 3: *S. milleri* B200 DNA; and 5: *S. aureus* DNA.

Page 148

LIST OF TABLES

- Table 1.1.** Murein hydrolases of *Escherichia coli*. Only enzymes whose genes have been mapped are indicated [Holtje, 1995]. **Page 12**
- Table 2.1.** Reagents used to prepare SDS-PAGE gels. **Page 66**
- Table 2.2.** Primer designation and sequence [Jarraud, S. *et al.* 2002 and Shopsin, B. *et al.* 2003]. **Page 75**
- Table 2.3.** Expected PCR product size [Shopsin, B. *et al.* 2003]. **Page 75**
- Table 2.4.** PCR Profile [Shopsin, B. *et al.* 2003]. **Page 76**
- Table 3.1.** N-terminal sequence similarity of the major autolytic enzymes from *Streptococcus milleri* 77. **Page 117**
- Table 3.2.** Concentration of the DNA samples from the bacterial isolates, analyzed using the NanoDrop Spectrophotometer. **Page 149**

LIST OF ABBREVIATIONS

2-D SDS PAGE	Two-dimensional Sodium Dodecyl Sulfate Polyacrylamide gel Electrophoresis
<i>agr</i>	Accessory gene regulator
<i>S. aureus</i>	<i>Streptococcus aureus</i>
<i>S. milleri</i> 77	<i>Streptococcus milleri</i> 77
<i>S. milleri</i> B200	<i>Streptococcus milleri</i> B200
<i>S. milleri</i> P35	<i>Streptococcus milleri</i> P35
AIP	Auto-Inducing Peptide
BCA	Bicinchoninic Acid
CAPS	3-cyclohexylaminol 1-propanesulfonic acid
CHAPS	3-[3 (Cholamidopropyl) dimethyl-ammonio] 1-propanesulfonate
DMAB	<i>p</i> -dimethylaminobenzaldehyde
DNP	N-dinitrophenyl
DTT	Dithiothreitol
EDC	<i>N</i> -ethyl- <i>N</i> '-[(3-dimethylamino)-propyl]-hydrochloride
EDTA	Ethylene Diamine Tetra-acetic Acid
E-HCl	Ethanolamine-hydrochloric Acid
HEPES	4-(2-Hydroxyethyl)-1-piperazineethansulfonic acid
HF	Hydrofluoric acid
IEF	Isoelectric Focusing
IPG	Immobilized Protein Gradient
IPG Buffer	Immobilized Protein Gradient Buffer
LTA	Lipoteichoic Acid
MIC	Minimum Inhibitory Concentration
NHS	<i>N</i> -hydroxysuccinimide
OD	Optical Density
PAGE	Polyacrylamide Gel Electrophoresis
PCD	Programmed Cell Death
PCR	Polymerase Chain Reaction
PITC	Phenylisothiocyanate

LIST OF ABBREVIATIONS

PTH	Phenythiohydantoin
PMSF	Phenylmethylsulfonyl
PVDF	Polyvinylidene membrane
RU	Response Units
SDS	Sodium Dodecyl Sulfate
SPR	Surface Plasmon Resonance
TA	Teichoic Acids
TEMED	Tetramethylethylenediamine
TSA	Tryptone Soy Agar
TSB	Tryptone Soy Broth
WTA	Wall Teichoic Acid

CHAPTER ONE

INTRODUCTION AND LITERATURE REVIEW

CHAPTER ONE

1.1. INTRODUCTION

The origin of the bacterial sacculus has in its entirety lead to the origin of the domain Bacteria. Manufacture of this exoskeleton is complex, mainly due to the fact that it involves the formation of polymerized peptidoglycan external to the cell membrane as a strong, stress resistant sacculus. This process involves the disaccharide pentamuropeptide, its transport through the membrane, and its polymerization in the glycan and peptide directions to form an intact fabric covering the cell. Beyond that, the precursor must be inserted into the wall without risk of lysis and the wall must be safely turned over. These complex processes imply that a set of diverse mechanisms arose and gave rise to variant mechanisms that functioned together to allow the formation of a strong covering or as it is commonly termed the, “bacterial cell wall”.

In both Gram-positive and Gram-negative Genera and species in which bacterial autolysins have been found, a variety of endogenous peptidoglycan hydrolases are self contained. The shape determining properties of peptidoglycan or murein are responsible for mechanically stabilizing a bacterial cell. Very specialized enzymes, allowing for the cleavage of the existing covalent bonds within the murein sacculus are required for the expansion of the bacterial cell wall during growth stages and the splitting of the septum prior to cell separation. It is these enzymes that are collectively know as murein hydrolases.

Peptidoglycan hydrolases have also been found in other micro organisms and even in higher organisms, with hen egg white lysozyme the best-known example. These lysozymes have been widely found in animals, tissues, tears, milk, cervical mucus, urine and most plants. The presence of peptidoglycan hydrolases in organisms other than bacteria may be considered as a natural antibacterial defence mechanism.

An important function of the peptidoglycan hydrolase is its role in cell wall metabolism hence most peptidoglycan hydrolases have been characterised as bacteriolytic enzymes by the various *in vitro* studies carried out to date. Many of the peptidoglycan hydrolases can

be classified on the basis of their cleavage specificities. The peptidoglycan hydrolases are characterised as *N*-acetylmuramidases (muramidases), *N*-acetylglucosamidases, *N*-acetylmuramyl-L-alanine amidases, endopeptidases and transglycosidases. Most of these enzymes display a modular structural organisation with two functional domains: 1, a catalytic domain containing the enzyme active site responsible for the enzymatic specificity and 2, a cell wall binding domain which provides the capacity to bind peptidoglycan of other cell wall polymers. Most of the enzymes responsible for cellular autolysis, that is, cell disintegration leading into the release of the intracellular content into the surroundings, are collectively termed autolysins.

The observation that bacteriolysis could be prevented, via the formation of spherical osmotically fragile bodies, by the provisions of iso-osmotic environments demonstrates that autolysis was the eventual result of hydrolysis of a sufficient number of bonds in the protective cell wall, peptidoglycan, to cause its dissolution and removal from the bacterial surface. Thus the conclusions attained were that these bacteria equipped themselves with their own endogenous enzymes, specifically peptidoglycan hydrolases, which possess the ability to eventually autolyse the cell, hence making their subsequent characterisation and isolation crucial to the understanding of their functioning, regulation and expression within cells.

1.2. ENDOGENOUS BACTERIAL ENZYMES

The peptidoglycan hydrolase enzymes, which are capable of hydrolysing the peptidoglycan of the bacterial cell envelope, are ubiquitous among bacteria. These peptidoglycan hydrolases which are involved in cell lysis are collectively termed autolysins [Tomasz, 1984]. Autolysins can be defined as endogenous enzymes that hydrolyse specific bonds in the bacterial cell wall (peptidoglycan), resulting in damage to the integrity and protective properties of the two- or three-dimensional structure of the peptidoglycan [Shockman *et al.*, 1983, 1988]. This definition excludes all the enzymes that are capable of hydrolysing bonds in the peptidoglycan. Enzymes such as DD-carboxypeptidases which are responsible for the removal of D-alanine residues are excluded from this definition as these enzymes do not hydrolyse bonds that are important in the mechanical stability of the murein sacculus [Holtje, 1995].

1.2.1. Cell wall hydrolase specificities

Bacteria elaborate various peptidoglycan hydrolases which include peptidases and glycosidases. Two types of glycosidases are known: β -*N*-acetylmuramidases (lysozymes) and β -*N*-acetylglucosidases, which hydrolyse the β -1,4-glycosidic bond between *N*-acetylmuramic acid (MurNAc) and acetylglucosamine (GlcNAc) and between GlcNAc and MurNAc, respectively [Holtje *et al.*, 1975; Holtje *et al.*, 1991]. Enzymes with muramidase-like capabilities from *Escherichia coli* as well as phage lamda [Taylor *et al.*, 1975; Bienkowska *et al.*, 1981], where similar to lysozyme, these enzymes cleave the β -1,4-glycosidic bonds between muramic acid and glucosamine. However unlike lysozyme, they transfer the muramyl bond onto the carbon-6-hydroxyl group of the same muramic acid, yielding a 1-6-anhydromuramic acid [Holtje *et al.*, 1975]. Amidases (*N*-acetylmuramoyl-*L*-alanine amidases) are found in many bacteria and effectively separate the peptide components from the amino sugar chain by cleaving the amide bonds between the lactyl group of muramic acid and the α -amino group of *L*-alanine, the first amino acid of the stem peptide [Harz *et al.*, 1990]. The peptide moieties of peptidoglycan are cleaved by exo- as well as endo- peptidases. DD-carboxypeptidases are responsible for the conversion of pentapeptide into tetrapeptide moieties by cleaving the terminal D-alanyl-D-alanine bond of crosslinked and uncrosslinked stem peptides. DD-endopeptidases cleave the DD-peptide at the bond that cross-links the stem peptides to yield the characteristic peptidoglycan network. Other peptidase specificities must exist, because of the existence of certain peptidoglycan turnover products, such as GlcAc-MurNAc-*L*-Ala-*D*-Glu [Gmeiner and Kroll, 1981].

The substrate specificities of these enzymes vary broadly, in that some enzymes will hydrolyse sensitive bonds only in low-molecular-weight wall fragments, while others will only hydrolyse sensitive bonds in intact insoluble cell wall preparations. Therefore, detection of the multiple activities amongst such enzymes greatly depends on the substrate been used.

1.2.2. Functions of peptidoglycan hydrolases

Autolytic peptidoglycan hydrolases present in cultures of rapidly growing and dividing bacteria led to the idea that such potentially suicidal enzymes may play an important role in cell wall assembly and bacterial growth [Shockman, 1965]. The capacity of bacterial cells to autolyse is maximal or near maximal during the exponential growth phase in several bacterial species [Mitchell and Moyle, 1957; Young, 1966; Coyette and Shockman, 1973]. Peptidoglycan hydrolases function in the processes involving the liberation of spores from mother cells and in germination of spores to form vegetative cells [Rogers *et al.*, 1980]. Autolysins may also be involved in cellular lysis following antibiotic inhibition of peptidoglycan synthesis. Similarly, the recycling of peptidoglycan must involve the action of several peptidoglycan hydrolase activities and the loss of wall by the process known as turnover [Shockman *et al.*, 1996]. Various other roles for peptidoglycan hydrolases include the hydrolytic action to provide new acceptor sites for the addition of peptidoglycan precursors in the bag-shape macromolecule surrounding the bacterium; the insertion of new subunits into the stress bearing peptidoglycan layer; the hydrolysis of bonds in selected areas of the cell wall surface causing modifications of the shape of previously assembled wall; cell division by compartmentalization into new cell units separated by both cell membrane and cell wall; and participation in the final stages of cell separation [Ghuysen and Shockman, 1973; Shockman, 1992].

In expanding the sacculus, new peptidoglycan subunits need to be inserted into the pre-existing network. For this process to occur, the existing covalent bonds must be broken to allow enlargement of the cell envelope. While high levels of lytic peptidoglycan hydrolases activities may not be required, some sort of peptidoglycan hydrolase is needed, even for the inside-to-outside growth mechanism for wall growth of gram-positive, rod-shaped bacteria [Pooley and Shockman, 1970; Koch and Doyle, 1985]. New peptidoglycan is first attached underneath the pre-existing peptidoglycan layer and this is followed by the specific cleavage of the covalent bonds in the stress-bearing layer by peptidoglycan hydrolases. As a result of this, the new material is automatically pulled into the layer under stress [Koch, 1990; Holtje, 1993].

Cell wall recycling is usually defined as the loss of previously assembled, insoluble wall from the bacterial cells. Loss of cell wall and cell wall peptidoglycan has been observed

during growth for a number of bacterial species including *B. subtilis*, *B. megaterium*, *Lactobacillus acidophilus*, *Staphylococcus aureus*, *Listeria monocytogenes*, *Escherichia coli* and *Neisseria gonorrhoeae* [Doyle *et al.*, 1998]. These findings dictate that peptidoglycan hydrolases must be involved in the loss of peptidoglycan fragments from assembled, peptide crosslinked wall. An amidase in *B. subtilis* appears to be the primary enzyme actively involved in the supernatant of cultures [Fiedler and Glaser, 1973]. Due to the lack of detection of the amidase in the growth medium, it was postulated that this enzyme was bound to the cell surface and catalysed the removal of wall material. In *L. acidophilus*, the only detectable peptidoglycan hydrolase activity is muramidase [Coyette and Ghuysen, 1970], which must therefore be responsible for the loss of peptidoglycan from the cells. In *E. coli*, lytic trans-glycosylases and endopeptidases are responsible for the turnover, whereas amidases, gulcosamidases and perhaps carboxypeptidases are involved in further hydrolysis of the turnover products to smaller units that can be re-utilized for peptidoglycan assembly after uptake back into the cytoplasm via active transport systems [Goddell and Higgins, 1987].

1.2.3. Regulation and control of peptidoglycan hydrolases

As expected, for such potentially suicidal activities, peptidoglycan hydrolases must be exquisitely regulated and integrated with other biosynthetic and degradative processes. Enzymes, like all proteins, synthesized on ribosomes in the cytoplasm must be transported through the cytoplasmic membrane to the sensitive bonds in the wall. In the cytoplasm they would only have access to cytoplasmic precursors or to wall degradation fragments that may be on a recycling path [Shockman, *et al.*, 1996]. Thus, control of general access to the insoluble substrate becomes an important factor.

Transmission of information to or from other cellular macromolecules in the cytoplasm would be through the cytoplasmic membrane “barrier” [Hartmann *et al.*, 1974]. This barrier was found to prevent access of peptidoglycan hydrolases to the peptidoglycan of *E. coli*. Autolytic transglycosylases can be overproduced to a 30-fold increase in *E. coli* without causing any lysis of the cell [Betzner and Keck, 1989]. Access can be limited to specific topologically located areas in the surface, such as at or near nascent cross walls as in the case of *E. hirae* or in the case of *E. coli*, to a periplasmic ring structure, formed by the periseptal annuli [Foley *et al.*, 1989]. Intact growing cells of *E. hirae* are known to be

resistant to the action of its muramidases, even though muramidase-2 is known to be present in an active form in the culture medium [Kariyama and Shockman, 1993]. In this instance, an exterior molecule could protect the peptidoglycan from hydrolysis. In at least one system, muramidase-1 of *E. hirea* appears to be synthesized and transported to the wall in protease activation, zymogen form. Thus activation of its processive muramidase activity occurs only after protease activation [Kariyama and Shockman, 1993]. This is a one-way mechanism of regulation that can only turn on enzyme activity.

The ability of such enzymes to bind to and maintain contact with the insoluble substrate, particularly outside of the cellular permeability barrier, is also important. This makes substrate binding and specificity very important in regulation. Hydrolysis of a specific bond is sometimes related to exact cell wall chemistry such as the presence or absence of a wall teichoic acid. For example, the presence of choline residues on the wall teichoic acid of pneumococci is important in the binding of an amidase and, therefore hydrolysis of the amidase-sensitive bonds. Several peptidoglycan hydrolases appear to possess noncatalytic modules that could be involved in binding to the wall substrate [Tuomanen and Tomasz, 1986]. Changes in the chemistry of the peptidoglycan may control the action of the peptidoglycan hydrolases. O- and N-acetylation of amino sugars of the peptidoglycan itself are two examples. O-acetylation decreases the susceptibility of the peptidoglycan to hydrolysis by hen egg white lysozyme but not to the *Chalaropsis* muramidase [Clark and Dupont, 1992]. An energized membrane appears to be important in the regulation of the amidase of *B. subtilis* [Jolliffe *et al.*, 1981]. Chaotropic and other agents such as ethanol, osmotic shifts up and down, and treatments with sucrose or salts have all been found to induce spontaneous bacteriolysis. Correlations have often been made with respect to the capacity of bacterial cells to autolyse and to the growth rate, the cell division cycle in synchronized cultures, and phase of growth [Pooley and Shockman, 1970].

1.3. PEPTIDOGLYCAN HYDROLASE SYSTEMS

1.3.1. *Escherichia coli* murein hydrolases

Murein hydrolases cleave bonds in the bacterial exoskeleton, the murein peptidoglycan sacculus, which is a covalently closed bag-shaped polymer made of glycan strands that are cross-linked by peptides. During growth and division of a bacterial cell, these enzymes are involved in the controlled metabolism of the murein sacculus. Murein hydrolases are believed to function as pacemaker enzymes for the enlargement of the murein sacculus since opening of bonds in the murein net is needed to allow the insertion of new sub units into the sacculus. Furthermore, they are responsible for splitting the septum during cell division. The murein turnover products that are released during growth are further degraded by these hydrolases to products that can be recycled by the biosynthetic enzymes. As potentially suicidal (autolytic) enzymes, murein hydrolases must be strictly controlled by the cell. Inhibition of murein synthesis, for example, by an antibiotic triggers an unbalanced action of murein hydrolases causing bacteriolysis. In *Escherichia coli*, 14 different murein hydrolases have been identified, each specific in their cleavage properties. The peptidases are responsible for the cleavage of the peptidyl structure, whilst the glycosidases interact with the polysaccharide chains (Figure 1.1.). The actual autolytic system, that is, the group of enzymes that could autolyse the cell via cleavage of bonds in the high molecular weight sacculus, consists of a variety of enzymes. Two of these enzymes are specialized and are termed endopeptidases and muramidases. The ability to concomitantly cleave bonds in the sacculus moiety to form an acid ring structure makes this system unique and very stable. It is scientifically evident that this reaction is very important in that it serves as a means of conserving the bond energy for further rearrangement reactions.

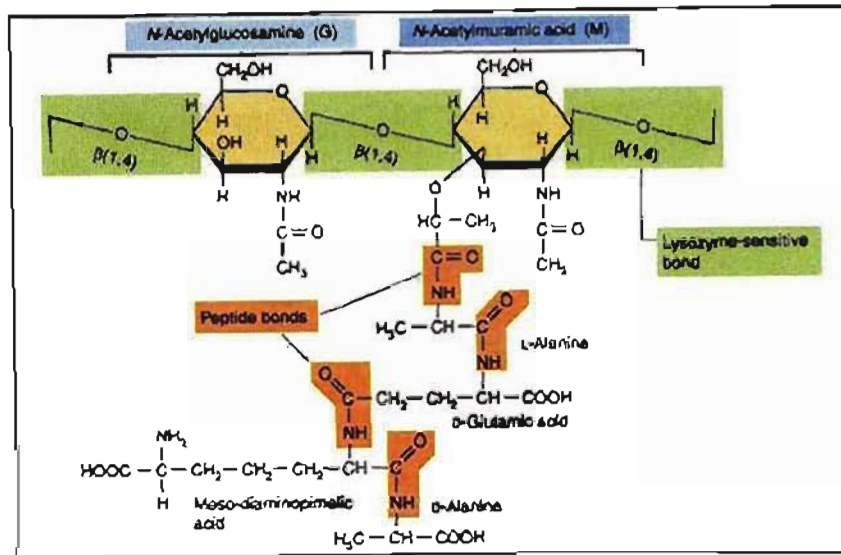


Figure 1.1. Structure of the murein sacculus of *Escherichia coli*. *N*-acetylglucosamine (GlcNAc) and *N*-acetylmuramic acid (MurNAc) are interlinked in an alternating sequence by β -1,4-glycosidic bonds forming polysaccharide chains which are cross linked by peptides of L- and D-alanine, D-glutamic acid and meso-diminopimelic acid (m-A₂pm). [Holtje, 1995].

1.3.1.1. Glycosidases

Romieis *et al.* in 1993 identified three different muramidase-like enzymes which catalyse a reaction (Figure 1.1), where like lysozyme they cleave the β -1,4-glycosidic bond between muramic acid and glucosamine. However, unlike lysozyme, they transfer the muramyl bond onto the carbon-6 hydroxyl group of the very same muramic acid, yielding an (1-6)-anhydromuramic acid [Holtje *et al.*, 1975]. Their intramolecular transglycosylation mechanism is responsible for these enzymes having been termed "lytic transglycosylases". A soluble lytic transglycosylase (Sl_t), with a molecular weight of 70kDa, has been isolated from the periplasm. Mapping of the gene (*sltY*) on the chromosome was achieved by Betzner and Keck in 1989. X-ray chromatography revealed a three-dimensional structure of Sl_t70m which showed a doughnut-shape, a super-helical ring of α -helices with a separate domain on top resembling the folding structure of lysozyme [Thunnissn *et al.*, 1994]. Ml_tA and Ml_tB are membrane-bound lytic transglycosylases, which have recently been identified and their genes mapped. Both these enzymes displayed characteristics to

that of lipoproteins residing in the outer membrane [Ursinus and Holtje, 1994, Ehler *et al.*, 1995]. The “soluble lytic transglycosylases 35” (Sly35), the proteolytic degradation product of MlyB, has previously been purified [Ehler *et al.*, 1995]. These three enzymes all function as exo muramidases, which, by starting at the nonreducing, (glucosamine end) cleave the glycan strands in a progressive manner, disaccharide peptide-by-disaccharide-peptide [Beachey *et al.*, 1981]. MlyA has been found to accept isolated muricin glycan strands as a substrate to high molecular weight murein sacculi, a specific feature not characterized in the other two lytic transglycosylases [Romesis *et al.*, 1993]. Present in the cytoplasm is β -*N*-acetylglucosaminidase which is active on soluble murein degradation products and catalytically releases *N*-acetylglucosamine from the isolated murein lipoprotein complex [Yem and Wu, 1976].

1.3.1.2. Peptidases, Amidases, Endopeptidases and Exopeptidases

Peptidases are often enzymes that hydrolyze peptide bonds and reduce proteins or peptides into amino acids.

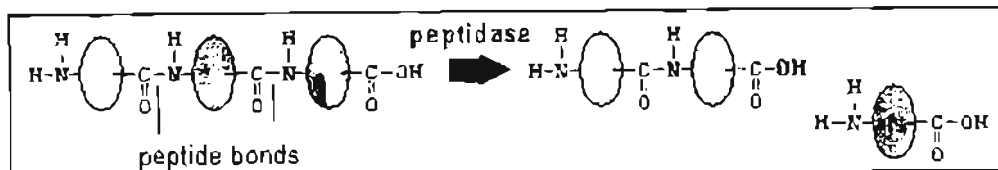


Figure 1.2. Cleavage properties of peptidases showing the reduction of proteins into single amino acids.

Endopeptidases act on the murein network by cleaving the peptide cross-bridges (Figure 1.2.). Characterization of three different muricin DD-endopeptidases showed that they hydrolyse the DD-peptide bonds between D-alanine and *meso*-diaminopimelic acid. Two of them are classified as penicillin-sensitive enzymes and therefore can be grouped in the family of penicillin binding proteins (PBPs) (Table 1.1.). Various studies have characterized the different PBPs molecularly, as well as the genes encoding it [Korat *et al.*, 1991]. The specific changes in the murein structure are observed when the cloned gene is overproduced. This indicates that it acts as both a DD-endopeptidase and a DD-carboxypeptidase *in vitro*. Accumulation of the overproduced enzyme in the active form in the soluble fraction is associated with the cytoplasmic membrane. This was seen in PBP4 characterization, and PBP7 displayed a similar profile where only recently it was shown to

have DD-endopeptidase activity [Romesis and Holtje 1994b]. PBP7 cleaves the D-alanyl-D-diaminopimelyl bond in high molecular weight murein, but not in soluble dimeric muropeptides, such as bis (disaccharide tetrapeptide), which is, however, cleaved by PBP4. PBP8 is the OmpT protease degradation product of PBP7 [Henderson *et al.*, 1994]. A third DD-endopeptidase is a penicillin-insensitive enzyme [Keck and Schwarz 1979]. The gene (*mepA*) encoding a 10kDa soluble protein has been mapped.

DD-carboxypeptidases and LD-carboxypeptidases form the two groups of carboxypeptidase's that have been identified thus far and exhibit exopeptidase functions. LD-carboxypeptidase is specifically inhibited by nocardicin A, a D-amino-acid-substituted β -lactam antibiotic. LD-carboxypeptidase has been purified by means of Nocardicin A-sepharose affinity chromatography as a 32kDa protein [Broome-Smith *et al.*, 1988]. Two additional LD-carboxypeptidases with molecular masses of 12 and 86kDa have been isolated for *E. coli* [Beck and Park, 1977]. PBP5 in contrast when overproduced results in the spherical growth of *E. coli* [Markiewicz *et al.*, 1982]. Therefore, it has been proposed that carboxypeptidase activity affects the amount of pentapeptides, the substrate for the transpeptidation reaction, and regulates the degree of cross linkage of murein.

Amidases are responsible for the cleavage of the amide bond between the lactyl group of muramic acid and L-alanine of the peptide moiety. Two *N*-acetylmuramyl L-alanine amidase have been identified in *E. coli* thus far. Located in the periplasmic space of the cell is the *N*-acetylmuramyl L-alanine amidase encoded for by the *amiA* gene [Van Heijenoort *et al.*, 1975]. This amidase is only active on muropeptides and does not accept the murein sacculus as a substrate.

Table 1.1. Murein hydrolases of *Escherichia coli*. Only enzymes whose genes have been mapped are indicated [Holtje, 1995].

Enzyme	Gene	Molecular mass (kDa)	Localization	Comments
[I]				
Lytic transglycosylases				
(It)				
Soluble It 70 (Slt70)	<i>sltY</i>	70.5	Periplasm	
Membrane-bound ItA (MltA)	<i>mltA</i>	38.9	Outer membrane	Lipoprotein
Membrane-bound ItB (MltB)	<i>mltB</i>	39.0	Outer membrane	Lipoprotein
(Soluble It35 (Slt35))		35	Periplasm	Proteolytic product of MltB
[II]				
<i>N</i>-acetylmuramyl-L-alanine-amidases				
AmiA	<i>amiA</i>	39	Periplasm	Does not accept whole sacculi
AmiD	<i>amiD</i>	20.3	Cytoplasm	Negative regulator of β -lactumase expression
[III]				
DD-Endopeptidases				
PBP4	<i>dacB</i>	49.6	Membrane associated	Additional DD-carboxypeptidases activity
PBP7	<i>pbhG</i>	32	Membrane associated	Inhibition by certain pnem antibiotics
MepA	<i>mepA</i>	30	Periplasm	Penicillin-insensitive
[IV]				
DD-Carboxypeptidases				
PBP4	<i>dacB</i>	49.6	Membrane associated	Additional DD-endopeptidases activity
PBP5	<i>dacA</i>	41.3	Inner membrane	
PBP6	<i>dacC</i>	40.8	Inner membrane	

1.3.2. Peptidoglycan hydrolases of *Bacillus subtilis*

Two major cell wall hydrolases, namely, *N*-acetylmuramyl-L-alanine amidase and the endo- β -*N*-acetylglucosamidases have been characterized as controlling the autolytic system in *Bacillus subtilis* [Rodgers *et al.*, 1980]. Studer and Karamata in 1988 found that these hydrolases belong to a specific class of cell-wall-bound proteins. Using sodium dodecyl sulfate-polyacrylamide gel electrophoresis (SDS-PAGE) mobility their molecular masses are about 49kDa and 90kDa respectively. *In vitro* and *in vivo* analyses have revealed that the 49kDa *N*-acetylmuramyl-L-alanine amidase activity is enhanced two-to threefold by another cell-wall-bound protein described as the modifier. This modifier, (*lyt B*) and a 49kDa amidase (*lyt C*), genes were mapped and cloned. Rashid *et al.*, in 1995 purified the 90kDa glucosamidase and the corresponding gene (*lyt D*) was cloned into *E. coli* and sequenced.

1.3.2.1. Genetic organisation of the *Bacillus* hydrolases

B. subtilis 168 has a regulatory unit encompassing the structural gene of the *N*-acetylmuramyl-L-alanine amidase and its modifier which has been sequenced and found to be a divergon consisting of divergently transcribed operons *lytABC* and *lytR*. Kuroda and Sekiguchi, in 1993 found that the *lyt C* gene, which codes for the 49kDa *N*-acetylmuramyl-L-alanine amidase, is part of an operon encoding a putative lipoprotein (*lyt A*), the modifier, *lyt B*, and *lyt R* genes. Transcription of this operon proceeds from a distal type to a proximal type promoter. The latter transcripts are predominant in the exponential growth phase [Kuroda and Sekiguchi, 1993].

LytA, in its mature state, has a molecular mass of 9.4kDa and is a highly acidic polypeptide whilst the modifier (LytB) and the amidase (LytC) are highly basic. Its derived amino acid sequence indicates that it has lipoprotein characteristics. These two proteins share considerable homology in their N-terminal moieties and have three GSNRY consensus motifs, characteristic nearly of all amidases. The expression of both *lytABC* and *lytR* operons is attenuated by *Lyt R*, a 35kDa protein [Kuroda and Sekiguchi, 1993].

The glucosamidase nucleotide region was sequenced and a monocistronic operon encoding a 95.6kDa protein was found. The amino acid sequence analysis of the glucosamidase showed two types of direct repeats, each type being present twice in the N-terminal to central region of the glucosamidase. These repeats probably represent the cell wall binding domain. Zymographic analysis revealed that the 90kDa glucosamidase is partly processed to several smaller proteins (35-39kDa), retaining lytic activity. Rashid *et al.* in 1995 showed that serial deletions from the N-terminus of the glucosamidase impacted in the loss of more than one repeating unit and drastically reduced its lytic activity towards cell walls. A novel cell wall hydrolase from *B. subtilis* 168, **LytE**, encoded for by *lytE*, which is often expressed during the exponential growth phase [Margot *et al.*, 1998], has been recently characterized. Amino acid similarity analysis of LytE revealed two domains. The N-terminal domain contains three repeats of a 44-amino-acid motif. It has been proposed that this motif found in a series of cell wall lytic enzymes is required for the binding of peptidoglycan. The C-terminal domain of LytE has sequence homology with several classes of proteins that are found outside the cytoplasmic membrane and surprisingly, are endowed with rather different enzymatic activities, such as endopeptidase or amylase. None of these motifs were similar to that characteristic of the main cell wall hydrolases [LytC and LytD] of *B. subtilis*; suggesting that *lytE* is a novel type of peptidoglycan hydrolase [Hourdou *et al.*, 1992]. LytE has a cysteine residue in a well-conserved motif, which may be compatible with an endopeptidase activity, since it has been proposed that the *B. sphaericus* peptidase is a cysteine enzyme [Bourgogone *et al.*, 1992].

1.3.3. *Bacillus licheniformis* peptidoglycan hydrolase

E. coli was used to clone the gene coding for a cell wall hydrolase of *B. licheniformis*. The gene, designated as *cwIM*, has a molecular mass of 27513kDa and encodes a polypeptide of 253 amino acids. Amino acid sequence analysis has indicated that there is a repeat sequence consisting of 33 amino acid residues in the C-terminal region. There is however no loss in cell wall lytic activity when there is a deletion in the C-terminal. The enzyme was found to be an N-acetylmuramoyl-L-alanine amidase via characterisation of the specific substrate bond cleaved by CwIM [Kuroda *et al.*, 1992]. Studies have shown that the enzyme hydrolyses the cell wall of *M. luteus* more efficiently than those of *B. licheniformis* and *B. subtilis*. However, when CwIM lacked its C-terminal region, this efficiency was lost.

1.3.4. The peptidoglycan hydrolases of *Enterococcus hirae* ATCC 9790

Studies have shown only one specific action of peptidoglycan hydrolases in *E. hirae* where the β -1,4 bond between MurNAc and GlcNAc is cleaved. Two muramidases, muramidases-1 and muramidases-2, have been characterized in *E. hirae* ATCC 9790 [Kawamura and Shockman, 1983]. Muramidases-1 is a glycoprotein, and it is reported to have hydrolytic properties with respect to the re-acetylation of peptidoglycan, as well as sodium dodecyl treated substrate cell walls of *E. hirae* ATCC 9790 [Kawamura and Shockman, 1983]. The addition of trypsin and a variety of other proteinases is responsible for the conversion of muramidase from a latent form of a 130kDa protein to an active form (87kDa) [Dolinger *et al.*, 1988]. Muramidase-2 differs from muramidase-1 in its substrate specificity and rapidly hydrolyses the nonacetylated peptidoglycan fraction of *E. hirae* walls of *Micrococcus luteus*, both of which are resistant to the action of muramidase-1 [Shockman *et al.*, 1983]. Highly purified preparations of muramidase-2, extracted from intact or disrupted bacteria, showed the presence of two polypeptides of about 125 and 74kDa [Dolinger *et al.*, 1989]. Both of these polypeptides possessed peptidoglycan hydrolase activities.

1.3.5. Peptidoglycan hydrolases from *Streptococcus pneumoniae*

Smith and Foster in 1995 purified and characterized an amidase enzyme found in *S. pneumoniae*. This pneumococcal amidase has a vast number of specific and unusual properties, in that it appears to recognize and interact with the choline-containing teichoic acid in the cell wall. The enzyme is synthesized in the 'E' form, which seems to be present only in the cytoplasm. It has negligible peptidoglycan hydrolase activity, and in the absence of a choline containing teichoic acid in the cell wall, is not transported through the membrane, nor is it converted to the active 'C' form. The formation of choline-amidase complexes and an allosteric change in the enzyme allows for the conversion from the 'E' form to the 'C' form. Studies by Doi in 1989 have allowed for the gene for pneumococcal amidase, *lytA*, to be cloned into *E. coli*, where it was sequenced and expressed in the E form. SDS-PAGE has shown that this gene codes for a 36.5kDa protein. A deleted *lytA* gene was found in a mutant strain, M13. The mutant displayed characteristics where it grew at a normal rate and could be transformed, however it failed to lyse in the stationary growth phase. M13 showed a tolerant response to the action of β -lactam antibiotics and

grew in chains of 6-8 cells. The amidase production rate increased five fold in the parental strain when the *lytA* gene carried on a plasmid was inserted. The ability to autolyze in stationary phase was also restored. In a similar study, insertional inactivation of the *lytA* gene failed to affect its phenotype, except for resistance to autolysis [Thunnissen *et al.*, 1994].

1.3.6. Cell wall hydrolases of *Staphylococcus aureus*

It is very necessary that bacteria with a compact peptidoglycan network have their own cell wall hydrolases, as in the case of *S. aureus* where, in order for it to divide and separate highly regulated control mechanisms aid these processes. Disturbance of these control mechanisms usually leads to cell lysis. These cell wall hydrolases are also a prerequisite for cell wall morphogenesis and turnover. *S. aureus* has three different autolytic enzymes: an *N*-acetylglucosaminidase, an *N*-acetylmuramidase and an endopeptidase [Giesbrecht *et al.*, 1998]. Examination of cell wall hydrolases by zymographic analysis has shown that several bands are capable of hydrolysing the peptidoglycan. This indicates that autolysins must be represented by more than the three characterized enzymes. The number of bacteriolytic enzymes, however, decreases when staphylococcal cells reach the stationary phase. The overall rate of murein hydrolase activity seems mainly to be regulated genetically by the *lytS-lytR* regulatory locus [Giesbrecht *et al.*, 1998]. In recent studies the *alt* gene encoding an autolytic enzyme with bifunctional activities was cloned and sequenced. The two domains contained an *N*-acetylmuramyl-L-alanine-amidase (AM) and an *N*-acetylglucosaminidase (GL). A gene for an additional amidase, encoding a polypeptide with a molecular weight of 23, 000 was cloned earlier. The two cell wall lytic enzymes AM and GL proved to be capable of acting as cluster-dispersing enzymes when externally added to cluster-forming mutant strains of *S. aureus* [Giesbrecht *et al.*, 1998].

1.3.7. Peptidoglycan hydrolases of other bacterial species

Peptidoglycan hydrolases are produced by a vast number of bacterial species. As progressive as science is, experimental data has shown that a number of additional bacterial species produce autolysin active enzymes. Evidence has shown that *Neisserhia gonorrhoeae*, *Pseudomonas aeruginosa*, and a species of Colstridia, staphylococci and

streptococci produce peptidoglycan hydrolases. In establishing the potential roles autolysins have in cell wall assembly and cell division, science must first establish whether or not all bacterial entities have and produce such hydrolases. Since some of the enzyme activities described are extracellular and others are coded for by genes of bacteriophages or plasmids, their role in the economy of the cell is reasonably questionable. In recent studies, the genes for several of these peptidoglycan hydrolases have been cloned and sequenced. Comparisons of these genes and their protein profiling will allow for further characterization.

1.4. D – ALANYL – TEICHOIC ACIDS IN GRAM POSTIVE BACTERIA

1.4.1. Teichoic acids as a cell wall constituent

The wall of the gram-positive bacterium constitutes a multifaceted fabric that is essential for survival, shape and integrity [Neuhaus and Baddiley, 2003]. Macromolecular assemblies of cross-linked peptidoglycan (murein), polyanionic teichoic acids (TAs), and surface proteins function within this envelope. TAs are composed of wall teichoic acid (WTA) and lipoteichoic acid (LTA). The WTA is covalently linked to the peptidoglycan whereas LTA is a macroamphiphile with its glycolipid anchored in the membrane and its poly (glycerol phosphate) chain extended into the wall (Figure 1.3.) [Baddiley, 2000]. One of the principle substituents of TAs is protonated D-alanyl ester residues. Many of the low G + C gram-positive bacteria are covalently linked to these chains and thus aid in the provision of counter ions for determining the net anionic charge of TA. Together with peptidoglycan, WTA and LTA make up a polyanionic network or matrix that provides functions relating to the elasticity, porosity, tensile strength, and electrostatic steering of the envelope [Archibald *et al.*, 1961]. This matrix is a polyelectrolyte gel with ion-exchange properties needed, for not only maintaining metal cation homeostasis and control, but also assisting in the “trafficking” of ions, nutrients, proteins and antibiotics [Neuhaus and Baddiley, 2003]. The wall matrix is therefore responsible for the permeability of proteins, the linkage of wall proteins, as well as being a determinant of cell

surface hydrophobicity, and of significant importance the presentation of peptidoglycan hydrolases (autolysins) and adhesins. Thus the peptidoglycan envelope provides the necessary functions needed for cellular growth of the gram-positive cell in its biological niche.

Although not all gram-positive bacteria have the conventional LTA and WTA, those that lack these polymers generally have functionally similar anionic ones. In *Micrococcus luteus*, LTA is replaced with lipomannan where succinyl groups esterify the mannosyl residues [Powell *et al.*, 1975]. The growth medium also plays an important role in the different types of WTA or LTA that the organism has. For example, *Bacillus subtilis* when grown in a phosphate-limiting medium results in the replacement of WTA with teichuronic acid, a phosphorus-free polysaccharide containing uronic acid residues [Ellwood, 1971]. Thus each of the above examples illustrates clearly the importance of wall anionic polymers during the growth of the organism.

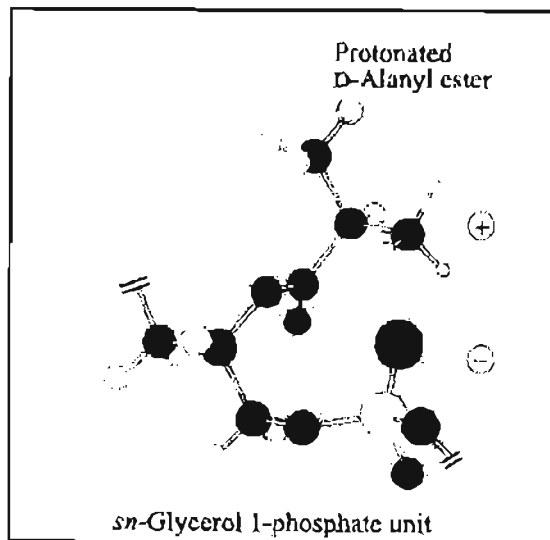


Figure 1.3. Protonated D-alanyl ester substituents linked to the 2' hydroxyl of a Gro-P unit (*sn*-glycerol 1-phosphate). Ion pairing of the phosphodiester with the protonated group occurs on rotation of the phosphodiester linkage [Neuhaus and Baddiley, 2003].

1.4.2. Structure of wall teichoic acids and lipoteichoic acids

Literature reveals a wide structural diversity of WTAs in gram-positive bacteria [Endl *et al.*, 1983]. Some of this diversity is confined to the presence and nature of the glycosyl substituents, D-alanyl esters, and repeating units, termed monomers [Archibald, 1974]. The monomers are joined via anionic phosphodiester linkages to form the linear chains that constitute between 30 to 60% of the cell wall. WTA is attached to peptidoglycan via the linkage unit (Gro-P)₂ or ₃ ManNAc (β 1-4) GlcNAc-P to C-6 of the MurNAc residues (Figure 1.4. A) [Coley *et al.*, 1978]. The major WTA for *B. subtilis* 168 is D-alanyl-[α -D-glucosylated poly (Gro-P)], with a chain length of 53 residues, whilst the degree of α -D-glucosylation has been shown to depend on the age of the cells and the P_i concentration in the growth medium. The genus *Bacillus* contains WTA with a variety of repeating units [Iwasaki *et al.*, 1986]. Staphylococci also contain either -Gro-P- or -Rbo-P as the repeating unit of WTA. *Staphylococcus aureus* contains D-alanyl-[α,β -GlcNAc-poly (Rbo-P) glycosylated on position 4 of the D-ribitol in either an α - or β -linkage (Figure 1.4. C) [Baddiley, *et al.*, 1962].

Without exception, the alanyl esters of TA are of the D-alanyl ester are found in position 2 of the -Rbo-P-monomer. In this WTA, a phosphodiester anionic linkage and the vicinal 3'-OH of the ribitol, flank the D-alanyl ester. In contrast, two phosphodiester linkages flank the D-alanyl ester of poly (Gro-P) TAs. When the 2'-OH of glycerol is substituted by a glycosyl unit as in the streptococci strains, the D-alanyl esters are substituents on the sugar [Neuhaus and Baddiley, 2003].

Many LTAs are macroamphiphiles, composed of poly (Gro-P) attached to the C-6 of the nonreducing glucosyl of the glycolipid anchor. The glycolipid is Glc (β 1-6) Glc (β 1-3) (gentobiosyl) diacyl-Gro in staphylococci, bacilli, and streptococci (Figure 1.4. A) [Neuhaus and Baddiley, 2003]. The poly (Gro-P) (Figure 1.4. B) chain length varies from 14 to 33 Gro-P units in LTA isolated from *Enterococcus faecalis* [Leopold and Fisher, 1992]. There seems to be a definite structure, however, microheterogeneity of LTAs often results in several variables, namely, in the fatty acid composition, the kind and extent of glycosyl substitution, the length of hydrophilic chains and the degree of D-alanylation.

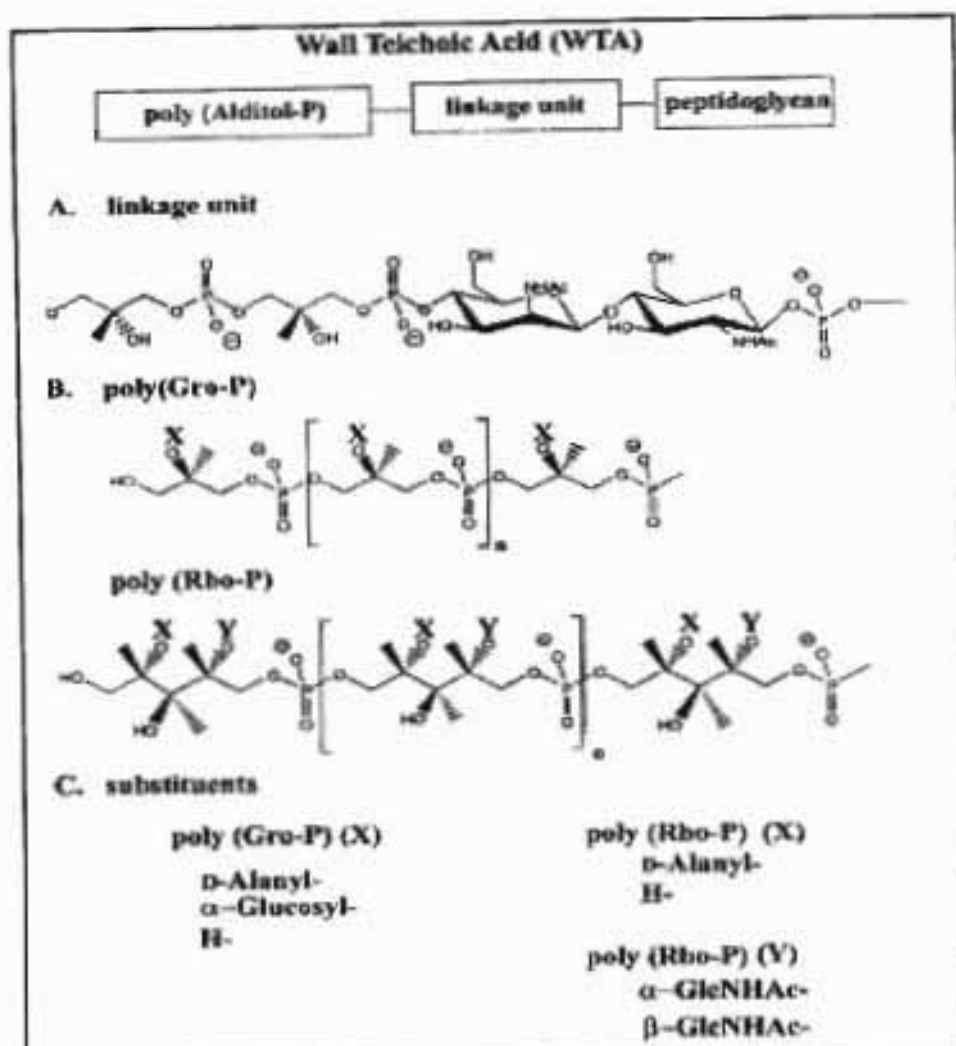


Figure 1.4. Wall teichoic acid. (A) Linkage unit. (B) Poly(Gro-P)(*sn*-glycerol 3-P) moiety from *Bacillus subtilis* 168 and poly(Rbo-P) from *Staphylococcus aureus* H. (C) Substituents on poly(Rbo-P) and poly(Gro-P) are characteristic of these bacteria [Neuhaus and Baddiley, 2003].

When the G+C content is greater than 55%, LTA is generally replaced by lipoglycans, as in the *Bifidobacterium bifidum*, which contains a macroamphiphile with single Gro-P units attached to the glycan backbone by phosphodiester linkages and substituted with succinyl substituents with ι -alanyl esters [Fisher, 1994]. The lipoglycan of *M. luteus* is a mannan substituted with succinyl substituents esterified to approximately 25% of the mannose residues. It has been proposed that the diversity of these cell surface components might be

useful in the classification of the high G+C and low G+C contents present in gram-positive bacteria [Sutcliffe and Shaw, 1991].

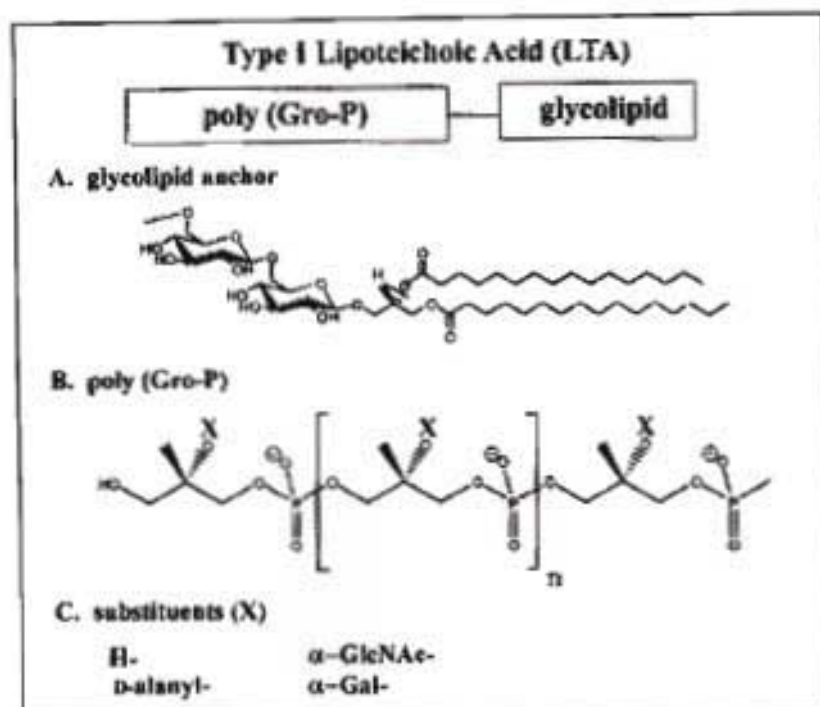


Figure 1.5. Type I lipoteichoic acid. (A) Glycolipid anchor. (B) Poly(Gro-P) (*sn*-glycerol 1-P). (C) Substituents (X) [Neuhaus and Baddiley, 2003].

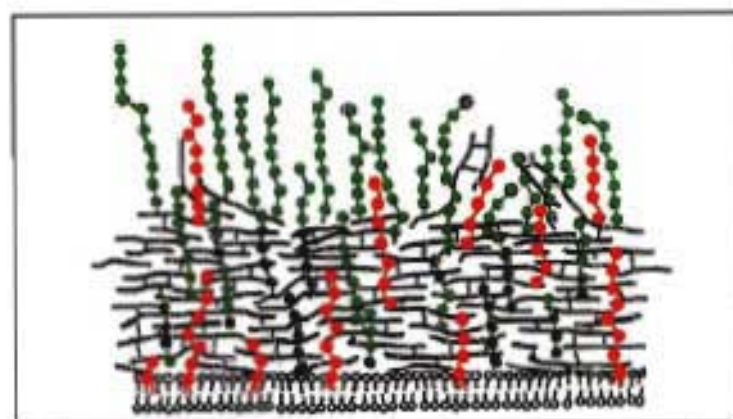


Figure 1.6. Topography of wall teichoic acid and lipoteichoic acid in *Staphylococcus aureus*. Peptidoglycan is shown as black lines whilst the wall teichoic acids are the green symbols. Topology of the lipoteichoic acids is depicted as red symbols [Neuhaus and Baddiley, 2003].

1.4.3. Topography of teichoic acids

Archibald *et al.* proposed that the chains of WTA in *B. subtilis* are arranged perpendicular to the surface of the wall. A fraction of this WTA is located in what has been termed as a “fluffy” layer region beyond the wall. It was postulated that this fibrous layer reflects a region of **autolysin-catalysed degradation** of outer non-stressed peptidoglycan [Archibald *et al.*, 1961]. A similar organisation was also observed in many strains of *S. aureus*. This topography is illustrated in Figure 1.6.

Many bacteriophages show a binding specificity for accessible WTA [Neuhaus and Baddiley, 2003]. By using pulsed incorporation of WTA in *B. subtilis*, it was observed that phage bind, initially, only to the inner surface of the wall. Maximal binding to the cell surface occurred after 0.75 to 1 generation. These findings seem to indicate that the assembly of WTA initiates at the wall-membrane interface at many sites and that this is followed by the movement of covalently linked WTA-peptidoglycan through the thickness of the cylindrical wall [Neuhaus and Baddiley, 2003]. At longer intervals after the pulse, phage binding was detected only at the polar region. The use of differential staining of WTA and teichuronic acid, allowed Merad *et al.*, to establish that in the transition from phosphate-limited to phosphate-replete growth, the new WTA is evenly distributed along the inner surface of the cylindrical region of the *B. subtilis* cells [Merad *et al.*, 1989]. Thus, the insertion of the new WTA occurs at the membrane concurrently with peptidoglycan in an “inside-to-outside” growth mode, with a slower appearance in the cell poles [Clarke-Sturman *et al.*, 1989].

LTA is found at the interface of the cytoplasmic membrane and wall. Via the use of immunoelectron microscopy, Aasjord and Grov established that LTA in *S. aureus* not only is attached to the membrane but also penetrates the wall [Aasjord and Grov, 1980]. In *Lactobacillus fermentum*, an organism that does not contain WTA, one portion of the LTA is exposed on the cell surface while a second portion is concentrated at the membrane. The surface-orientated LTA is responsible for the serological specificity of the species [van Dreil *et al.*, 1973]. Based on turnover experiments, the LTA is released from the cell surface during growth. This transient LTA is non-covalently associated with wall components such as peptidoglycan and proteins, through the ionic interactions. In group-A streptococci, the glycolipid moiety of the LTA becomes surface orientated as a result of interaction of the M protein [Neuhaus and Baddiley, 2003]. Thus, one of the determinants

of cellular hydrophobicity in this bacterium is the anchoring of LTA with the hydrophobic moiety to the medium.

1.4.4. Teichoic acids and the glycocalyx

Many bacteria are enveloped with an additional matrix of polymers known as the glycocalyx [Costerton *et al.*, 1981]. This matrix is distal to the wall peptidoglycan and in some cases includes an S layer, capsule, or a slime layer. These highly hydrated structures, almost 99%, play a role in adherence, access of macromolecules and ions, and virulence [Neuhaus and Baddiley, 2003]. In several bacteria, coalescence of adjacent glycocalyxes leads to biofilm formation. The glycocalyx is composed of exopolysaccharides, WTA and LTA, wall-associated proteins, and a variety of membrane constituents. A major function of the LTA-antibodies-protein A-gold complexes in group B streptococci is located within the glycocalyx (capsule) and organised as long, fibrous threads [Orefici, *et al.*, 1986]. These threads appear to be fibrillar in the glycocalyxes of several organisms. In *Staphylococcus epidermidis* the solid component of the slime layer is approximately 80% (wt/wt) TA and 20% protein. Based on immunochemical labelling studies and LTA turnover experiments, Wicken *et al.* in 1986 concluded that LTA would be expected to be a component of the glycocalyx and thus play an important role in its function. It was proposed that the spatial divisions of the wall and glycocalyx are not rigid but rather “represent regions in a continuum and individual types of cell-wall-associated polymers may be distributed across the continuum both spatially and also temporally if they are in transit” [Wicken *et al.*, 1986].

1.4.5. Functions of teichoic acids

1.4.5.1. Role of D-alanyl esters

In understanding the basic function of teichoic acids in their entirety, the role of D-alanyl esters must first be established. Three functions of D-alanyl-TAs have thus been proposed: (i) to modulate the activities of autolysins, (ii) to maintain cation homeostasis and assist in the assimilation of metal cations for cellular function, and (iii) to define the electromechanical properties of the cell wall. These functions however, maybe limited and therefore depending on the species, additional roles in adhesion, biofilm formation, acid tolerance, intrgeneric co-aggregation, protein folding, antibiotic resistance, UV sensitivity, and virulence are important [Neuhaus and Baddiley, 2003]. A stereoisomer opposite to proteins, D-alanine, plays a unique role as a metabolite in both the peptidoglycan cross-linking as well as the TA functioning in the bacterial envelope. D-Alanine may very well be an integral component of a regulatory system connecting the D-alanyl esters of TA in the one hand, and the D-Ala- D-Ala moiety of the peptidoglycan on the other. It is thus possible that by sensing responding changes in the D-alanine concentration, some bacteria gain a competitive advantage for growth in certain conditions or habitats [Neuhaus and Baddiley, 2003].

The ease of D-alanyl ester migration strongly suggests that this feature is related to D-alanyl-TA function in the living cell. Although this has not being proven as yet, the migration or transacylation of the D-alanyl esters to specific locations or regions within the wall matrix provides a unique mechanism for transmitting signals that could very well determine the activities of proteins requiring a specific ionic micro-environment for function, e.g., an autolysin. Thus, the absence or presence of these esters within the wall matrix at specific locations might constituent a targeting mechanism for proteins that are regulated by localized ionic charge. In this way, D-alanyl-LTA is envisaged to be a communicator of cellular needs during growth of the bacterium [Neuhaus and Baddiley, 2003].

1.4.5.2. Lipoteichoic acid and wall teichoic acid in the content of the envelope

The growing cell possesses a wall with a unique mixture of microenvironments, anion and cation composition, proton gradient, proteins, TAs and peptidoglycan [Neuhaus and Baddiley, 2003]. Each of these contributes to the functions of the envelope as the cell undergoes growth, binary division and cell-cell separation. In this milieu, the protonated D-alanyl esters of TS provide the counter-ions for the interactions with the adjacent anionic sites of TAs, peptidoglycan and proteins. Hydrogen bonds, electrostatic forces and “van de Waals” attractions provide the necessary forces that determine the properties and organization of the TAs as well as the functions of these constituents within the envelope [Neuhaus and Baddiley, 2003].

The matrix can thus be seen as an elastic polyelectrolyte gel that swells or shrinks in its response to a variety of factors, signals, environmental stresses, and protons [Doyle and Marquis, 1994]. The molecular basis for the expansion and contraction of this gel results in part from the charge-charge repulsion of the phosphodiester anionic linkages of TA. One of the determinants of charge distribution in the envelope of the respiring cell is the proton gradient, where a low pH causes the polyelectrolyte gel matrix to contract. To demonstrate the charge effects on the cell wall, studies have shown that the proton gradient plays a major role in the binding of cations and the regulation of autolysin activity in *B.subtilis* [Calamita and Doyle, 2002]. Competition between protons and mobile counter-ions in the matrix thus determines a gradient packing density, as well as a gradient of cations and active autolysins within the wall of the growing, respiring cell [Millward and Reaveley, 1974].

It has been shown that, in certain instances, when the D-alanyl esters were removed from the WTA of *S. aureus*, it caused an expansion of the wall, where such a volume change as a result of charge-charge repulsion, impacted on the electromechanical interactions within the wall [Ou and Marquis, 1970]. Thus the D-alanyl esters, as well as the protons, determine the density or compactness of the wall and hence also constitute factors that regulate autolysin and cation binding.

1.4.5.3. D-Alanyl esters in autolysin control

The inhibitory action of LTA on autolysins (peptidoglycan hydrolases) has been widely acknowledged [Fisher *et al.*, 1981]. It has been suggested that the degree of D-alanylation influenced this inhibitory activity and that alanine-free LTA and alanine-substituted LTA represented active and inactive forms of an autolysin inhibitor respectively [Fisher *et al.*, 1981]. The arguments for and against this proposal were summarized for *B. subtilis*, and it was concluded that there is “no real evidence suggesting that LTA modifies the N-acetylmuramic acid L-alanine amidase activity *in vivo* or *in vitro*”. Herbold and Glaser found, however, that the high affinity of this amidase for walls requires WTA [Herbold and Glaser, 1975]. The induction of autolysis in *Staphylococcus simulans* 22 by the cationic antibiotics Pep5 and nisin suggested that these cationic substances and autolysins compete for the anionic sites on the LTA [Bierbaum and Sahl, 1987]. Higher levels of these antibiotics were required to initiate lysis when the D-alanyl esters were removed. Therefore, the esters would appear to determine the number of binding sites on LTA for autolysins. The action of hemolysin or bacteriocin of *E. faecalis* was inhibited by the D-alanyl-WTA of this organism [Davie and Brock, 1966]. Removal of D-alanyl esters inactivated this inhibitory activity and induced autolysis. Therefore, the number of binding sites for hemolysin or bacteriocin in *S. simulans* would also appear to determine the degree of D-alanylation. It is recognised that the autolysin binding to LTA and WTA determined in part by D-alanyl esters, constitutes only one of the factors that may regulate and present these potentially lethal hydrolases [Calamita and Doyle, 2002].

The ability to isolate D-alanyl ester-deficient mutants [Perego, *et al.*, 1995] thus provides a novel approach to the examination of the role of esters in the regulation of autolysis. However, the observed increase in autolysin activity in certain *B. subtilis* mutants was an unexpected occurrence [Wecke *et al.*, 1997]. This contradiction was resolved with the work of Wecke *et al.*, who suggested that the inhibitory effect of LTA micelles, observed in the earlier work, is actually the result of autolysin entrapment, preventing lysis [Wecke *et al.*, 1997]. A physical analysis of the LTA micelle revealed that it is assembled from approximately 150 molecules with the hydrophilic poly(Gro-P) chains extending the core [Labischinski *et al.*, 1991]. It was proposed that the heavily coiled chains of the micelle trap, the cationic autolysin molecules and thus inhibit autolysis [Wecke *et al.*, 1997].

However, it was further postulated that the packing density of LTA in these micelles is too high to reflect their actual organization in the bacterial membrane. To address these proposals, LTA was diluted into Triton X-100 micelles and tested as an inhibitor of autolysin action [Cleveland *et al.*, 1976]. Under these conditions, the inhibitory activity was abolished. Micelles, with a decreased LTA concentration, do not trap or sequester autolysins. Therefore, the inhibitory action of LTA that has originally been described with high-density micelles may have led to an equivocal conclusion. A molecule of membrane associated LTA in the cell is surrounded, on average, by eight phospholipid molecules [Gutberlet *et al.*, 1997]. Under these conditions, LTA binds autolysin for presentation to the susceptible peptidoglycan linkages. For species with D-alanyl esters, Wecke *et al.* proposed that the ester content determines the number of anionic sites in LTA and WTA for autolysin binding [Wecke *et al.*, 1997]. Thus it is this binding capacity increase that also results in an increase in the rate of autolysis.

1.4.6. D-Alanyl esters and pathogenicity

Pathogenicity defines the ability of a bacterium to inflict damage on the host [Maurer and Mattingly, 1991]. In this contrast, TAs function as inducers of proinflammatory mediators, immunogens, complement activators, adhesions and mitogens [Thiemermann, 2002]. Therefore, in establishing the role of D-alanyl esters of TAs implicated in host responses, the correlation between pathogenicity and the ester content of its LTA and WTA is important. It thus becomes conceivable that the inhibitors of D-alanylation may be efficacious in modulating some of these responses. There are three roles for polyanionic TAs: (i) D-alanyl-TAs can provide the scaffolding for the presentation of adhesins and surface proteins that initiate the infectious process, (ii) TAs can interact directly, both specifically and non-specifically, with host receptors to elicit their responses; and (iii) TAs can determine the effectiveness of innate cationic inhibitors, as well as cationic antibacterial agents [Neuhaus and Baddiley, 2003].

The correlation of D-alanyl-ester content with the actions of cationic antimicrobial peptides, β -lactams and glycopeptide antibiotics, is an unexpected finding [Peschel *et al.*, 1999]. The antibacterial activities of the glycopeptides vancomycin, teicoplanin, and

balhimycin are increased in mutants, which lack D-alanyl esters [Peschel *et al.*, 2000]. The antibacterial action of human group IIA phospholipase A₂ is facilitated by the increased anionic charge in the gram-positive organism. For example, PLA₂ has been identified as one of the principle mediators of anti-staphylococcal activity in human tears [Neuhaas and Baddiley, 2003]. This protein works in concert with lysozyme and other antibacterial peptides as part of an innate response of the host. Insertional mutagenesis of a *dlt* operon in a methicillin-resistant *S. aureus* (MRSA) strain increased the resistance from 16µg/ml to 128µg/ml in the mutant strain [Nakao *et al.*, 2000]. For expression of low-level resistance in this strain, the product of the *mecA* element, penicillin-binding protein 2a is essential. Thus, *dltABCD* is a member of a group of genes whose inactivation leads to increased resistance when the element is present. These are distant from the more than 20 *aux* or *fem* genes, whose inactivation leads to a decreased resistance. Previously, O'Brien *et al.* observed that mutagenized strains of MRSA, defective for D-alanyl ester formation, have increased methicillin resistance [O'Brien *et al.*, 1995]. These results correlated with the enhanced expression of methicillin resistance when MRSA is grown in either 7.5% NaCl or at a pH of 8, both conditions which lead to reduced D-alanylation. In studies of the *mecA* element in *S. aureus*, Jenni and Berger-Bachi found that although *mecA* altered the autolytic behaviour, it had no effect on the cellular content, chain length, or D-alanine substitution of LTA and WTA [Jenni and Berger-Bachi, 1998]. In addition, Peschel *et al.* observed no differences in methicillin sensitivity in the *S. aureus* mutants [Peschel *et al.*, 2000]. Growth of MRSA, in the presence of NaCl also leads to increased resistance and thus mimics the phenotype of the inactivated *dlt* mutant of this strain.

Komatsuzawa *et al.* and Ohta *et al.* found that LTA plays an important role in the sensitivity of MRSA to oxacillin and methicillin [Komatsuzawa *et al.*, 1994; Ohta *et al.*, 2000]. Growth of a variety of clinical isolates, in the presence of 0.02% Triton X-100 increased both the release of LTA and the sensitivity of the strain to these β-lactams. For example, a 4.2-fold increase in the release of LTA resulted in 2.048-fold increase in the susceptibility (MIC ratio) to oxacillin. These findings strongly suggest that LTA released during growth in the presence of the detergent, is associated with a reduction in resistance to the antibiotic. The D-alanyl-ester-deficient mutants of *B. subtilis* not only have a higher rate of autolysis, but also have a higher susceptibility to methicillin [Wecke, *et al.*, 1997]. This was expressed by a faster loss of viability and a slower recovery in the post-antibiotic

phase. The addition of magnesium ions protected both the mutant as well as the parental strains from methicillin-induced lysis.

The cationic tear protein, lactoferrin, binds to the LTA of *S. epidermidis*, blocking the cationic sites on the cell surface [Leitch and Wilcox, 1999]. Studies suggest that this binding decreases the negative charge, providing the tear lysozyme with greater accessibility to the peptidoglycan of the organism. In addition, lactoferrin increases the susceptibility of this organism to vancomycin [Leitch and Wilcox, 1999]. Therefore, the actions of a number of antibacterial agents targeted to wall assembly, membrane disruption, and protein synthesis, would appear to depend, initially on the anionic binding sites of LTA and WTA for their assimilation by the cell wall.

1.4.7. Future possibilities using teichoic acids as regulators

LTA and WTA, together with peptidoglycan, define the polyelectrolyte properties of the periplasm that provides the conduit- the continuum of anionic charge- between the cell membrane, wall, glycocalyx and the environment (Figure 1.7.). Not only is this matrix responsible for cation homeostasis and assimilation, but also for trafficking of metal cations, nutrients, proteins and antibiotics. While there is not a discreet, defined space for this periplasm, as in the case of gram-negative organisms, there is nevertheless a “compartment” or environment, where a myriad of cellular processes occur. While this is not a compartment in the strict sense of the word, the use of a less stringent definition allows us to define a functional entity [Mayer, 1993], where the ionic composition is regulated, enzymes and other proteins are tethered, and energy is provided by a non-diffusible, intermediate, D-alanyl ester. Within the context of this compartment or periplasm, peptidoglycan functions to protect the integrity of the cell against turgor pressure. The D-alanyl esters of LTA and WTA allow many low G+C gram-positive organisms to modulate the polyanionic charge and surface properties of this compartment.

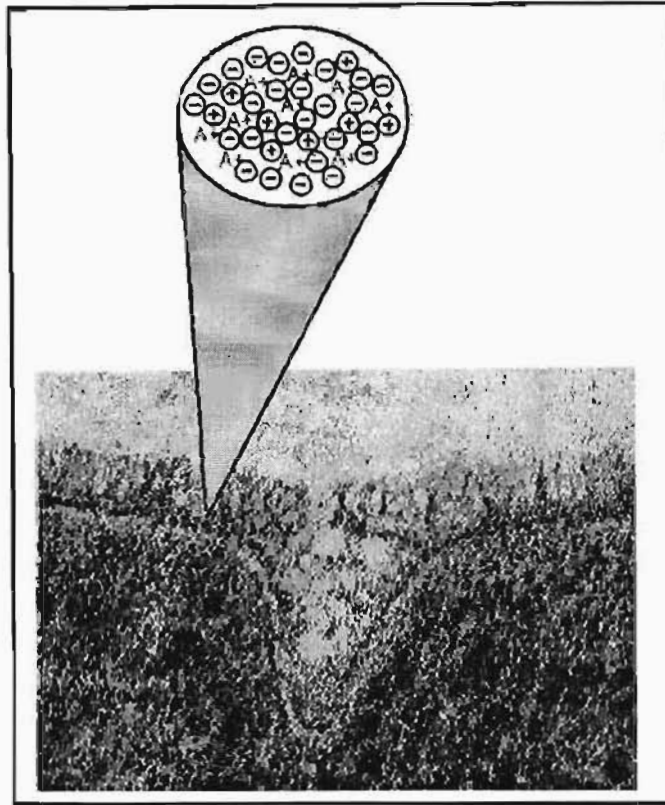


Figure 1.7. Continuum of ionic charge. A high-magnification, freeze-substituted image of the septal region of an exponentially growing *Bacillus subtilis* 168 cell is shown. The tripartite structure of the walls shows the fibrous nature of the outer layer. The electron photomicrograph is a reprint where A^+ represents the D-alanyl esters of teichoic acids, \oplus represents mobile cations and other fixed cationic functions in peptidoglycan, and \ominus represents the phosphodiester anionic linkages of teichoic acids and anionic groups of peptidoglycan [Neuhaus and Baddiley, 2003].

Questions that address (i) the functions the D-alanyl-TAs, (ii) the mechanism of D-alanylation, and (iii) the role of D-alanyl esters in pathogenicity as well as how do these D-alanyl esters function in the presentation of autolysins and adhesions, all provide an interesting insight into the roles of the D-alanyl esters of LTA and WTA in microbial physiology as well as in host interaction and responses [Neuhaus and Baddiley, 2003].

1.5. PROGRAMMED CELL DEATH IN BACTERIAL DEVELOPMENT

1.5.1. Defining programmed death in bacteria

In animals, apoptosis serves to eliminate cells in the course of development and to eradicate defective cells [Metzstein *et al.*, 1998]. Cancerous transformation, microbial infection, and lethal factors such as heat, mutagens, oxidants and chemical toxins, all lead to apoptosis. Cell damage is sensed by receptors activating apoptotic signal transduction pathways that converge mainly at the level of caspase proteases. As in metazoa, programmed cell death (PCD) plays an important role in a number of developmental processes in bacteria, such as lysis of the mother cell in cell sporulation, lysis of vegetative cells in myxobacterial fruiting body formation, and DNA transformation liberated from cells of streptococci undergoing spontaneous autolysis [Lewis, 2000]. A considerable amount of data suggests that microorganisms also evolved programmed death of defective cells. Perhaps the most common observation of possible PCD in bacteria is autolysis of cells exposed to antibiotics and other harmful conditions. Autolysis is a self-digestion of the cell wall by the peptidoglycan hydrolases, where both the synthesis as well as the hydrolysis of the peptidoglycan is necessary for building the cell wall and at least some autolysins are part of this normal cell growth activity. Traditionally, autolysis has been viewed as a maladaptive disbalance in the processes caused by the inhibition of cell growth. However, research now suggests that autolysis may very well also represent PCD in bacteria [Lewis, 2000].

It may not be immediately apparent, but a defective unicellular organism will benefit from committing suicide. At the very same time, it is also known that bacteria live and die in complex communities that in many ways resemble a multi-cellular organism. The release of pheromones induces bacteria in a population to respond in concert by changing patterns of gene expression, a phenomenon termed quorum sensing, and reactive oxygen species cause self-aggregation in *Escherichia coli*, a behaviour thought to provide mutual protection to the cells [Fuqua and Greenberg, 1998]. From this perspective PCD of damaged cells may be beneficial to a multi-cellular bacterial community [Lewis, 2000]. For example, suicide could limit the spread of a viral infection. In the case of serious

damage by toxic factors, cells will donate their nutrients to their neighbours instead of draining resources from their kin in a futile attempt to repair themselves. Finally, elimination of cells with damage DNA, would contribute to maintenance of a low mutation rate.

1.5.1.1. Sporulation

Apoptosis in eukaryotic cells was discovered in studies of *Caenorhabditis elegans* development, the death of certain cells is a necessary stage in ontogenesis [Metzstein *et al.*, 1998]. Similarly, autolysis is part of the development process in a number of bacterial species. In sporulating *B. subtilis*, the mother cell is actively lysed prior to release of the spore. Three autolysins have been identified that participate in mother cell lysis [Nugroboho *et al.*, 1999]. CwlB is the major autolysin produced at the end of the exponential growth phase. A double *cwlB cwlC* mutant was defective in mother cell lysis, but single mutants showed lysis. Similarly, double but not single *cwlC cwlH* mutants were defective in lysis. CwlC becomes the major autolysin at late sporulation stage, whilst both CwlC and a minor autolysin, CwlH, are transcribed by a sporulation-specific $E\sigma^K$ RNA polymerase and requires a coat protein transcriptional activator for expression. Expression of σ^K in the process of sporulation has shown that σ^K is the final regulator in a complex pathway that begins with Spo0A, a transcriptional factor that integrates signals from nutritional status and cell cycle. In turn, it activates a cascade of interdependent sigma factors in the forespore and mother cell (Figure 1.8.) [Levin and Grossman, 1998]. σ^K is responsible for spore coat and cortex formation and for mother cell lysis. It might seem that the knowledge of the signal transduction pathway controlling PCD of the mother cell is fairly complete. However, the mere presence of autolysin is not sufficient for lysis. Autolysis usually requires an additional unidentified factor to activate the autolysin. Indeed, an autonomously active CwlB, for example, would exterminate cells at the end of the exponential stage of growth. An additional activator released after the spore is formed would allow for specific targeting of the mother cell for autolysis. This therefore establishes that the mother cell functions in the elimination of the barrier that could potentially interfere with the outgrowth of a germinating spore. There might be an

additional function of autolysins-nutrients released by the mother cell could be used by kin cells, helping them complete the energy-demanding process of sporulation. In *B. subtilis* rapid autolysis is also observed if cells are transferred into a medium lacking a carbon source [Lewis, 2000]. Autolysis is activated by a decrease in proton motive force rather than by a drop in ATP. Apparently, sporulation cannot proceed in the complete absence of nutrients. Altruistic lysis under such conditions might provide some of the kin cells with enough of an energy source to allow for sporulation. A simpler explanation would be that *B. subtilis* cannot cope with a sudden decrease in energy, and cell lysis is a maladaptive consequence of a breakdown in the control of the cell wall synthesis machinery [Lewis, 2000].

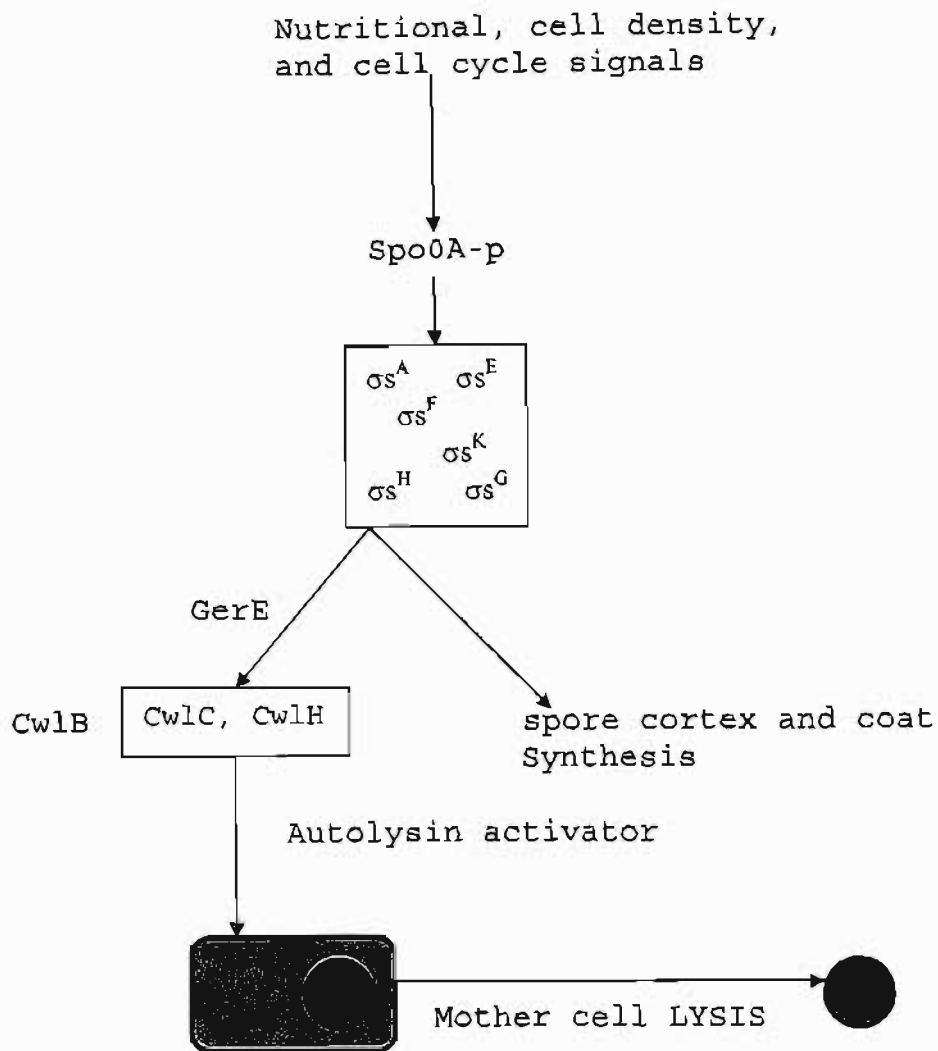


Figure 1.8. Programmed death of mother cell in sporulation development of *B. subtilis*. Environmental as well as internal signals are integrated at level of Spo0A, which in turn activates a cascade of sporulation sigma factors. The terminal sigma factor σ^K controls the final stages of sporulation-formation of the spore cortex, coat synthesis and expression of autolysins CwlC and CwlH. Activation of autolysins by an unknown factor causes mother cell lysis and liberation of the spore [Lewis, 2000].

1.5.1.2.1. Programmed death and sex

Yet another example of specialized adaptive autolysis, related to development, comes from the studies of genetic exchange. In a number of species, autolysis is part of a well-controlled mechanism of natural transformation. Cells that did not lyse pick up the released DNA. The gene for the main autolysin in *Streptococcus pneumoniae*, *lytA*, is located in the same operon with *recA*, which is responsible for homologous recombination with the incoming DNA [Mortier-Barriere *et al.*, 1998]. Both RecA and LytA are induced by the quorum-sensing factor, a peptide pheromone that accumulates at high cell density (Figure 1.9).

1.5.2. Two-component regulatory systems

Monitoring and adapting to changing environmental conditions, is the key function of bacterial signal transduction, which is generally carried out by the so-called two-component systems. Two-component signal transduction systems have evolved to allow cells to monitor their environment and respond appropriately to a wide variety of stimuli, including nutrient deprivation, chemical changes, host-pathogen interactions, osmotic shock and other stresses. Despite the great diversity in the types of signals detected and responses elicited, two-component systems utilize a common molecular mechanism that is based on the conversion of signal recognition into a chemical entity (Figure 1.9.).

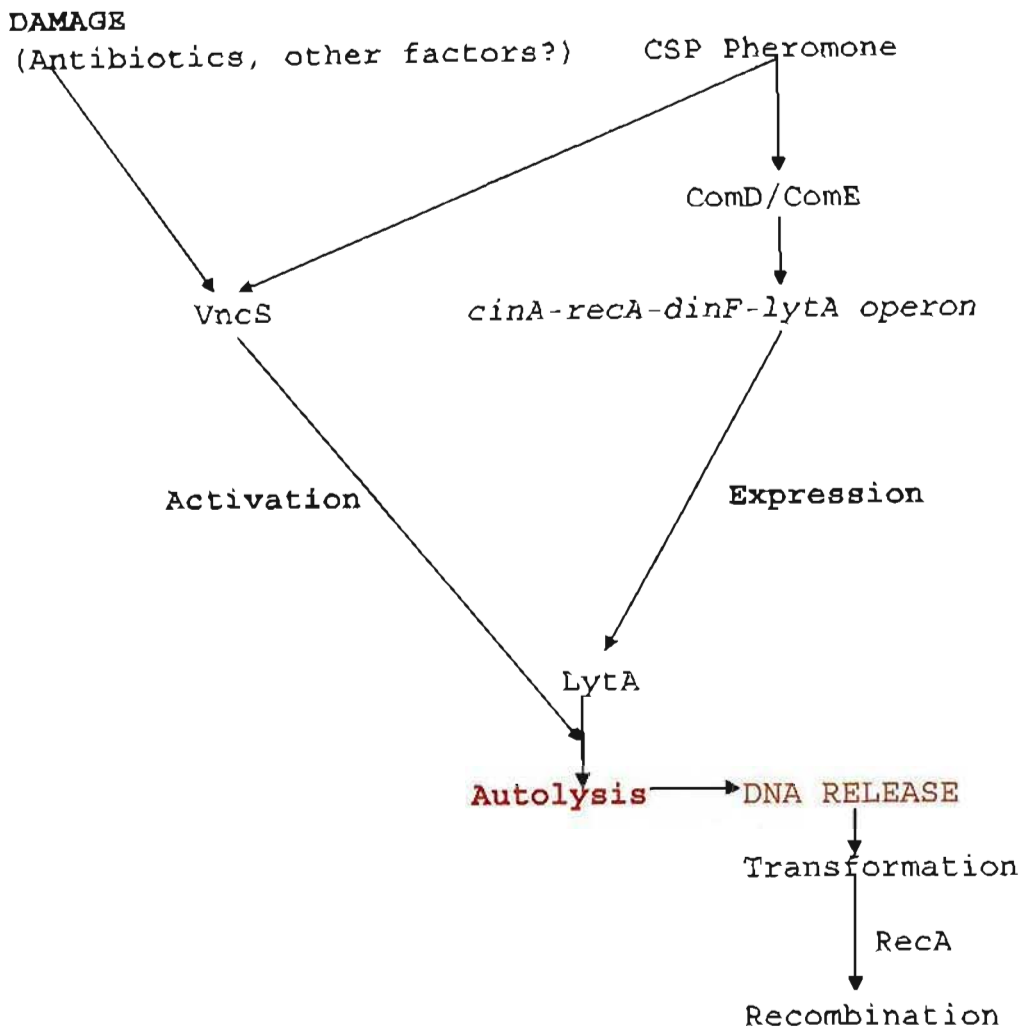


Figure 1.9. PCD in autolysis of *S. pneumoniae*. At a high cell density of, the concentration of a released pheromone (CSP) increases and activates a two-component signal transduction kinase (ComD) and its response regulator (ComE). Phosphorylated ComE in turn activates transcription of a competence operon containing the genes required for recombination of incoming DNA and the *lytA* gene, responsible for autolysis. Released DNA is picked up by other cells and recombined with the aid of RecA. *LytA* requires activation, which is controlled by the sensory kinase VncS. Signals originating from cell damage by antibiotics and possibly by other factors converge prior to or at the level of VncS and activate *LytA*, causing elimination of defective cells [Lewis, 2000].

1.5.2.1. Two-component regulatory systems in *Staphylococcus aureus*

Staphylococcus aureus infections are a major cause of morbidity and mortality in community and hospital environments. Consequently, the emergence of methicillin-resistant strains, and more recently of vancomycin-resistant strains of *S. aureus* represents an enormous threat to public health. *S. aureus* pathogenesis primarily involves the secretion of toxins that damage or lyse the host cells or interfere with the immune system. Enzymes that degrade tissue components and cell wall-associated proteins that may be involved in adhesion and protection against host defences are also affected. Synthesis of many of these virulence factors are controlled by a two-component regulatory locus, *agr*, an accessory gene regulator [Gholson *et al.*, 2000]. This locus contains a two-component module that is activated by a secreted auto-inducing peptide (AIP) in a cell density dependant manner. This type of regulation falls under the rubric of the ever-broadening field of quorum-sensing, whereby a population of bacteria responds in concert, when a critical cell density is reached. In the case of *S. aureus*, as cells enter post-exponential phase, the AIP reaches a threshold concentration that turns on the *agr* (virulence) response. This process is mediated by the five genes in the *agr* locus, namely *agrB*, *D*, *C*, *A*, and *RNAIII* (Figure 1.10.) [Gholson *et al.*, 2000]. The P2 promotor drives the transcription of the *agrB*, *C*, and *A* genes, which provide the cytosolic, transmembrane, and Extracellular components of a quorum-sensing/autoinducing circuit. The *agrD* gene product is also a propeptide that is probably processed and secreted by AgrB, an integral membrane protein. The resultant mature AIP binds to the transmembrane receptor-histidine kinase coded by *agrC*. Binding of the AIP triggers phosphorylation of AgrC on a histidine residue. The response regulator accepts the phosphate group from AgrC and, in conjunction with a second transcription factor, SarA, activates transcription from the *agr* P2/P3 promoters. The P3 transcript, RNAIII, mediates up-regulation of secreted virulence factors as well as down-regulates certain surface proteins [Gholson *et al.*, 2000].

The AIP-AgrC receptor pair shows considerable interstrain sequence variation, which must have resulted from evolutionary covariation of this region of the chromosome to retain the specificity of the receptor-ligand interaction. *S. aureus* strains can be divided into at least four *agr* specificity groups. These strains appear to compete with each other at the level of *agr* expression, as each AIP inhibits the *agr* response in strains belonging to other groups. This type of bacterial interference is unusual, because it affects the expression of a subset

of genes rather than inhibiting growth. Due to the intergroup inhibitory effects of the AIPs, the AIP itself needs somewhat of a re-defining status, since the acronym for “autoinducing peptide,” to mean the mature AgrD peptide and their synthetic or modified variants. The usage thus becomes irrespective of whether the AIP acts as an inhibitor or *agr* expression. Structure-activity analysis of the AIPs from *S. aureus* has begun to elucidate their mechanism of action. These peptides contain a thiolactone ring structure in which the α -carboxyl group of the C-terminal amino acid is linked to the sulfhydryl group of a cysteine, which is always the fifth amino acid from the C-terminus of the peptide (Figure 1.10.) [Gholson *et al.*, 2000]. There are usually three or four amino acids N-terminal to the cysteine, which are collectively referred to as the “tail” of the AIP. The high-energy thiolactone linkage appears to be necessary for activation; the corresponding lactone and lactam analogues (but not the linear version) are potent intergroup inhibitors, arguing that the high-energy thiolactone linkage is not required for intergroup inhibition, but that the ring structure is important for both types of activity. There are two remarkable features of this system. Firstly, the AIPs show major sequence diversity yet explicitly cross-inhibit *agr* activation.

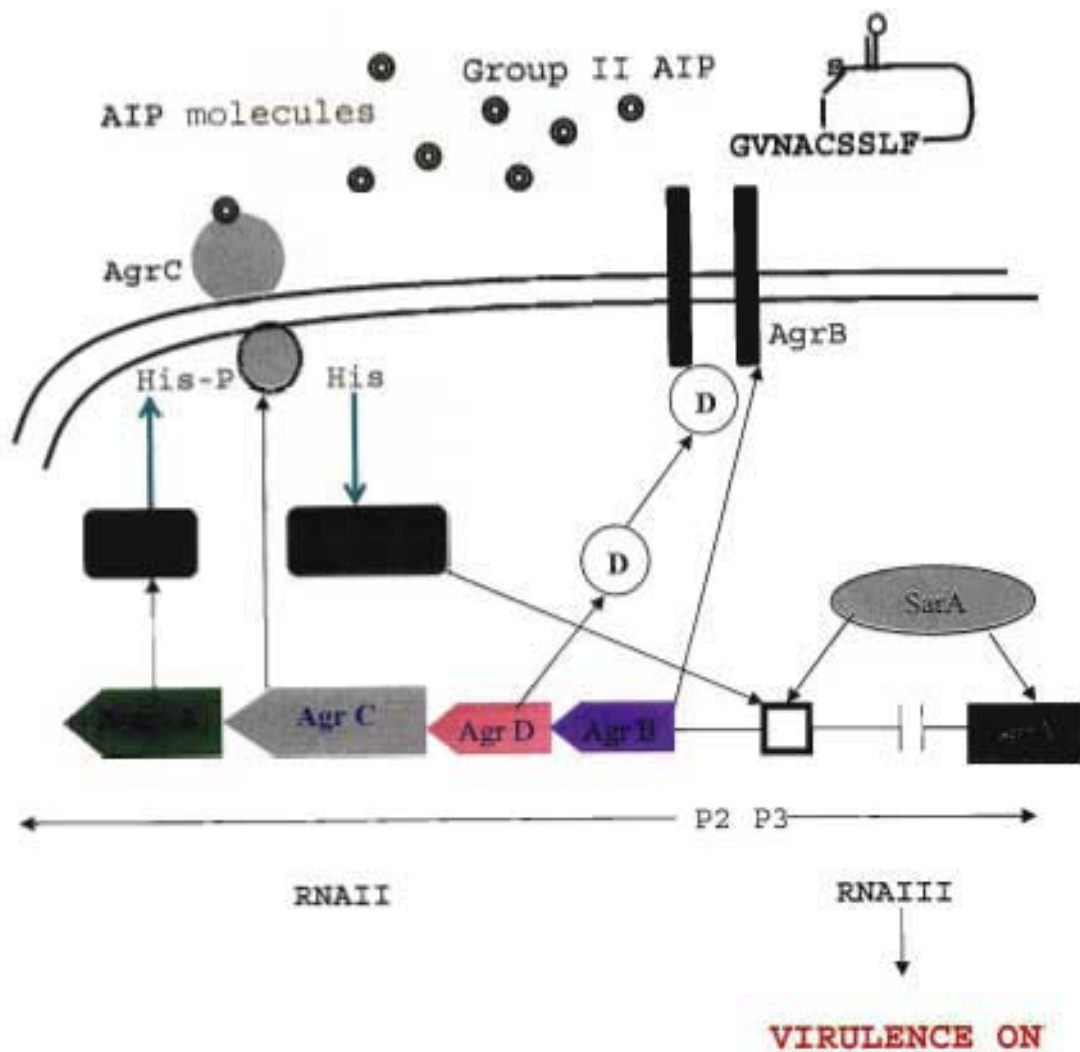


Figure 1.10. The *agr* locus showing the various components and their putative actions in the signalling network for *S. aureus* [Gholson *et al.*, 2000].

Secondly, analogs with oxygen or nitrogen in place of sulphur in the ring structure (i.e.; the lactone or lactam vs. the thiolactone) are potent intergroup inhibitors, but neither activates nor inhibits their cognate receptors, at least when tested at concentrations a hundred-fold higher than the activating and inhibiting concentrations of the natural ligands. In the Agr signalling system the signal acceptor is the AgrC gene, whilst the response regulator is the AgrA gene. AgrB and AgrD are both responsible for the excision of the small peptide from the AgrD protein, which becomes modified and secreted as the agr pheromone peptide into the surrounding medium. This peptide serves as the autoinducer signal of the

agr system. AgrB seems to be involved in the maturation and secretion processes of the modified peptide. The pheromone activates the AgrC/AgrA two-component regulatory system, which in turn activates transcription of the *agrB*, *agrD*, *agrC*, and *agrA* as well as the RNA III genes. When triggered the genes are transcribed forming the mRNA, RNA II and the regulatory RNA III molecule. RNA III controls the expression of target genes via an unknown mechanism (Figure 1.10.) [Gholson *et al.*, 2000].

The quorum-sensing capabilities of the bacteria are now able to provide promising targets in anti-microbial therapies. Many of the virulence factors are in turn regulated by these quorum systems. Unlike conventional antibiotics, drugs interfering with the quorum-sensing system are advantageous in that they specifically allow for the suppression of the expression of virulence factors without killing the bacteria, thereby minimizing the selection for resistant strains.

1.5.2.2. Two-component signal transduction in *Enterococcus faecalis*

Enterococci are gram-positive constituents of the normal human micro flora, typically colonizing the intestinal tract and skin [Jett *et al.*, 1994]. However, these organisms are capable of causing diseases mimicked as opportunistic pathogens, mainly in immunocompromised individuals. In the past decade the problem of Enterococcal infection has been aggravated by the emergence of multiple antibiotic resistances. This has converted some Enterococci from being difficult to treat medically, to being completely refractory to all antimicrobial regimens [French, 1998]. The signal recognition function is carried out by a histidine protein kinase. Its auto-phosphorylation activity in response to a signal output is followed by phosphotransfer to a mated response regulator, thus activating its function. Response regulators are, for the most part, transcription regulators that, upon phosphorylation, activate and/or repress genes involved in the adaptive response [Hancock and Perego, 2002]. The length of the amino acid sequence of the sensing domain of histidine kinases, are highly variable from one protein to the other, reflecting the variety of signals to which these kinases respond. The sensing domain is coupled to a C-terminal cytoplasmic catalytic domain, which, by contrast, consists of an invariant histidine residue, and an ATP-binding domain, showing high levels of sequence conservation. The response

regulator contains a conserved, amino-terminal regulatory, domain that is phosphorylated on an aspartic acid residue, by the histidine kinase to which it is paired. Phosphorylation of the regulatory domain activates the associated C-terminal or effector domain [Hancock and Perego, 2002].

Enterococci are organisms capable of adapting to a number of host environments as either commensals or pathogens. Thus, it is not surprising that key regulators of physiological functions were identified together with putative pathogenic modulators. The literature available clearly indicates that most, but not all, two-component signal transduction systems are common to related species analysing the bacterial genomes [Hancock and Perego, 2002]. This suggests that the progenitor of the diverse present day gram-positive genera had already amplified by gene duplication the two-component systems, presently found in these bacteria, before speciation. The conservation of catalytic domains of sensor kinases with the response regulators, their virtually invariant gene order, and the conserved interaction surfaces, provide strong evidence for such a conclusion. As the present day genera evolved from the progenitor, the putative signalling domains became highly variable in sequence and structure, suggesting that the unique ecological niche that each species occupies contains specific signals that drive the diversity of the signal input domain [Hancock and Perego, 2002]. Furthermore, in any given species, one environment may activate a subset of two-component systems and, as a consequence, a certain pattern of genes, whereas a second environment may induce an expression of another subset of genes. Thus, for an opportunistic pathogen such as Enterococci, and its relatives, the capacity to survive in an environment depends on the signals and the genes that are connected to the two-component system that responds to those signals [Hancock and Perego, 2002].

1.5.3. Genes controlling cell death and survival

1.5.3.1 *Staphylococcus pneumonia* lysis by antibiotics and survival of cells

The three types of specialized bacterial autolysis participating in development and genetic exchange are clearly adaptive and are controlled by programmed death pathways. A number of intriguing observations suggest that programmed death in bacteria also occurs in response to damage, analogously to apoptosis of defective cells [Lewis, 2000]. What can be established from these experiments is that VncS is a component of the autolytic pathway and is required for autolysis induced by antibiotics. How antibiotics induce autolysis, is possibly due to the fact that the normal pathway of VncS-dependent autolysis in *S. pneumoniae* is somehow unnaturally activated by different antibiotics. Alternatively, elimination of defective cells damaged by antibiotics could represent programmed cell death [Lewis, 2000].

One potentially severe problem with PCD in bacteria is that suicide could very well eliminate all cells of a clonal population in response to damage. Indeed, a chemical toxin diffusing into a population can reach and equally damage all cells. A resulting PCD of the entire population would be counter-productive. However, it appears that the bacteria devised an intelligent strategy to avoid such a disastrous outcome [Lewis, 2000]. In the process of developing such mechanisms, it seems that the bacterial population strategically responded to external damaging factors. The majority of cells have a program that will determine whether to repair damage or activate suicide. The suicide program is disabled in a small fraction of persistors, in the case of the damaging factor and reaches the entire population. The nature of persistence is unknown, but it does not seem likely that only a special regulatory program is able to assign as few as 10^{-6} cells to perform a particular function, in this case survival. If one or more of the regulators controlling cell survival were present in small amounts, a random variation in the number of these proteins would produce rare persisting variants. The rate of persistors would then depend on the mean number of molecules of a regulator produced and on the variation of the mean. The evolved setting of this mean and its variation would depend on the need for making persister cells [Lewis, 2000].

1.5.3.2. Genes controlling the survival of *Escherichia coli*

A number of regulatory genes have been found to, dramatically, affect cell survival in *E. coli* without influencing the ability of the cell to grow in the presence of a lethal factor [Lewis, 2000]. An important locus affecting the cell survival is *relA*. It is well established that tolerance to killing by a wide variety of factors, (virtually all cidal antibiotics, for example), correlates inversely with growth rate. Slow growth rate activates the RelA-dependant synthesis of a synthase, guanosine 3', 5'-bispyrophosphate (ppGpp), which hereby inhibits anabolic processes in bacterial cells [Lewis, 2000]. Interestingly, ppGpp suppressed the activity of a major *E. coli* autolysin, soluble lytic transglycosylase (SLT), which would make the cells more resistant to autolysis and could explain the mechanism of tolerance to antibiotics in slow-growing cells [Betzner *et al.*, 1990]. A mutation in *relA*, the gene coding for ppGpp synthase, while not affecting growth rate, made non-growing cells sensitive to killing by antibiotics that inhibit cell wall synthesis [Rodionov and Ishiguro, 1995]. Guanosine 3', 5'-bispyrophosphate (ppGpp) inhibits, peptidoglycan synthesis, which thus complicates interpretation of this finding. RelA is a potentially very interesting cell death regulator, since homologs of RelA have been found in all bacteria so far, and all species studied became tolerant to killing when growth rate decreased. Suppression of cell death by ppGpp probably allows the cell to avoid mistaking a starvation state for an unrepairable defect [Lewis, 2000]. Cell survival is also modulated by heat shock proteins that function as molecular chaperons in refolding and degradation of damaged polypeptides. Induction of heat shock proteins suppressed autolysis of *E. coli* by a number of β -lactams that inhibits the synthesis of peptidoglycan [Powell and Young, 1991]. This inhibition was observed in a *relA* background, indicating that the effect was independent of a possible activation of a stringent response.

The immediate cause of death in bacteria is often autolysis, and autolytic enzymes are the likely ultimate targets for possible programmed death pathways. In *S. pneumoniae*, mutation of the LytA autolysin prevents autolysis and causes tolerance to killing by antibiotics inhibiting the cell wall synthesis [Tomasz *et al.*, 1970]. The recent finding of the VncS kinase, regulating autolysis in response to antibiotics *S. pneumoniae* will undoubtedly facilitate the identification of a pathway linking damage to autolysin. A particular autolysin tied to killing factors has not yet been identified in gram-negative

species. It can be noted though that unrelated cidal antibiotics (β -lactams, aminoglycosides and fluoroquinolones), might trigger autolysis in gram-negative bacteria [Vincent *et al.*, 1991], although inhibitors of peptidoglycan synthesis produce the most dramatic and complete hydrolysis of the cell wall. It is important to note that even cell wall inhibitors do not always produce a clear-cut picture of lysis when they kill bacteria [Fujimoto and Bayles, 1998], including cases when killing does not depend on the presence of a functional autolysin [Tomasz *et al.*, 1970]. It is possible that in some instances lysis is limited and localized; it is also possible that cells might die independently of lysis or autolysins, although this is not as yet known. Several autolysins have been identified in *E. coli*, and two of them seem to be good candidates for a role in programmed cell death. AmiB is a particularly interestingly *E. coli* autolysin [Tsui *et al.*, 1996], whose over-expression sensitises cells to autolysis by cell wall inhibitors. An *amiB* mutant had no discernible phenotype (tolerance to antibiotics has not been tested). *amiB* forms a “super-operon” with several genes, including *mutL*, a mismatch repair protein that protects cells from mutagenesis, and *hfq*, a global regulator that protects cells from stresses, including high temperatures and oxidants, via activation of the expression of the stationary-phase sigma factors [Tsui *et al.*, 1996]. It thus appears that this super-operon harbours elements that can either protect the cell from death and repair is insufficient to control the damage. The linking of the repair to the death elements in one operon is suggestive of a program that thus determines cell fate [Lewis, 2000].

1.6. TWO-DIMENSIONAL GEL ELECTROPHORESIS

1.6.1. An introduction to two-dimensional gel electrophoresis

Two dimensional polyacrylamide gel electrophoresis (2-D PAGE) is a technique that allows proteins to be separated according to charge (pI) by isoelectric focusing (IEF) in the first dimension, and then according to size (Mr) by SDS-PAGE, in the second dimension. In general 2-D electrophoresis can refer to any electrophoretic method capable of resolving protein mixtures on the basis of two independent separation criteria. This technique has the unique capacity to allow for the resolution of complex mixtures of proteins, permitting the simultaneous analysis of a variety of gene products. Since the original description of 2-D electrophoresis, the most extensive modifications to the technique have been in the first dimension of separation [Cash, 1998].

Two-dimensional electrophoresis has provided an opportunity to investigate gene expression on a global scale for a number of different bacteria organisms via the study and analysis of their complete genome nucleic acid sequences. The method of two-dimensional analysis has been rapidly developed in order to permit reproducible analyses of complex protein mixtures between laboratories and for the development of micro-sequencing technologies which ultimately are capable of analysing the small amounts of protein recovered by 2D-PAGE [Cash, 1998].

1.6.2. Principle of two-dimensional polyacrylamide gel electrophoresis

Initially, one-dimensional PAGE allows for the separation of proteins based only on molecular size. In 2D-PAGE, proteins are resolved in the first dimension according to their pI charge value by a method known as iso-electric focusing. The pH gradient instability and irreproducibility are overcome by the use of immobilized pH gradients (IPG) [O'Farrell, 1975]. Immobilized protein gradients (IPGs) are based on the principle

that the pH gradient is generated by a limited number of well-defined chemicals known as immobilines which are co-polymerized within the acrylamide matrix. Thus, cathodic drift is eliminated, reproducibility enhanced, and pattern match and inter-laboratory comparisons simplified [Cash, 1998]. IPGs allow the generation of pH gradients of any desired range between 3 and 12. Protein mixtures, when applied via active rehydration or cup loading, are focused during the application of a current. Depending on their charge value, either positive or negative; they will migrate along the IPG strip until they reach a net charge of zero (Figure 1.11.). Once they have reached a true net charge of zero, no further migration along the strip is possible. Thus the proteins become embedded within the IPG, and are then ready for separation in the second dimension, via SDS-PAGE. In the second dimension, polyacrylamide gel electrophoresis is used to resolve the proteins according to their molecular weight. The IPG are equilibrated prior to electrophoresis, and large SDS-PAGE is carried out. The final visualization of the gels is achieved via different staining protocols, each merited against different optimizations. The most popular and widely used is the standard Coomassie brilliant blue method. However, increasing in popularity includes a variety of new fluorescent dye stains [Schmid *et al.*, 1997].

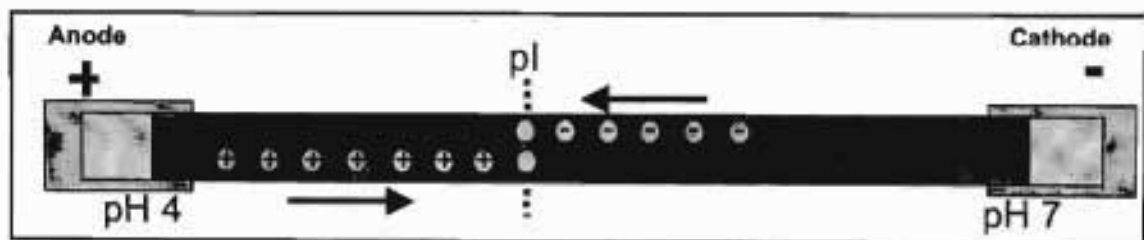


Figure 1.11. Diagrammatic representation of the principle of Iso-electric focusing, allowing complex protein mixtures to be separated via their pI values.

1.6.3. Two-dimensional polyacrylamide technique

1.6.3.1. Bacterial protein sample preparation

Various methods have been used to prepare bacterial proteins for analysis by 2D- PAGE. Many proteomic studies use a crude preparation of soluble proteins by the disruption of bacterial cells. Depending on the purpose of the experiments, the bacteria can be grown in nutrient media as either a broth culture or solid media. Bacteria grown in broth culture are collected by centrifugation, whereas bacterial colonies on solid media can be removed with a swab or plating loop. Flooding the surface of the agar plate with buffer can also help to remove the bacteria from the agar surface. Subsequent sample processing requires the same attention to detail, as for any sample prepared for analysis by 2D electrophoresis [Schmid *et al.*, 1997]. Problems often arise in the disruption of the cells due to the presence of thick cell walls, as in the case of Gram-positive bacterial cells. Lysis with a non-ionic detergent such as NP40, in the presence of 8M urea and an inhibitor of proteolysis, can be employed to disrupt such cells [Rabilloud, 1996]. It is advised that for Gram-positive encapsulated bacterial cells, that brief sonication be applied to the protein mixture, to aid in the disruption of the cells (Figure 1.12.). Heating samples in low molarities of SDS buffer (0.3%) can be used to solubilize the proteins, providing that the urea is omitted from the lysis buffer in order to prevent protein carbamylation at high temperatures [Rabilloud, 1996]. Alternative cell disruption procedures include a French pressure cell and homogenization in the presence of zirconium beads. Contaminating nucleic acids which might interfere with protein migration in the first dimension are removed by incubating the sample in the presence of DNAase and RNAse [Cash, 1998].

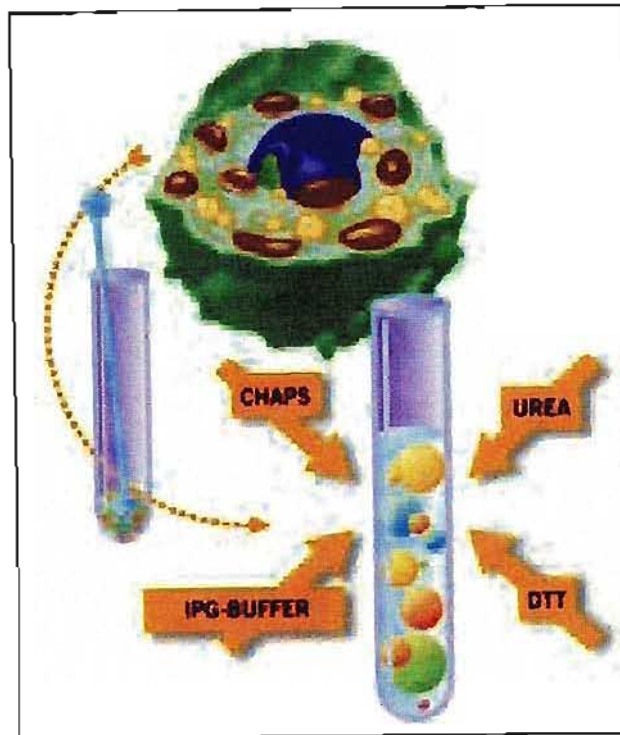


Figure 1.12. Incorporation of different chemicals to facilitate the disruption of bacterial cells, where each component allows for the solubilization of the protein mixture [Rabilloud, 1996] .

1.6.3.2. Two-dimensional protein electrophoresis

Since the original description of 2D electrophoresis, the most extensive modifications to the technique have been in the first dimension of separation. Carrier ampholytes were originally used to establish the pH gradient in 2D electrophoresis for the separation of proteins according to charge [Neidhardt *et al.*, 1989]. However, carrier ampholytes have a number of drawbacks, including the inability to load the large amounts of protein required for micro-sequencing minor proteins, poor stability of the pH gradient during electrophoresis, and relatively, poor gel-to-gel reproducibility particular between laboratories. The use of immobilized pH gradients for the charge separation, helped overcome this problem. IPGs are prepared using immobilines made by, covalently linking the buffering components to the acrylamide monomers [Neidhardt *et al.*, 1989]. The pH

gradient is generated by casting a gradient gel using immobilines with the desired pH extremes. Immobilized pH gradients are stable and capable of simultaneously focussing both, acidic and basic proteins on a single gel prepared with a broad pH gradient. Methods to analyse the very basic proteins with iso-electric points of >10 on IPG gels, have been described. An important feature of IPG strips is their high reproducibility between laboratories, a characteristic which makes them ideal for developing 2D protein databases [Neidhardt *et al.*, 1989]. The second dimension of 2D electrophoresis separates proteins on the basis of their apparent molecular masses on polyacrylamide in the presence of SDS. The gels, in the form of slab gels, are prepared as either single-concentration or gradient-polyacrylamide gels which can be optimized to separate proteins over a specific M_r range [Neidhardt *et al.*, 1989].

1.6.3.3. Staining and detection of 2-Dimensional gels

One objective of 2D electrophoresis for proteome analysis is to maximise the number of proteins amenable to analysis. This requires the optimisation of both, the gel resolution and protein detection [Cash, 1998]. The method of post-electrophoretic detection of the proteins depends upon the nature of the original protein sample. Non-radioactive proteins are stained with either Coomassie brilliant blue or silver stains, the latter being a more sensitive method for protein detection. A limitation of these staining methods for quantitative protein synthesis analysis is that proteins differ in their response to the two stains. Radio-labelled proteins are detected by autoradiography. The use of computerised phosphor-imaging systems in place of the film improves the linearity of detection, which is particularly important for quantitative studies of protein synthesis [Prasad *et al.*, 1999]. The final product of analysis is the production of protein profiles for the bacteria under study, which are both, reproducible and suitable for further analysis in characterising protein biosynthesis and in identifying the expressed proteins.

1.7. SURFACE PLASMON RESONANCE (SPR)

1.7.1. An introduction to Surface Plasmon Resonance

In the past decade surface plasmon resonance (SPR) sensing has been demonstrated to be an exceedingly powerful and quantitative probe of the interactions of a variety of biopolymers with various ligands. SPR spectroscopy is an evanescent wave biosensor technology that monitors the interaction of two or more molecules in a label-free, real-time environment [Liedberg *et al.*, 1995]. The SPR biosensors are sensitive to changes in mass bound to the sensor surface, in that they detect changes in the refractive index. This technique can be used to measure biomolecular interactions of peptides, proteins, nucleic acids, carbohydrates and phospholipid vesicles [Green *et al.*, 2000].

1.7.2. Principle of SPR technology

The underlying principle of SPR is that one binding partner is immobilized on the surface of a sensor chip, whereas the other binding partner is carried in a flow of buffer solution through a miniature flow cell. The immobilization is carried out on an SPR-active gold-coated glass slide which forms one wall of a thin flow-cell [O'Shannessy *et al.*, 1993]. When light (visible or infrared) is shone through the glass slide and onto the gold surface, at angles and wavelengths near the so called "surface plasmon resonance" condition, the optical reflectivity of the gold changes very sensitively with the presence of biomolecules in the gold surface or in a thin coating on the gold [Maynard and Georgiou, 2000]. The high sensitivity of the optical response is due to the fact that it is a very efficient, collective excitation of conduction electrons near the gold surface [Alaedini and Latov, 2002]. Any binding event on the surface of the sensor chip, leads to a change in the refractive index at the surface layer and is monitored by a detector (Figure 1.13.). Time-dependent changes in the refractive index are recorded as sensograms (Figure 1.14.). Association and dissociation is measured in arbitrary units and displayed over a given period of time.

These response values are generally expressed in resonance units (RU) [O'Shannessy *et al.*, 1993]. One RU represents a change of 0.0001° , in the angle of the intensity minimum. The exact conversion factor between RU and surface concentration depends on properties of the sensor surface and the nature of the molecule responsible for the concentration change. Sensograms not only provide information about the binding or non-binding, but they also contain information about the kinetics and the strength of the interaction. An advantage of SPR is its high sensitivity without any fluorescent or other labelling interactants [O'Shannessy *et al.*, 1993].

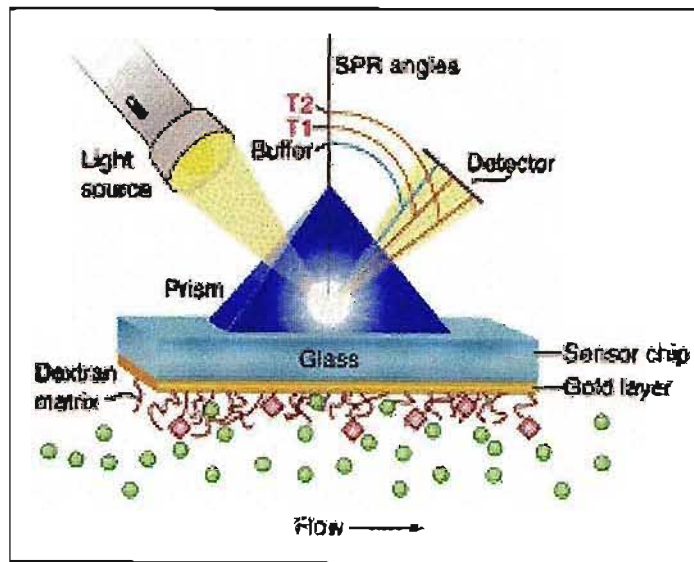


Figure 1.13. Basic components of an instrument for SPR biosensing: A glass slide with a thin gold coating is mounted on a prism. Light passes through the prism and slide, reflects off the gold and passes back through the prism to a detector. Changes in reflectivity versus angle or wavelength give a signal that is proportional to the volume of biopolymer bound near the surface.

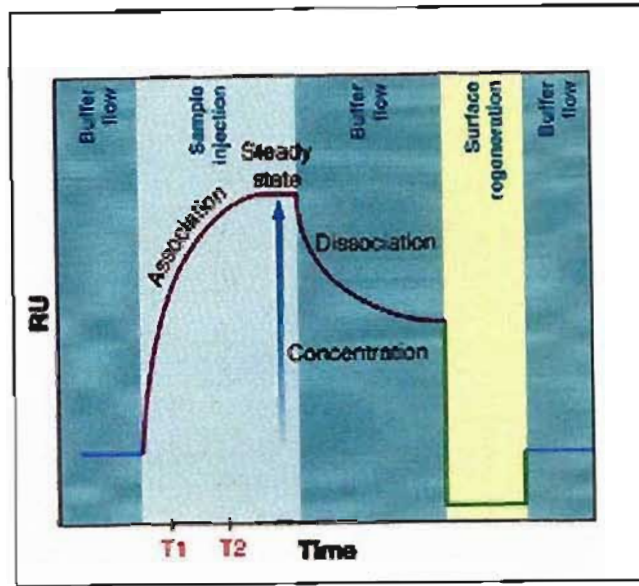


Figure 1.14. A typical SPR biosensing experiment showing the optical response versus time. The gold surface with immobilized interactants starts in pure buffer. At T1, solution containing the other interactant is introduced to produce an association. At T2 the flow cell is flushed with pure buffer, after which the dissociation is measured. Lastly the starting surface is regenerated with a sequence of reagents.

1.7.3. Commercialization of SPR technology

Biacore AB introduced the first commercial biosensor in 1990, and has since maintained a leading position as a supplier of the technology for investigating the interactions between biomolecules. Biacore offers systems, reagents and applications of SPR-based biosensor technology in life science research, drug discovery and development and food analysis. The ease of Biacore lies in its ability to allow for highly specific interactions to occur over a faster time frame, while still keeping the interaction binding affinities at a steady level [Biacore AB, Uppsala, Sweden].

1.7.3.1. Biacore's SPR technology

Biacore's SPR technology has been designed to investigate the functional nature of binding events. Its reliability and success is built on Biacore's unique expertise in three cornerstone technologies. These technologies are the sensor chips, which provide the surface conditions for SPR for attaching molecules of interest. A Microfluidics system delivers the sample to the surface and surface plasmon resonance ultimately detects the mass concentrations at the surface.

1.7.3.1.1. Sensor chip technology

The Biacore's sensor chip is at the heart of the technology. Quantitative measurements of the binding interaction between one or more molecules are dependent on the immobilization of a target molecule to the sensor chip surface [McDonnell, 2001]. The sensor chip consists of a glass surface, coated with a thin layer of gold. This forms the basis for a range of specialized surfaces designed to optimize the binding of a variety of molecules [Alaedini and Latov, 2002]. . In the most widely used sensor chip, the gold surface is modified with a carboxymethylated dextran layer (Figure 1.15.). This dextran hydrogel layer forms a hydrophilic environment for the attachment of biomolecules, preserving them in a non-denatured state. A range of other derivatized surfaces is also available to enable various immobilization chemistries. Stability is such that the sensor chip can be regenerated for many cycles depending on the nature of the immobilized ligands. The chips can also withstand high salt concentrations, extremes in pH and organic solvents [Green *et al.*, 2000]. Most important is that Biacore sensor chips are easily interchangeable and this provides great flexibility in the research environment.

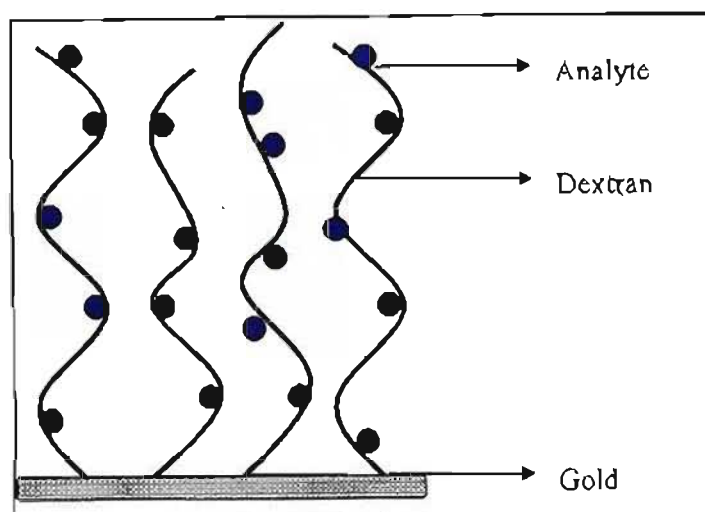


Figure 1.15. The sensor chip surface.

1.7.3.1.2. Microfluidics

Biacore has developed a flexible Microfluidics system for its SPR technology, based around the Integrated micro Fluidics Cartridge (IFC), which is specific to defined instrument series. All IFC's allow analyte to pass over the sensor surface in a continuous, pulse-free and controlled flow-maintaining a constant analyte concentration at the sensor chip surface [McDonnell, 2001]. The benefits of the Microfluidics system is:- the low sample concentration; the absence of an air-solution interface, where samples can evaporate and proteins can be denatured. The concentration of free analyte is constant and therefore known at all times and since no washing steps are needed to replace the sample with buffer, a range of surface ligand concentrations and contact times can be analysed in one experiment improving on the kinetic and concentration analysis tool. Screening large number of samples and channels can be used in different configurations, so that more than one experiment can be run at the same time [McDonnell, 2001].

1.7.3.1.3. Surface plasmon resonance detection

The gold layer in the sensor chip, creates the physical conditions required for SPR. Essentially, SPR detects changes in mass in the aqueous layer close to the sensor chip surface by measuring changes in the refractive index [Alaedini and Latov, 2002]. When molecules in the test solution bind to a target molecule the mass increases, when they dissociate, the mass falls. Molecules as small as 100 Daltons can be studied.

1.7.3.2. Choice of coupling chemistry

There are three main types of coupling chemistry, which utilize amine (lysine), thiol (cysteine) or aldehyde (carbohydrate) functional groups on glycoproteins, respectively. All covalent coupling methods utilize free carboxymethyl groups on the sensor chip surface [Alaedini and Latov, 2002]. They can, therefore, be used for any of the sensor chips that have such carboxymethyl groups. If the protein to be immobilized has a surface-exposed disulphide or a free cysteine, ligand-thiol coupling is probably the method of choice. Failing this, amine coupling could instead be used. If the amine coupling inactivates the protein (as assessed by ligand and/or antibody binding), aldehyde coupling can be attempted, provided that the protein is glycosylated.

1.7.3.3. Advantages of Biacore

Biacore does not require any labels or reporter groups to detect biomolecular interactions. This eliminates the work associated with the purification and labelling of material, also removing the risk that labels may interfere with the interaction being studied [Rich and Myszka, 2000]. In addition, Biacore follows every step in a multi-step analysis procedure, in contrast to label-based methods that often only report one final step. The progress of interactions is displayed directly on the computer screen in Biacore, as a plot of response against time. Immediate feedback on the status of an interaction speeds up assay development and analysis. The result can of course be processed further after the run, for

example to extract kinetic constants for the interaction. SPR-based technology is based on measurement of light reflected from the side of the sensor surface that is not in contact with the sample [Rich and Myszka, 2000]. The light does not penetrate the sample so that the measurements can be made on turbid or opaque samples with no interference from light absorption or scattering.

1.7.4. Applications of Biacore

Biomolecular binding interactions are fundamental to research, not only within life sciences, but also for drug discovery and food analysis. Biacore's SPR technology is been used in laboratories around the world as a tool for the functional analysis of biomolecular binding events. In research applications, SPR has allowed for the identification of DNA damage, as well as the binding partners, to any target molecule via ligand fishing. Elucidation of functional novel proteins in proteomics research; determination of the nature of protein complexes and their functions and the optimization of therapeutic antibodies has made SPR such a powerful tool. SPR has also been implicated in the identification of disease markers in clinical samples and in the evaluation of ion selectivity in signalling pathways as well as in the study of membrane associated molecules in near native environments [Myszka, 1999]. On the drug discovery and development frontier, SPR has been successful in proteomics via target identification and ligand fishing and clinical trails, studying the stratification of patient responses to therapeutics. In food analysis, applications quality control is studied via rapid and reliable vitamin analysis, in health and nutrition food manufacturing; food safety, if achieved in the optimization of screening assays for monitoring hazardous natural toxins in food and feed; on-site screening for veterinary drug residues such as antibiotics and hormones in dairy and meat production plants and in process control to monitor specific analytes in food and beverage plants [Myszka, 1999].

1.8. CONCLUSION

Until now, convincing proof showing that peptidoglycan hydrolases are indispensable for the growth of bacteria containing peptidoglycan in their walls, fails to exist. However, it is difficult to think of a mechanism by which the peptidoglycan network could be enlarged and divided upon without the help of hydrolytic enzymes. Thus, theoretically, peptidoglycan hydrolases must be considered as the peacemakers of the cell wall for growth and therefore for bacterial growth in general. In accepting such a concept, it is indeed that this class of enzymes represents unique bacterial proteins. On the one hand, they enable the cell to grow, but on the other hand, they can also kill the cell by means of autolysis. It is based on these two features that these enzymes provide the basis for a vested interest in the development of chemotherapeutics.

Although the molecular details are still not understood in its entirety, it is clear that the bacteriolytic action of cell wall synthesis inhibitors, such as the penicillins, is due to the uncontrolled action of endogenous peptidoglycan hydrolases. In addition to inhibition of peptidoglycan synthesis, other ways of uncontrolled action of these enzymes are feasible. The mode of action of certain low molecular weight phage-coded lysis proteins is just one example.

As peacemaker enzymes for bacterial growth, peptidoglycan hydrolases thus provide the ideal target for antibiotics. The problem, however, is the multiplicity of hydrolases found in bacteria. This fact has, not only inhibited the isolation of mutants completely lacking peptidoglycan hydrolytic activity, but also is an obstacle in attempts to demonstrate that a complete block of these hydrolases results in bacteriostasis as would be expected for true peacemaker enzymes.

Peptidoglycan hydrolases, which appear to be involved in the growth of the shape maintaining structure of the bacterial cell, necessarily have to be under strict topological and temporal control. Thus by studying the cellular control mechanisms for peptidoglycan hydrolases, a fundamental problem in biology can be addressed, namely, how a specific shape is realized, maintained and modified in a well controlled fashion, in a biological system. One clue for an understanding of these mechanisms may very well turn out to be the specific subcellular distribution of the enzymes. Since some of them are tightly bound

to peptidoglycan, it is possible that the sacculus serves as a matrix to guarantee synthesis of a peptidoglycan network identical in shape to the pre-existing structure. In analogy to DNA replication, it is quite likely that multi-enzyme complexes are involved in these processes. In particular, for a coordination of the insertion of new peptidoglycan subunits with the cleavage of bonds to provoke enlargement of the sacculus, holoenzyme-like complexes are reasonable possibilities.

With the emergence of tolerant strains worldwide, it has become extremely important to study the control mechanisms employed by bacteria in the functioning of their hydrolytic enzymes. Seemingly as not all autolysins are lethal to the cells that created them, the emphasis now lies in the identification and regulation of such autolysins. Attempts to produce completely autolysin-negative bacteria have not been successful, as generated mutants simultaneously deficient in the two major autolysins of *B. subtilis* could not produce a totally autolysin-negative cell. Although the major autolysin in pneumococci that causes lysis of stationary cultures can be ablated, it may not be essential for vegetative growth.

Analogy of the effects of antibiotics to the stringent response has been made, but this analogy is far from perfect. In the original context, stringent cells deprived of a needed amino acid had mechanisms to shut down RNA metabolism. A cell treated with an antibiotic against the cell wall in principle, has resources for the synthesis of protein, RNA and DNA. In establishing the regulatory genes that affect autolysin, will open the pathway to developing antimicrobial chemotherapeutics. This will reduce the development of resistant strains, as regulatory systems may now be employed to work against the bacterium when in the presence of a specific antibiotic, thereby not killing the bacterium, hence not allowing the bacterium to acquire resistance to that antibiotic.

Increasing bacterial resistance to virtually all available antibiotics causes an urgent need for new antimicrobial drugs, drug targets and therapeutic concepts. The focus now turns to strategies, which can render bacteria highly susceptible to the antimicrobial arsenal of the immune system by targeting bacterial immune escape mechanisms that are conserved in a major number of pathogens. Virtually all innate molecules that inactivate bacteria, ranging from antimicrobial peptides such as defensins and cathelicidins to bacteriolytic enzymes such as lysozyme and group IIA phospholipase A2, are highly cationic in order to facilitate

binding to the anionic bacterial cell envelopes. Bacteria have found ways to modulate their anionic cell wall polymers such as peptidoglycan, lipopolysaccharide, teichoic acid or phospholipids by introducing positively charged groups. Two of these mechanisms involving the transfer of D-alanine into teichoic acids and of L-lysine into phospholipids, respectively, have been identified and characterized in *Staphylococcus aureus*. Inactivation of the responsible genes, *dltABCD* for alanylation of teichoic acids and *mprF* for lysinylation of phosphatidylglycerol respectively, renders *S. aureus* highly susceptible to many human antimicrobial molecules and leads to profoundly attenuated virulence. The *dltABCD*- and *mprF*-related genes are found in the genomes of many bacterial pathogens indicating that the escape from human host defences by modulation of the cell envelope is a general trait in pathogenic bacteria. Thus studies suggest that inhibitors of DltABCD or MprF should have great potential in complementing or replacing the conventional antibiotic therapies. By allowing for these studies to form the basis of current research, similar mechanisms maybe identified in the *Streptococcus milleri* organism and regulation and expression of the particular hydrolytic enzymes present will lead to novel therapeutics been established.

1.9. AIMS AND OBJECTIVES OF THE RESEARCH

Therefore, progress in understanding growth and division of the bacterial cell wall, which is the molecular basis for the morphogenesis of the bacterium during its cell cycle, opens the investigation of the interplay of peptidoglycan-synthesizing and peptidoglycan-hydrolysing enzymes. The main aim of this study will be to characterize the major cell wall autolysins found in the Streptococcal isolates. This characterization would thereby allow for the subsequent identification of the regulatory mechanisms present in autolysin activity, and link those mechanisms to antibiotic stresses as well as the presence or absence of charged groups within the bacterial cell wall. Biacore techniques will aim to better understand the protein interaction of the autolysins with the specific charged group, teichoic acid, a noteworthy component of the bacterial cell wall. A proteomic approach aims to establish a two-dimensional map for the selected Streptococcal isolate. Characterization of these autolytic systems present in the Streptococcal isolates on a molecular and regulatory level forms the basis for the research carried out in this study. Ultimately, this study aims to develop novel therapeutics beneficial to society as a whole.

CHAPTER TWO

MATERIALS AND METHODS

CHAPTER TWO

2.1. Bacterial strains, culture and growth conditions

Streptococcus milleri and *Staphylococcus aureus* strains were isolated from clinical samples at a pathology laboratory in Pietermaritzburg, South Africa. *Streptococcus milleri* P35 (*S. milleri* P35), *Streptococcus milleri* 77 (*S. milleri* 77), *Streptococcus milleri* B200 (*S. milleri* B200) and *Staphylococcus aureus* (*S. aureus*) was grown in tryptone soy broth (TSB) or tryptone soy plates (TSA, BioLab) containing 1.4% agar per litre. Cultures were checked for purity on 5% defibrillated sheep blood-agar plates. All working cultures were sub cultured fortnightly and stored at 4°C until needed. Stock cultures were maintained on TSB in a 30% glycerol suspension at -70°C. Overnight *Streptococcus* cultures were incubated at 37°C in 5% carbon dioxide (CO₂) atmosphere. Overnight *Staphylococcus* cultures were incubated at 37°C.

2.2. Minimal inhibitory concentration (MIC)

Micro broth dilution was used to determine the MIC for each strain. Optical density (OD) at 600nm of overnight cultures were monitored in a Beckman DU 640 spectrophotometer and used as a 1% inoculum into microtitre plates containing Mueller Hinton broth (Becton, Dickson and Company). Antibiotics (Ampicillin, Penicillin G and Vancomycin [SIGMA]) were prepared as 10mg/ml stock solutions from which appropriate concentrations were prepared. Antibiotic concentrations ranging from 0 to 80µg/ml were tested respectively. Plates were incubated for 36 hours at 37°C in 5% CO₂ atmosphere.

2.3. Disk diffusion assay to determine antibiotic susceptibility

Cultures of each strain were spread on the surface of TSA plates and antibiotic susceptibilities were tested with paper disks containing the antibiotics ampicillin, penicillin and vancomycin ranging from 0 to 30 µg/ml. The sizes of inhibition zones were evaluated after incubation for 24 hours at 37°C in 5% CO₂ atmosphere.

2.4. Relative Fitness Assay

Overnight starter cultures were prepared in 10ml TSB. Erlenmeyer flasks (250ml) containing 100ml of medium were inoculated with 1ml of the overnight starter culture. Growth was monitored at 600nm with the optical density read at hourly intervals. The relative fitness was also determined in the presence of an antibiotic. Ampicillin (SIGMA) at a concentration of 5µg/ml was incorporated into 100ml culture volumes of inoculated TSB. Growth was monitored at an optical density of 600nm at hourly intervals. Growth curves were plotted using SIGMA PLOT, 2000 and relative fitness for each strain determined respectively.

2.5. Gram stain morphology and microscopy

Slides were sterilized in 70% alcohol and a small drop of water placed onto it. A small amount of bacterial culture was transferred using an inoculating loop onto the slide, spread evenly and heat fixed. The smear was covered with Hucker's ammonium oxalate crystal violet stain, (0.2% crystal violet (wt/vol) in 95% ethanol and 0.01% ammonium oxalate (wt/vol) in distilled water) and allowed to stain for 1 minute. The dye was washed off with distilled water. A second dye, iodine (1% potassium iodine (wt/vol) and 0.5% iodine (wt/vol) in distilled water) was applied to the smear and allowed to develop for 1 minute. The dye was washed off with distilled water. The smear was decolorized with 95% ethanol for 30 seconds before been counterstained with safranin (10ml of a saturated solution of safranin in 95% ethanol added to 10ml distilled water) for 1-2 minutes. Slides were washed and blot dried with filter paper. The smears for each strain were examined microscopically, using a 100X magnification oil emersion lens, and photographed.

2.6. Protein and autolysin extraction

Overnight cultures of each strain were diluted into 200ml TSB at a 1% concentration and incubated at 37°C in 5% CO₂. Extraction was performed at different stages of the growth cycle; cells were pelleted at 7700 x g for 10 minutes in a Beckman J2-21M centrifuge using a JA14 rotor. The resultant pellets were resuspended in 4% sodium dodecyl sulfate (SDS) (wt/vol) and incubated for 16 hours with gentle agitation at room temperature. Large scale autolysin extraction was carried out with a 1% inoculation of an overnight

culture into 500ml TSB aliquots and grown to an OD_{600nm} of approximately 0.8. Cells were harvested by centrifugation (9000 rpm for 15 minutes at 4°C) and pellets were resuspended in 5ml of 4% SDS (wt/vol) and incubated at room temperature for 20 hours with gentle agitation. Cells were pelleted at 12 400 x g for 15 minutes at 4°C. Supernatants containing autolytic proteins were stored at -20°C until required.

2.7. Protein concentrations

Protein concentrations were determined using a Micro BCA Assay Kit (Pierce Biotechnology, Rockford, USA) according to manufactures instructions. Briefly, working reagent was prepared as a 25: 24: 1 ratio of MA: MB: MC respectively. A 1: 1 ratio of sample to working reagent was prepared. Samples were incubated along with standards at 60°C for 1 hour. Optical densities were monitored at an OD of 562nm. Bovine serum albumin served as a standard in all assays. Standard curve analysis using a computational package, SIGMA PLOT 2000, allowed for the exact protein concentrations to be determined.

2.8. Sodium dodecyl sulfate - Polyacrylamide Gel Electrophoresis (SDS-PAGE)

Proteins were resolved by SDS-polyacrylamide gel electrophoresis (SDS-PAGE) on a Hoefer Mighty Small SE260 (Amersham) using the Laemlli buffer system (Laemlli, 1970). The electrode buffer contained 0.05 M Tris-glycine (pH 8.3) and 0.1% SDS. Polyacrylamide gels at a 10% concentration were prepared. The separating gel contained 7.5% acrylamide, 0.15 M Tris hydrochloride (pH 8.8), 0.1% SDS, 0.05% *N, N, N', N'*-tetramethylethylenediamine (TEMED), 1% glycerol and 0.1% ammonium persulfate (APS). The stacking gel contained 5% acrylamide, 0.0625 M Tris hydrochloride (pH 6.8), 0.1% SDS, 0.05% TEMED, and 0.1% APS. The sample loading buffer contained 0.125 M Tris hydrochloride (pH6.8), 4% SDS, 0.02% bromophenol blue, 0.2 M dithiothreitol (DTT), and 20% (v/v) glycerol. Samples were solubilized in sample loading buffer in a boiling water bath for 5 minutes prior to loading. Recombinant molecular weight marker (BioRad) was included ranging from 15 to 150 kDa. Electrophoresis occurred at 18mA per gel, until the Bromophenol blue tracker dye ran off the gel. Following electrophoresis, gels were stained for 90 minutes in a solution of 0.025%

Coomassie Brilliant Blue, 40% methanol, and 7% acetic acid. Gels were destained initially in 40% methanol and 7% acetic acid for 30 minutes and transferred to a 7% acetic acid and 5% methanol solution for 24 hours whilst on a rotary shaker at room temperature. Gels were visualized under white light and photographed using a VERSADOC 3000 gel documentation system (BioRad Inc.).

2.9. Two Dimensional sodium sulfate - Polyacrylamide Gel Electrophoresis (2-D SDS-PAGE)

2.9.1. Sample preparation

Total protein analysis was carried out following the methods of Wilkins *et al.*, 2001 with minor modifications. Briefly, cells were collected at the middle of exponential phase by centrifugation at 4000 rpm for 10 minutes at 4°C. Pelleted cells were washed in 0.9% sodium chloride (NaCl) and immediately suspended in 25mM Tris HCl (pH 7.5) containing 0.01% lysozyme, 0.026% phenylmethylsulfonyl (PMSF), 0.005% chloramphenicol and 18% sucrose and allowed to incubate for 15 minutes at 37°C (Giard *et al.*, 1997). The bacterial cells were again pelleted at 5000 rpm for 5 minutes at 4°C and resuspended in 50mM Tris HCl (pH 7.5) solution with 0.3% sodium dodecyl sulfate and 0.3% dithiothreitol (DDT) and incubated for 5 minutes in a boiling water bath. Samples were then vortexed and centrifuged at 9500 rpm for 5 minutes at 4°C. The resulting supernatants was retained and incubated at 4°C for 15 minutes following the addition of 24ul of 0.5M Tris HCl (pH 7.5) containing 0.5% anhydrous magnesium chloride (MgCl₂) and 4U each of RNase A and DNase. Protein was precipitated by the addition of four volumes of ice-cold acetone and collected by centrifugation at 10 500 rpm at 4°C for 10 minutes. The resulting pellet was resuspended in a minimal volume of 7M deionized urea combined with 2M thiourea in a 2% Tergitol NP-40 and 62mM DDT. A 2% solution of pH 3-10 carrier ampholytes was added to the final suspension. Protein concentrations were determined using a Micro BCA Assay Kit (Pierce Biotechnology, Rockford, USA) according to manufactures description. Protein concentrations were determined prior to the addition of DTT, as this compound interferes with the working solution. Protein samples were stored at -20°C until further needed.

2.9.2. First-dimension electrophoresis

Iso-electric focusing was carried out by using 11cm precast Immobiline DryStrips (BioRad Inc) with a linear pH gradient off 4 to 7 and a Multiphor II apparatus (Amersham Pharmacia). Initially, 20 μ g of protein was rehydrated in a rehydration buffer (8M urea, 2% 3-[3 (Cholamidopropyl) dimethyl-ammonio] 1-propanesulfonate (CHAPS) and 2% Immobilized Protein Gradient Buffer (IPG buffer); [20mM DTT was added before use]) in a 1:1 ratio in the Immobiline DryStrip Reswelling tray (Amersham Pharmacia) overnight. For total protein gels, another 20 μ g of protein was cup loaded at the anodic end for Coomassie blue- and silver-stained gels, respectively. Samples were solubilized in sample buffer (9M urea, 0.5% Triton X-100, 0.5% Pharmalyte [pH 4-10], 250mg DTT or 0.5% 2-mercaptoethanol and traces of Bromophenol Blue) in a 1:4 ratio. The Bromophenol blue acts as a tracking dye allowing the migration of the sample to be visualized within the first 5 to 10 minutes of the run. The following voltage gradient was applied: from 0 to 300 volts in 0.1 hour; 300 volts for 6 hours; from 300 to 3500 volts for 5 hours; and 3500 volts for 5.5 hours. Focusing was performed at 5°C, using a cooling system.

2.9.3. Second-dimension electrophoresis

Focused Immobiline DryStrips were equilibrated in 0.4M Tris HCl (pH 6.8) containing 6M urea, 30% (v/v) glycerol, 2% SDS and 1% DTT for 15 minutes and subsequently for 15 minutes in the same buffer containing 2.5% iodoacetamide prior to loading onto second-dimension SDS-polyacrylamide gels. Gels were set (Table 2.1.) and allowed to polymerize overnight at 4°C prior to been run. No stacking gel was set. Equilibrated strips were incorporated into the SDS gel. BioRad molecular weight marker was electrophoresed in the second-dimension at the acidic end to determine the relative molecular masses of the proteins. The pI was deduced by linearity of the Immobiline DryStrip. Electrophoresis was carried out at 5°C, at 60 mA and maximum voltage. Proteins were visualized initially by Coomassie Blue- and thereafter by silver-staining.

Table 2.1. Reagents used to prepare SDS-PAGE gels.

REAGENTS	Running Gel (10%)
Acrylamide	12.6 ml
Distilled water	21.6 ml
0.5 M Tris HCl (pH 6.8)	-
3 M Tris HCl (pH 8.8)	5.0 ml
50% (v/v) Glycerol	0.8 ml
20% (v/v) SDS	0.2 ml
TEMED	0.06 ml
10% ammonium persulfate	0.144 ml

2.9.4. Silver staining

Silver staining was used to enhance the visualization of the protein spots in the two-dimensional polyacrylamide gels. Silver stain is several orders of magnitude more sensitive for detection of protein than the Coomassie stain. The method used was that of Morrisey (1981) with minor modifications, where DTT reduction was incorporated to improve the reproducibility. The gel was initially placed in 100ml of Destain solution I [40% (v/v) methanol and 7% (v/v) acetic acid] and allowed to destain overnight. This solution was replaced with 100ml of Destain solution II [5% (v/v) methanol and 7% (v/v) acetic acid]. Gels were gently agitated at room temperature for 30 minutes. The Destain solution II was discarded and replaced with 100ml of cross-linking solution [10% (v/v) glutaraldehyde] for 2 hours, and after several washes in distilled water, 100ml DTT (5 μ g/ml) was added and incubated for 30 minutes. Once the DTT solution was discarded, a silver nitrate solution [0.1% (w/v)] was added and the gels were gently agitated at room temperature for 30 minutes. The gels were finally rinsed under running deionized water before developing solution [3% (w/v) sodium carbonate and 0.019% formaldehyde] was added, with slow shaking until the bands became visible. Staining was stopped with Destain solution II. Gels were visualized under white light, and photographed using a VERSADOC 3000 gel documentation system (BioRad Inc.).

2.10. Preparation of cell wall material

Crude cell walls were prepared from overnight cultures grown in TSB. The overnight culture was diluted into 200ml TSB as a 1% inoculation and incubated at 37°C to an OD_{600nm} of approximately 0.8. Cells were pelleted at 8000 x g for 10 minutes at 4°C and resuspended in 3ml of double distilled water. The suspension was placed in a boiling water bath for 30 minutes and centrifuged at 12 100 x g for 15 minutes. The pellet was washed twice with 50 mM phosphate buffer (pH 7.5), centrifuged and resuspended in a minimal volume of the same buffer. This served as the crude cell wall substrate in renaturation SDS-PAGE (Zymogram).

2.11. Renaturing SDS-PAGE (Zymogram)

Renaturing SDS-PAGE was performed according to the method of Sugai *et al.*, 1990 with minor modifications. Polyacrylamide SDS gels (10%) containing 0.1% (wt/vol) of the crude cell wall substrate, specific to the strain been analyzed, was used for the detection of lytic activity. Samples were mixed 1:1 (v/v) with sample buffer. Samples were heated for 5 minutes in a boiling water bath prior to loading on the gel. Upon completion of electrophoresis, gels were soaked for 2 hours in 250ml-distilled water at room temperature with gentle agitation, changing the distilled water every half hour. For the final half hour the gels were soaked in 250ml fresh distilled water and incubated at 37°C. Gels were transferred to 150ml of renaturation buffer (50 mM phosphate buffer [pH7.5] containing 0.01% Triton-X100) and incubated for 16 hours at 37°C. Bands with lytic activity were observed as clear in the opaque gel. To enhance the detection of the lytic bands, gels were stained for 5 minutes in 0.1% methylene blue in 0.01% Potassium hydroxide and destained extensively in distilled water.

2.12. Two Dimensional Zymographic analysis

Autolytic extracts from the mid exponential phase of *S. milleri* 77 were prepared as previously explained (2.6. Protein and autolysin extraction).

2.12.1. First-dimension electrophoresis

First dimension electrophoresis was carried out by using 11cm precast Immobiline DryStrips (BioRad Inc) with a linear pH 4 to 7 gradient and a Multiphor II apparatus (Amersham Pharmacia). Initially, 20µg of autolytic protein extract was rehydrated in a rehydration buffer (8M urea, 2% CHAPS and 2% IPG buffer [20mM DTT was added before use]) in a 1:1 ratio in the Immobiline DryStrip Reswelling tray (Amersham Pharmacia) overnight. A further 20µg of protein was cup loaded at the anodic end. Autolytic samples were solubilized in sample buffer (9M urea, 0.5% Triton X-100, 0.5% Pharmalyte [pH 4-10], 250mg DTT or 0.5% 2-mercaptoethanol and traces of Bromophenol Blue) in a 1:4 ratio. The Bromophenol blue acts as a tracking dye allowing the migration of the sample to be visualized within the first 5 to 10 minutes of the run. The following voltage gradient was applied: from 0 to 300 volts in 0.1 hour; 300 volts for 6 hours; from 300 to 3500 volts for 5 hours; and 3500 volts for 5.5 hours. Focusing was performed at 5°C, using a cooling system.

2.12.2. Second-dimension electrophoresis

Focused Immobiline DryStrips were equilibrated in 0.4M Tris HCl (pH 6.8) containing 6M urea, 30% (v/v) glycerol, 2% SDS and 1% DTT for 15 minutes and subsequently for 15 minutes in the same buffer containing 2.5% iodoacetamide prior to loading onto second-dimension SDS-polyacrylamide gels. Polyacrylamide SDS gels (10%) containing 0.2% (wt/vol) of *S. milleri* 77 crude cell wall substrate, specific to the strain been analyzed, was used for the detection of lytic activity in the second dimension. Gels were set (Table 2.1.), the modification been the incorporation of 0.2% extracted crude cell wall material as a part of the distilled water component, and allowed to polymerize overnight at 4°C prior to been run. No stacking gel was set. Equilibrated strips were incorporated into the SDS gel.

2.12.3. Staining and visualization of Two-dimensional Zymographic profile

Upon completion of electrophoresis, the gel was soaked for 4 hours in 300ml-distilled water at room temperature with gentle agitation, changing the distilled water every half hour. For the final half hour the gel was soaked in 300ml fresh distilled water and incubated at 37°C. The gel was then transferred to 300ml of renaturation buffer (50 mM phosphate buffer [pH7.5] containing 0.01% Triton-X100) and incubated for 5 days at 37°C. To enhance the detection of the lytic spots, gels were stained for 5 minutes in 0.1% methylene blue in 0.01% Potassium hydroxide and destained extensively in distilled water. Spots with lytic activity were observed as clear in the opaque gel. Gels were visualized under white light and photographed using a VERSADOC 3000 gel documentation system (BioRad Inc.).

2.13. Elution of lytic proteins from zymograms

Protein bands showing lytic enzyme action were excised from the zymogram. Gel slices were placed in a Model 422 electro-eluter (BIO-RAD, California) and extracted according to manufacturers instructions. Eluted proteins were stored in 50mM phosphate buffer (pH 7.5) at -20°C until further use.

2.14. N-terminal sequencing

Proteins were resolved on SDS-PAGE and transferred to Sequi-Blot polyvinylidene (PVDF) membrane (BIO-RAD) in 10mM 3-cyclohexylaminol 1-propanesulfonic acid (CAPS) buffer (Sigma) using a Mini-Trans-Blot Cell (BIO-RAD) according to manufactures instructions. Blot transfer lasted 90 minutes at maximum current and 90 volts. Blots were stained with Coomassie Blue and individual bands corresponding to lytic activity when compared to the zymograms were excised for N-terminal sequencing. N-terminal amino acid sequences were obtained with a model 491 Procise automated sequencer (PE, Applied Biosystems) using Edmund chemistry.

2.15. Appearance of N-acetyl amino sugars and free amino groups in soluble fragments during lysis of bacterial cell walls

The appearance of reduced sugars and the liberation of free amino groups were assayed by the Morgan-Elson assay and the N-dinitrophenyl (DNP) assay (according to the methods of Ghuysen *et al.*, 1966) respectively. Purified *S. milleri* cell walls (1mg) were digested, at 37°C, with gel extracted autolytic enzyme (1ug/ml) in 50mM phosphate buffer, pH 7. *S. milleri* cell walls digested with mutanolysin (Sigma) under the same conditions served as a control in both assays. Reaction mixtures were centrifuged and the supernatants was dried under vacuum and re-dissolved in 1% potassium tetraborate (K₂B₇O₄) (Sigma). This mixture was then used to assay for reduced sugars (Morgan Elson) and free amino groups (DNP) respectively [Beukes *et al.*, 2000].

2.16. Autolytic assays with whole cells

Triton X-100-stimulated autolysis was measured at OD₆₀₀ in glycine buffer at pH 8 [Gardete *et al.*, 2004]. Cultures were rapidly chilled on ice; cells were pelleted by centrifugation at 9 500 x g at 4°C for 10 minutes, and washed in phosphate buffer (pH 7.5) to remove traces of nutritive media. Cells were suspended in 50mM glycine-0.01% Triton X-100 buffer to an OD₆₀₀ of 0.3. The effect of antibiotic stress on autolysis was measured at hourly intervals at 37°C. Two types of buffers were employed, phosphate buffer (pH 7.5) and phosphate buffer in 0.01% Triton X-100 (pH 7.5) to monitor their effect on the rates of autolysis. In separate assays, whole cells were resuspended in Triton X-100 – glycine buffer and extracted autolysin for each strain was added to a final concentration of 100µg/ml respectively, to monitor the rate of autolysis. Autolytic assays were also carried out using 0.01% deoxycholate incorporated into the buffer.

2.17. Autolytic assay on cell wall fractions

Peptidoglycan with intact teichoic acid and that without teichoic acid were used to assay for the role that teichoic acids play in the rate of autolysis. Fractions were resuspended to an OD₆₀₀ of 0.3 in Triton X-100 – 50mM glycine buffer (pH 8) and a series of assays were performed. The rate of autolysis was measured in the presence of the respective autolysin at a final concentration of 100µg/ml. The rate of autolysis was measured at

hourly intervals at 37°C to monitor the effect of antibiotic stress, when incorporate at sub-minimal MIC values.

2.18. Preparation of peptidoglycan fractions

Peptidoglycan was isolated according to the methods of Hakenbeck *et al.*, 1998. A 500ml volume of an exponentially growing culture was rapidly chilled in an ethanol-ice bath. Cells were harvested by centrifugation at 8000 x g for 15 minutes at 4°C, resuspended in double distilled water, and immediately boiled in 4% SDS (Roche). Cells were then washed in distilled water and boiled at 90°C to remove bacterial cellular enzymes. This was followed by a 1 M NaCl buffer-wash (Merck Chemicals) to remove any traces of SDS. Samples were then incubated at 37°C with 200µg/ml of pronase E (SIGMA) for 16 hours followed by treatment with 200µg/ml trypsin (SIGMA) and further incubated for 16 hours at 37°C. The mixture was washed three times with 1% SDS, 8 M lithium chloride (LiCl) solution (Merck Chemicals), and 100 mM ethylene diamine tetra-acetic acid (EDTA) solution (Associated Chemical Enterprises) and washed at least twice with distilled water. After centrifugation cells were resuspended in 1ml of distilled water and separated into two 500µl aliquots. The one aliquot which served as intact teichoic acid peptidoglycan was centrifuged at 12 100 x g for 5 minutes, washed in acetone, and dried for 15 minutes under laminar flow conditions. From the second aliquot, teichoic acids were removed with 7% (vol/vol), final concentration of hydrofluoric acid (HF) for 36 hours at 4°C. HF was removed by centrifugation at 8000 x g for 5 minutes at 4°C and the resultant pellet was washed in acetone and dried in a laminar flow bench. These fractions served as starting material for the peptidoglycan autolytic assays.

2.19. Molecular interaction measurements

The interaction between peptidoglycan and autolytic extract were analyzed with a model X system from Biacore (Uppsala, Sweden). An amine-coupling kit containing *N*-hydroxysuccinimide (NHS), *N*-ethyl-*N*'-[(3-dimethylamino)-propyl]-hydrochloride (EDC), and ethanolamine-hydrochloric acid [E-HCl] (Amersham Pharmacia Biotech) was used to immobilize the ligand to the chip. This kit is designed to allow ligands to

be attached via primary amine groups to the sensor surface for subsequent analysis. EDC and NHS are prepared by adding 10ml of filtered and deionized water to dissolve each chemical. Both reagents are stored at -18°C, whilst ethanolamine is stored at 4°C. A mixture of NHS and EDC (1:1) was injected into the dextran matrix on the sensory chip to activate it at the flow rate of 5µl/ min at 25°C, and different concentrations of autolysin (100µg/ml) in HBS buffer (pH 7.5 - 8.5) was immobilized on the matrix. Samples with and without teichoic acid were digested with 15µg/µl Lysozyme (Roche) overnight at 37°C and centrifuged to remove any traces of lysozyme. The peptidoglycan in 0.1M sodium acetate (NaOH) buffer was immobilized on the sensory chip, CM5, to measure its interaction with autolytic protein. The excess active sites of the matrix were blocked with 1M ethanolamine-HCl and washed with 0.1M NaOH regeneration buffer. Autolysin was injected at a flow rate of 10µl/min at 25°C, and the binding capacity of the autolysin to the peptidoglycan in the presence and absence of teichoic acids was monitored and presented as a sensogram (a plot of Response Units versus Time). Chips were undocked and stored in 4-(2-Hydroxyethyl)-1-piperazineethansulfonic acid [HEPES] buffered saline solution [HBS] at 4°C for further use.

2.20. Preparation of Auto-inducing peptide (AIP) containing supernatants

S. aureus strains were grown in CYGP Broth (10g/litre casamino acids; 10g/litre yeast extract; 5g/litre glucose; 5.9g/litre NaCl; and 60mM β-glycerol phosphate) with shaking at 37°C for 9 hours starting with an inoculum of $\sim 3 \times 10^7$ cells/ml in 5ml of broth [Novick, 1991]. Cells were removed by centrifugation at 13 000 x g for 5 minutes at 4°C, and the supernatant was filtered (0.22-µm filter, Gelman). Ammonium sulfate precipitation was performed on the filtrate according to the method of Green and Hughes in 1955. A gradient decreasing concentration of ammonium sulfate allowed for differing concentrations of the AIP to be precipitated out of the solution. This filtrate was left for 16 hours at room temperature with gentle agitation to facilitate the precipitation. These solutions were centrifuged at 10 000 rpm for 10 minutes at 4°C. The resultant pellet was

retained and resuspended in 500µl distilled water. The AIP concentrate was stored at -70°C and used as a source of AIP.

2.21. *Agr* auto-induction assay

Overnight cultures for each strain were used to carry out a 1% inoculation into 50ml TSB volumes. Cultures were split into 25ml aliquots prior to been harvested via centrifugation at 13 000 x g for 5 minutes. One aliquot served as the control to which no AIP supernatant was added, whilst the other had 200µl of AIP supernatant incorporated into the suspension of cells in Triton X-100 glycine buffer. Rates of autolysis were monitored at 30 minute intervals. The data was analyzed using SIGMA PLOT 2000. The regression curve for each plot was determined and a respective bar chart established in relation to the percentage AIP additive incorporated into the assay.

2.22. Molecular manipulations

DNA was isolated using the Nucleospin Tissue Kit (Macherey-Nagel, Düren Germany). Overnight cultures of each strain were incubated at 37°C in 5% CO₂ atmosphere to an OD₆₀₀ of approximately 0.8. A 5ml aliquot of bacterial culture was centrifuged at 8000 x g for 5 minutes and the supernatant discarded. Pre-lysis was achieved by resuspension of the pellet in 80% lysis buffer (T1) and 20% proteinase K. Samples were vortexed vigorously and then incubated at 56°C for one hour until complete lysis were obtained. After the addition of a double volume of lysis buffer B3, samples were incubated for a further 10 minutes at 70°C. The DNA binding conditions were adjusted by the addition of double volume 100% ethanol. The samples were then applied to a column and centrifuged for 1 minute at 11 000 x g and the flow-through discarded. Two wash steps were included with different buffers to clean the silica membrane. The membrane was dried and residual ethanol removed. Highly pure DNA was eluted with pre-warmed elution buffer (BE). Samples were incubated at room temperature and centrifuged for 1 minute at 11 000 x g. Quantification of DNA was achieved via spectrophotometric analysis (NanoDrop Spectrophotometer) as well as agarose gel electrophoresis. Isolated DNA was stored at -20°C or used directly for amplification.

2.23. Construction and design of primers for Polymerase Chain Reaction (PCR)

To identify the accessory gene regulator (*agr*) alleles present in the Streptococcal isolates, universal primers used in *Staphylococcus aureus* *agr* allele characterization was also employed in this study [Jarraud *et al.*, 2002]. The universal primers Pan-1 (forward) and Pan-2 (reverse) (Table 2.2.) were designed from *agr* group I to IV to amplify a 1234-base pair (bp) *agr* fragment encompassing the 3' end of *agrB*, all of *agrD*, and the 5' of *agrC* [Jarraud *et al.*, 2002]. The 5' ends were synthesized with phosphorylation. To identify *agr* specificity groups, PCR amplification of the hyper variable domain of the *agr* locus using oligonucleotide primers specific for each of the four major specificity groups was used [Shopsin *et al.*, 2003]. Four reverse primers, each specific for amplification of a single *agr* group based on *agrD* or *agrC* gene nucleotide polymorphism were designed [Shopsin *et al.*, 2003]. All primers were synthesized at the Department of Biochemistry, University of Cape Town, South Africa (Table 2.2.). The *agr* specificity groups were identified by the size of the amplicons expected (Table 2.3.). PCR was performed by adding 1µl of a 1:200 dilution of chromosomal template DNA to 50µl of a PCR mixture that included 2.5U perpetual OptiTaQ DNA polymerase (Eur_x), 2mM magnesium chloride (MgCl₂), 350µM (total) deoxynucleoside triphosphates, and 25mM potassium chloride [PCR Core Kit – Roche] in sterilized 0.2ml PCR tubes. A positive control of isolated *S. aureus* DNA was included. Reactions were performed in a GeneAmp 9700 thermocycler (Perkin-Elmer Applied Biosystems Division). The PCR profile was as described in Table 2.4. PCR samples were stored at -20°C prior to agarose gel electrophoresis. Molecular weight marker III (Roche) was included to determine the size of the PCR amplicons. Samples were diluted at a 1:5 ratio of loading buffer (0.25% bromophenol blue, 0.25% xylene cyanol in 30% glycerol) to sample. Agarose gels were stained with ethidium bromide (0.5µg/ml) and visualized under ultra violet light (VERSADOC 3000, gel documentation system (BioRad Inc.).

Table 2.2. Primer designation and sequence [Jarraud *et al.*, 2002 and Shopsin *et al.*, 2003].

Primer	Sequence
Pan-1	5'- ATG CAC ATG GTG CAC ATG CA-3'
Pan-2	5'- CAT AAT CAT GAC GGA ACT TGC TGC GCA-3'
Agr R1	<i>agr</i> group I 5'- GTC ACA AGT ACT ATA AGC TGC GAT-3' (in the <i>agrD</i> gene)
Agr R2	<i>agr</i> group II 5'- GTA TTA CTA ATT GAA AAG TGC CAT AGC-3' (in the <i>agrC</i> gene)
Agr R3	<i>agr</i> group III 5'- CTG TTG AAA AAG TCA ACT AAA AGC TC-3' (in the <i>agrD</i> gene)
Agr R4	<i>agr</i> group IV 5'- CGA TAA TGC CGT AAT ACC CG -3' (in the <i>agrC</i> gene)

Table 2.3. Expected PCR product size [Shopsin, B. *et al.*, 2003].

Reverse Primer	Expected PCR Product (base pairs)
Agr R1	440
Agr R2	572
Agr R3	406
Agr R4	588

Table 2.4. PCR Profile [Shopsin *et al.*, 2003].

Number of Cycles	Conditions	Temperature (°C)	Time (Minutes)
1	Denaturation	95	5
35 {	Denaturation	94	1
	Annealing	55	1
	Extension	72	1
1	Extension	72	10

CHAPTER THREE

RESULTS AND DISCUSSION

CHAPTER THREE

3.1. Minimal inhibitory concentrations (MIC)

To accurately establish the MIC's for the bacterial strains used, two different techniques were employed. Initially, the micro titre technique was used. When exposed to ampicillin, *S. milleri* P35 had a MIC value of 5µg/ml; *S. milleri* 77 a MIC value of 15µg/ml and *S. milleri* B200 a MIC of 10µg/ml (Figure 3.1.). Exposure to the antibiotic penicillin revealed that the MIC for *S. milleri* P35 and B200 was 20µg/ml respectively. *S. milleri* 77 had a MIC of 70µg/ml. These MIC values were in accordance as ampicillin is a derivative of penicillin. The bacterial strains were therefore susceptible at higher antibiotic levels of ampicillin as compared to its penicillin derivative. The values obtained using the micro-titre dilution methods were higher to those obtained in the disk diffusion assay method. This is expected since the media type used in each technique was different. More so, for the fact that MIC values should be higher when in a liquid medium such as the tryptone soy broth as compared to the tryptone soy agar plates (Figure 3.1. and Figure 3.4.).

Comparing the above results to those obtained in the disk diffusion assay, it could be established that *S. milleri* P35 was susceptible at a concentration of 5µg/ml for ampicillin, whilst doubling to 10µg/ml when in the presence of penicillin. *Streptococcus milleri* B200 exhibited the same profile, where again its MIC values were similar to *S. milleri* P35. *S. milleri* 77 was susceptible at a concentration of 10µg/ml for ampicillin [Figure 3.3. (A)]. In the presence of penicillin *S. milleri* 77 showed high levels of resistance, growing in antibiotic concentrations of 30µg/ml and greater [Figure 3.3. (B)]. Figure 3.4. clearly suggests these trends.

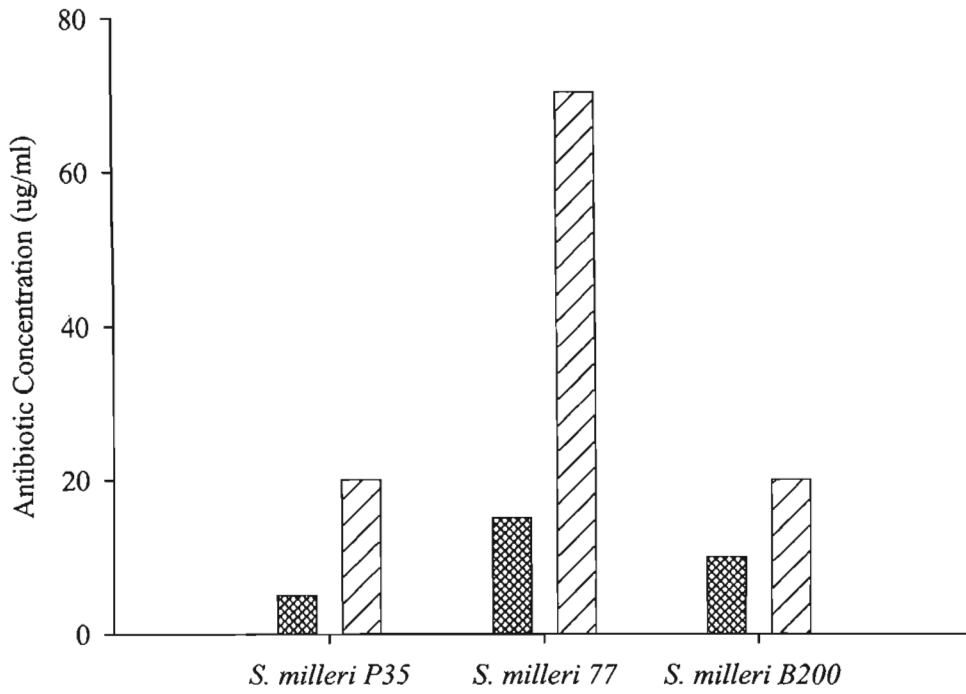


Figure 3.1. Minimal inhibitory concentration determined by the micro titre dilution assay, of Ampicillin and Penicillin against the Streptococcal strains *S. milleri* P35, *S. milleri* 77 and *S. milleri* B200. Antibiotics are represented as follows: (▨) – Ampicillin and (///) – Penicillin.

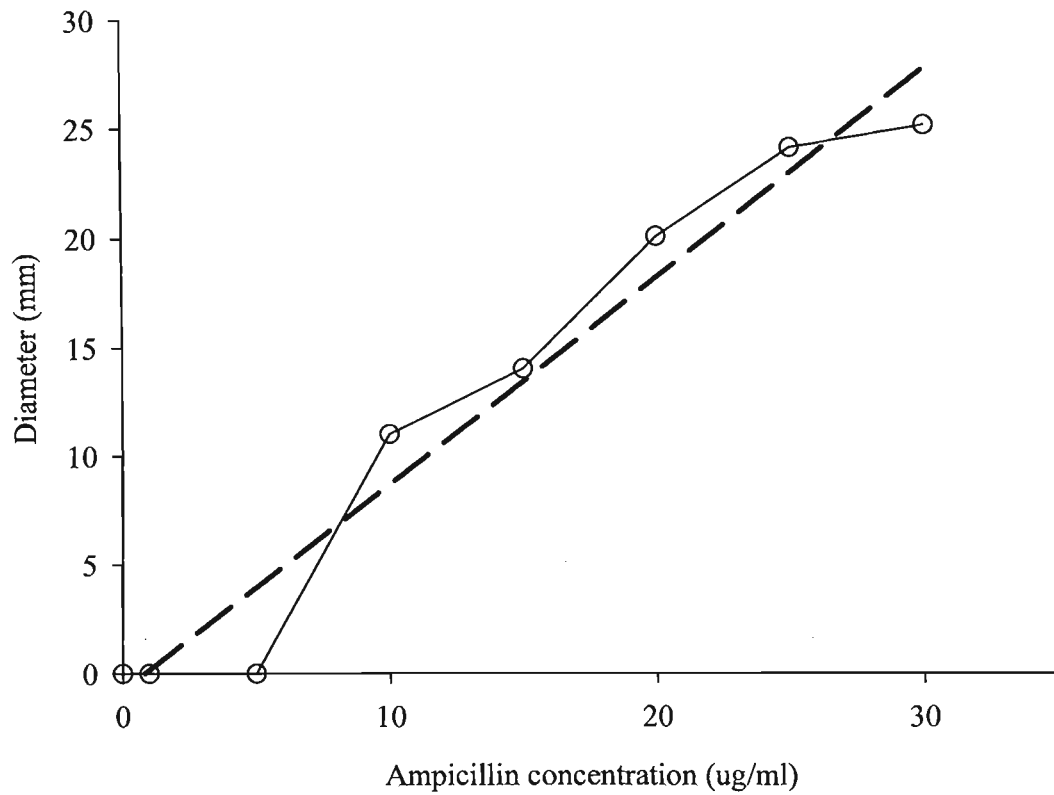


Figure 3.2. Plot of the radius diameter (mm) of the zone of inhibition versus the concentration of Ampicillin ($\mu\text{g/ml}$) tested for *S. milleri* 77. MIC was determined on tryptone soy agar plates, where 200 μl of starter culture was inoculated into sloppy agar and overlaid. Plots are represented as: Raw data (\circ) and Fit curve (—).

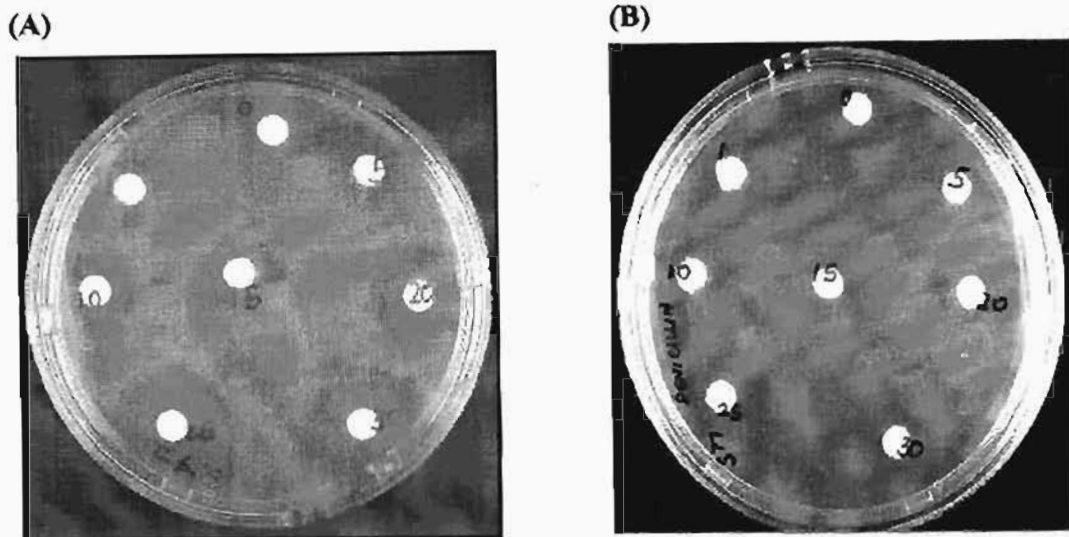


Figure 3.3 Disk diffusion assay for *S. milleri* 77 tested against specific antibiotic concentrations ranging from 0 to 30µg/ml. (A) Disk diffusion assay tested against the antibiotic Ampicillin, establishing the MIC value at 10µg/ml. (B) Disk diffusion assay tested against the antibiotic Penicillin, establishing the MIC value greater than 30µg/ml.

Using the disk diffusion assay technique, the radius of each zone of inhibition was measured and plotted against the concentration of the antibiotic, to establish the relationship between minimum inhibitory concentration and increasing values of antibiotic stress (Figure 3.3.). Based on the data obtained, radii diameters could be directly correlated to the MIC values. In each instance the zone diameter is taken into consideration when classifying each bacterial strain according to its susceptibility or resistance. A directly proportional relationship was observed, where increasing levels of antibiotic produced an increase in the diameter of the zone of inhibition (Figure 3.2.). Depending on the antibiotic used, there were differential changes in the diameter size.

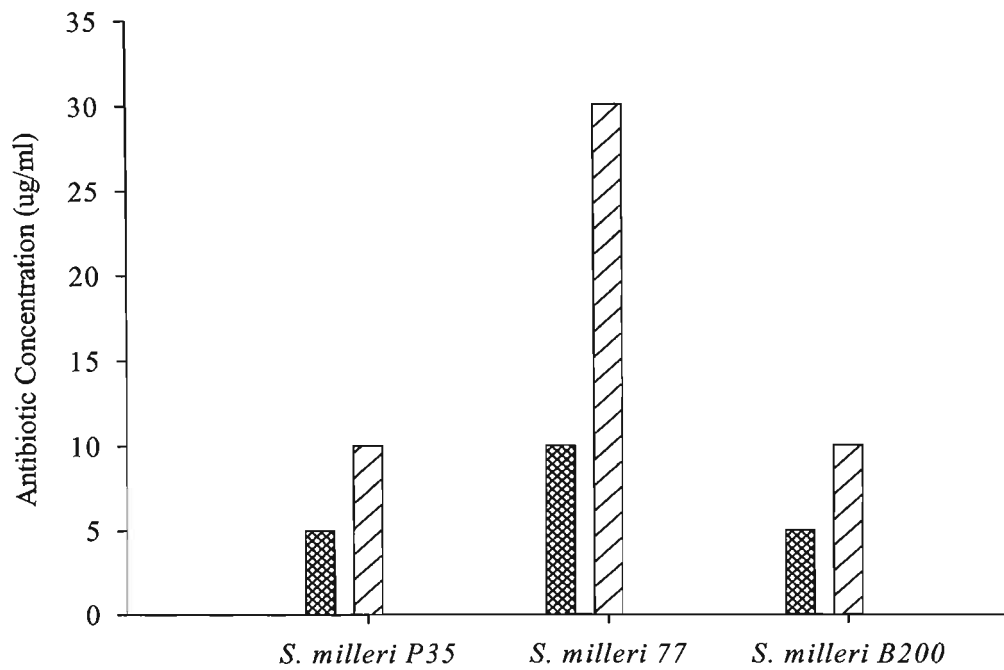


Figure 3.4. Minimal inhibitory concentration determined by the disk diffusion assay of Ampicillin and Penicillin against the Streptococcal strains, *S. milleri* P35, *S. milleri* 77 and *S. milleri* B200. Antibiotics are represented as follows: (▨) – Ampicillin and (///) – Penicillin.

3.2. Relative fitness assay

Relative fitness establishes a complete growth cycle of the bacterial organism, over the period of time taken for the bacterial cells to go from the lag phase to the death phase. Expressed as changes in the optical density, the specific phases within the sigmoid growth cycle can be established with a corresponding time frame taken to reach that phase (Figure 3.5.).

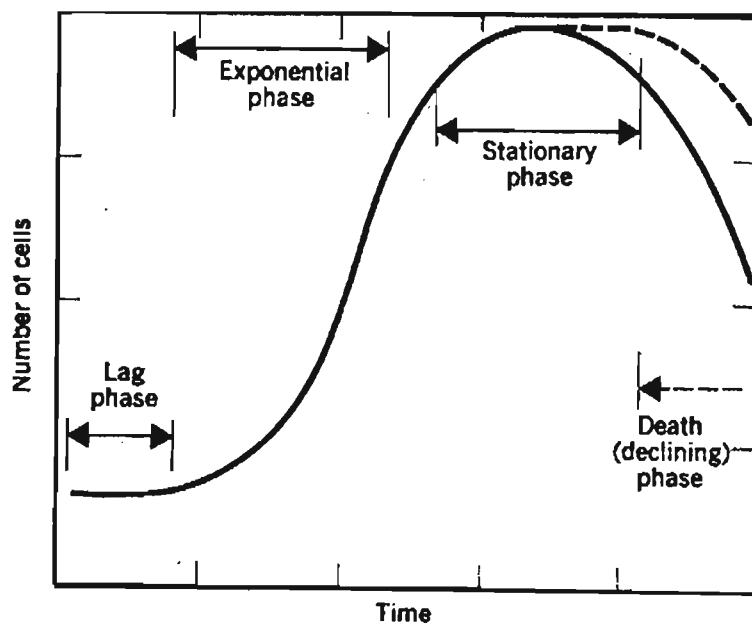


Figure 3.5. Diagrammatic representation of a typical growth cycle during one generation of a bacterial population. The different phases are shown progressively as a sigmoidal curve.

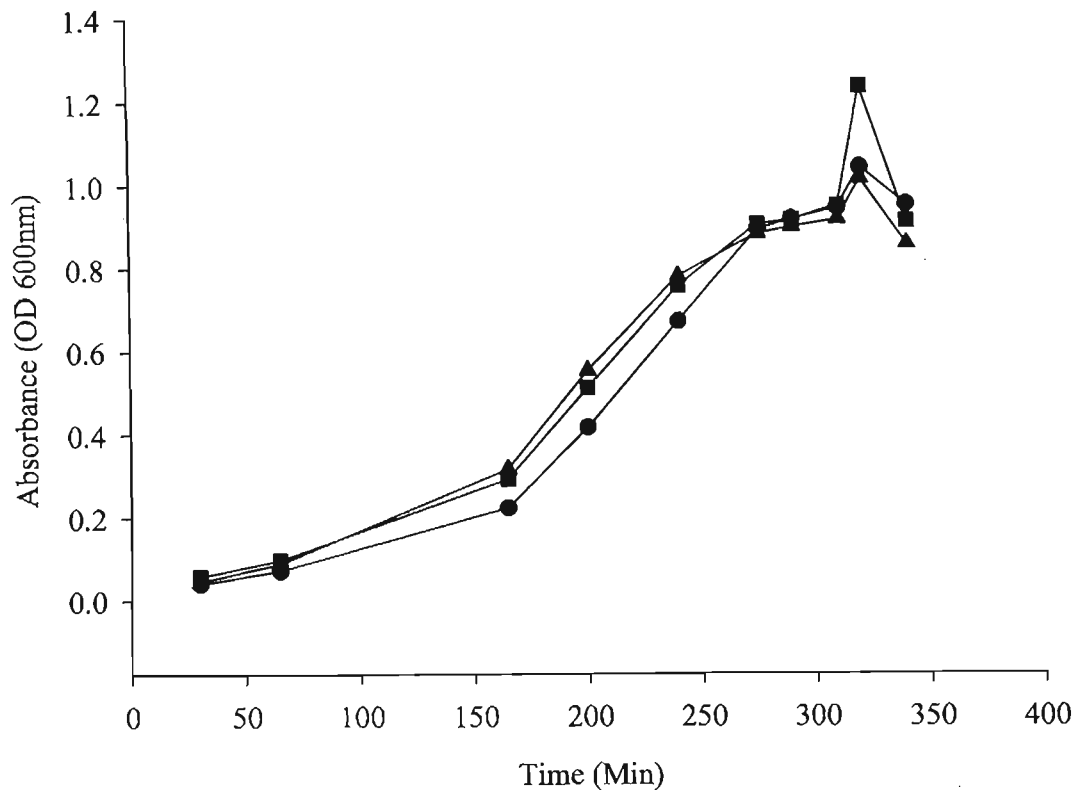


Figure 3.6. Relative fitness profiles (raw data) for each Streptococcal strain, in the absence of antibiotic stress. Bacterial growth cycle was monitored as changes in the optical density at 600_{nm} over Time. The plots are represented as follows: *S. milleri* P35 – (●); *S. milleri* 77 – (■); and *S. milleri* B200 – (▲).

Monitoring the relative fitness in the absence of antibiotic stress (Figure 3.6. and Figure 3.7.) it was clear that strains *S. milleri* P35 and B200 exhibited a very similar profile. *S. milleri* B200 had a slightly higher relative fitness as compared to *S. milleri* P35. Progressively, *S. milleri* 77 had an overall higher relative fitness during its exponential growth phase, but in the death phase of growth its relative fitness decreased, lower than *S. milleri* P35 and B200 respectively.

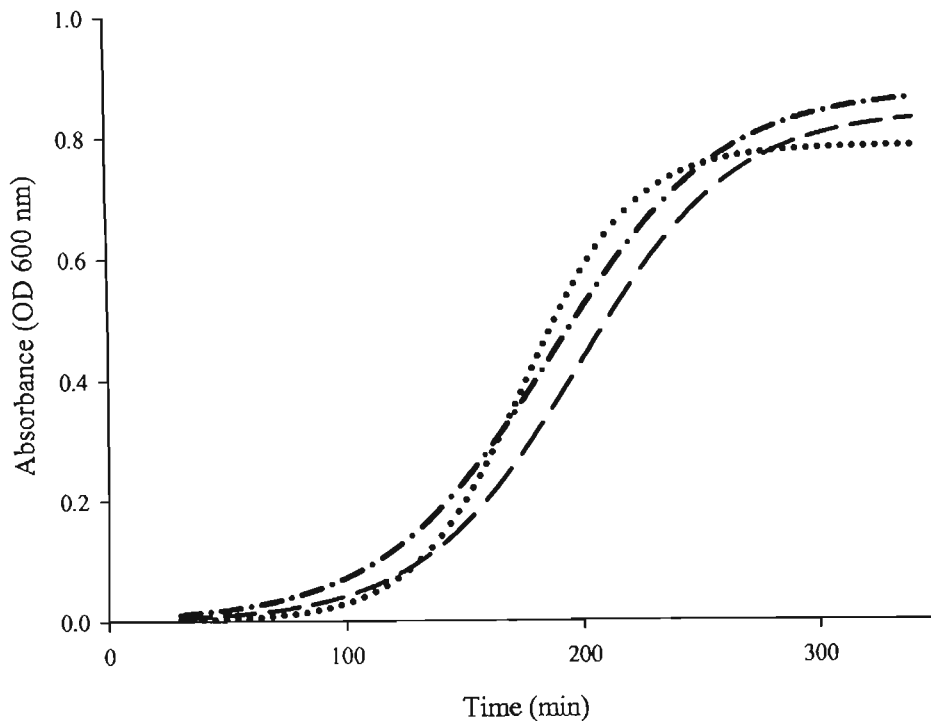


Figure 3.7. Relative fitness profiles (fit curves) for each Streptococcal strain, in the absence of antibiotic stress. Bacterial growth cycle was monitored as changes in the optical density at 600_{nm} over Time. The plots are represented as follows: *S. milleri* P35 – (— —); *S. milleri* 77 – (...); and *S. milleri* B200 – (— · —).

Bacteria can become resistant via *de novo* mutation or by the acquisition of foreign genetic material. Typically, resistant bacteria suffer a loss of fitness seen as reduced growth rate and/or a loss of virulence. Thus, most antibiotic-resistant bacteria risk being out-competed by antibiotic-sensitive bacteria. However, if the resistant bacteria can acquire mutations restoring fitness, without losing antibiotic resistance, then they can be stabilised in the population. Profiling these strains showed that in the presence of sub-minimal inhibitory concentrations of Ampicillin, the relative fitness was compromised (Figure 3.8. and Figure 3.9.). Ampicillin is a

cell wall acting antibiotic, targeting the peptidoglycan layer within the murein sacculus, thereby stressing the bacterial cell to such an extent that lysis occurs. Strains *S. milleri* P35 and *S. milleri* B200 were unable to, in the presence of the antibiotic, reach an optical density of 1. This could very well be due to the presence of the antibiotic, stressing the bacterial population, thereby causing a staggered growth pattern. Progressively *S. milleri* 77, had in comparison to the other two strains, a higher relative fitness. *S. milleri* 77 was able to successfully grow and reach an optical density of 1; however as compared to its relative fitness pattern in the absence of antibiotic, its fitness was reduced because the bacterial strain would be unable to reach an optical density of 1 in the same time frame. Profiles for *S. milleri* P35 and *S. milleri* B200 show a similar pattern. The relative fitness for *S. milleri* B200, increased in the late exponential phase, but also could not reach an optical density of 1.

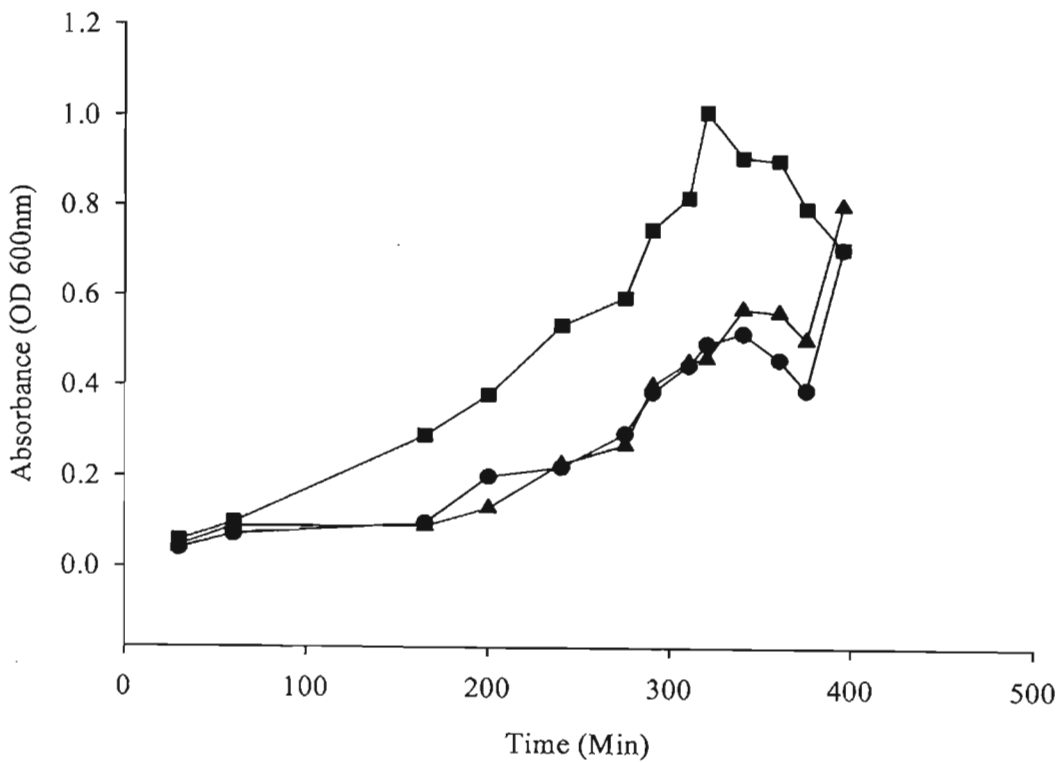


Figure 3.8. Relative fitness profiles (raw data) for each Streptococcal strain, presence of Ampicillin at sub minimal inhibitory concentrations. Bacterial growth cycle was monitored as changes in the optical density at 600_{nm} over Time. The plots are represented as follows: *S. milleri* P35 – (●); *S. milleri* 77 – (■); and *S. milleri* B200 – (▲).

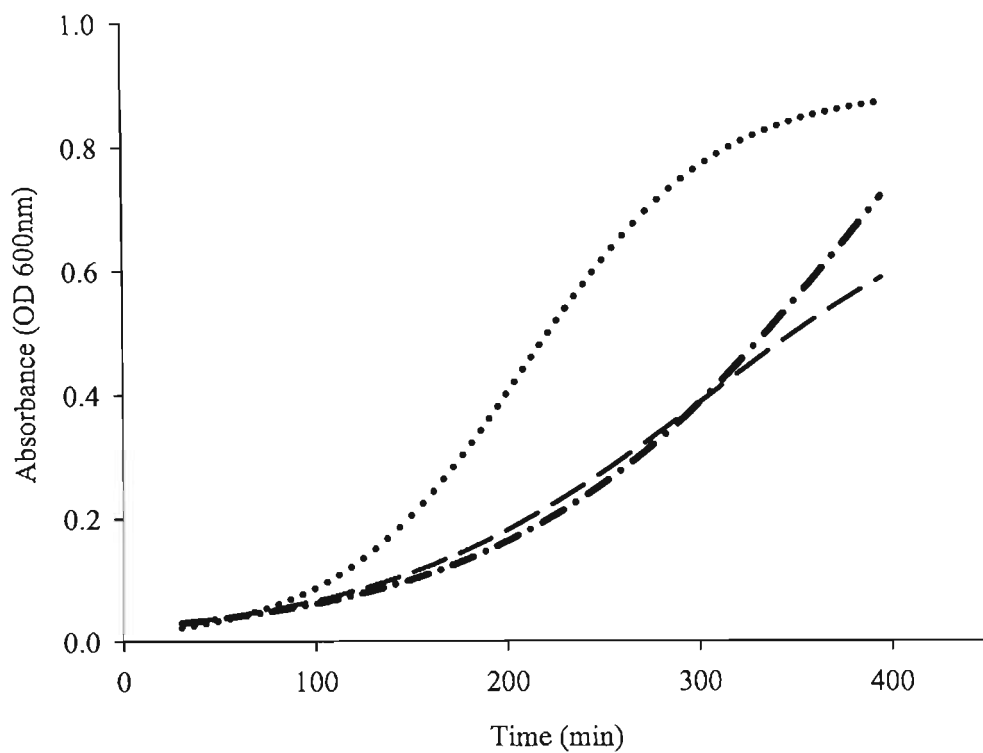


Figure 3.9. Relative fitness profiles (fit curves) for each Streptococcal strain, presence of Ampicillin at sub minimal inhibitory concentrations. Bacterial growth cycle was monitored as changes in the optical density at 600_{nm} over Time. The plots are represented as follows: *S. milleri* P35 – (—); *S. milleri* 77 – (···); and *S. milleri* B200 – (-·-).

3.3. Autolytic protein and Zymographic profiles

A protein profile for each strain was established. Autolytic extracts were extracted using 4% SDS at different stages of the growth cycle. Total protein concentrations were calculated using the bicinchoninic acid (BCA) method [Stoscheck, 1990]. This assay is a detergent-compatible bicinchoninic acid formulation for the colorimetric detection and quantification of total protein. This technique utilizes BCA as the detection reagent for copper⁺¹ which, is formed when copper⁺² is reduced by protein in an alkaline environment [Stoscheck, 1990]. A purple-coloured product is formed by the chelation of two molecules of BCA with one cuprous ion. This water-soluble complex exhibits a strong absorbance at 562nm that is linear with the increasing values of protein concentrations [Stoscheck, 1990]. A standard curve is plotted and relative protein concentrations can be calculated (Figure 3.10.).

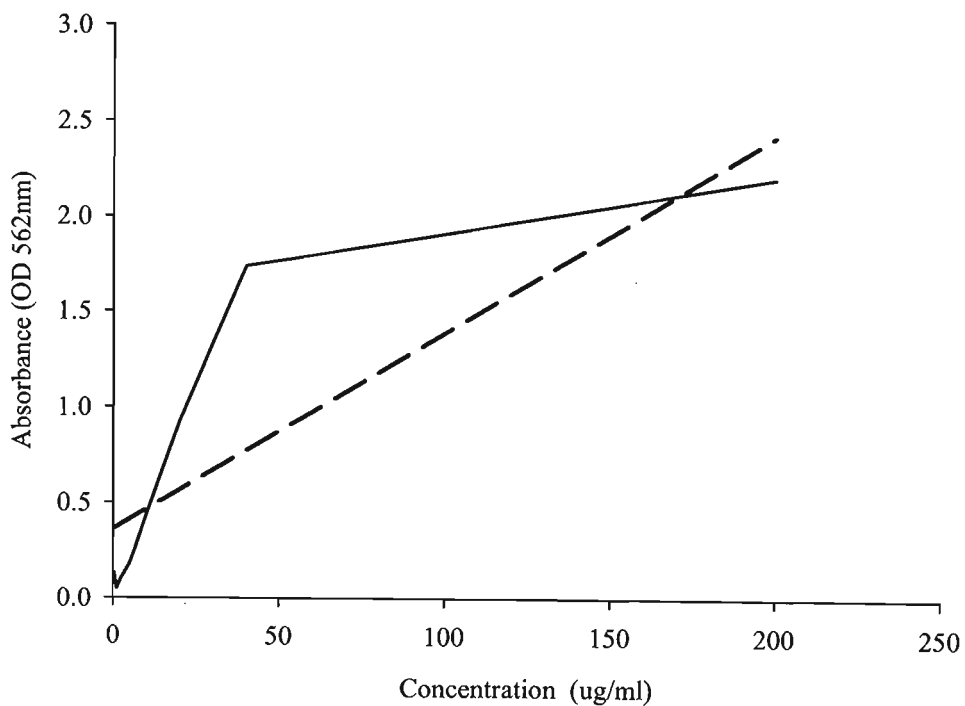


Figure 3.10. Standard curve. Different concentrations of Bovine serum albumin (0.5 - 200 μ g/ml) were used as the standard. The plots are represented as follows: Raw data - Black and Fit Curve - Dashed solid line.

S. milleri P35 exhibited increasing activity levels for the autolytic extracts (Figure 3.11.). There was a direct increase in the activity of autolysins along the growth cycle, the highest activity being for the mid stationary and death phases. This can be associated to previously characterized autolysin profiles, which show high expression and activity levels of autolysins in the late stationary and/ or death phases [Beukes and Hastings, 2001].

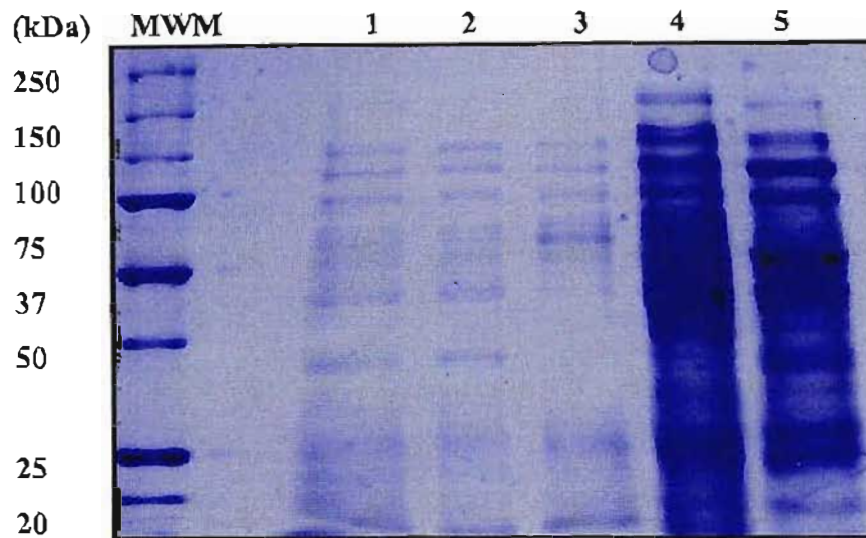


Figure 3.11. Polyacrylamide (10%) gel of proteins extracted with 4% SDS from whole cells of *Streptococcus milleri* P35. Lanes 1-5: Represents extractions from stages within the growth cycle. Lanes: 1, mid lag phase; 2, early exponential phase; 3, mid exponential phase; 4, mid stationary phase; and 5, death phase. MWM: BioRad Precision Plus unstained protein standards.

Zymogram profiles were established by the incorporation of strain specific crude cell wall material, which forms the substrate for degradation by the autolysin. These zymographic profiles allowed for the identification of the possible autolytic enzymes present.

Different samples, each from the specific stages within the growth cycle, were analyzed using renaturation SDS-PAGE through the incorporation of crude *S. milleri* cell wall material into the gel matrix [Strating and Clark, 2001]. *S. milleri* P35 initially exhibited characteristics of a putative autolytic-free strain. This was as a result of the lack of lytic bands in the zymogram

profile after an overnight incubation period which allowed for renaturation. The zymogram was repeated. However, this time the incubation period in the renaturation buffer was extended to 96 hours. The longer incubation period allowed for better renaturation and lytic bands could then be visualized (Figure 3.12.). This showed that *S. milleri* P35 had a lowered autolysin activity, and was not an autolytic-free strain as deduced from the electron morphology result (Figure 3.25). This correlates to the autolytic assays previously established, which showed *S. milleri* P35 to behave in a similar way. Four clear lytic bands were observed. These ranged from 150kDa to 25kDa. There was an increase in the expressional levels of these autolysins from the mid exponential phase to the death phase. In the mid stationary phase the 25kDa autolysin is dominant. The 100kDa sized autolysin was present during the first four phases in the growth cycle, but it was most prominent in the mid exponential phase. Profiles for the lag and early exponential phases are identical.

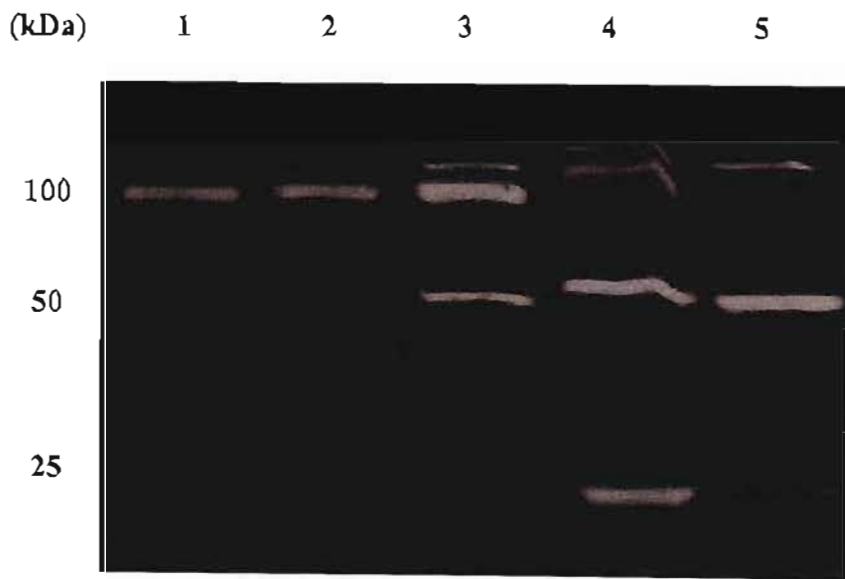


Figure 3.12. Zymogram analysis of proteins extracted with 4% SDS from different stages within the growth cycle of *Streptococcus milleri* P35. The gel contains 0.1% *S. milleri* P35 crude cell wall stained with 0.1% methylene blue in 0.01% KOH. Lanes: 1, mid lag phase; 2, early exponential phase; 3, mid exponential phase; 4, mid stationary phase; and 5, death phase.

The protein profile and zymogram established for *S. milleri* 77 had a very similar pattern. In the SDS-PAGE analysis (Figure 3.13.), there were specific identified autolysins which were present throughout the growth cycle. At a molecular weight of approximately 60kDa, a specific autolysin could be identified (Figure 3.13.). In relation to the corresponding zymogram, this same autolysin was shown to have a similar profile, constitutively expressed through all the growth phases. Other extracts showed that these autolysins were produced along the growth cycle. However, their increased autolytic activity was seen during specific stages within the growth cycle (Figure 3.13.).

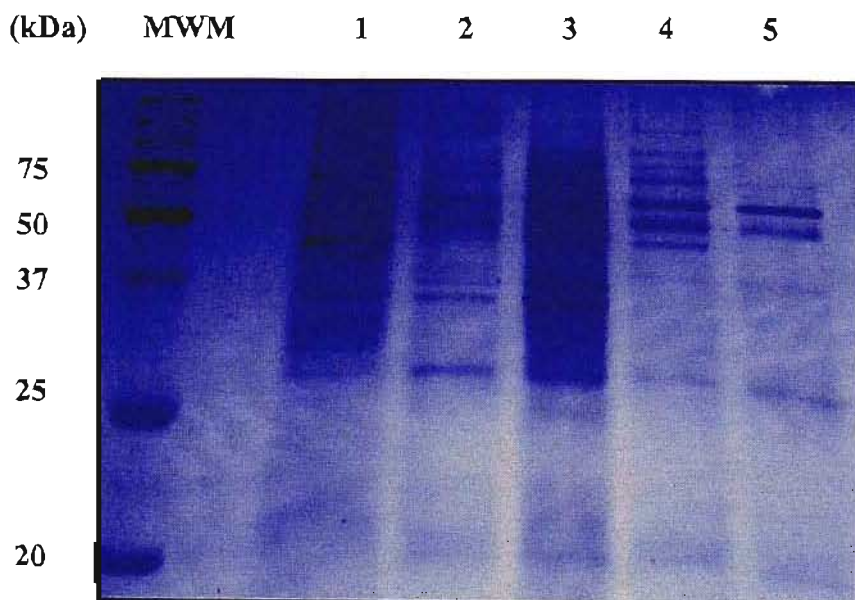


Figure 3.13. Polyacrylamide (10%) gel of proteins extracted with 4% SDS from whole cells of *Streptococcus milleri* 77. Lanes 1-5: Represents extractions from stages within the growth cycle. Lanes: 1, mid lag phase; 2, early exponential phase; 3, mid exponential phase; 4, mid stationary phase; and 5, death phase. MWM: BioRad Precision Plus unstained protein standards.

Following the renaturation of SDS extracted proteins and incubation in gels containing *S. milleri* 77 crude cell wall material as a substrate, several bands of autolytic activity could be identified (Figure 3.14.). The profiles were obtained from different stages of the growth cycle [Strating and Clark, 2001]. In the lag phase only two bands could be observed, one dominant band with a molecular weight of 60kDa and a minor band of 55kDa. The profiles for the early and late exponential phases were very similar and showed the presence of five autolytic bands (Figure 3.14.). The lytic band at 15kDa however, was much more dominant in the mid exponential phase than in the early exponential growth phase. The autolytic profile for the stationary and death phases were exactly the same (Figure 3.14.). Both profiles showed three dominant lytic bands at 60kDa, 50kDa and 25kDa. The number of bands found in each profile may not reflect the enzymes that may exist. Proteolytic processing of autolytic enzymes has been shown to occur as a means of regulation by activation.

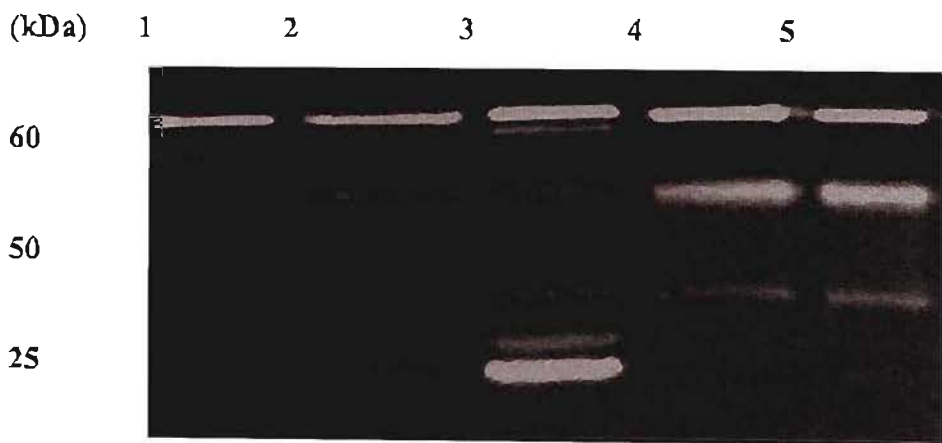


Figure 3.14. Zymogram analysis of proteins extracted with 4% SDS from different stages of the growth cycle of *Streptococcus milleri* 77. The gel contains 0.1% *S. milleri* 77 crude cell wall stained with 0.1% methylene blue in 0.01% KOH. Lanes: 1, mid lag phase; 2, early exponential phase; 3, mid exponential phase; 4, mid stationary phase; and 5, death phase.

The protein profile for *S. milleri* B200 showed a substantial increase in autolytic activity, as seen by the increase in the banding profile obtained (Figure 3.15.). The highest autolytic activity was monitored in the mid stationary phase of the growth phase. The autolytic extract isolated from the mid stationary and death phase also showed the highest rate of autolysis from the autolytic assays.

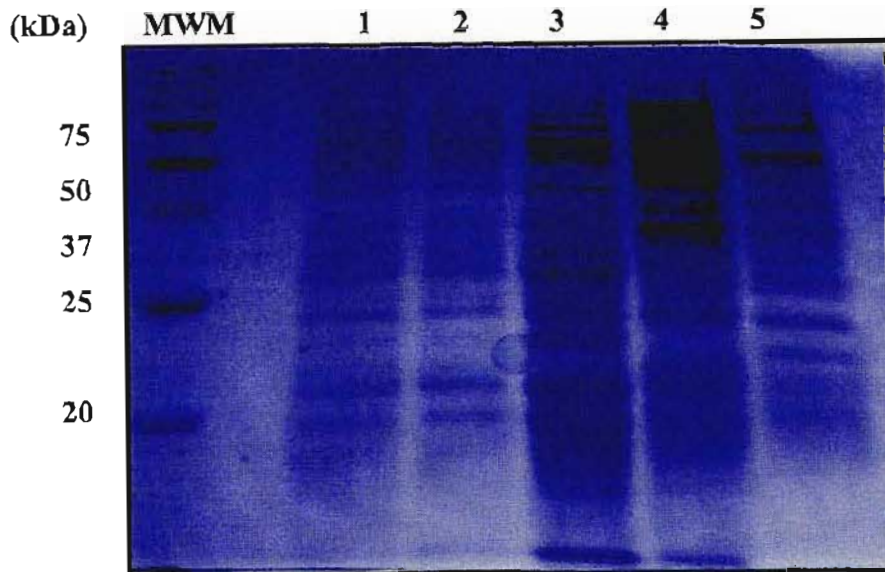


Figure 3.15. Polyacrylamide (10%) gel of proteins extracted with 4% SDS from whole cells of *Streptococcus milleri* B200. Lanes 1-5: Represents extractions from stages within the growth cycle. Lanes: 1, mid lag phase; 2, early exponential phase; 3, mid exponential phase; 4, mid stationary phase; and 5, death phase. MWM: BioRad Precision Plus unstained protein standards.

S. milleri B200 showed a zymographic profile which had only one distinct lytic band present at a molecular weight of approximately 50kDa (Figure 3.16.). This lytic band was dominant throughout the growth cycle of the bacterium. Lytic activity was achieved after an initial overnight incubation in the renaturation buffer, with Triton X-100 incorporated to increase the rate of autolytic activity. There seems to be an increase in activity along the growth cycle, reaching its highest activity levels from the mid exponential phase all the way to the death phase (Figure 3.16.).



Figure 3.16. Zymogram analysis of proteins extracted with 4% SDS from different stages of the growth cycle of *Streptococcus milleri* B200. The gel contains 0.1% *S. milleri* B200 crude cell wall stained with 0.1% methylene blue in 0.01% KOH. Lanes: 1, mid lag phase; 2, early exponential phase; 3, mid exponential phase; 4, mid stationary phase; and 5, death phase.

3. 4. Two Dimensional sodium sulfate - Polyacrylamide Gel Electrophoresis (2D SDS-PAGE)

3.4.1. 2D SDS-PAGE

Two dimensional SDS-PAGE allowed for the analysis of total protein in the presence and absence of an antibiotic stress. Initially, specific bands as seen in Figure 3.17., when in the presence of the antibiotic, had a fainter profile compared to the banding profile of the antibiotic free cultured cells. Superficially it can be established that the presence of the ampicillin at the sub-minimal MIC value contributes to certain protein expression been decreased or to a certain extent even absent. This was further examined using the two dimensional SDS-PAGE technique.

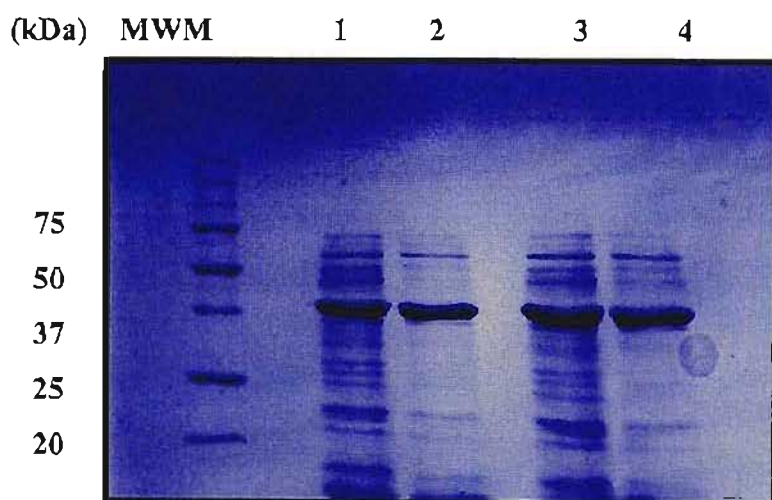


Figure 3.17. Polyacrylamide (10%) gel of total protein extracted from whole cells of *Streptococcus milleri* 77. Lanes 1-4: Represents extractions from mid exponential cell cultures, grown in the presence or absence of antibiotic stress. Ampicillin at MIC value of $10\mu\text{g/ml}$ was incorporated into the growing culture. Lanes: 1, $0.5\mu\text{g}$ protein in the absence of antibiotic; 2, $0.5\mu\text{g}$ protein in the presence of $10\mu\text{g/ml}$ ampicillin; 3, $0.5\mu\text{g}$ protein in the absence of antibiotic; and 4, $1\mu\text{g}$ protein in the presence of $10\mu\text{g/ml}$ ampicillin. MWM: BioRad Precision Plus unstained protein standards.

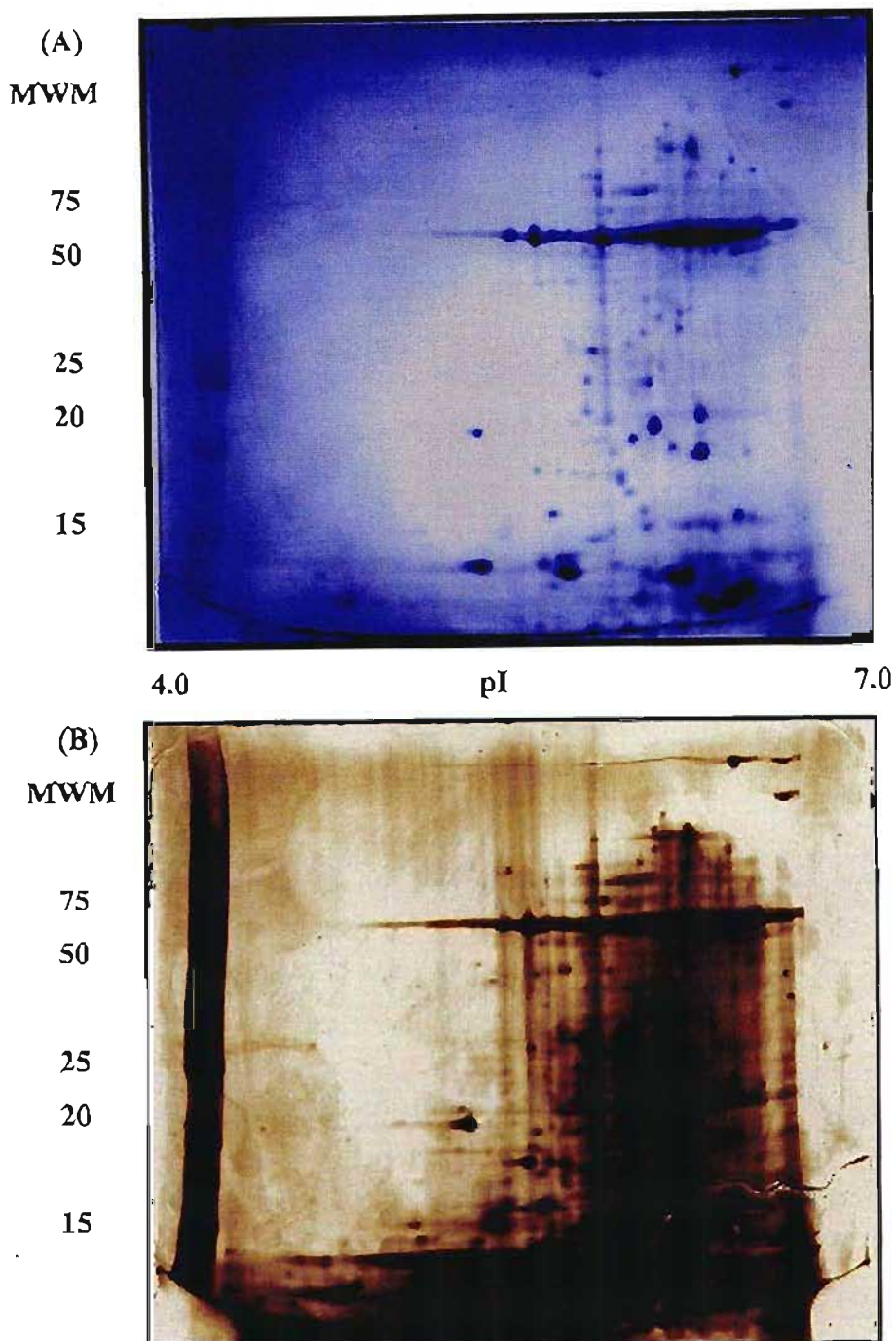


Figure 3.18. 2-D PAGE analysis of cellular proteins of *S. milleri* 77 cultured in the absence of antibiotic. Extracted proteins were separated by isoelectric focusing in the pI range of 4 to 7 in the first dimension and a gradient (10%) SDS-PAGE in the second dimension. Resolved proteins were visualized following (A) Coomassie Blue staining and (B) Silver staining. MWM: BioRad Precision Plus unstained protein standards indicated on the extreme left.

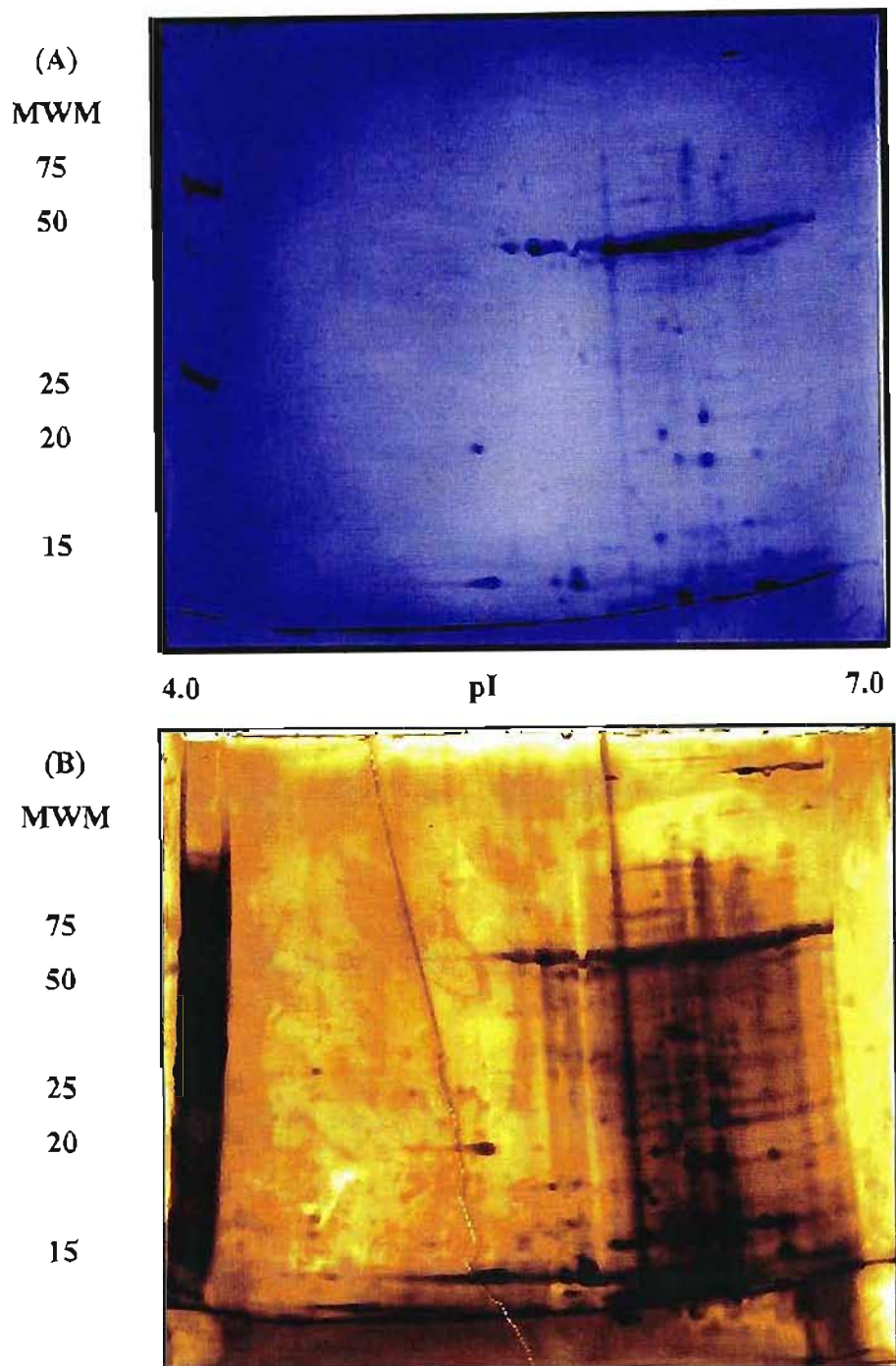


Figure 3.19. 2-D PAGE analysis of cellular proteins of *S. milleri* 77 cultured in the presence of antibiotic (Ampicillin - 10 μ g/ml). Extracted proteins were separated by isoelectric focusing in the pI range of 4 to 7 in the first dimension and a gradient (10%) SDS-PAGE in the second dimension. Resolved proteins were visualized following (A) Coomassie Blue staining and (B) Silver staining. MWM: BioRad Precision Plus unstained protein standards indicated on the extreme left.

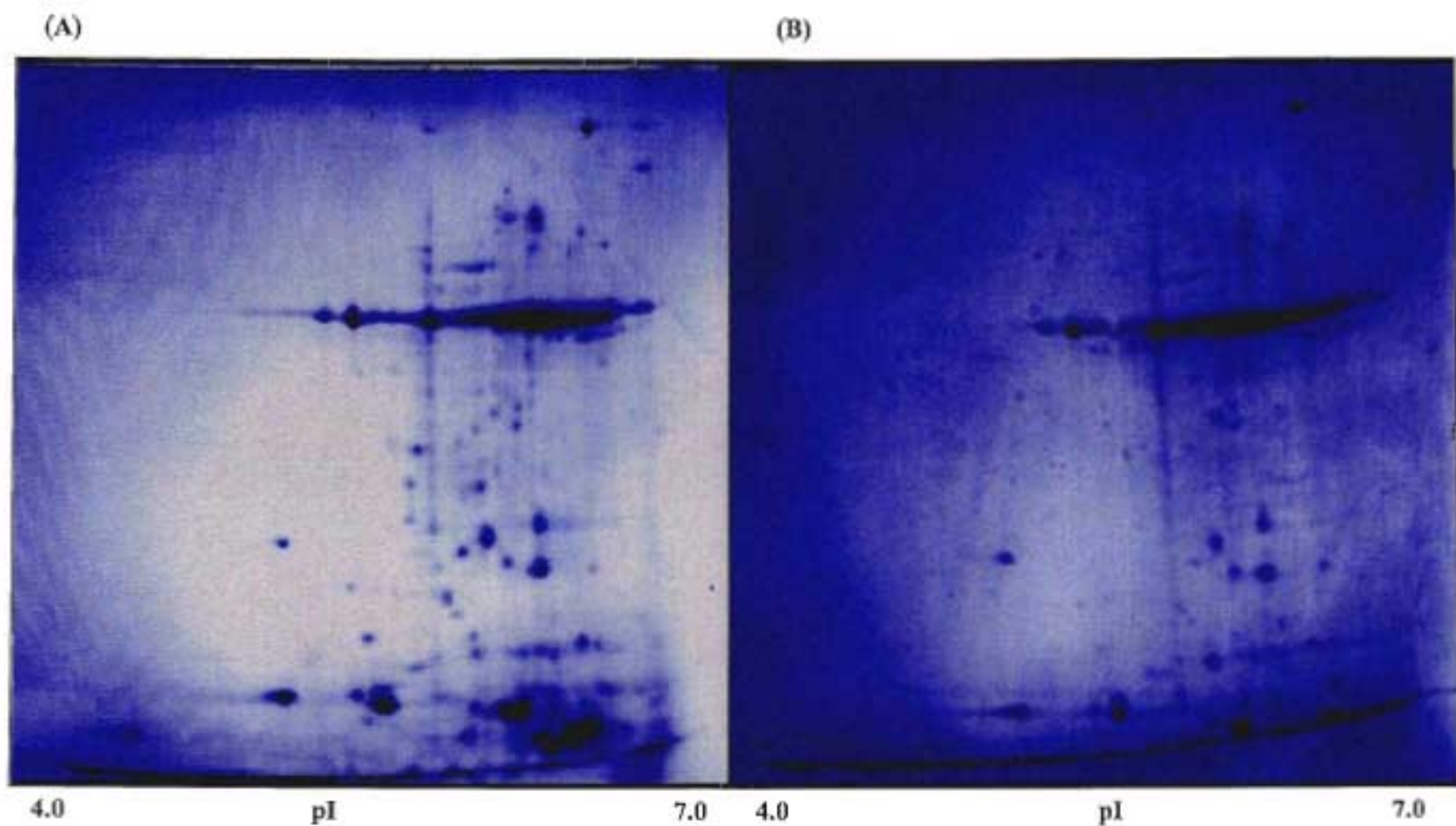


Figure 3.20. Comparative analysis of the 2-D PAGE gels of the cellular proteins of *S. milleri* 77. **(A)** Resolved proteins with cells cultured in the absence of antibiotic stress. **(B)** Resolved proteins with cells cultured in the presence of antibiotic (Ampicillin - 10µg/ml).

A major number of spots were analyzed using PD Quest (Figure 3.20.), and many showed a difference in either their presence or absence, when cultured in the presence of the antibiotic. The intensity of the spots also diminished in the antibiotic cultured protein extracts, as seen in the initial one-dimensional SDS-PAGE analysis (Figure 3.17.).

The sensitivity of the staining processes allowed a higher number of spots to be identified when the gels were silver stained (Figure 3.18. [B] and Figure 3.19. [B]). However, the silver staining method produces a very high background, hence for image analysis, Coomassie stained gels were used in the PD Quest software. In establishing the respective increase or decrease in the fold intensity, different computational parameters were changed in accordance with the analysis software package.

In comparison to the zymographic analysis (Figure 3.14.), which showed autolytic bands at a molecular mass of 60kDa, 50kDa and 25kDa respectively, spots within this molecular range was characterized (Figure 3.21.). At 70kDa a conglomerate of spots within a pI range of 6.0 to 6.5 clusters for both profiles (Figure 3.21.). Autolytic spots can therefore be associated with this clustered group. The broad molecular mass range in which autolysins can be characterized shows that the two-dimensional profiles incorporates all of the putative autolysins (Figure 3.21.). Three specific spots were identified with a molecular weight of approximately 25kDa, were observed as unclassified in the comparative analysis (Figure 3.22.). These spots can now be further implicated as markers in the identification of putative proteins which are targeted when in the presence of antibiotic stress. These proteins (seen as red circles in [Figure 3.22.]) when excised using the spot cutter tool, available in the PD QUEST analysis package will aid in the characterization process. A possible reason for these spots been unclassified can be attributed to the presence of the antibiotic when culturing the cells, implicating ampicillin in the down regulation of those putative autolysins.

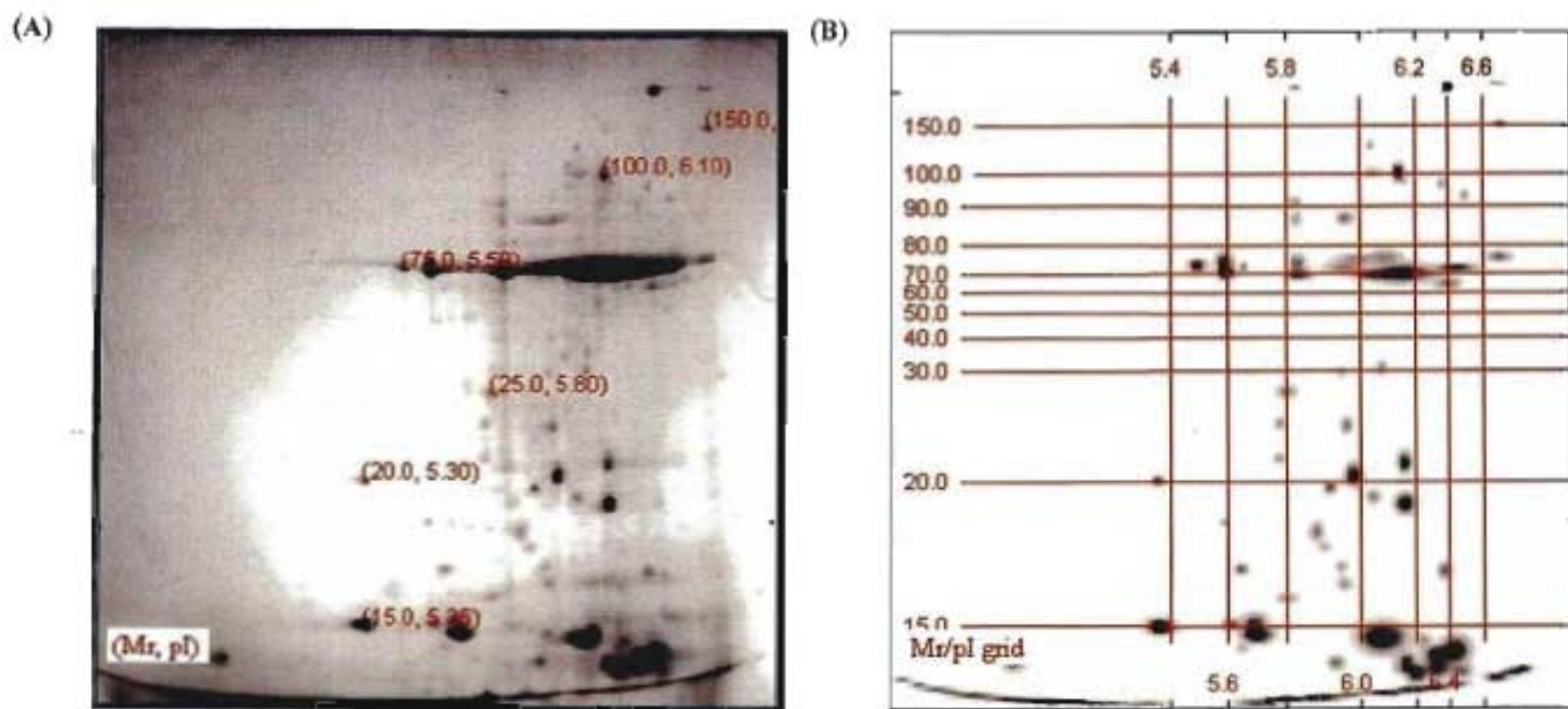


Figure 3.21. (A) Molecular weight standards were based on the BioRad Precision Plus unstained protein standards run in second dimension electrophoresis. (B) Molecular weight and pI grid analysis of the Master gel established using PD QUEST software.

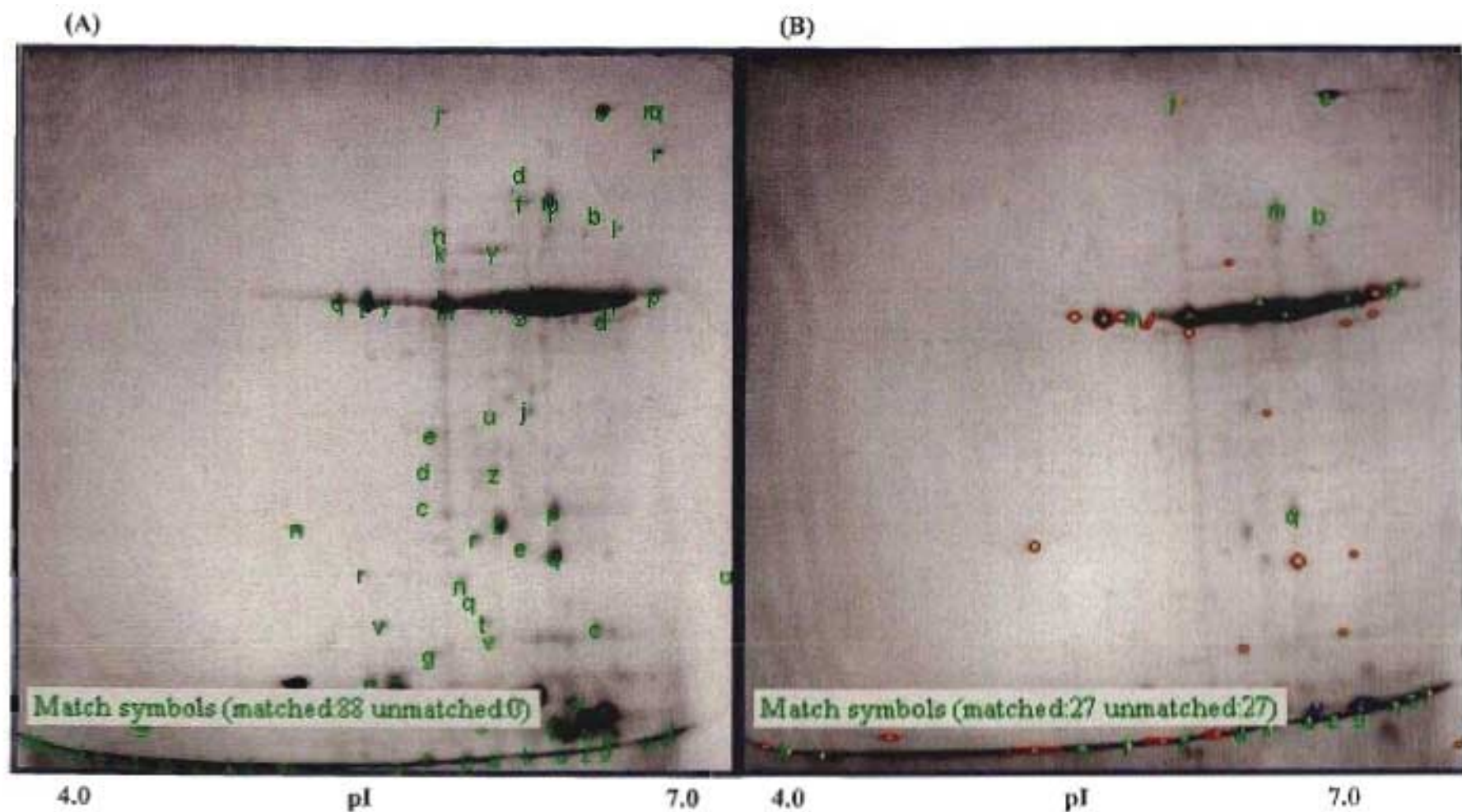


Figure 3.22. Comparative analysis of the 2-D PAGE gels of the cellular proteins of *S. milleri* 77. (A) Resolved proteins with cells cultured in the absence of antibiotic stress. (B) Resolved proteins with cells cultured in the presence of antibiotic (Ampicillin - 10 μ g/ml). Images obtained using PD Quest Software. Green shows spots matched to the master gel, whilst red depicts unmatched spots.

Conglomerates of spots situated towards the lower molecular mass spectrum were observed as a presence or absence of those particular spots when cells are cultured in the presence of the antibiotic (Figure 3.23.). These spots averaged at a molecular weight of approximately just below 15kDa. In the presence of the antibiotic stress, these spots were absent. Seen in Figure 3.23, the pop-up marginal analysis revealed that these spots when compared to the Master gel, were absent in the antibiotic stressed 2-D profile. In this instance a three-fold down regulation of these proteins was observed. A variety of other spots were similarly identified on the basis of the effect the antibiotic has on protein expression.

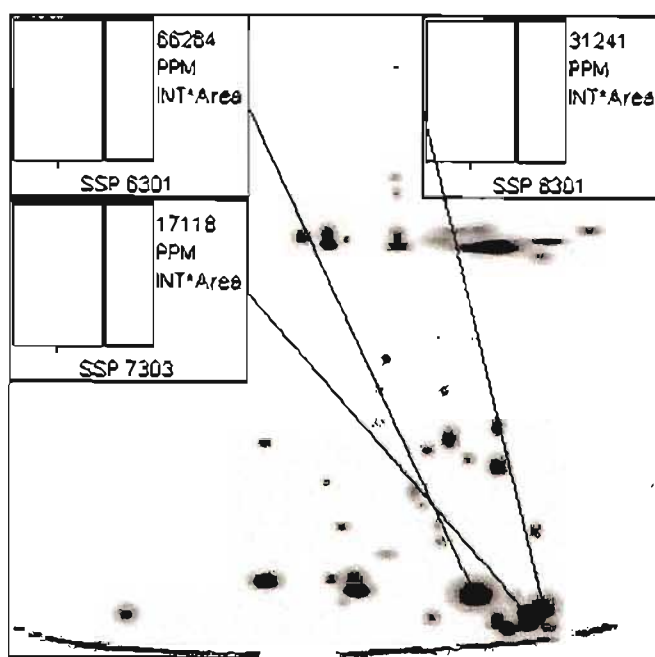


Figure 3.23. Pop-up margin graphic analysis obtained using PD QUEST software, showing three specific spots at an approximate molecular weight just below 15kDa on the Master Gel (2-D PAGE gel of the cellular proteins of *S. milleri* 77 in the absence of antibiotic stress). Spot number is identified as SSP, the thick black bar (■) in the graph shows these specific spots to be present when cells are cultured in the absence of an antibiotic stress.

3.4.2. Two Dimensional SDS - Zymographic analysis

This is the first report using the 2D SDS-PAGE technique to differentiate the presence of lytic spots based on both their pI value as well as their molecular size. Initially, standard zymographic analysis allowed for the molecular size of the lytic band to be approximately identified. Referring to Figure 3.24, it is clear that six visible lytic spots were detected at a pI value of 7.0 following renaturation of the autolytic enzymes. This is the physiologically neutral pH range for which most lytic enzymes have been successfully characterized to function optimally. This profile was obtained only for autolytic enzymes found in the mid exponential phase of the growth cycle. This stage of the growth cycle was chosen as it contained the most number of lytic bands as seen in the conventional zymogram (Figure 3.14.)

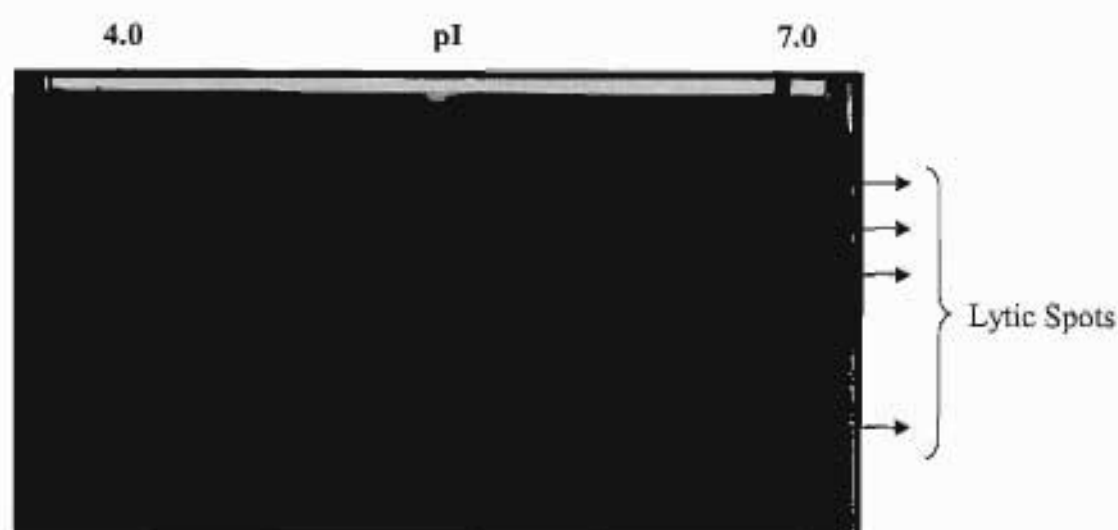


Figure 3.24. Zymogram analysis of mid exponential phase proteins of *Streptococcus milleri* 77 extracted with 4% SDS. The gel contains 0.2% *S. milleri* 77 crude cell wall material. Extracted proteins were separated by isoelectric focusing in the pI range of 4 to 7 in the first dimension and a gradient (10%) SDS-PAGE in the second dimension. Gels were stained with 0.1% methylene blue in 0.01% KOH.

This zymogram revealed six dominant lytic spots, in correlation to the conventional zymogram (Figure 3.14.). The dominant lytic spot in the 2D zymogram seen at a molecular range of approximately 15kDa was also a significant lytic band in the conventional zymogram (Figure 3.14.). The number of lytic spots found for the mid exponential stage in this profile may not necessarily reflect the enzymes that may exist. Proteolytic processing of autolytic enzymes has been shown to occur as a means of regulation by activation. These lytic spots represent the most significant and highly active enzymes in this stage.

The incubation period in the renaturation buffer was at a physiologically neutral pH, and future experiments can investigate the effect different pH's have on the detection of the lytic spots. The incubation in renaturation buffers with a gradient pH range may very well allow for the detection of more lytic spots present in specific stages. Often, 2D SDS-PAGE analysis requires a specific method for the preparation of the samples prior to focusing of the proteins on the strip. In this instance a high percentage of SDS (4%) was used to extract the autolytic enzymes. Traces of SDS greater than 0.25% have been know to affect the overall rehydration and focusing of the proteins due to the presence of this high concentration [Cash, 1998]. Future research in the detection of lytic spots two dimensionally can employ a new approach which effectively isolates crude autolytic extracts in a reduced SDS environment to monitor the true effect the high percentage of SDS had on the running conditions for the zymogram.

3.4. Gram stain morphology and microscopy

Gram stain morphology and microscopy was conducted to determine if *S. milleri* P35 and *S. milleri* B200 differed in their morphological appearance, as they seem to exhibit profiles of a very similar nature as shown in their respective relative fitness assays. *S. milleri* P35 did exhibit a lower relative fitness than *S. milleri* B200 and in relation to its zymographic profile, also had a lower autolytic expression (Figure 3.16.).



Figure 3.25. *S. milleri* P35 cell morphology from a 48 hour culture. 100X magnification achieved using oil emersion.

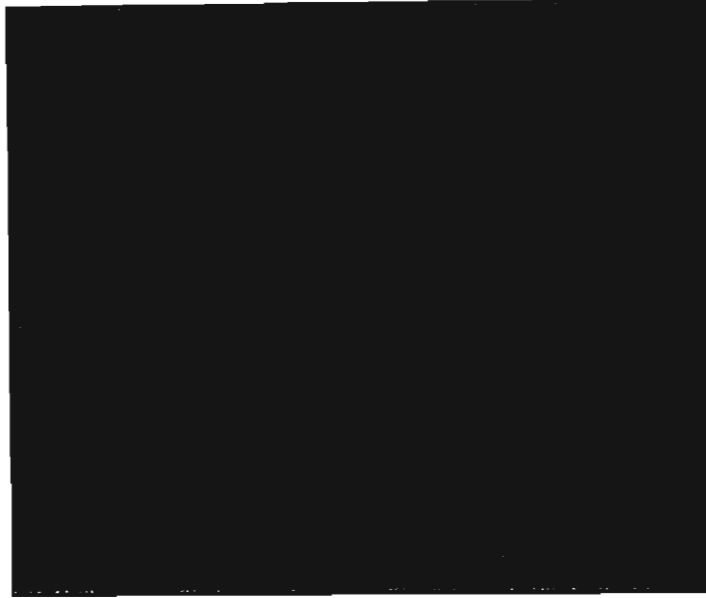


Figure 3.26. *S. milleri* B200 cell morphology from a 48 hour culture. 100X magnification achieved using oil emersion.

Gram positive bacterial cells have a characteristically thicker cell wall, due to a higher presence of peptidoglycan in the murein sacculus. Gram stain analysis revealed that *S. milleri* P35 appeared to have a chain-like morphology, characteristic of incomplete cell wall synthesis (Figure 3.25.). This is generally accounted to the lack of or decreased autolytic activity. Previously characterized autolysins have been implicated in the cell wall separation process where enzymatic hydrolases are responsible for the cleavage of specific bonds within the murein sacculus, arising in the separation of the septum. The *S. milleri* P35 strain seems to lack such characteristics.

S. milleri B200 has clearly well defined cocci cells (Figure 3.26.). In this instance the defined cell separation as seen in *S. milleri* B200 is indicative of a higher autolytic presence and activity as compared to the *S. milleri* P35 strain.

3.5. Autolytic Assays

Analysis of the rates of autolysis, based on the regression pattern, shows that some buffers had a more desired effect compared to others (Figure 3.27.). Regression patterns show a direct proportionality to the rate of autolysis. The higher the regression the higher the autolytic rate observed. The assay buffer of choice was 50mM glycine in 0.01% Triton X-100 at a pH of 8. This buffer however did not show the fastest rate of autolysis. However, the 50mM phosphate buffer which is a physiologically neutral buffer, allowed for the greatest rate of autolysis (Figure 3.27. – Clear Bars).

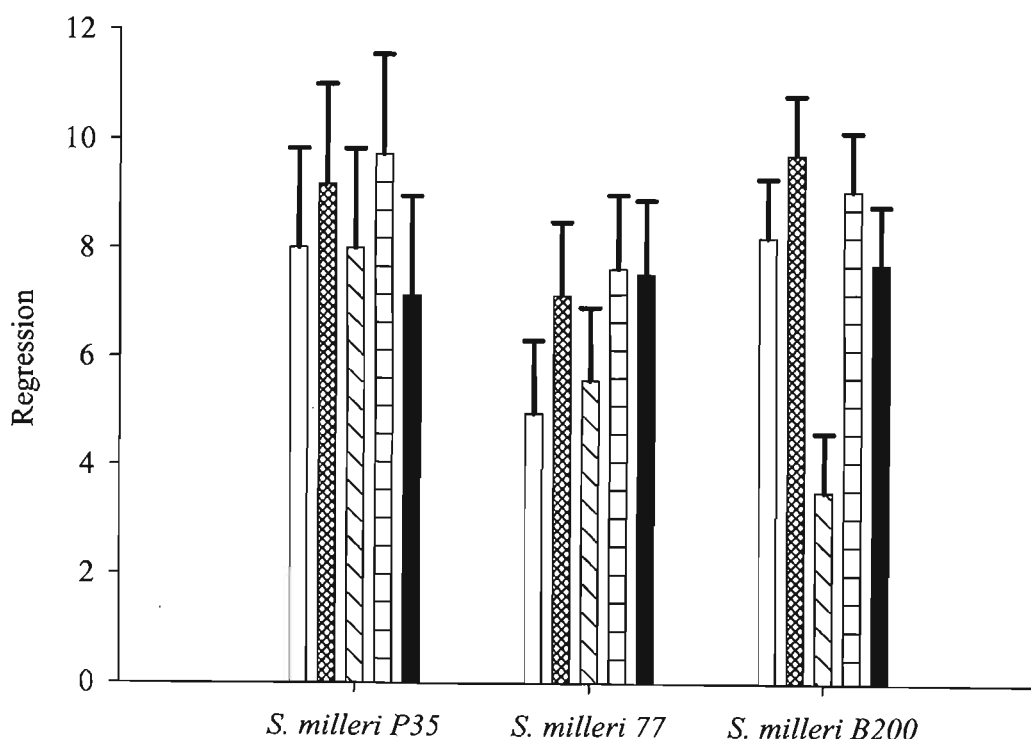


Figure 3.27. Autolytic rate shown as a regression plot, with the standard deviation (τ) plotted above the bar. Different buffers for each assay are shown as follows:

Clear bars – 50mM Phosphate buffer (pH 7.2); (●●) – 50mM Phosphate buffer in 0.01% Triton X-100 (pH 7.2); (\\) – 50mM Phosphate buffer in 0.01% Deoxycholate (pH 7.2); (=) – 50mM Glycine buffer in 0.01% Triton X-100 (pH 8) and Black bars – Ampicillin induced lysis in 50mM Phosphate buffer (pH 7.2).

Overall phosphate buffer promoted the highest rate of autolysin activity for all the strains in the presence of the detergent, Triton X-100 (Figure 3.27. – [▣] Bars). This suggests that the detergent has access to the cell wall material and promotes the degradation of the bacterial cell wall. This is not the case when deoxycholate, which also has detergent-like characteristics, was used as an autolysis buffer (Figure 3.27. – [∖] Bars). A possible explanation for this is that the detergent cannot gain access to facilitate or promote the enzymatic breakdown of the bacterial cell wall.

Comparatively, the regression pattern for strains *S. milleri* P35 and B200, correlated to the morphological observations in the gram stain. *S. milleri* P35 showed distinct chain-like cocci cells, indicative that the activity of its autolysins was lower than that of *S. milleri* B200. The *S. milleri* B200 strain had clearly defined cocci cells. Structurally, due to the lowered activity of the autolysins in *S. milleri* P35, cell wall separation becomes compromised resulting in the chain-like appearance of the bacterial cells.

Autolytic degradation in *S. milleri* P35 was staggered as compared to *S. milleri* B200. In correlation to the zymogram profiles, it was shown that *S. milleri* P35 had a much lower autolysin activity, as the renaturation period which shows lytic presence occurred over 96 hours instead of 24 hours. This correlates to the level observed from the assay. From the regression pattern, it can be established that the 50mM glycine in the presence of Triton -X100 promoted autolysis, for *S. milleri* P35 (Figure 3.27. – [=] Bar). This could be due to the positively ion-charged environment created by the presence of the glycine in the buffer. Charge groups are known to play an important role in the regulatory process of autolysins, where changes in the charge balance can affect the rate of autolysis. This pattern holds true also for *S. milleri* 77 which displayed a similar profile (Figure 3.27. – [=] Bar). Deductively, *S. milleri* strains possessing higher autolytic activity, such as *S. milleri* B200, display the adverse of autolysis when in the presence of the glycine buffer. Their rate of autolysis is compromised, and a more neutrally physiologically stable buffer such as the phosphate buffer is preferred.

The presence of an antibiotic in the assay buffer did not relate to previous studies carried out [Winslow, *et al.*, 1983]. Antibiotics which target the cell wall, such as beta-lactams, when used in the assay buffer at sub-minimum inhibitory conditions did not show an increased autolytic profile [Koch, 2001]. Rather, the regression pattern suggests that the presence of ampicillin did not affect autolysis at all (Figure 3.27. – Black Bars). These β -lactams and other glycopeptide antibiotics inhibit cell wall synthesis, which results in the arrest of bacterial growth. Bacteria are stabilized by the peptidoglycan that completely encloses the cell. The specific binding of the antibiotic to the bacterial target should lead to death of the bacterial cell by the deregulation of the extra cellular autolytic enzymes [Koch, 2001]. This is not observed in these assays (Figure 3.27. – Black Bars). During normal growth, autolysin activity is believed to be subjected to strong, prolonged down-regulation as suggested by literature [Gardete *et al.*, 2004]. Initially the expression of most hydrolases is constitutive throughout the cell cycle, but the enzymes are only physiologically active during stationary phase lysis. Autolysin activity during the exponential phase remains curtailed even when the gene is constitutively expressed. This indicates that the regulation of autolysin activity is independent from the transcription of the autolysin itself. Cells used in these assays were harvested in the late exponential phase, which showed the fastest rate of autolytic degradation as compared to other stages within the cell cycle. This is the first report to suggest that antibiotic stress does not promote the lysis of the bacterial cell, indicative that more stringent mechanisms must be in place to protect the cell from lysis and ultimate self destruction.

3.7. Autolysin identification

S. milleri 77 was selected for further autolytic characterization. Three bands appeared consistently, from the early exponential phase through to the death phase (Figure 3.28.) in the zymogram profile. These bands were named as autolysins A, B and C. A fourth band, named autolysin D, was only present in the mid exponential phase (Figure 3.28.). Expressional activities of the autolysins differed along the phases within the growth cycle. This indicates that autolysins are present throughout the cell growth cycle, and only expressed at certain times within the specific stages. As stated in literature, the highest level of autolytic expression can be observed in the late exponential and death phases [Beukes and Hastings, 2001].

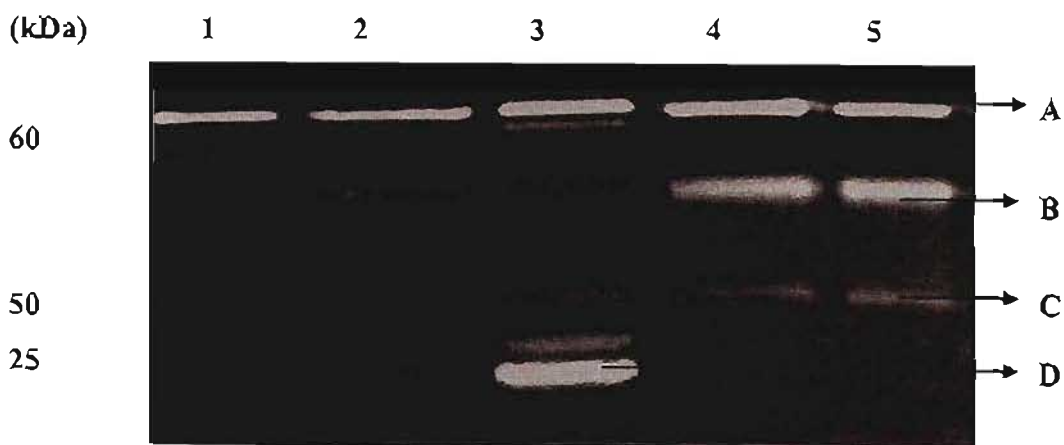


Figure 3.28. Zymogram analysis of proteins extracted with 4% SDS from different stages of the growth cycle of *Streptococcus milleri* 77. The gel contains 0.1% *S. milleri* 77 crude cell wall stained with 0.1% methylene blue in 0.01% KOH. Lanes: 1, mid lag phase; 2, early exponential phase; 3, mid exponential phase; 4, mid stationary phase; and 5, death phase. A, B, C and D indicate the different putative autolysins selected for further characterization.

3.8. N-terminal Sequencing

N-terminal sequencing was employed to determine the specific amino terminal sequence of the identified autolysins. N-terminal sequencing uses a chemical process based on the technique developed by Pehr Edman in the 1950's [Edman and Henschen, 1975]. In this technique the N-terminal amino acid reacts with phenylisothiocyanate (PITC) (Figure 3.29.). The cleavage reaction occurs in the presence of trifluoroacetic acid. Derivatization results in a phenylthiohydantoin (PTH) – amino acid. This amino acid is then sequentially removed while the rest of the peptide chain remains intact (Figure 3.29.). Each derivatization process is a new cycle and within each cycle a new amino acid is removed. The amino acids are sequentially analyzed to give the sequence of the protein or peptide [Edman and Henschen, 1975]. This is achieved by reverse-phase high pressure liquid chromatography. This is a highly sensitive process, where as little as 10 pica moles of starting material is sufficient to produce a desired result [Edman and Henschen, 1975]. N-terminal protein sequencing plays a significant role in modern structural and molecular biology [Edman and Henschen, 1975]. It has been successfully used in the identification of novel proteins and has allowed for the design of oligonucleotide primers / or probes. This technique has also shown degrees of identity between proteins and the confirmation of recombinant protein identity and fidelity [Edman and Henschen, 1975].

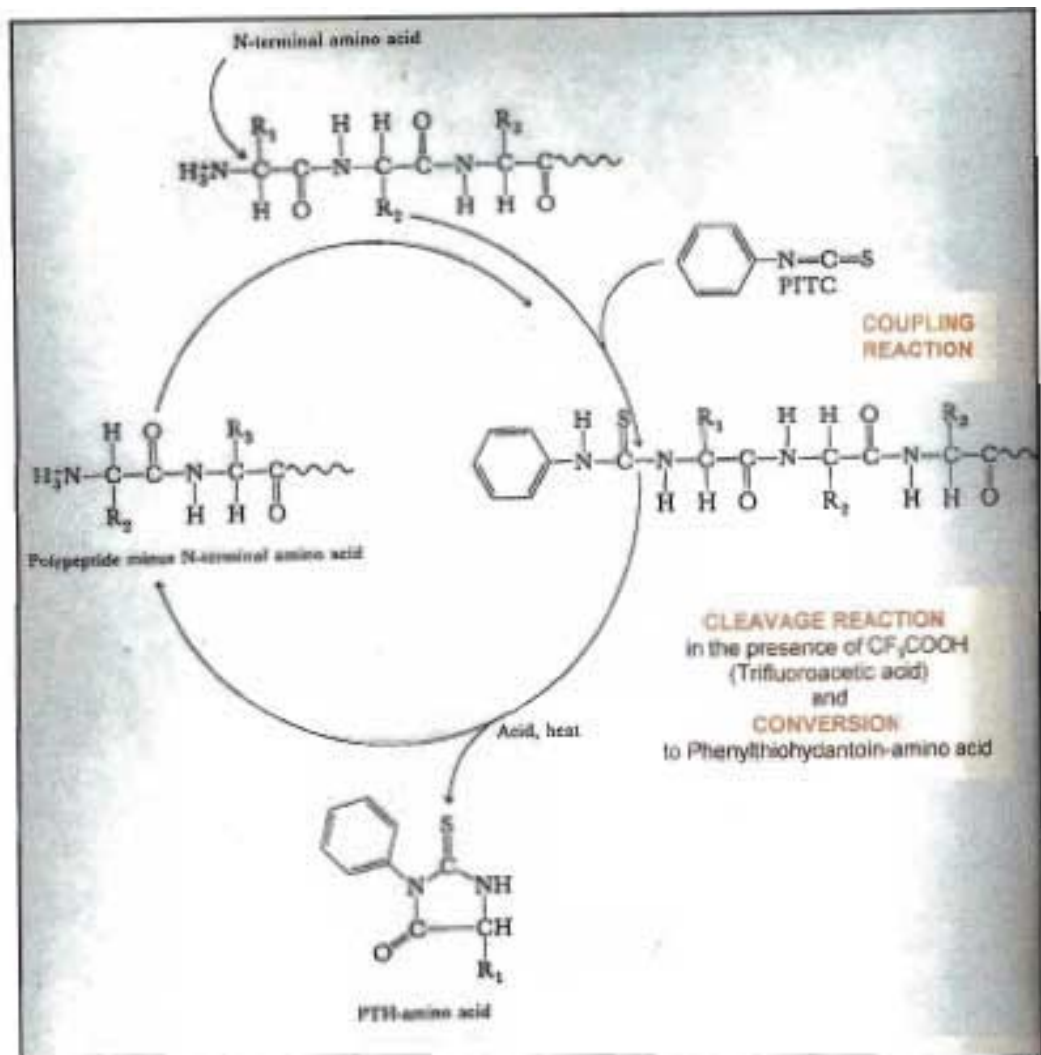


Figure 3.29. Illustrative representation demonstrating N-terminal sequencing using Edman chemistry [Edman and Henschen, 1975].

S. milleri 77 autolytic protein extracts were transferred onto PVDF membrane as described in chapter two (Figure 3.30.). Lytic bands identified as putative autolysins were excised and used as the starting material for N-terminal sequencing. An Applied Bio systems Procise protein sequencer was used.

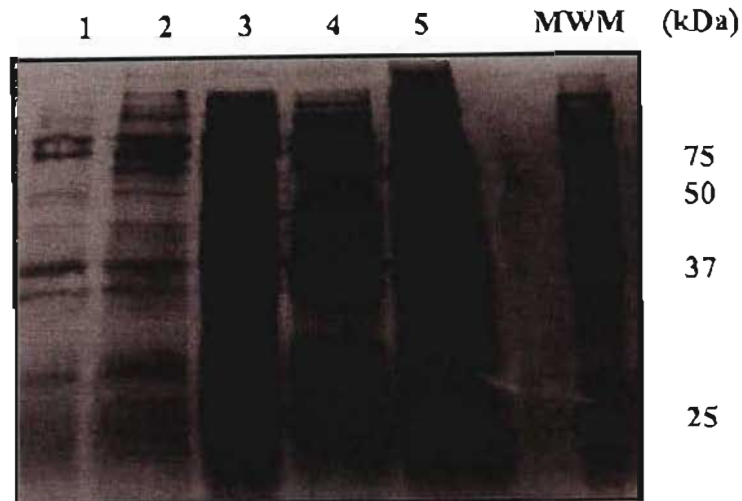


Figure 3.30. PVDF blot of protein extracts from *Sireptococcus milleri* 77. Blot was stained with Coomassie Blue. Lanes: 1, death phase; 2, mid stationary phase; 3, mid exponential phase; 4, early exponential phase; and 5, mid lag phase. MWM: BioRad Precision Plus unstained protein standards.

The hydrophobicity of the PVDF membrane makes it an ideal support for binding of proteins in electrophoretic applications in that the proteins were tightly bound and quantitatively retained during exposure to acidic, basic, or organic solvents. In binding the proteins onto the membrane, thioglycolate solution was incorporated into the upper running buffer to scavenge reactive compounds left in the gel which could subsequently cause N-terminal blocking.

The N-terminal sequencing using Edmund chemistry resulted in the following amino acid sequences: - Autolysin A: SGGLADKNKK, Autolysin B: SDGTWTGKQ, Autolysin C: VLLNLIVSM and Autolysin D: SENDFSKAMVL. The N-terminal sequences were searched for sequence similarities on the Swiss-Prot/TrEMBL protein database. The N-termini of

autolysins A, B, C and D revealed between 100% and 80% sequence similarity to several previously identified putative autolysins (Table 3.1.).

The N-terminus of autolysin A showed 90% homology to a putative N-acetyl-muramidase from *Streptococcus mutans*. Autolysin B revealed 100% homology to a putative peptidoglycan hydrolase Mur1 found in *Streptococcus pyogenes* serotypes M1, M3 and M13. Autolysin C displayed an 88% homology to a putative endo-beta-N-acetylglucosaminidase LytB, precursor of the murein hydrolase system in *Streptococcus pneumoniae* R6. LytB has been shown to have an important cell dispersing function in *S. pneumoniae*. The N-terminal sequence of Autolysin D showed an 80% sequence similarity to that of Millericin B from *Streptococcus milleri* NMSCC 66, an endopeptidase containing two autolytic domains previously characterized in our laboratory. Of interest, these enzymes are proposed to have a defensive function and act as a bacteriocin-like cell wall hydrolase, active against other species that share the same niche. Furthermore, the molecular weight of Autolysin D was estimated to be half of that of Millericin B. It can be deduced that perhaps Autolysin D, possibly only contains one of the two catalytic domains found in Millericin B.

Table 3.1. N-terminal sequence similarity of the major autolytic enzymes from *Streptococcus milleri* 77.

Protein	N-terminal Sequence	Sequence Identity	Strain Identity	Percentage Sequence Identity
Autolysin A	SGGLADKNKK	N-acetyl muramidase	<i>Streptococcus mutans</i>	90
Autolysin B	VLLNLIVSM	Mur 1.1	<i>Streptococcus pyogenes</i> (M1, M3, M13)	100
Autolysin C	SDGTWTGKQ	LytB	<i>Streptococcus pneumoniae</i> R6	88
Autolysin D	SENDFSKAMVL	Millericin B	<i>Streptococcus milleri</i> NMSCC 66	80

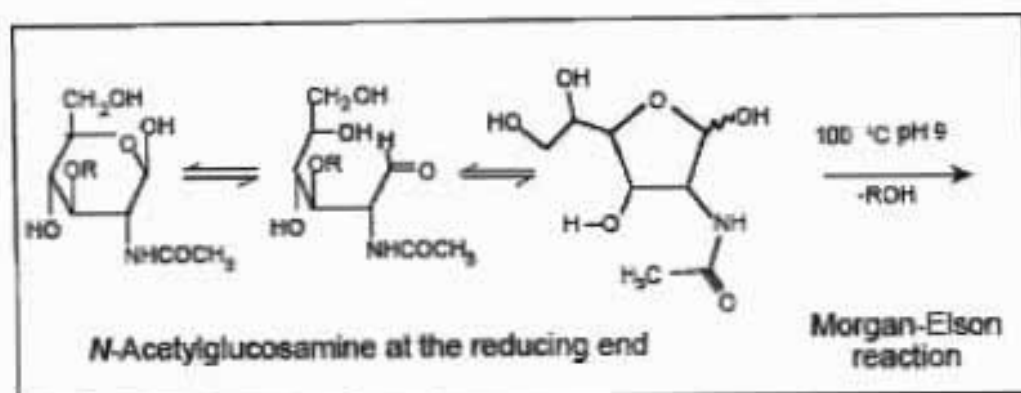
3.9. Colorimetric Assays

After renaturation SDS-PAGE the specific enzymes were extracted from the gel and their activities were characterized. Peptidoglycan is insoluble as a result of extensive cross-linking. Hydrolysis of sufficient cross-links will allow for the solubilization of the cell wall and consequent lysis. Several methods exist to detect the enzymatic nature of the hydrolysis reaction, most of which measures the increase in optical density of a particular component released via a colorimetric assay. The two assays employed were the Morgan-Elson assay and DNP assay. The application of these assays in the present study allowed for the detection of the activity of autolysins A, B, C and D.

3.9.1. Morgan-Elson Assay

The Morgan-Elson assay tested for the appearance of reduced sugars. *N*-Acetyl-2-amino sugars are assayed using the Morgan-Elson assay. This assay requires a 1-aldo-2-acetamido-4-hydroxy combination for reactivity. The interference of hexoses and amino acids are greatly reduced in this assay. *N*-acetylation is quantitatively carried out on the free amino sugars via the treatment with acetic anhydride in a slightly alkaline solution. Differences in the colour yield of the various 2-acetamido sugars are direct functions of both the alkalinity of the buffer and the heating time used in the step for pro-chromogen formation. The product is then allowed to react with Ehrlich's *p*-dimethylaminobenzaldehyde (DMAB) reagent (Figure 3.31.). Substitution of borate buffer for sodium carbonate has also allowed differentiation between 2-acetamido-glucose, 2-acetamino-galactose and 2-acetamino-mannose. Both the latter compounds yield approximately 30-50% the colour value of the glucose analog, the colour yield being roughly proportional to the heating time used.

(A)



(B)

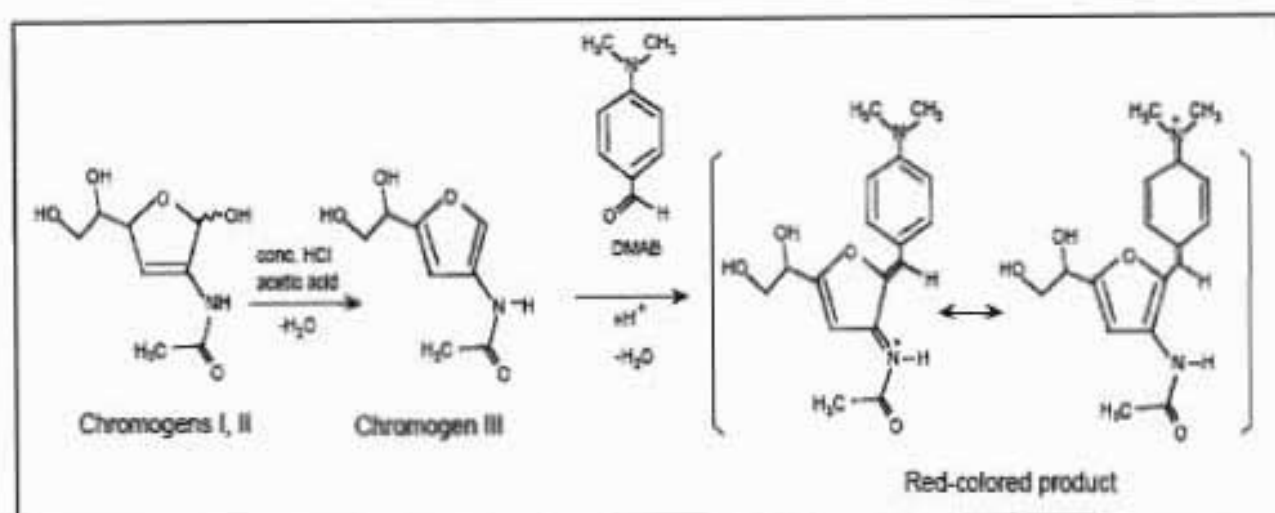


Figure 3.31. Morgan-Eelson chemistry showing the *N*-acetylglucosamine at the reducing end (A). Proposed structures of the coloured product and chromogens I, II and III in the Morgan-Eelson assay reaction (B). Chromogen I depicts the α configuration and chromogen II shows the β configuration described by Takahashi *et al.*, 2003.

The autolysins were tested for the hydrolysis of the glycan bond between *N*-acetylmuramic acid and *N*-acetylglucosamine repeating subunits of peptidoglycan by the Morgan-Elson assay. The liberation of free reducing sugar derivatives were monitored photometrically. An increase in the liberation of free reducing sugars was detected for Autolysin A as well as for the control, mutanolysin (Figure 3.32.). There was no noteworthy increase in the liberation of free reducing sugars in the presence of Autolysins B, C and D. It can be established that Autolysin A does indeed have muramidase activity, based on its ability to liberate reducing sugars from a cell wall substrate.

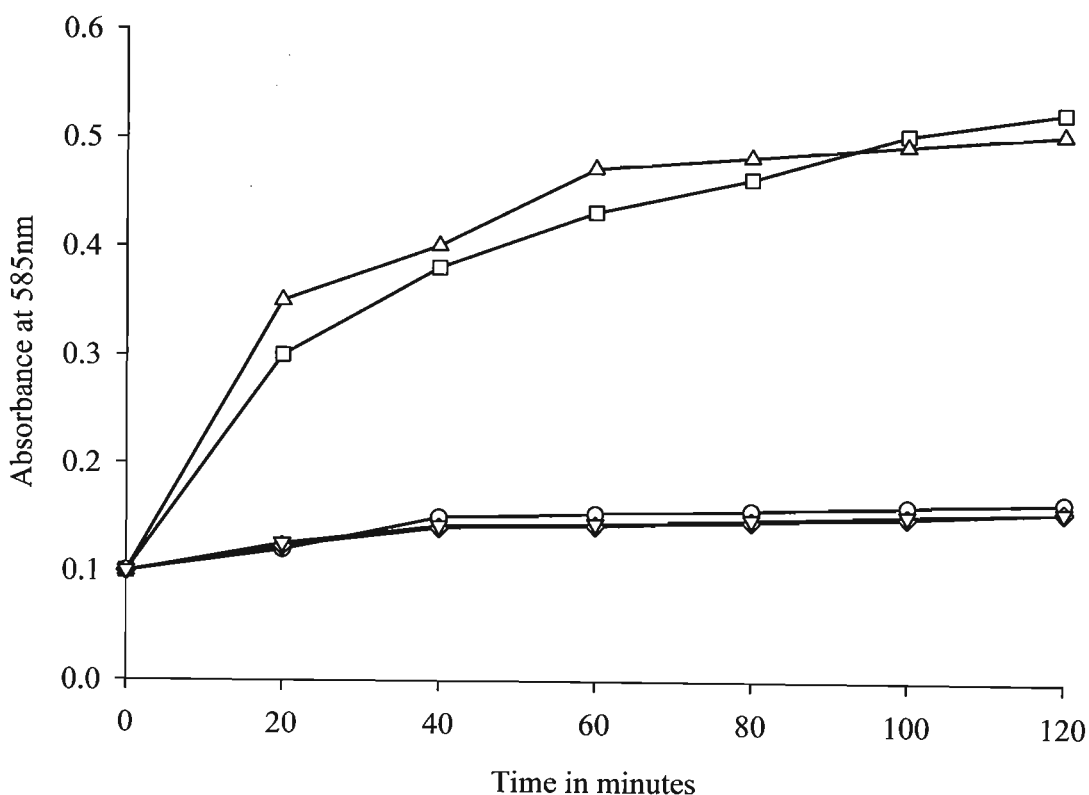


Figure 3.32. Liberation of free reducing sugars from the cell walls of *Streptococcus milleri* 77 after digestion with autolysins analyzed by the Morgan-Elson assay. Symbols: □, cell walls digested with Autolysin A; Δ, cell walls digested with mutanolysin; ◇, cell walls digested with Autolysin B; and ○, cell walls digested with Autolysin C; and ▼, cell walls digested with Autolysin D.

3.9.2. N-dinitrophenyl Assay

The detection of endopeptidase activity was done by a colorimetric assay with N-dinitrophenyl (DNP) derivatization. In this procedure, the appearance of free amino groups is tested for during the lysis of bacterial cell walls. The reagent used in this assay is fluorodinitrobenzene; together with potassium tetraborate which when acidified produces a colour change readable at a wavelength of 405nm. At this wavelength and pH, dinitrophenol derived from the excess reagent has negligible absorption while *N*-dinitrophenol derivatives of amino acids can be read at a wavelength of 405nm. Cell wall substrates digested with the three autolysins showed an increase in the liberation of free amino groups for Autolysins B, C and D. There was no significant increase in the liberation of free amino groups in the presence of Autolysin A (Figure 3.34.) Autolysins B, C and D are thus classified as having peptidase activity (Figure 3.34.). Peptidases are characterized as enzymes that hydrolyze peptide bonds and reduce proteins or peptides to amino acids (Figure 3.33.). Autolysin C however displayed endopeptidase activity (Figure 3.34.). Endopeptidases act on the murein network by cleaving the peptide cross-bridges. The experiments carried out however did not elucidate the exact bonds been cleaved.

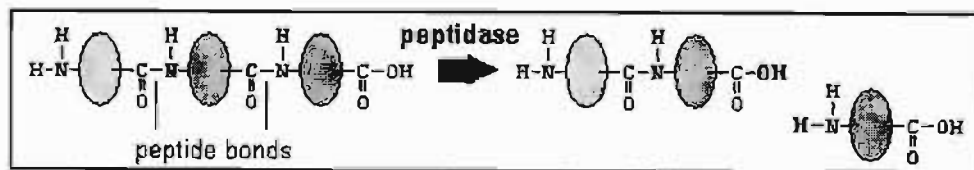


Figure 3.33. Cleavage properties of peptidases showing the reduction of proteins into single amino acids.

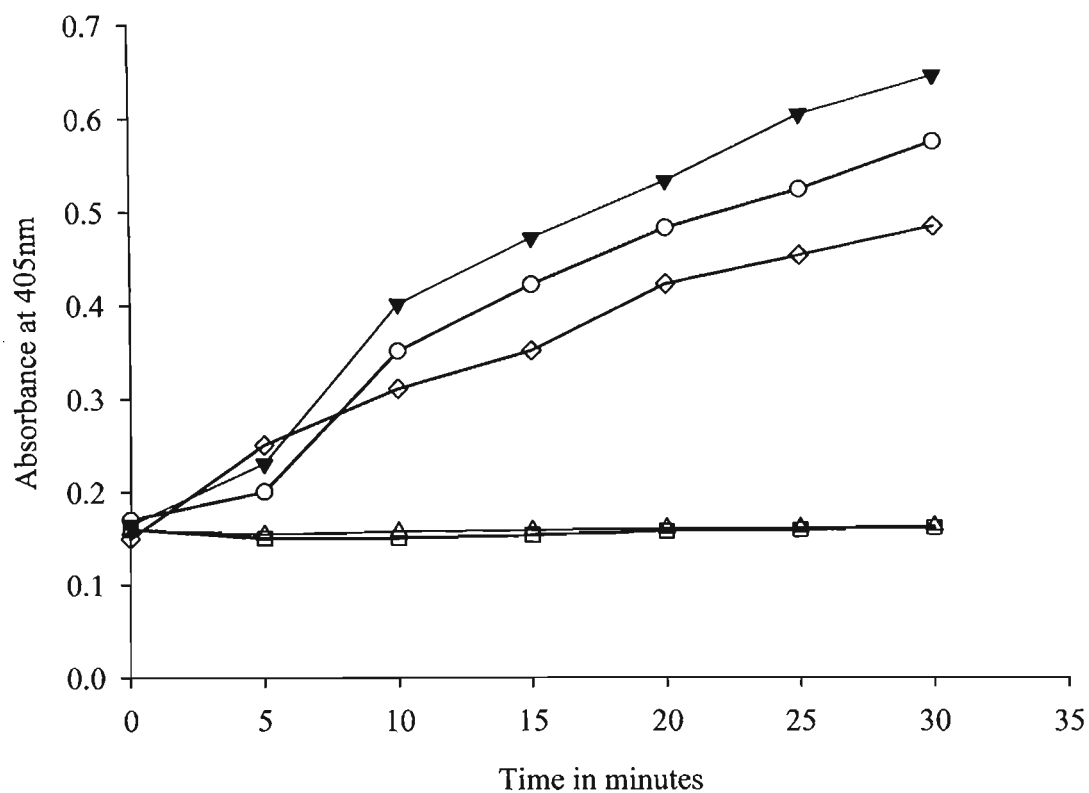


Figure 3.34. Liberation of free amino groups for the digestion of *Streptococcus milleri* cell walls with Autolysins extracted from *Streptococcus milleri* 77 analyzed by the DNP assay. Symbols: □, cell walls digested with Autolysin A; Δ, cell walls digested with mutanolysin; ◇, cell walls digested with Autolysin B; ○, cell walls digested with Autolysin C; and ▼, cell walls digested with Autolysin D.

3.10. Peptidoglycan Assays

Gram-positive bacteria are characterised by a multifaceted fabric essential for the survival, shape and general integrity of the cell. Macromolecular assemblies of peptidoglycan, cell wall polymers and surface proteins function within this envelope. An important cell wall constituent, teichoic acids play a vital role in the charged environment within this membrane. These assays were designed to establish the role such polymers play in relation to cell wall degradation and lysis.

Peptidoglycan isolated in the presence and absence of teichoic acids formed the basis of these assays. Initially, monitoring the autolytic patterns obtained, it was observed that autolysis was promoted when the charged group, teichoic acid, was present in the peptidoglycan isolate. Strains *S. milleri* P35 and *S. milleri* 77 showed an increase in their respective autolytic rate (Figure 3.35.). This relates to literature, which has found that cell wall polymers are responsible for altering the proton gradient creating an anionic environment allowing for the binding of autolysins to the cell wall [Neuhaus and Baddiley, 2003]. An interesting finding was that the highly autolytic producing *S. milleri* B200 strain displayed an opposite response in its autolytic regression. In this instance, the absence of teichoic acids actually promoted the rate of autolysis (Figure 3.35.). This may be associated to the fact that these cell wall polymers act to down regulate the binding of autolysins in strains that show high levels of autolytic activity as in the case of *S. milleri* B200 (Figure 3.35.). Teichoic acids can now be implicated directly as targets for cell lysis and degradation.

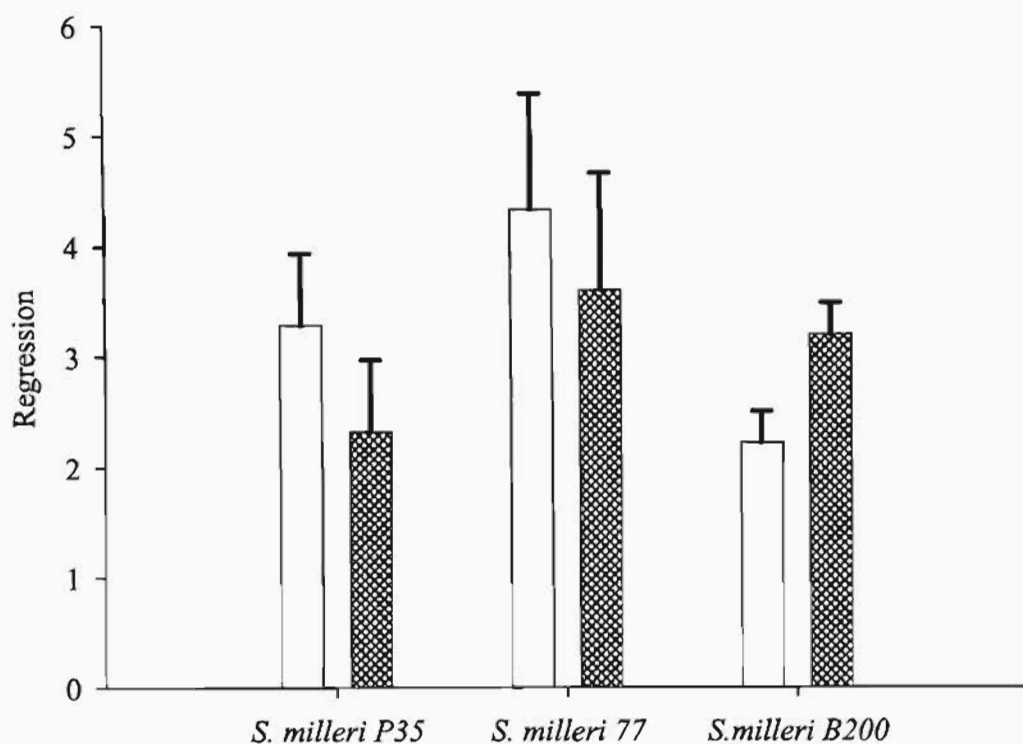


Figure 3.35. Regression patterns monitoring the presence versus the absence of teichoic acids (a charged group) in the peptidoglycan for each of the Streptococcal strains, with the standard deviation (\top) plotted above the bar. Peptidoglycan in the presence of teichoic acids is shown as clear bars whilst (▨) represents the absence of teichoic acids.

To further investigate the effect such groups have on the autolytic rates, the regression profiles for *S. milleri* P35 and *S. milleri* B200 were compared. For these assays autolytic extract from each respective strain was also incorporated. Autolytic extract has a similar mode of action as lysozyme, which degrades the peptidoglycan constituents within the cell wall. Hence, the autolytic extracts should in theory increase the rates of autolysis. Comparing the regression profiles obtained, *S. milleri* P35 displayed a 0.5 fold increase in its autolytic rate when the autolytic extract was incorporated (Figure 3.36.). Again, the absence of the charged group promoted autolysis (Figure 3.36.).

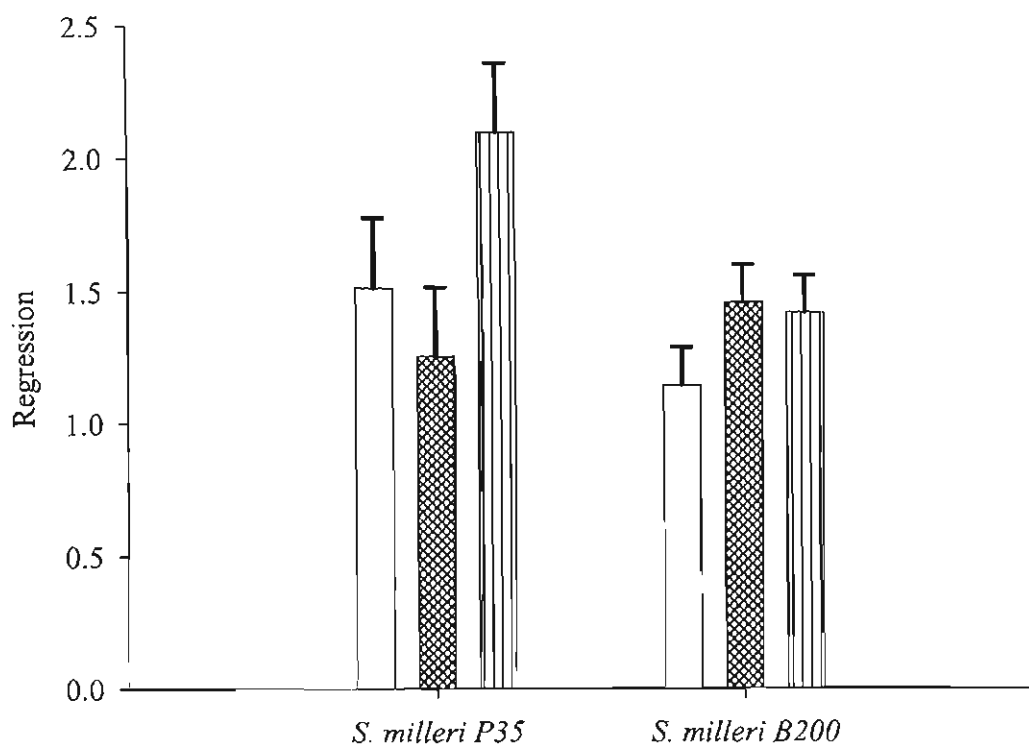


Figure 3.36. Regression patterns monitoring the presence versus the absence of teichoic acids (a charged group) in the peptidoglycan for each of the Streptococcal strains, with the standard deviation (τ) plotted above the bar. Autolytic extract (100 μ g/ml) of each respective strain was incorporated. Peptidoglycan in the presence of teichoic acids is shown as clear bars whilst (⊗) represents the absence of teichoic acids. The control peptidoglycan, containing no autolytic additives in the presence of teichoic acids is shown as (||).

The incorporation of the autolytic extract in *S. milleri* B200 showed no noteworthy change to its autolytic pattern. These results cumulatively indicate that strains with an increased autolytic activity have a regulatory mechanism in place to counter act upon the binding sites of the cell wall. Hence, charged groups, such as teichoic acids do not have the same effect as they would when present in strains exhibiting lower autolytic activity, such as *S. milleri* P35.

To study the effect antibiotic stress has on the lysis capability of the cell wall, an assay was designed to monitor the regression patterns. The role of charged groups was also monitored. A similar profile as previously obtained was seen for all the strains (Figure 3.37.). *S. milleri* 77 displayed a staggered decrease in its autolytic pattern, where the highest rate of autolysis was obtained for teichoic acid containing peptidoglycan isolate (Figure 3.37.). No substantial difference was observed. However, autolysis was least promoted when subjected to antibiotic stress and the absence of the charged group polymer. Strains *S. milleri* P35 and B200 displayed a significant change in their autolytic pattern (Figure 3.37.). Marginally, increases in the autolytic profile for *S. milleri* P35 was observed. It can be deduced that potentially dangerous strains, which are found to also have a low autolytic activity, can be targeted by initially removing their charge group polymers and then subjecting these strains to antibiotic stress. This minimizes the development of antibiotic resistance. Overall, the autolytic rate was increased for both strains when in the presence of an antibiotic, as well as in the absence of the teichoic acids (Figure 3.37.). A combined effect of antibiotic and the removal of the charged groups can be responsible for increasing the rate of autolysis. Thus, antibiotic stress can now be implicated in the increased lysis capability in these strains.

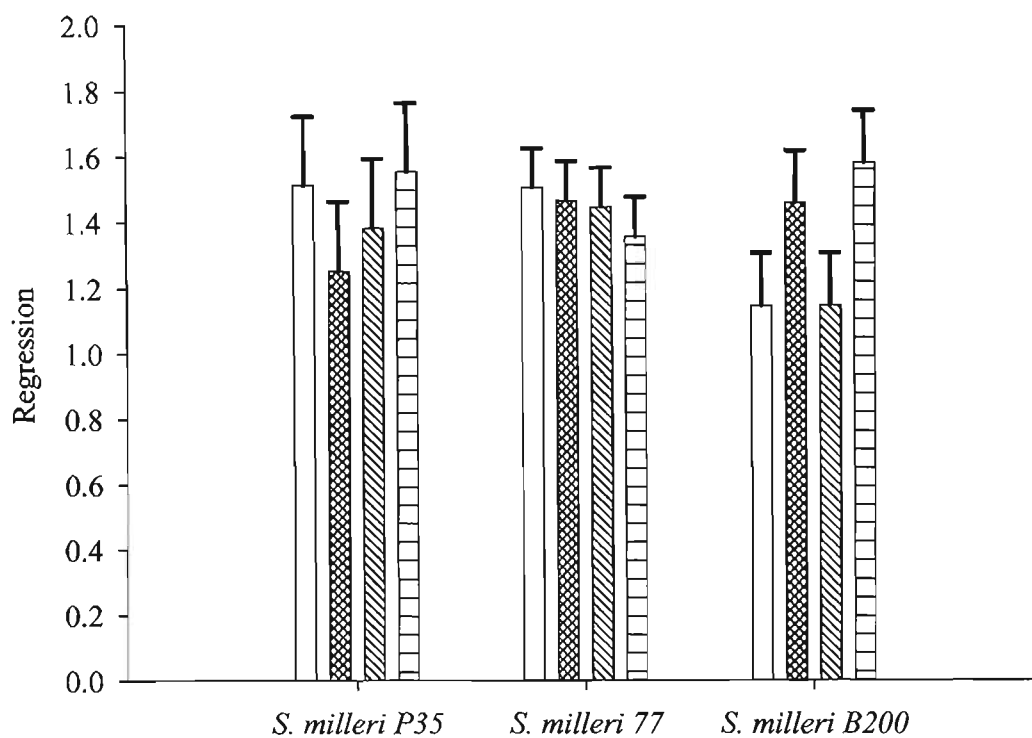


Figure 3.37. Regression patterns monitoring the presence versus the absence of teichoic acids (a charged group) in the peptidoglycan for each of the Streptococcal strains, with the standard deviation (\top) plotted above the bar. Antibiotic (Ampicillin) below the MIC value was incorporated. Peptidoglycan in the presence of teichoic acids is shown as clear bars whilst (●) represents the absence of teichoic acids. The peptidoglycan containing antibiotic in the presence of teichoic acids are indicated as (\\). The peptidoglycan containing antibiotic in the absence of teichoic acids are shown as (=).

3.11. Molecular interaction analysis (Biacore)

Lysozyme is a known enzyme that attacks the bacterial cell wall. Lysozyme is a common constituent of biological tissues and secretions; it has been found in egg whites, tears and sweat. This enzyme can be characterized as antibacterial because it degrades the polysaccharide component that is found in the cell walls of many bacteria. Lysozyme is most effective against Gram positive bacteria since the peptidoglycan layer is relatively accessible to the enzyme. Lysozyme achieves this by catalyzing the insertion of a water molecule to the glycosidic bond between *N*-acetylmuramic acid and *N*-acetylglucosamine at the position indicated in Figure 3.38. by the red arrow. This disrupts the glycosidic bond resulting in the chain breaking at that point. In each hydrolysis step, the two fragments separate from the enzyme, the enzyme is freed, and able to attach to a new location on the bacterial cell wall. It is in this similar way that autolysins function, thus lysozyme serves as a good control in the Biacore assays. The sensogram deduced should be a reflection of that generated when autolytic extract is immobilized onto the sensor chip in subsequent assays.

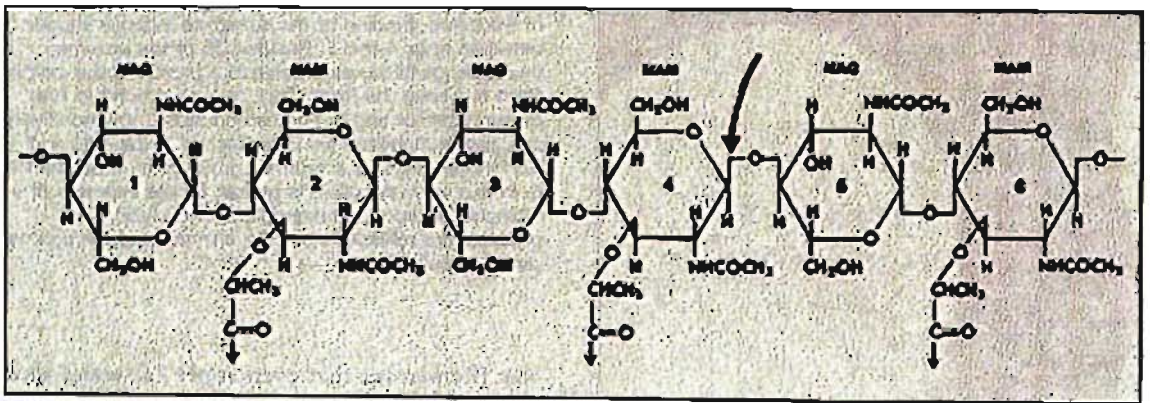


Figure 3.38. Enzymatic degradation of the polysaccharide component of the bacterial cell wall by the enzyme Lysozyme [Holtje, 1995].

Figure 3.39. represents the sensogram generated during the immobilization of lysozyme onto a CM5 sensor chip. This served as the control assay, as lysozyme would have a profile similar to that of an autolytic injection. The individual section (1-4) of the sensogram shows the different steps during the immobilization process (Figure 3.39). Lysozyme was immobilized via amine coupling. This coupling chemistry allows for the activation of carboxyl groups on the matrix by adding *N*-hydroxysuccinimide (NHS) and *N*-ethyl-*N*'-[3-dimethylamino]-propyl]-hydrochloride (EDC) to form active esters which react spontaneously with amine groups on the ligand. Initially, during phase 1, a mixture of NHS and EDC (1:1) was injected into the dextran matrix on the sensory chip to activate it at a flow rate of 5 μ l/ min at 25°C. After the first injection of lysozyme, an initial relative value of 13 000 Response Units (RU) was observed during phase 2. To increase the yield of lysozyme attached to the matrix, a second injection was performed. Phase 3 depicts an increase in the response value by 1 000 RU to approximately 14 000 RU. It can be established that the amount interacted is thus proportional to the relative response value. The excess active sites of the matrix were blocked with 1M ethanolamine-HCl. This was followed by several regeneration steps (phase 4), using sodium hydroxide buffer, to prepare the surface for the Biacore assays.

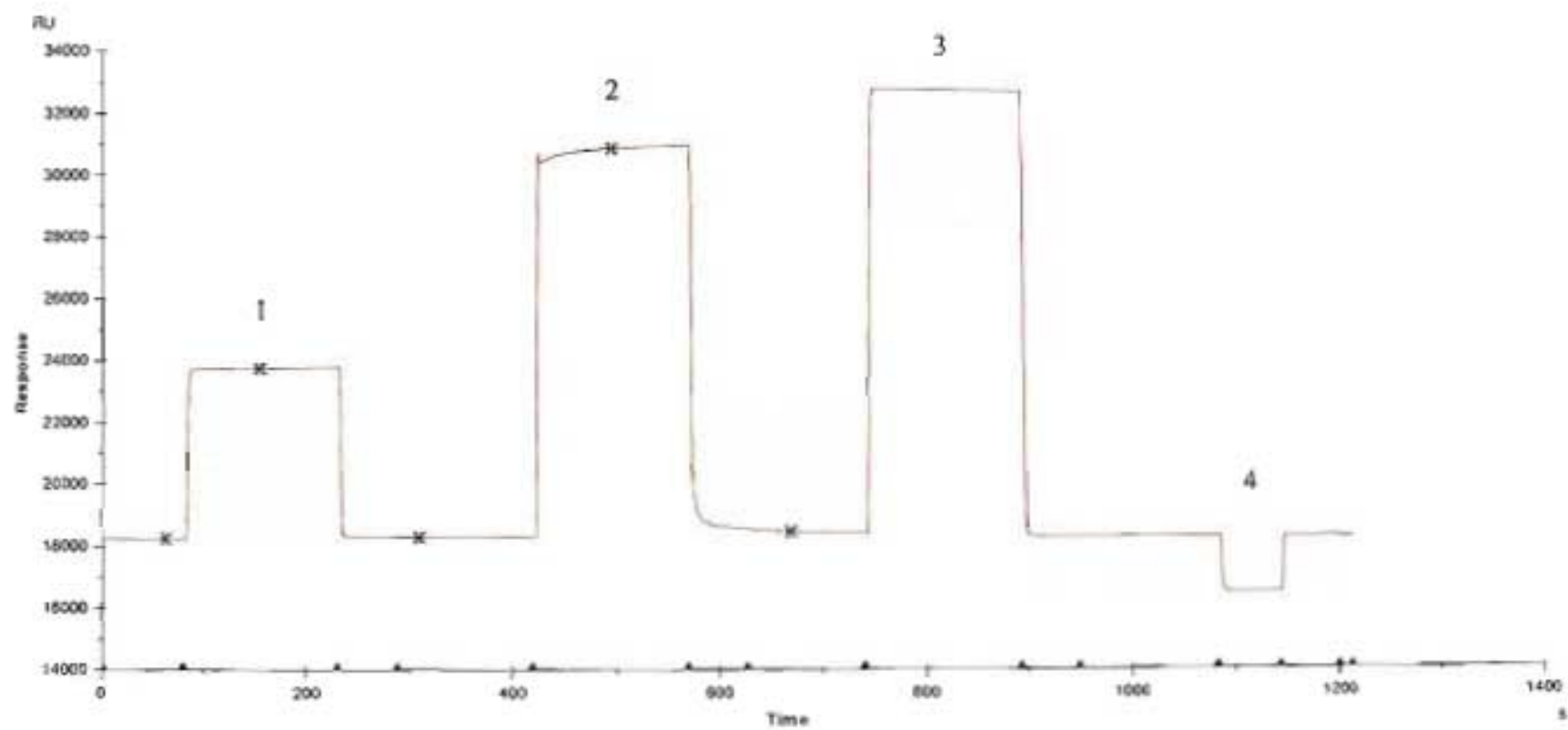


Figure 3.39. Sensogram showing the immobilization of Lysozyme onto a CM5 sensor chip using amine coupling.

During the immobilization of the peptidoglycan samples onto the sensor chip, negative charges of the carboxylated dextran on the sensor chip are used to concentrate the ligand close to the surface for the actual coupling. This is known as pre-concentrating the sensor surface chip. To achieve this, the substance to be immobilized onto the sensor chip should have an iso-electric point above 3.5. In these experiments the pI value was unknown; therefore the pre-concentrating step mentioned was recommended, using a non-active sensor chip surface. Initially, peptidoglycan with intact teichoic acids were immobilized onto flow cell 1, and peptidoglycan isolated in the absence of teichoic acids were immobilized onto flow cell 2. For each experiment, the autolytic extract was allowed to pass over both flow-cells to comparatively analyze the interactions.

From analyzing the sensograms generated for each of the injections of the crude autolytic extracts, for strains *S. milleri* P35 and B200, the profile suggests that there is a very quick saturation of the sensor chip surface. This occurs immediately after the sample was injected. In each instance, for the above mentioned strains, the interaction between the autolysin to the coupled peptidoglycan in the presence of the charged group, teichoic acids, occurs at a higher rate, seen as the red line in the sensogram (Figure 3.40., Figure 3.41., Figure 3.42., Figure 3.46., Figure 3.47. and Figure 3.48.). The green line depicts the overall interaction of the crude autolytic extract with the coupled peptidoglycan in the absence of the teichoic acids. The interaction is gradually slower in comparison to the peptidoglycan with intact teichoic acids present. In each instance, the rate of dissociation is directly proportional to the rate of association. The relative response units (RU) measuring the strength of the interaction in the case of *S. milleri* P35 averaged at 12000 RU. In correlation to the control experiment where lysozyme was coupled onto the sensor chip, this value is within the range of response units which will allow for a stable interaction to subsequently be detected. It was observed that when varying the concentrations of the autolytic extract, it produced a more stable interaction. However, after the threshold was reached, no more binding could occur and an immediate dissociation was observed (Figure 3.42.). A plateau effect was observed when saturation occurred and no further binding could be significantly measured.

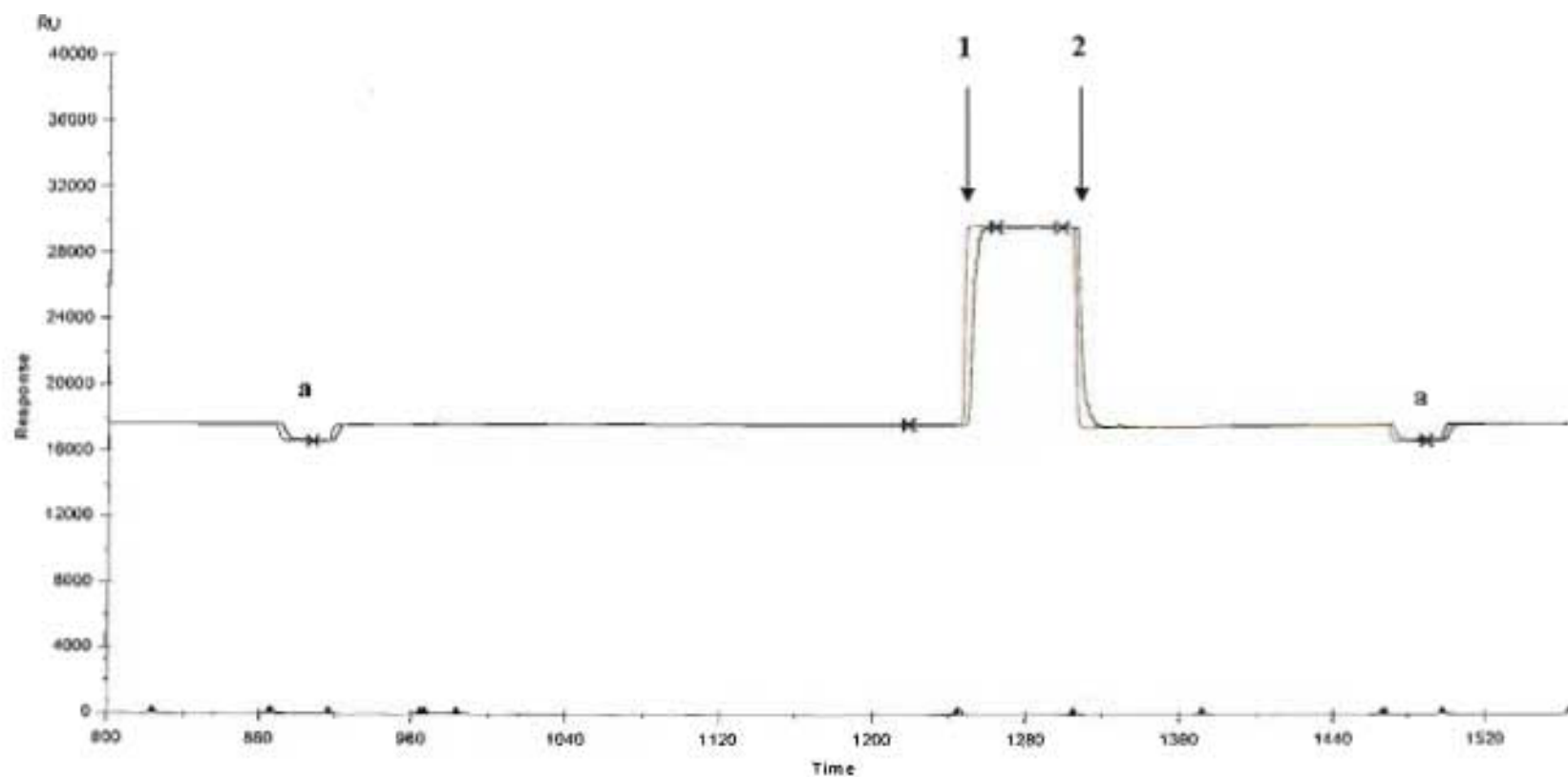


Figure 3.40. Sensogram showing the interaction between the Peptidoglycan with intact teichoic acids (shown in Red) and Peptidoglycan without teichoic acids (shown in Green) in the presence of a 10 μ l crude autolytic extract for *Streptococcus milleri* P35. The arrows (\downarrow) 1 and 2 indicate the start and end of the injection of the autolysin sample. The symbol (a) depicts the regeneration of the sensor chip with 5 μ l NaOH.

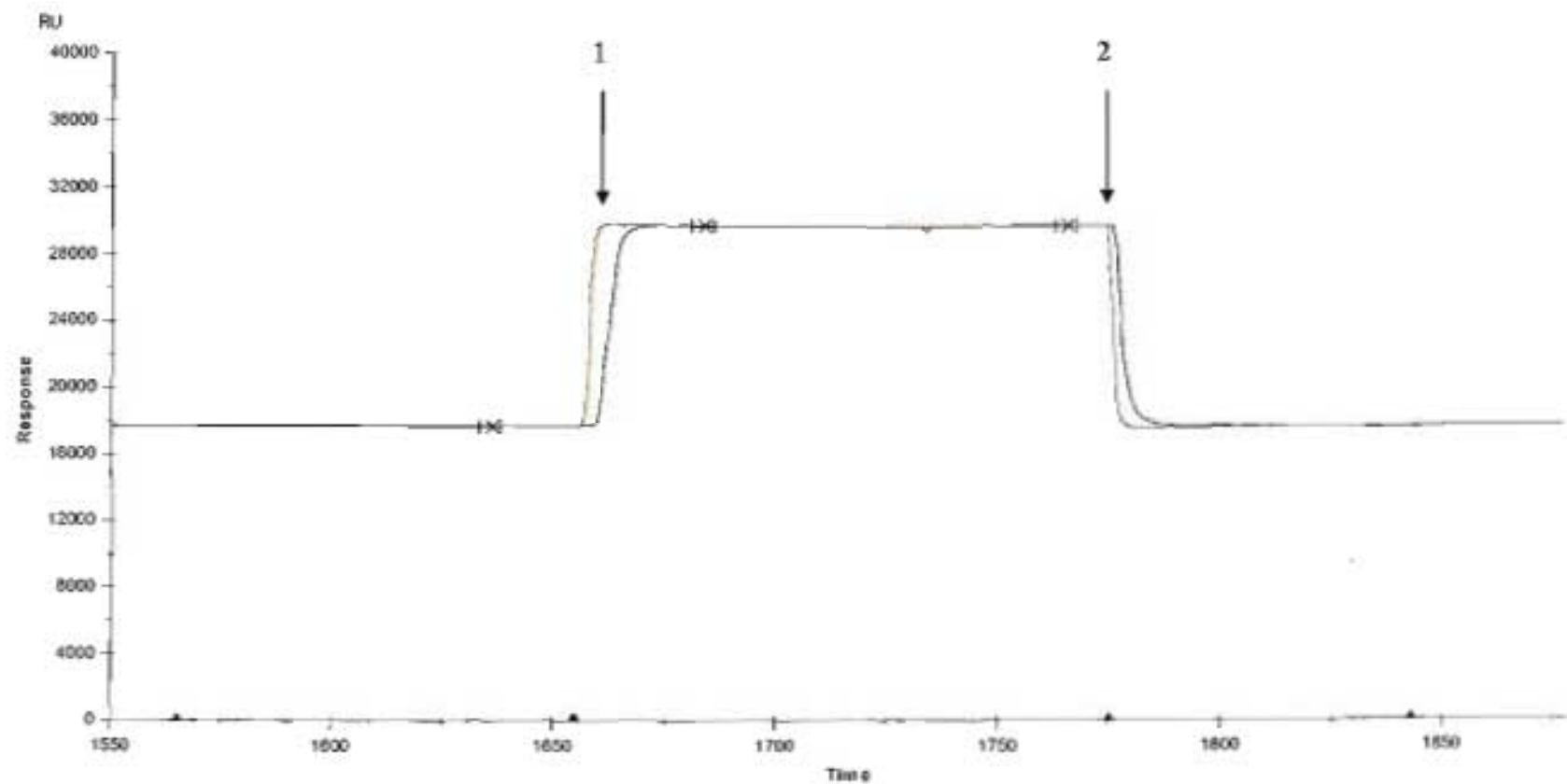


Figure 3.41. Sensogram showing the interaction between the Peptidoglycan with intact teichoic acids (shown in Red) and Peptidoglycan without teichoic acids (shown in Green) in the presence of a 20 μ l crude autolytic extract for *Streptococcus milleri* P35. The arrows (↓) 1 and 2 indicate the start and end of the injection of the autolysin sample.

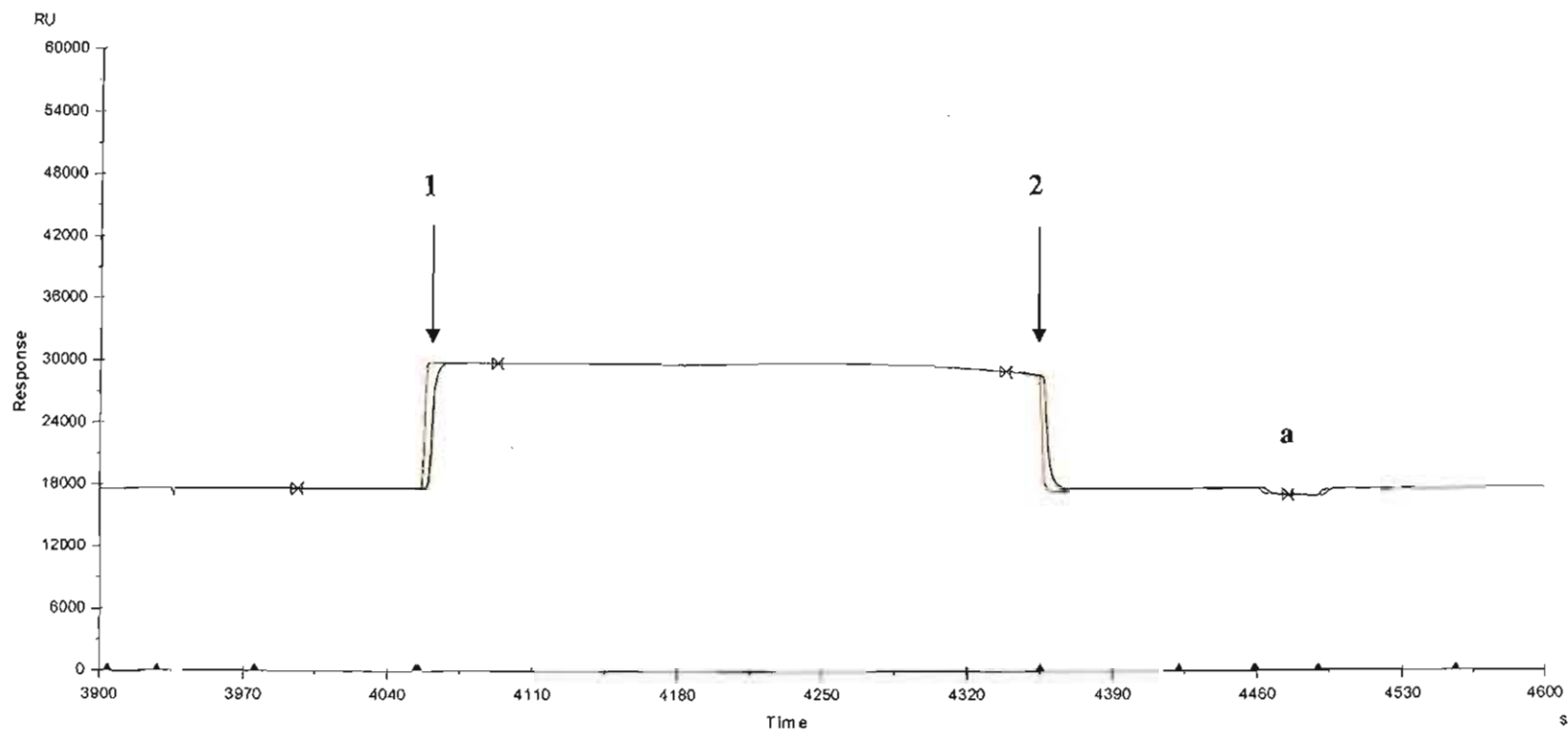


Figure 3.42. Sensogram showing the interaction between the Peptidoglycan with intact teichoic acids (shown in Red) and Peptidoglycan without teichoic acids (shown in Green) in the presence of a 50 μ l crude autolytic extract for *Streptococcus milleri* P35. The arrows (\downarrow) 1 and 2 indicate the start and end of the injection of the autolysin sample. The symbol (a) depicts the regeneration of the sensor chip with 5 μ l NaOH.

The binding of crude autolytic extract of *S. milleri* 77 did not produce a similar sensogram as seen for strains *S. milleri* P35 and B200 (Figure 3.43., Figure 3.44., and Figure 3.45.). The sensograms generated for this strain showed that the interaction between the autolytic extract and the peptidoglycan was very weak. Varying the concentration of the autolytic extract did not enhance or promote the interaction. On average, a total of approximately 2000 RU was achieved for each interaction. This was significantly different from the peptidoglycan assays previously carried out, which showed *S. milleri* P35 and *S. milleri* 77 to behave in a similar manner when monitoring the effect of presence versus the absence of the charged groups on the autolytic rates. The Biacore analysis suggests that strain *S. milleri* 77 could not produce a stable interaction to demonstrate the binding of autolysins to the peptidoglycan sub-units. However, it was observed that again the presence of the charged group in the peptidoglycan had a quicker relative response (seen in Red [Figure 3.43.]) as compared to the charge group been absent (seen in Green [Figure 3.43.]). The low value of RU obtained can directly be attributed to the fact that the response units is directly proportional the rate of interaction, thus in the case of *S. milleri* 77, the rate of interactive binding was extremely poor, and therefore the response units obtained were very low. At the highest concentration range tested (50 μ l of crude autolytic extract) no interaction could be measured (Figure 3.45.).

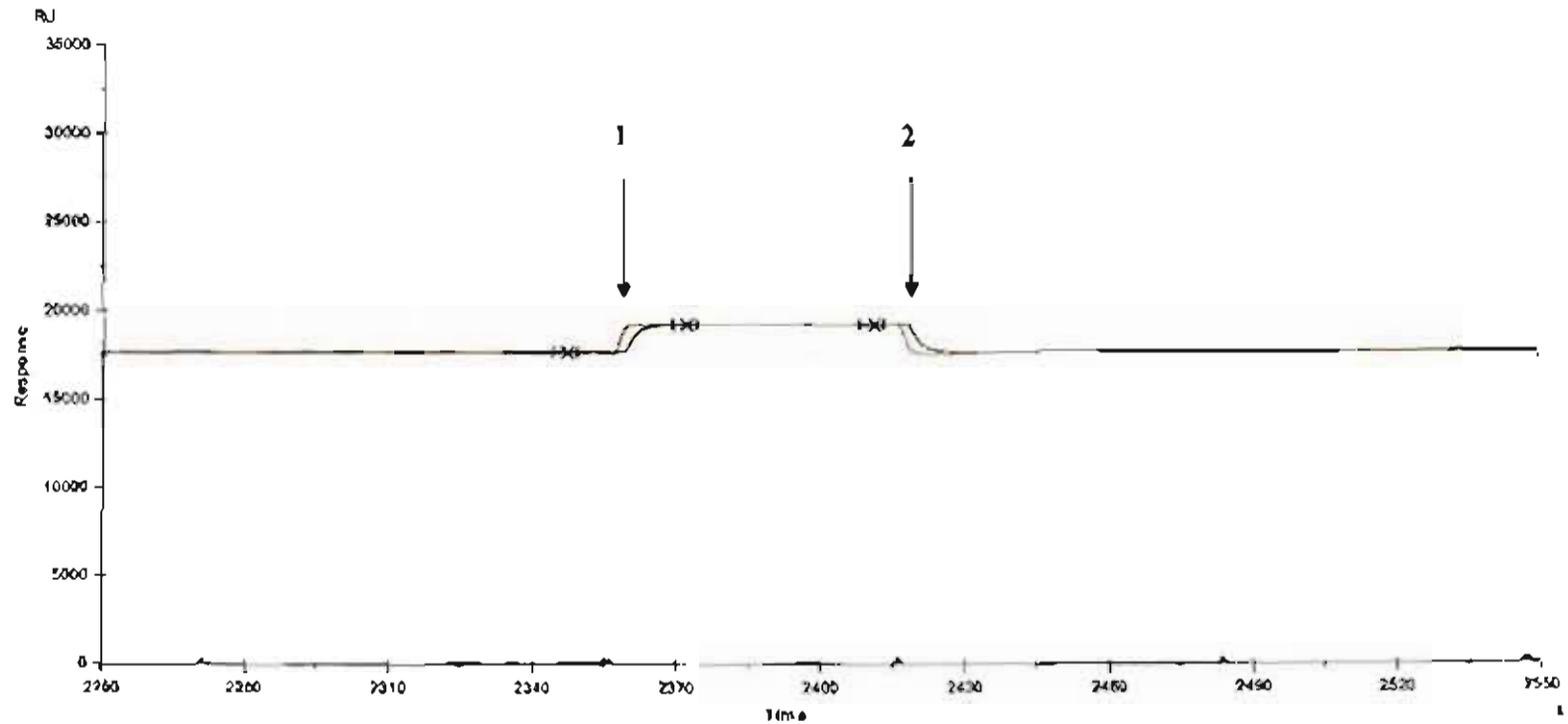


Figure 3.43. Sensogram showing the interaction between the Peptidoglycan with intact teichoic acids (shown in Red) and Peptidoglycan without teichoic acids (shown in Green) in the presence of a 10µl crude autolytic extract for *Streptococcus milleri* 77. The arrows (↓) 1 and 2 indicate the start and end of the injection of the autolysin sample.

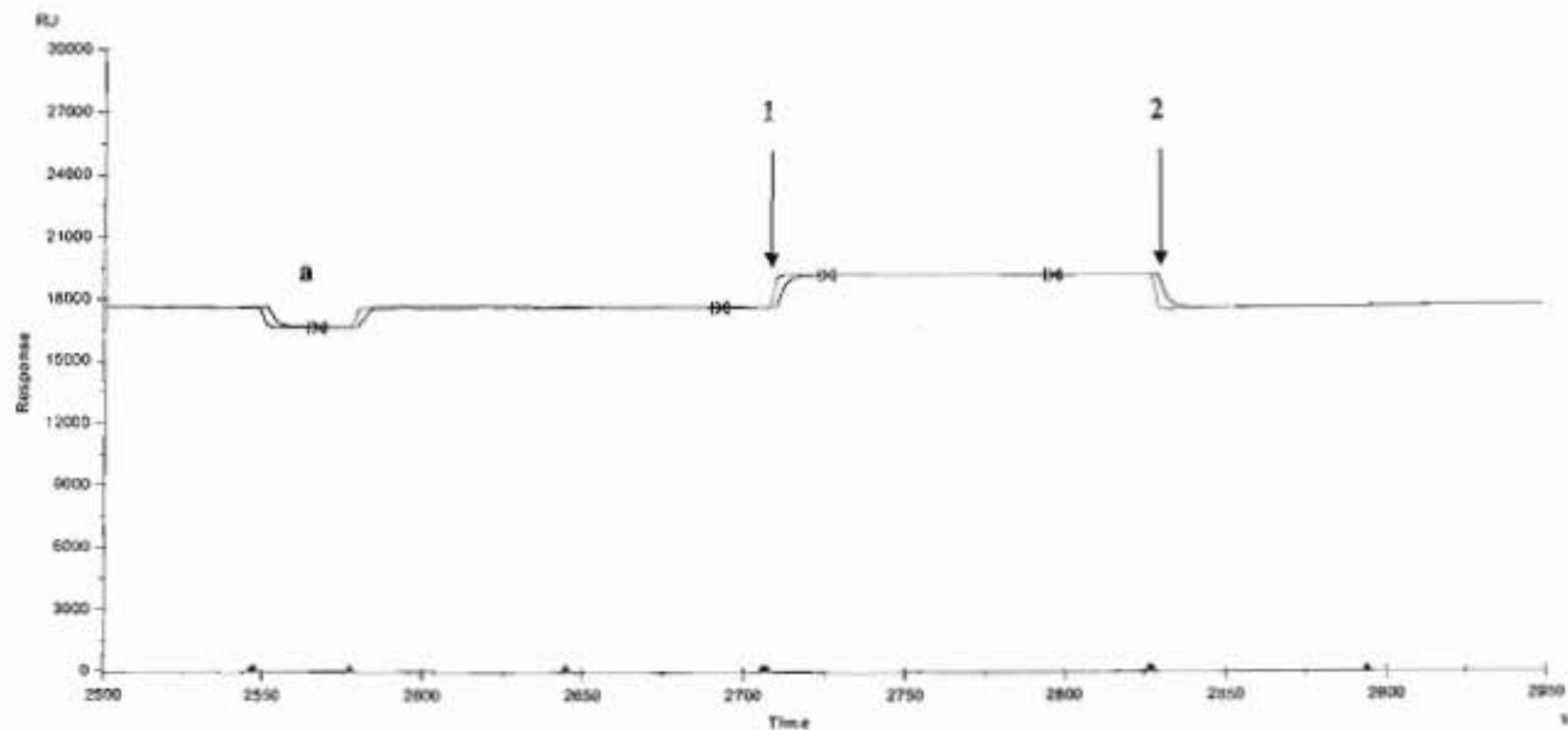


Figure 3.44. Sensogram showing the interaction between the Peptidoglycan with intact teichoic acids (shown in Red) and Peptidoglycan without teichoic acids (shown in Green) in the presence of a 20 μ l crude autolytic extract for *Streptococcus milleri* 77. The arrows (\downarrow) **1** and **2** indicate the start and end of the injection of the autolysin sample. The symbol (**a**) depicts the regeneration of the sensor chip with 5 μ l NaOH.

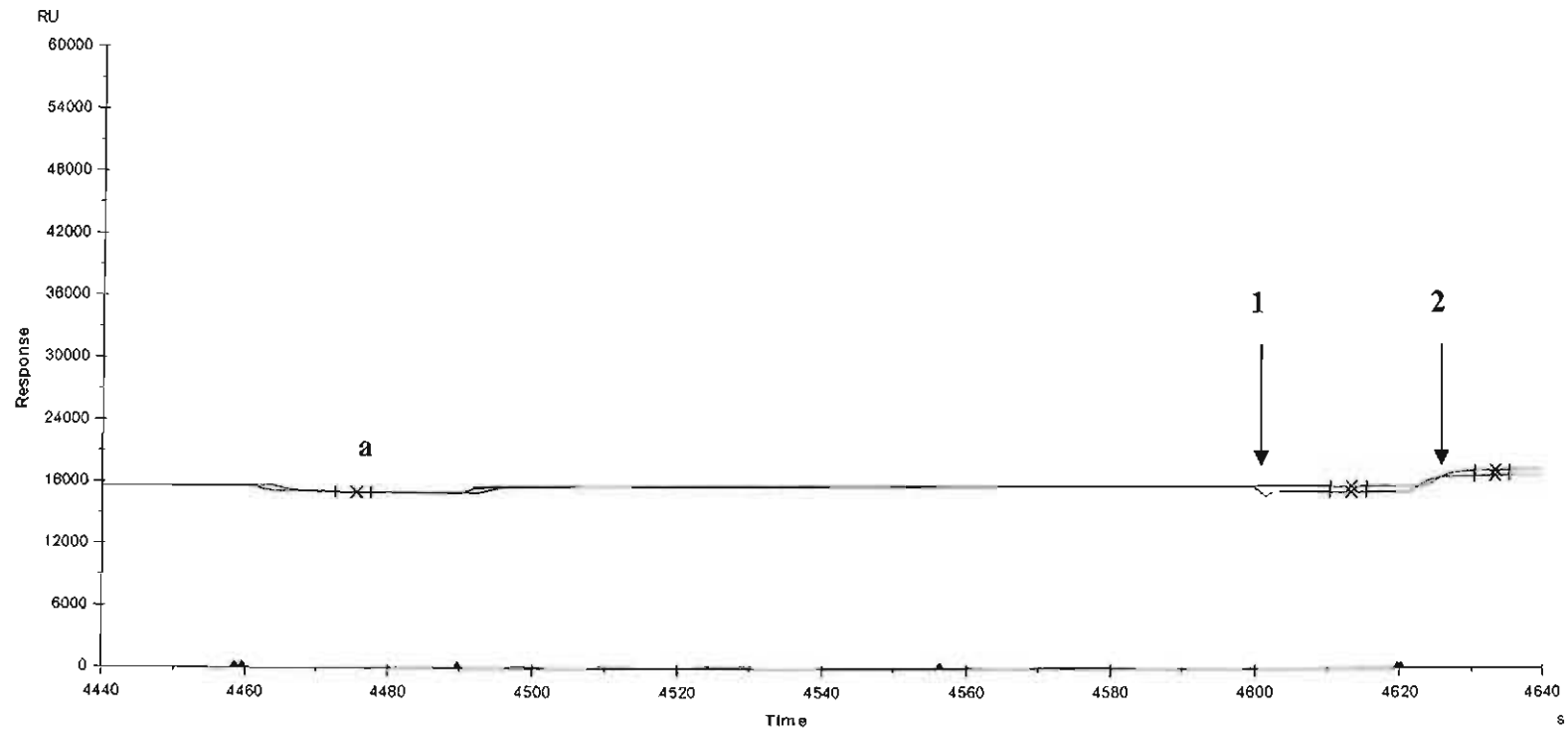


Figure 3.45. Sensogram showing the interaction between the Peptidoglycan with intact teichoic acids (shown in Red) and Peptidoglycan without teichoic acids (shown in Green) in the presence of a 50 μ l crude autolytic extract for *Streptococcus milleri* 77. The arrows (\downarrow) 1 and 2 indicate the start and end of the injection of the autolysin sample. The symbol (a) depicts the regeneration of the sensor chip with 5 μ l NaOH.

The relative response units averaged approximately 10 000 RU for *S. milleri* B200 (Figure 3.46.), slightly lower than that seen for the interactive studies for *S. milleri* P35 (Figure 3.46.). It was also observed that the presence of the charged groups promoted the binding of the autolytic extract to the peptidoglycan. It was noticed that the presence of the charged group in the peptidoglycan, had a quicker relative response (seen in Red [Figure 3.48.]) as compared to when the charged groups were absent (seen in Green [Figure 3.48.]). These results correlated with the previous assays, indicating again that the presence of teichoic acids does affect the binding capacity of the autolysin to the peptidoglycan sub-units and consequentially affecting the autolytic rate.

These interactive studies show, in correlation to the assays conducted, that the presence of the charged groups does play an important role in the binding of the autolysins to the peptidoglycan sub-units for their eventual degradation or lysis. Teichoic acids aid in providing a balanced ionic environment, which allows autolysins to bind optimally and promote lysis.

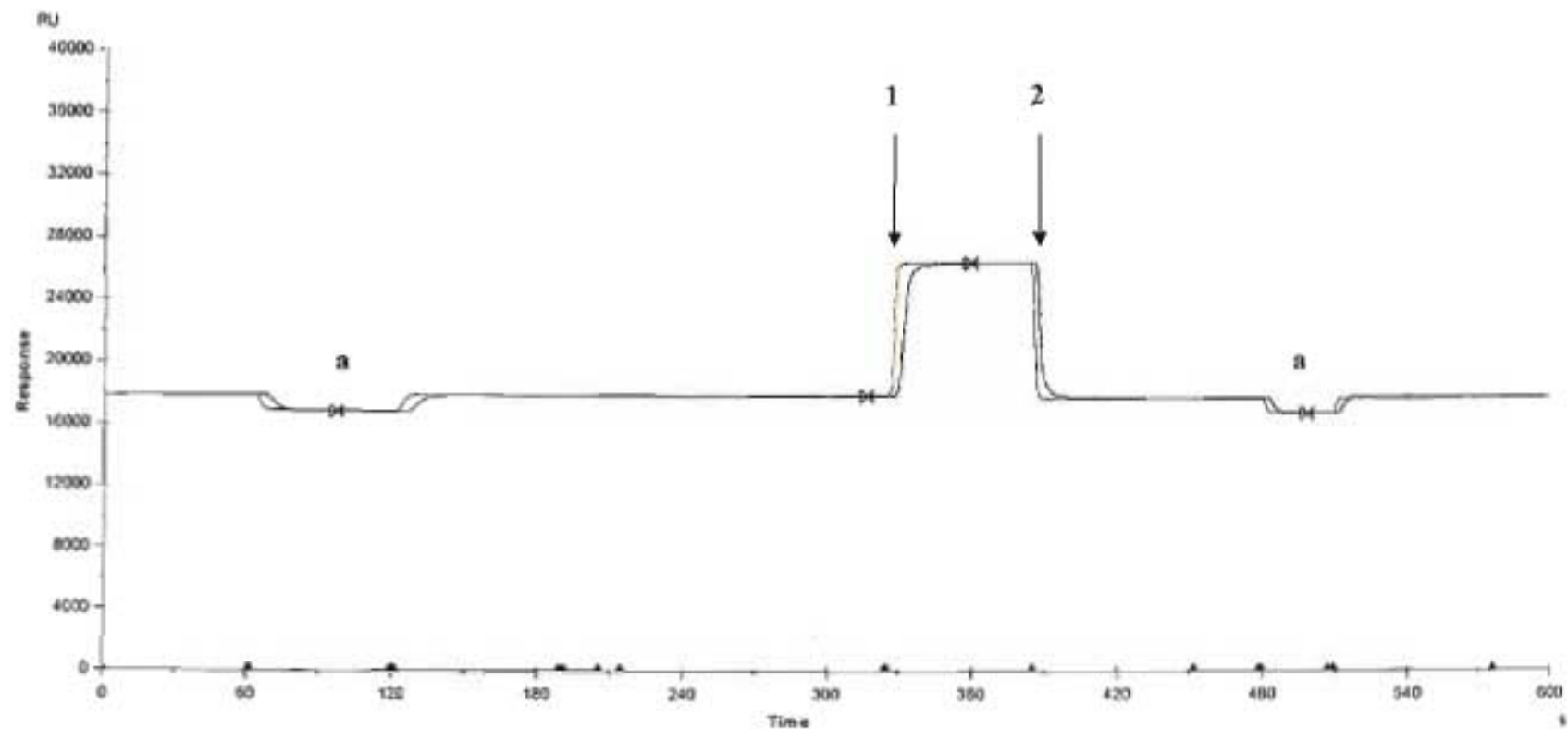


Figure 3.46. Sensogram showing the interaction between the Peptidoglycan with intact teichoic acids (shown in Red) and Peptidoglycan without teichoic acids (shown in Green) in the presence of a 10 μ l crude autolytic extract for *Streptococcus milleri* B200. The arrows (↓) 1 and 2 indicate the start and end of the injection of the autolysin sample. The symbol (a) depicts the regeneration of the sensor chip with 5 μ l NaOH.

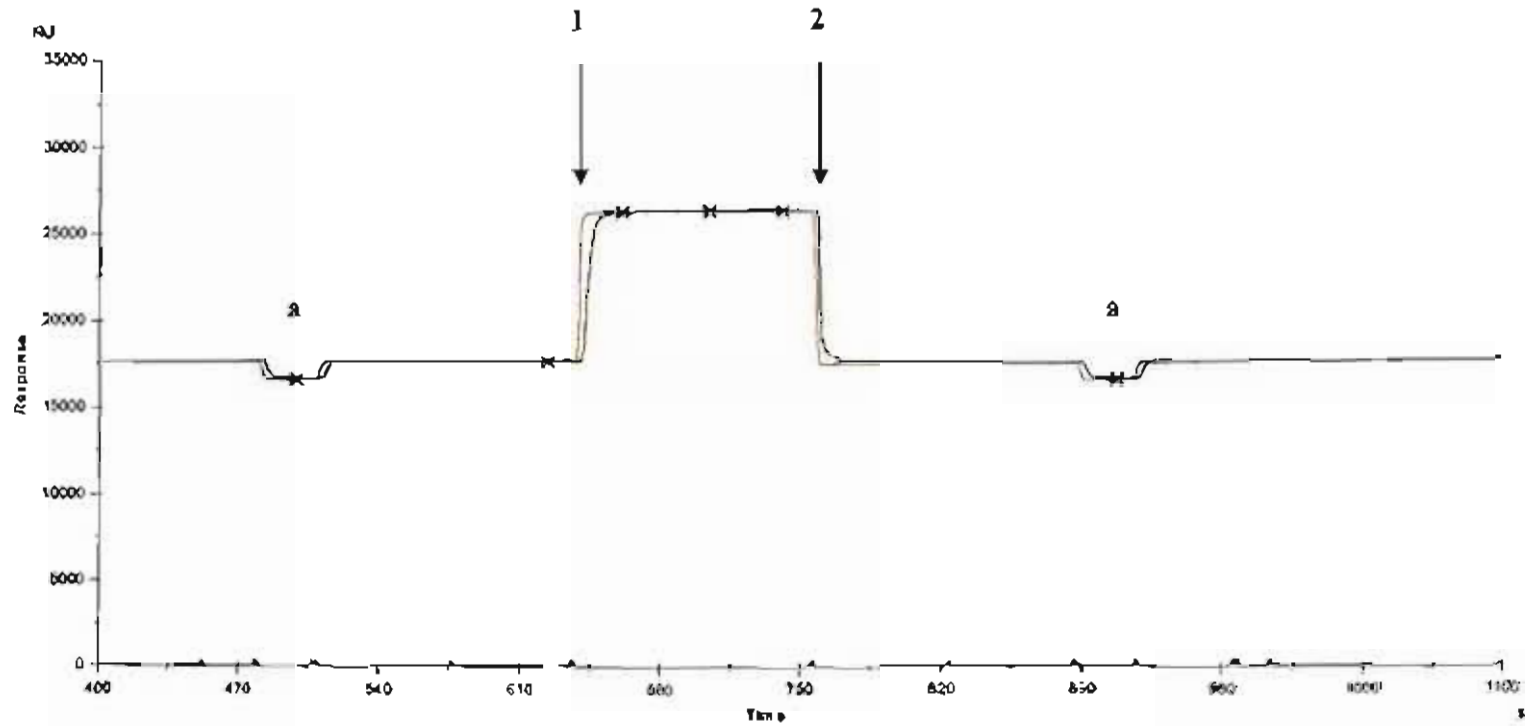


Figure 3.47. Sensogram showing the interaction between the Peptidoglycan with intact teichoic acids (shown in Red) and Peptidoglycan without teichoic acids (shown in Green) in the presence of a 20 μ l crude autolytic extract for *Streptococcus milleri* B200. The arrows (1) 1 and 2 indicate the start and end of the injection of the autolysin sample. The symbol (a) depicts the regeneration of the sensor chip with 5 μ l NaOH.

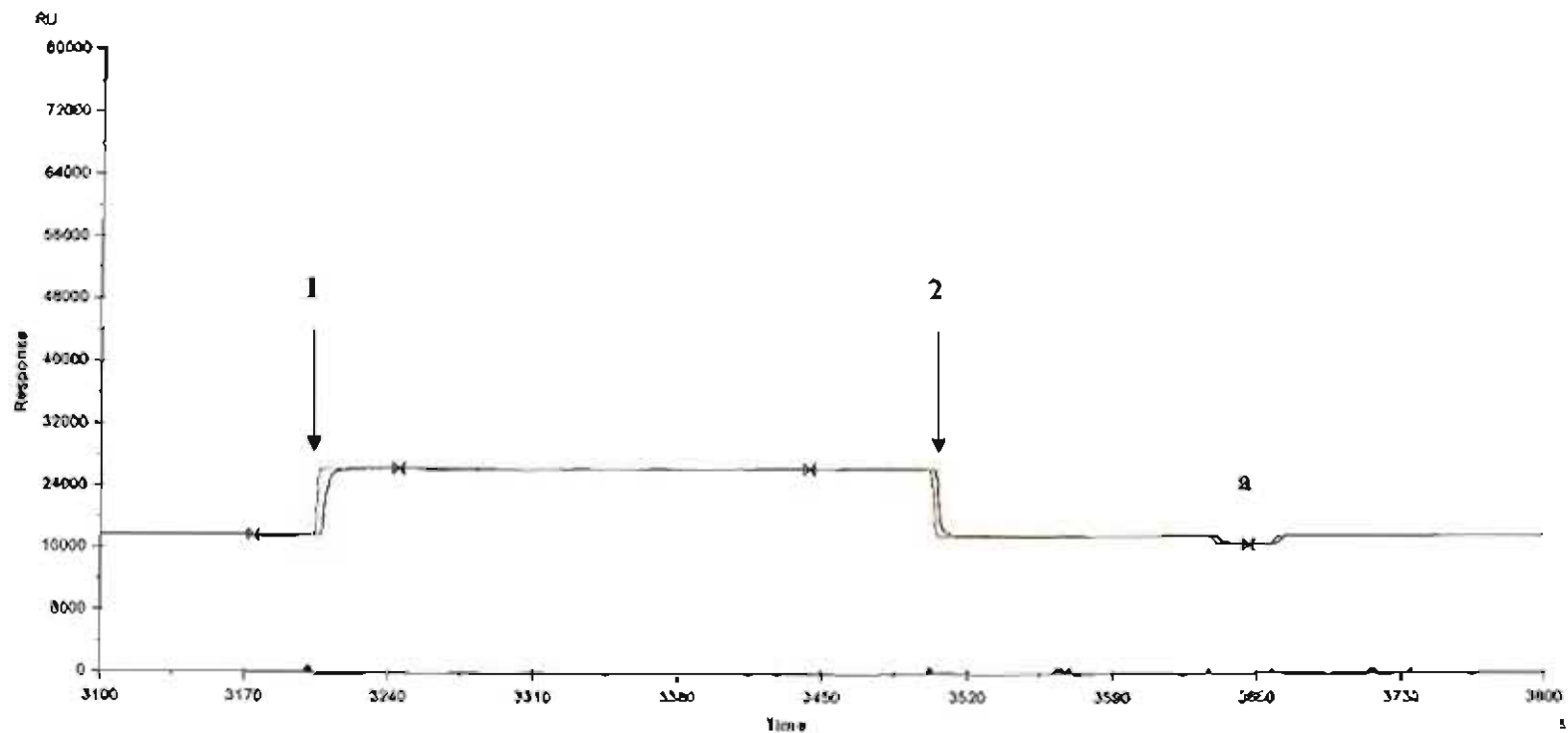


Figure 3.48. Sensogram showing the interaction between the Peptidoglycan with intact teichoic acids (shown in Red) and Peptidoglycan without teichoic acids (shown in Green) in the presence of a 50µl crude autolytic extract for *Streptococcus milleri* B200. The arrows (↓) 1 and 2 indicate the start and end of the injection of the autolysin sample. The symbol (a) depicts the regeneration of the sensor chip with 5µl NaOH.

3.12. Auto Inducing Peptide (AIP) Assays

It has been shown in bacteria that a variety of physiological changes in the bacterial population are dependent on specific cell densities and growth phases. Peptides are the most common and well studied signalling molecules in Gram positive bacteria, often referred to as auto-inducing peptides (AIP). These peptides show a variety of structures but share in that they are a small size, ribosomally synthesized, and are in certain instances subjected to post-translational modifications that add to their stability and functionality (Figure 3.49.).

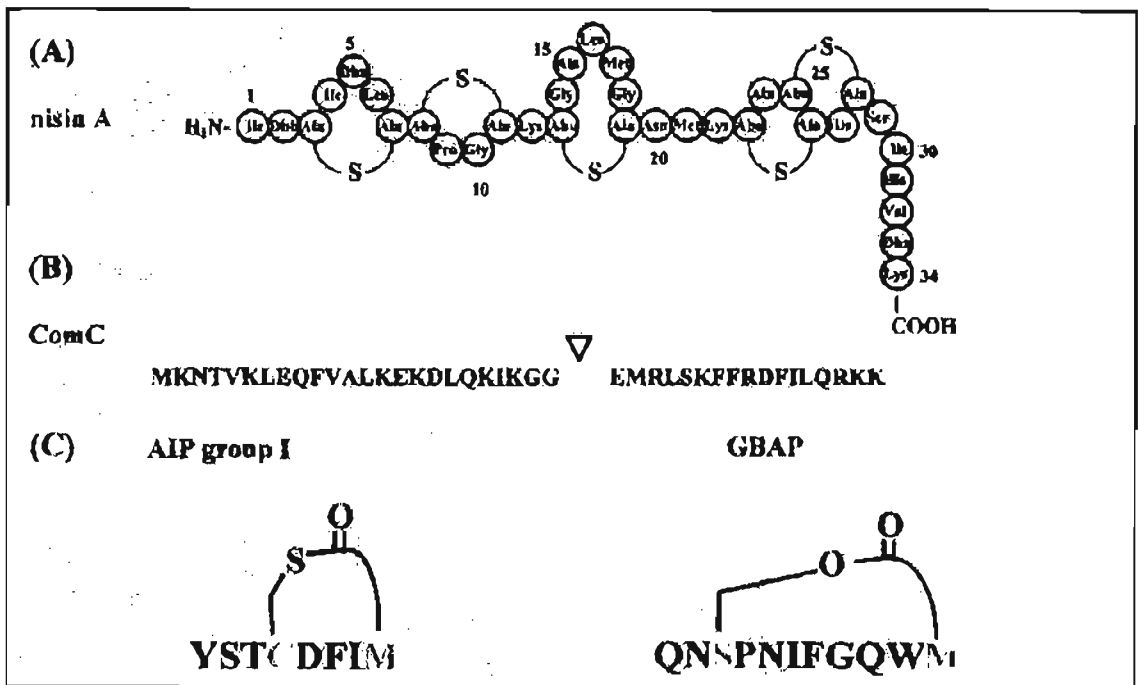


Figure 3.49. Structural diversity of auto-inducing peptides found in Gram positive bacteria. (A) Lantibiotic nisin of *Lactococcus lactis*; (B) Competence development (ComC) found in *Streptococcus pneumoniae* and (C) Cyclic thiolactone- and lactone- peptides, AIP group I of *Staphylococcus aureus* and GBAP (gelatinase biosynthesis-activating pheromone) found in *Enterococcus faecalis*. [Strume *et al.*, 2002]

Staphylococcal pathogenesis is regulated by a two-component quorum-sensing system, accessory gene regulator (*agr*), activated upon binding of a self-coded auto-inducing peptide to the receptor-histidine kinase, AgrC. The expression of most virulence factors in *Staphylococcus aureus* strains is controlled by the *agr* locus. This locus encodes a two-component signalling pathway whose activating ligand is an *agr*-encoded auto-inducing peptide (AIP). The AIPs consist of a thiolactone macrocycle and an exocyclic "tail", both of which are important for its functionality. Within a given group, each strain produces a peptide that can activate the *agr* response in the other member strains, whereas the AIP's belonging to different groups are mutually inhibitory. This assay was designed to establish the effect that AIP would have on the autolytic rate of the *Streptococcus milleri* P35 and B200 respectively. A control *Staphylococcus aureus* strain was used to isolate the auto-inducing peptide to be incorporated as the AIP additive in the respective assays.

The regression patterns obtained in these assays show evidence that the incorporated AIP additive does affect the autolytic rate. In most instances the respective rates were increased (Figure 3.50.). Auto-inducing peptide was precipitated out of its culture supernatant using a gradient decreasing ammonium sulphate concentration method. This method allowed for decreasing values of AIP to be collected prior to been incorporated into the assays. The cross-reactive nature of the AIP should in theory also be able to induce an autolytic response when introduced into the assay buffer with whole bacterial cells of the *Streptococcus* strains. The regression patterns obtained clearly indicates a higher autolytic rate for each assay when in the presence of both the AIP additive as well as the antibiotic stress, Ampicillin (Figure 3.51.).

Monitoring the regression pattern in Figure 3.51., it can be estimated that the rate of autolysis is actually increased by 10-fold. The incorporation of the AIP additive at 80, 60 and 20% respectively showed an increase in the autolytic rates for both the Streptococcal and the Staphylococcal isolates. This establishes that the AIP does indeed possess a cross-reactive nature in that an autolytic expression is induced when the peptide is present. The most significant increase in the autolytic pattern was seen when the 60% AIP additive was introduced to each assay. At this percentage concentration of the peptide overall lysis for each

bacterial strain was promoted. The AIP acts as a signalling molecule in each case, inducing an increased rate of autolysis.

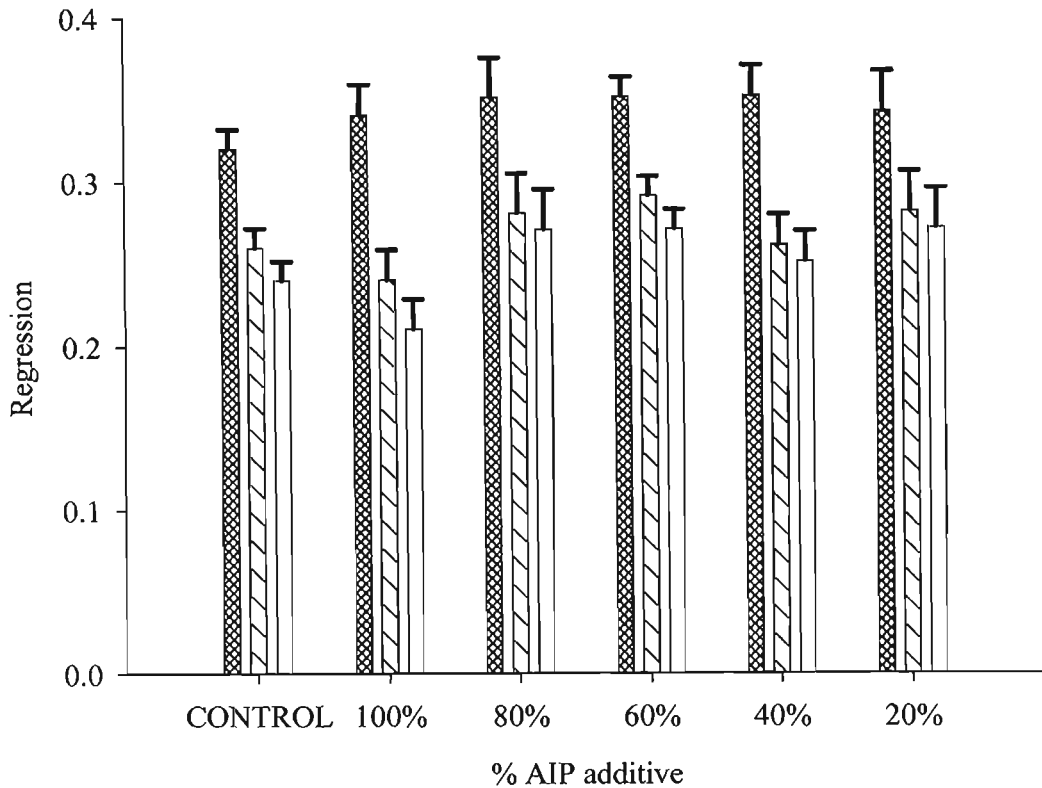


Figure 3.50. Regression patterns monitoring the rate of autolysis in the presence of differing percentages of Auto-Inducing Peptide additives (% AIP) isolated from a control *Staphylococcus aureus* strain. The standard deviation (\top) is plotted above the bar. The plots are represented as follows: (▨) – *S. aureus*; (▧) – *S. milleri* P35 and clear bars – *S. milleri* B200. The control plots represent no percentage of AIP added to the assay. This assay was conducted in the absence of antibiotic stress.

Figure 3.51. shows that the presence of the antibiotic works in correlation with the peptide to create an overall increase in the autolysis pattern. It is more significant in the Streptococcal isolates, seen as the (//) and clear bars in Figure 3.51. The peptide seems to signal the lysis of the bacterial cells creating such a steep increase in the slope of autolysis. The 80 and 60% additive promoted the highest increase in the autolytic rate for *S. milleri* P35, which has been know to be morphologically different in its structure to that of *S. milleri* B200. In comparison to the zymogram analysis which showed *S. milleri* P35 to have a lowered activity of its autolysins, a direct correlation can now be established that the AIP does promote autolytic processing, and subsequent lysis. Thus it can be established that in the case of *S. milleri* P35, lysis can be increased significantly when in the presence of an antibiotic stress as well as the incorporation of the signalling peptide. Thus a similar two component system as previously explained could very well be identified in the Streptococcal isolates.

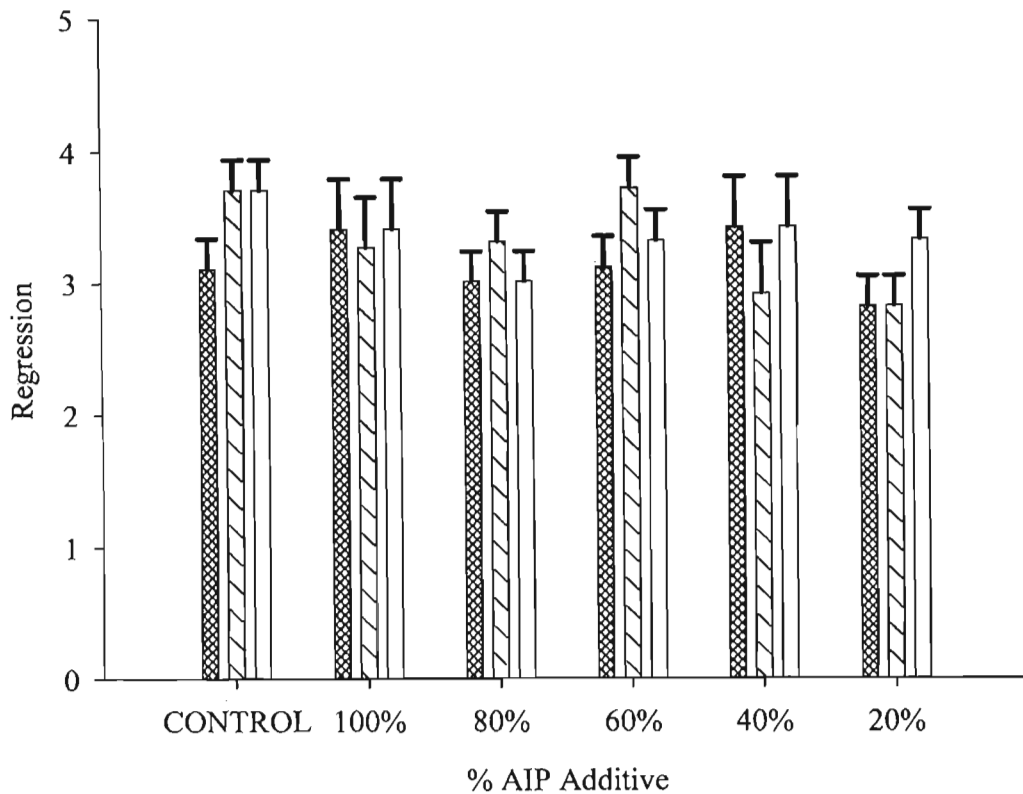


Figure 3.51. Regression patterns monitoring the rate of autolysis in the presence of differing percentages of Auto-Inducing Peptide additives (% AIP) isolated from a control *Staphylococcus aureus* strain. The standard deviation (\top) is plotted above the bar. The plots are represented as follows: (⊗) – *S. aureus*; (\\) – *S. milleri* P35 and clear bars – *S. milleri* B200. To each of the reactions ampicillin below the MIC value at $5\mu\text{g/ml}$ was incorporated. The control plots represent the autolytic rates in the absence of auto-inducing peptide.

3.13. Molecular manipulations

DNA was isolated using the Nucleospin Tissue Kit and analyzed via agarose gel electrophoresis. The isolated DNA was visualized as a single bright band under ultra violet light as seen in Figure 3.52. Spectrophotometric analysis was also employed to determine the concentration of the DNA (Table 3.2.). This DNA provided the template for the polymerase chain reactions which aimed to establish if the *agr* system present in *S. aureus* is also found in the Streptococcal isolates. Both types of analysis showed that a high yield of DNA was obtained for the isolations using the Nucleospin Tissue Kit and that PCR could be carried out.

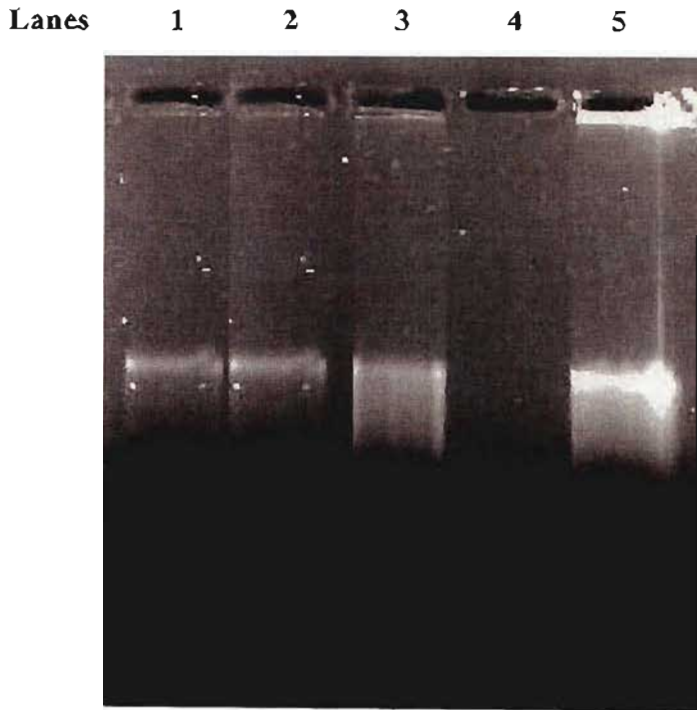


Figure 3.52. Isolated DNA from *Streptococcus milleri* and *Staphylococcus aureus* strains. Lanes 1: *S. milleri* P35 DNA; 2: *S. milleri* 77 DNA; 3: *S. milleri* B200 DNA; and 5: *S. aureus* DNA.

Table 3.2. Concentration of the DNA samples from the bacterial isolates, analyzed using the NanoDrop Spectrophotometer.

Bacterial Isolate	Concentration (ng/μl)	A₂₆₀ Value	A₂₆₀ / A₂₈₀ Ratio
<i>S. milleri</i> P35	141.37	1.027	1.8
<i>S. milleri</i> 77	104.64	2.093	1.27
<i>S. milleri</i> B200	417.84	8.357	1.70
<i>S. aureus</i>	708.11	14.162	1.24

Analyzing the agarose gel, Figure 3.52. and the spectrophotometric analysis (Table 3.2.), the concentration of the DNA isolated could be directly correlated. Brighter DNA bands as seen in Figure 3.52. are indicative of a higher yield and higher DNA concentrations. Traces of impurities in the DNA sample can be accounted for as an inflated A₂₆₀ value (Table 3.2.), seen for *S. aureus*.

The primers chosen were based on the universal PAN set, designed to amplify distinct areas within the *agr* locus [Jarraud, *et al.*, 2002]. These primers were successfully used in clinical isolates to determine their *agr* type. The four different *agr* reverse primers were used to evaluate the *agr* locus nucleotide polymorphism for the identification of *agr* auto-inducer receptor specificity groups [Shopsin *et al.*, 2003]. In this investigation the PCR analysis was unsuccessful. The protocol could not be optimized to reveal the desired amplicons. Optimization involved profiling the magnesium chloride concentrations, DNA template concentrations, primer concentrations as well as reducing the stringency of the reaction by reducing the annealing temperature from 45°C to 35°C. No amplification was obtained for the control *S. aureus* strain, which theoretically contains the *agr* system. Amplicons at the specified base pair value should have been observed in the control strain. For future studies, Real Time PCR maybe employed to obtain the desired amplicons. More stringent parameters can be incorporated and perhaps new primers can be designed using Primer Express software analysis.

CHAPTER FOUR

CONCLUSION AND FUTURE STUDIES

This investigation has allowed for the partial characterization of the autolytic system in *Streptococcus milleri* 77. *S. milleri* 77 had a low autolytic expression during the early and late exponential phases of its growth cycle. The autolytic expression of strain 77 was concentrated to the late exponential phase of growth and continued into the stationary phase. The autolytic profile of *S. milleri* strain 77 was characterized to have four major autolysins, a muramidase, a peptidase, an aminidase and an endopeptidase. This is the first report on the autolytic system of *Streptococcus milleri*.

Two-dimensional analysis revealed a number of proteins that can now be implicated as antibiotic sensitive constituents. Autolytic proteins have been identified in this map by virtue of their differences or absence. Proteomic analysis can now further be explored, to generate a complete 2-Dimensional map of the *Streptococcus milleri* proteome on the basis of their autolysins. The regulation of the autolysins monitored in the presence of antibiotic stress can hold the key to the understanding of how these genes are expressed and subsequently regulated.

Bacteria have found ways to modulate their anionic cell wall polymers. This investigation has shown that teichoic acids play a vital role in the regulation of autolysins. These polymers are responsible for altering the ion charged environment within the bacterial cell wall, facilitating the binding of autolysins to the anionic bacterial cell envelopes. The autolytic assays and the molecular interactive studies showed that teichoic acids promote the rates of autolysis within the bacterial cell. The absence of these polymers in the peptidoglycan layer resulted in lowered rates of autolysis. Lowered rates of autolysis were observed in strains which exhibited putative-free autolysin content. *S. milleri* P35 displayed such results, and in this instance the absence of teichoic acids promoted autolysis.

The incorporation of an AIP additive in the autolysis patterns indicates that, as in the case of *Staphylococcus aureus*, most virulence factors are controlled by signaling pathways activated by these peptides. The cross-reactive nature of the AIP, isolated from the *S. aureus* strain, was able to induce an increased autolytic response in the *S. milleri* strains. Although, the PCR analysis, to determine if a two component-system was present in *Streptococcus milleri*

strains, was unsuccessful futures studies can employ Real Time PCR analysis in order to optimize the protocol. This makes for interesting discoveries, should a similar system be present in *Streptococcal* strains. Subsequent molecular characterization can be established.

Drug resistance has been identified as the key problematic area in most infectious diseases. This makes the various resistance mechanisms, very important, in its capacity to combat the spread of these infectious agents.

Thus the application of this research has great potential in the development of antibiotics in relation to multiple drug resistance. Employing the knowledge attained from the characterization of these autolysins, their proteomic profiles as well as their autolytic pathways by means of their regression patterns, the genomes of the bacterial strains can now be sequenced and the genes responsible for the switching on or off of these autolysins can be established. A detailed molecular and biochemical approach to study this autolytic system by cloning and expression of the autolytic genes will contribute in the future to fully explain the physiological role of the enzymes.

CHAPTER FIVE

REFERENCES

REFERENCES

1. **Aasjord, P., and A. Grov.** 1980. Immunoperoxidase and electron microscopy studies of Staphylococcal lipoteichoic acid. *Acta. Pathol. Microbiol. Scand. Sect. B* **Volume 88**: 47-52.
2. **Alaedini, A., and N. Latov.** 2002. Measurements of antibody levels in autoimmune neuropathies using SPR technology. *Biacore Journal.* **Volume 1**: 12-13.
3. **Archibald, A.R.** 1974. The structure, biosynthesis and function of teichoic acid. *Adv. Micro. Physio.* **Volume 11**: 53-95.
4. **Archibald, A.R., Armstrong, J.J., Baddiley, J., and J.B. Hay.** 1961. Teichoic acids and the structure of bacterial walls. *Nature.* **Volume 191**: 570-572.
5. **Baddiley, J., Buchanan, J., Martin, G., and U.L. RajBhandary.** 1962. Teichoic acids from the walls of *Staphylococcus aureus* H: location of the phosphate and alanine residues. *Biochem. J.* **Volume 82**: 439-448.
6. **Baddiley, J.** 2000. Teichoic acids in bacterial co-aggregation. *Micobiol.* **Volume 146**: 1257-1258.
7. **Beachely, E.H., Keck, W., De Pedro, M., and U. Schwarz.** 1981. Exoenzymatic activity of transglycosylases isolated from *Escherichia coli*. *Eur. J. biochem.* **Volume 116**: 355-358.
8. **Beliveau, C., Potvin, C., Trudel, J., Asselin, A., and G. Bellemare.** 1991. Cloning, sequencing and expression in *Escherichia coli* of a *Streptococcus faecalis* autolysin. *J. Bacteriol.* **Volume 173**: 5619-5623.
9. **Betzner, A.S., Ferreira, L.S.C., Holtje, V.D., and W. Keck.** 1990. Control of the activity of the soluble lytic transglycosylase by the stringent response in *Escherichia coli*. *FEMS Microbiol. Lett.* **Volume 55**: 161-164.

10. **Betzner, A.S., Ferreira, L.S.C., Holtje, V.D., and W. Keck.** 1990. The R gene product of bacteriophage λ is the murein transglycosylase. *FEMS Microbiol. Lett.* **Volume 67:** 161-164.
11. **Betzner, A.S., and W. Keck.** 1989. Molecular cloning, over-expression and mapping of the *slt* gene encoding the soluble lytic transglycosidases of *Escherichia coli*. *Mol. Gen. Genet.* **Volume 219:** 489-491.
12. **Beukes, M., Bierbaum, G.S., and J.W. Hastings.** 2000. Purification and partial characterization of a murein hydrolase, Millericin B, produced *Streptococcus milleri* NMSCC 061. *Appl. Environ. Microbiol.* **Volume 66:** 23-28.
13. **Beukes, M., and J.W. Hastings.** 2001. Self-protection against cell wall hydrolysis in *Streptococcus milleri* NMSCC 061 and analysis of the Millericin B operon. *Appl. Environ. Microbiol.* **Volume 67:** 3888-3896.
14. **Bienkowska-Szewczyk, K., Lipinska, B., and A. Taylor.** 1981. The R gene product of bacteriophage λ is the murein transglycosylase. *Mol. Gen. Genet.* **Volume 184:** 111-114.
15. **Bierbaum, G., and H.G. Sahl.** 1987. Induction of autolysis of *Staphylococcus simulans* 22: influence of cationic peptides on activity of N-acetylmuramoyl-L-alanine amidase. *J. Bacteriol.* **Volume 169:** 5452-5458.
16. **Bourgogne, T., Vacheron, M.J., Guimand, M., and G. Michel.** 1992. Purification and partial characterization of the gamma-D-glytanyl-L-di-amino acid endopeptidase II from *Bacillus sphaericus*. *Int. J. Biochem.* **Volume 24:** 471-476.
17. **Calamita, H.G., and R.J. Doyle.** 2002. Regulation of autolysins in teichuronic acid-containing *Bacillus subtilis* cells. *Mol. Microbiol.* **Volume 44:** 601-606.
18. **Cash, P.** 1998. Characterization of bacterial genomes by two-dimensional electrophoresis. *Analy. Chimica ACTA.* **Volume 372:** 121-145.

19. **Clark, A.J., and C. Dunpont.** 1992. O-Acetylated peptidoglycan: its occurrence, pathobiological significance and biosynthesis. *Can. J. Microbiol.* **Volume 38:** 85-91.
20. **Clark-Sturman, A.J., Archibald, A.R., Hancock, I.C., Harwood, C.R., Merad, T., and J.A. Hobot.** 1989. Cell wall assembly in *Bacillus subtilis*: partial conversion of polar wall material and the effect of growth conditions on the pattern of incorporation of new material at the polar caps. *J. Gen. Microbiol.* **Volume 135:** 657-665.
21. **Cleveland, R.F., Wicken, A.J., Daneo-Moore, L., and G.D. Shockman.** 1976. Effect of lipoteichoic acid and lipids on lysis of intact cells of *Streptococcus faecalis*. *J. Bacteriol.* **Volume 127:** 1582-1854.
22. **Coley, J., Tarelli, E., Archibald, A.R, and J. Baddiley.** 1978. The linkage between teichoic acid and peptidoglycan in bacterial cell walls. *FEBS Lett.* **Volume 88:** 1-9.
23. **Costerton, J.W., Irvin, R.T., and K.-J. Cheng.** 1981. The bacterial glycocalyx in nature and disease. *Annu. Rev. Microbiol.* **Volume 35:** 299-324.
24. **Coyette, J., and J.M. Ghusen.** 1970. Wall autolysin of *Lactobacillus acidophilus* strain 63 AM Gasser. *Biochemistry.* **Volume 9:** 2952-2955.
25. **Coyette, J., and G.D. Shockman.** 1973. Some properties of the autolytic N-acetylmuramidases of *Lactobacillus acidophilus*. *J. Bacteriol.* **Volume 114:** 31-41.
26. **Davie, J.M., and T.D. Brock.** 1966. Effect of teichoic acid on resistance to the membrane-lytic agent of *Streptococcus zymogenes*. *J. Bacteriol.* **Volume 92:** 1623-1631.
27. **Doi, R.H.** 1989. *In Bacillus.* Harwood. C.R. Sporulation and germination. London: Plenum Press. 169-215.

28. **Dolinger, D.L., Daneo-Moore, L., and G.D. Shockman.** 1989. The second peptidoglycan hydrolase of *Streptococcus faecium* ATCC 9790 covalently binds penicillin. *J. Bacteriol.* **Volume 171:** 4355-4361.
29. **Dolinger, D.L., Schramm, V.L., and G.D. Shockman.** 1988. Covalent modification of the β -1,4-N-acetylmuramoylhydrolase of *Streptococcus faecium* with 5-mercaptouridine monophosphate. *Proc. Natl. Acad. Sci. USA.* **Volume 85:** 6667-6671.
30. **Doyle, R.J., and R.E. Marquis.** 1994. Elastic, flexible peptidoglycan and bacterial cell wall properties. *Trends Microbiol.* **Volume 2:** 57-60.
31. **Edman, P. and A. Henschen.** 1975. Needleman S.B. In Protein sequence determination: a sourcebook of methods and techniques. New York Springer-Verlag. 211-279.
32. **Ellwood, D.C.** 1971. The anionic polymers in the cell wall of *Bacillus subtilis* var. *niger* grown in phosphorus-limiting environments supplemented with increasing concentrations of sodium chloride. *Biochem. J.* **Volume 118:** 367-373.
33. **Endl, J., Seidl, H.P., Fiedler, F., and K.H. Schleifer.** 1983. Chemical composition and structure of teichoic acids of *Staphylococci*. *Arch. Microbiol.* **Volume 135:** 215-223.
34. **Engel, H., Kazemeir, B., and W. Keck.** 1991. Murein-metabolising enzymes from *Escherichia coli*: sequence analysis and controlled over-expression of the *sly* gene, which encodes the soluble lytic transglycosylases. *J. Bacteriol.* **Volume 175:** 120-210.
35. **Engel, H., Smink, J., van Wijngaarden, L., and W. Keck.** 1992. Murein-metabolising enzymes from *Escherichia coli*: on the existence of second lytic transglycosylases. *J. Bacteriol.* **Volume 175:** 130-210.
36. **Fiedler, F., and L. Glaser.** 1973. Assembly of bacterial cell walls. *Biochem. Biophys. Acta.* **Volume 300:** 467-485.

37. **Fisher, W.** 1994. Lipoteichoic acids and lipoglycans. *New Compr. Biochem.* **Volume 27:** 199-215.
38. **Fisher, W., Rosel, P., and H.U. Koch.** 1981. Effect of alanine ester substitution and other structural features of lipoteichoic acids on their inhibitory activity against autolysins of *Staphylococcus aureus*. *J. Bacteriol.* **Volume 146:** 467-475.
39. **Foley, M., Brass, J.M., Birmingham, J., Cook, W.R., Garland, P.B., Higgins, C.F., and L.I. Rothfield.** 1989. Compartmentalization of the periplasm at cell division sites in *Escherichia coli* as shown by fluorescence photo-bleaching experiments. *Mol. Microbiol.* **Volume 3:** 1329-1336.
40. **Foster, S.J.** 1992. Analysis of the autolysins of *Bacillus subtilis* 168 during vegetative growth and differentiation by using renaturation polyacrylamide gel electrophoresis. *J. Bacteriol.* **Volume 174:** 464-470.
41. **French, G.L.** 1998. *Enterococci* and vancomycin resistance. *Clin. Infect. Dis.* **Volume 27:** 75-83.
42. **Fujimoto, D.F., and K.W. Bayles.** 1998. Opposing roles of the *Staphylococcus aureus* virulence regulators, Agr and Sar, in Triton X-100- and penicillin-induced. *J. Bacteriol.* **Volume 180:** 3724-3726.
43. **Fuqua, C., and E.P. Greenberg.** 1998. Self perception in bacteria: quorum sensing with acylated homoserine lactones. *Curr. Opin. Microbiol.* **Volume 3:** 132-137.
-
44. **Gardeye, S., Ludovice, A.M., Sobral, R.G., de Lencastre, H., and A. Tomasz.** 2004. Role of *murE* in the expression of β -lactam antibiotic resistance in *Staphylococcus aureus*. *J. Bacteriol.* **Volume 186:** 1705-1713.
45. **Gholson, J.L., Mayville, P., Muir, T.W., and R.P. Novick.** 2000. Rational design of a global inhibitor of the virulence response in *Staphylococcus aureus*, based in part on localization of the site of inhibition to the receptor-histidine, AgrC. *Proc. Natl. Acad. Sci. USA.* **Volume 91:** 13330-13335.

46. **Ghuysen, J.-M., Tripper, D.J., and J.L. Stroinger.** 1966. Enzymes that degrade cell walls, p. 685-699. In E.F. Neufeld (ed.), *Methods. Enzymology. Volume VII.* Academic Press Inc.
47. **Ghuysen, J.M., and G.D. Shockman.** 1973. In: Leive (Ed.) *Bacterial membranes and walls.* New York: Marcel Dekker, 37-130.
48. **Giesbrecht, P., Kersten, T., Maidhof, H. and Wecke, J.** 1998. *Staphylococcal* cell wall: morphogenesis and fatal variations in the presence of penicillin. *Micro. and Molec. Bio. Reviews.* **Volume 62:** 1371-1414.
49. **Gmeiner, J., and H.P. Kroll.** 1981. Membranes of the protoplast L-form of *Proteus mirabilis*. *FEBS. Lett.* **Volume 129:** 142-144.
50. **Goddell, E.W., and C.F. Higgins.** 1987. Uptake of cell wall peptides by *Salmonella typhimurium* and *Escherichia coli*. *J. Bacteriol.* **Volume 169:** 3861-3865.
51. **Green, A.A. and W.L. Hughes.** 1955. Protein fractionation on the basis of solubility in aqueous solutions of salts and organic solvents. *Methods. Enzymology.* **Volume I:** 68- 96.
52. **Green, R.J., Frazier, R.A., Shakesheff, M., Davies, M.C., Roberts, C.J., and S.J.B. Tendler.** 2000. Surface plasmon resonance analysis of dynamic biological interactions with biomaterials. *Biomaterials.* **Volume 21:** 1823-1835
53. **Gutberlet, T., Frank, J., Bradacek, H., and W. Fisher.** 1997. Effect of lipoteichoic acid on thermotrophic membrane properties. *J. Bacteriol.* **Volume 179:** 2879-2883.
54. **Hakenbeck, R., König, A., Kern, I., van der Linden, M., Keck, W-G., Billot-Klien, D., Legrand, R., Schoot, B., and L. Gutmann.** 1998. Acquisition of five high M_r Penicillin binding protein variants during transfer of high β -lactam resistance from *Streptococcus mitis* to *Streptococcus pneumoniae*. *J. Bacterio.* **Volume 180:** 1831-1840.

55. **Hancock, L., and M. Perego.** 2002. Two-component signal transduction in *Enterococcus faecalis*. *J. Bacteriol.* **Volume 184:** 5819-5825.
56. **Hartmann, R., Bock-Hennig, S.B., and U. Schwartz.** 1974. Murein hydrolases in the envelope of *Escherichia coli*. Properties *in situ* and solubilization from the envelope. *Eur. J. Biochem.* **Volume 41:** 203-208.
57. **Harz, H., Burgdorf, K., and J.V. Holtje.** 1990. Isolation and separation of the glycan strands from murein of *Escherichia coli*. By reversed-phase high performance liquid chromatography. *Anal. Biochem.* **Volume 190:** 120-128.
58. **Heijne, G.** 1986. A new method for predicting signal sequence cleavage sites. *Nucleic Acids Res.* **Volume 14:** 4693-4690.
59. **Henderson, T.A., Dombrosky, P.M., and K.D. Young.** 1994. Artificial processing of penicillin-binding proteins 7 and 1b by the Omp T protease of *Escherichia coli*. *J. Bacteriol.* **Volume 103:** 504-512.
60. **Herbold, D.R., and L. Glaser.** 1975. *Bacillus subtilis* N-acetylmuramic acid L-alanine amidase. *J. Biol. Chem.* **Volume 250:** 519-521.
61. **Higgins, M.L., Pooley, H.M., and G.D. Shockman.** 1970. Site of initiation of cellular autolysis in *Streptococcus faecalis* as seen by electron microscopy. *J. Bacteriol.* **Volume 103:** 504-512.
62. **Holtje, J.V.** 1995. From growth to autolysis: the murein hydrolases in *Escherichia coli*. *Arch. Microbiol.* **Volume 164:** 243-254.
63. **Holtje, J.V., Mirelman, N.S., and U. Schwarz.** 1975. Novel types of murein transglycosylase in *Escherichia coli*. *J. Bacteriol.* **Volume 124:** 1067-1076.
64. **Holtje, J.V., and A. Tomasz.** 1976. Purification of the pneumococcal N-acetyl-muramyl-L-alanine amidase to biochemical homogeneity. *J. Biol. Chem.* **Volume 251:** 4199-4207.
65. **Holtje, J.V., and E.I. Tuomanen.** 1991. The murein hydrolases of *Escherichia coli*: properties, functions and impact on the course of infection *in vitro*. *J. Gen. Microbiol.* **Volume 137:** 441-454.

66. **Hourdou, M.L., Duez, C., Joris, B., Vacheron, M.J., Guinand, M., Michel, G., and J.M. Ghuysen.** 1992. Cloning and nucleotide sequence of the gene encoding the γ -D-glutamyl-L-diamino- acid endopeptidase II of *Bacillus sphaericus*. FEMS Microbiol. Lett. **Volume 91**: 165-170.
67. **Ingavale, S., van Wamel, W., Luong, T.T., Lee, C.Y., and A.L. Cheung.** 2005. Rat/MgrA, a regulator of autolysis, is a regulator of virulence genes in *Staphylococcus aureus*. Infect. and Immunity. **Volume 73**: 1423-1431.
68. **Iwasaki, H., Shimada, A., Yokoyama, K., and E. Ito.** 1986. Structure and glycosylation of lipoteichoic acids in *Bacillus* strains. J. Bacteriol. **Volume 171**: 424-429.
69. **Jarraud, S., Mougel, C., Thioulouse, J., Lina, G., Meugnier, H., Forey, F., Nesme, X., and F. Vandenesch.** 2002. Relationship between *Staphylococcus aureus* genetic background, Virulence factors, *agr* groups (Alleles, and Human disease). Infect. and Immunity. **Volume 70**: 631-641.
70. **Jenni, R., and B. Berger-Bachi.** 1998. Teichoic acid in different lineages of *Staphylococcus aureus* NCTC8325. Arch. Microbiol. **Volume 170**: 171-178.
71. **Jett, B.D., Huycke, M.M., and M.S. Gilmore.** 1994. Virulence of *Enterococci*. Clin. Microbiol. Rev. **Volume 7**: 462-478.
72. **Jolliffe, L.K., Doyle, R.J., and U.N. Streips.** 1981. The energized membrane and cellular autolysis in *Bacillus subtilis* cell. **Volume 25**: 753-763.
73. **Joseph, R., and G.D. Shockman.** 1947. Autolytic formation of protoplast (autoplast) of *Streptococcus faecalis* 9790: Release of cell wall, autolysin and formation of stable autoplast. Antimicro. Agents Chemother. **Volume 40**: 789-801.
74. **Kariyama, R., and G.D. Shockman.** 1992. Extracellular and cellular distribution of muramidase-2 and muramidase-1 of *Escherichia hirae*. J. Bacteriol. **Volume 174**: 3236-3241.

75. **Kawamura, T., and G.D. Shockman.** 1983. Evidence for the presence of a second peptidoglycan hydrolase in *Streptococcus faecium*. FEMS. Microbiol. Lett. **Volume 19:** 65-69.
76. **Keck, W., and U. Schwartz.** 1979. *Escherichia coli* murein DD-endopeptidase insensitive to β -lactam antibiotics. J. Bacteriol. **Volume 139:** 770-774.
77. **Koch, A.** 2001. Autolysis Control Hypothesis for Tolerance to wall antibiotics. Antimicro. Agents Chemo. **Volume 45:** 2671-2675.
78. **Koch, A.L., and R. J. Doyle.** 1985. Inside-to-outside growth and turnover of the wall of gram-positive rods. J.Theor. Biol. **Volume 117:** 132-157.
79. **Komatsuzawa, H., Suzuki, J., Sugai, M., Miyake, Y., and H. Suginaka.** 1994. The effect of Triton X-100 on the in vitro susceptibility of methicillin-resistant *Staphylococcus aureus* to oxacillin. J. Antimicrob. Chemother. **Volume 34:** 885-897.
80. **Korat, B., Mottl, H., and W. Keck.** 1991. Penicillin-binding protein 4 of *Escherichia coli*: molecular cloning of the *dacB* gene controlled over-expression, and alterations in the murein composition. Mol. Microbiol. **Volume 5:** 675-684.
81. **Kuroda, A., Rashid, M.H., and J. Sekiguchi.** 1992. Molecular cloning and sequencing of the upstream region of the major *Bacillus subtilis* autolysin gene: a modifier protein exhibiting sequence homology to the major autolysin and the *spoIID* product. J. Gen. Microbiol. **Volume 139:** 1067-1076.
82. **Labischinski, H., Naumann, D., and W. Fisher.** 1991. Small- and medium-angle X-ray analysis of bacterial lipoteichoic acid phase structure. Eur. J. Biochem. **Volume 202:** 1269-1274.
83. **Laemmli, U.K.** 1970. Cleavage of structural proteins during the assembly of the head bacteriophages T4. Nature. **Volume 227:** 680-685.

84. **Leitch, E.C., and M.D.P. Willcox.** 1999. Elucidation of the antistaphylococcal action of lactoferrin and lysozyme. *J. Med. Microbiol.* **Volume 48:** 867-871.
85. **Leopold, K., and W. Fisher.** 1992. Hydrophobic interaction chromatography fractionates lipoteichoic acid according to the size of the hydrophilic chain: a comparative study with anion-exchange and affinity chromatography for suitability in species. *Anal. Biochem.* **Volume 201:** 350-355.
86. **Levin, P.A., and A.D. Grossman.** 1998. Cell cycle and sporulation in *Bacillus subtilis*. *Curr. Opin. Microbiol.* **Volume 1:** 630-635.
87. **Lewis, K.** 2000. Programmed death in bacteria. *Microbiol. Mol. Biol. Rev.* **Volume 64:** 503-514.
88. **Liedberg, B., Nylander, C., and I. Lundström.** 1995. Biosensing with surface plasmon resonance – how it all started. *Bioanalytical History Report.* **Volume 10:** i-ix.
89. **Margot, P., Wahlen, M., Gholamhuseinian, P., and D. Karamata.** 1998. The *lytE* gene of *Bacillus subtilis* 168 encodes a cell wall hydrolase. *J. Bacteriol.* **Volume 180:** 749-752.
90. **Markiewicz, Z., Broome-Smith, J., Schwartz, U., and B-G. Spratt.** 1982. Spherical *Escherichia coli* due to alleviated levels of D-alanine carboxypeptidase. *Nature.* **Volume 297:** 702-704.
91. **Maurer, J.J., and S.J. Mattingly.** 1991. Molecular analysis of lipoteichoic acid from *Streptococcus agalactiae*. *J. Bacteriol.* **Volume 173:** 487-494.
92. **Mayer, F.** 1993. Principles of functional and structural organisation in the bacterial cell: 'compartments' and their enzymes. *FEMS Microbiol. Rev.* **Volume 104:** 327-346.
93. **Maynard, J., and G. Georgiou.** 2000. Antibody Engineering. *Annual Review Bio. Engineering.* **Volume 2:** 339-376.

94. **McDonnell, J.M.** 2001. Surface plasmon resonance: towards an understanding of the mechanisms of biological molecular recognition. *Curr. Opinion Chem. Bio.* **Volume 5**: 572-577.
95. **Merad, T., Archibald, A.R., Hancock, I.C., Harwood, C.R., and J.A. Hobot.** 1989. Cell wall assembly in *Bacillus subtilis*: visualization of old and new wall material by electron microscopic examination of samples stained selectively for teichoic acid and teichuronic acid. *J. Gen. Microbiol.* **Volume 135**: 645-655.
96. **Metzstein, M.M., Stanfield, G.M., and H.R. Horvitz.** 1998. Genetics of programmed cell death in *C. elegans*: past, present and future. *Trends Genet.* **Volume 14**: 410-416.
97. **Millward, G.R., and D.A. Reaveley.** 1974. Electron microscope observations on the cell walls of some gram-positive bacteria. *J. Ultrastruct. Res.* **Volume 46**: 309-326.
98. **Mitchell, P., and J. Moyle.** 1957. Autolytic release and osmotic of 'protoplast' from *Staphylococcus aureus*. *J. Gen. Microbiol.* **Volume 16**: 184-194.
99. **Morrissey, J. H.** 1981. Silver stain for proteins in polyacrylamide gels: a modified procedure with enhanced uniform sensitivity. *Anal. Biochem.* **Volume 117**: 307-310.
100. **Mortier-Barriere, I., de Saizieu, A., Claverys, J.P., and B. Martin.** 1998. Competence-specific induction of *recA* is required for full recombination proficiency during transformation in *Streptococcus pneumoniae*. *Mol. Microbiol.* **Volume 27**: 159-170.
101. **Myszka, D. G.** 1999. Improving biosensor analysis. *J. Mol. Recog.* **Volume 12**: 279-284.

102. **Nakao, A., Imai, S.-I., and T. Takano.** 2000. Transposon-mediated insertional mutagenesis of the D-alanyl-lipoteichoic acid (*dlt*) operon raises methicillin resistance in *Staphylococcus aureus*. *Res. Microbiol.* **Volume 151:** 823-829.
103. **Neidhardt, F.C., Appleby, D.B., Sankar, P., Hutton, M.E., and T.A. Phillips.** 1989. Genomically linked cellular protein databases derived from 2-Dimensional polyacrylamide gel electrophoresis. *Electrophoresis.* **Volume 10:** 116.
104. **Neuhaus, F.C., and J. Baddiley.** 2003. A continuum of anionic charge: structure and functions of D-alanyl-teichoic acids in gram-positive bacteria. *Microbiol. Mol. Biol. Rev.* **Volume 67:** 686-723.
105. **Nugroho, F., Yamamoto, H., Kobayashi, Y., and J. Sekiguchi.** 1999. Characterization of a new sigma K-dependant peptidoglycan hydrolase gene that plays a role in *Bacillus subtilis* mother cell lysis. *J. Bacteriol.* **Volume 181:** 6230-6237.
106. **Ohta, K., Komatsuzawa, H., Sugai, M., and H. Suginaka.** 2000. Triton X-100-induced lipoteichoic acid release is correlated with the methicillin resistance in *Staphylococcus aureus*. *FEMS Microbiol. Lett.* **Volume 182:** 77-79.
107. **Orefici, G., Molinari, A., Donelli, G., Paradisi, S., Teti, G., and G. Arancia.** 1986. Immuno-location of lipoteichoic acid on group B streptococcal surface. *FEMS Microbiol. Lett.* **Volume 34:** 111-115.
108. **Ou L.-T., and R.E. Marquis.** 1970. Electrochemical interactions in cell walls of gram-positive cocci. *J. Bacteriol.* **Volume 101:** 92-101.
109. **O'Brien, M.J., Kuhl, S.A., and M.J. Starzyk.** 1995. Correlation of teichoic acid D-alanyl esterification with the expression of methicillin resistance in *Staphylococcus aureus*. *Microbios.* **Volume 83:** 119-137.

110. **Peschel, A., Otto, M., Jack, W., Kalbacher, H., Jung, G., and F. Gotz.** 1999. Inactivation of the *dlt* operon in *Staphylococcus aureus* confers sensitivity to defensins, protegrins, and other antimicrobial peptides. *J. Biol. Chem.* **Volume 274**: 8405-8410.
111. **O'Farrell, P.H.** 1975. High resolution Two-Dimensional Electrophoresis of proteins. *Journ. Biol. Chem.* **Volume 250**: 4007.
112. **O'Shannessy, D.J., Brigham-Burke, K., Soneson, K., and P. Hensley.** 1993. Determination of rate and equilibrium binding constants for molecular interactions using surface plasmon resonance: Use of non-linear least squares analysis methods. *Analytical Biochemistry.* **Volume 212**: 457-468.
113. **Peschel, A., Vuong, C., Otto, M., and F. Gotz.** 2000. The D-alanine residues of *Staphylococcus aureus* teichoic acids alter the susceptibility to vancomycin and the activity of autolytic enzymes. *Antimicrob. Agents Chemother.* **Volume 44**: 2845-2847.
114. **Pooley, H.M., and G.D. Shockman.** 1970. Relationship between the location of autolysin, cell wall synthesis, and the development of resistance to cellular autolysis in *Streptococcus faecalis* after inhibition of protein synthesis. *J. Bacteriol.* **Volume 103**: 457-466.
115. **Perego, M., Glaser, P., Minutello, A., Strauch, M.A., Leopold, K., and W. Fisher.** 1995. Incorporation of D-alanine into lipoteichoic and wall teichoic acid in *Bacillus subtilis*: identification of genes and regulation. *J. Biol. Chem.* **Volume 270**: 15598-15606.
116. **Powell, D.A., Duckworth, M., and J. Baddiley.** 1975. A membrane associated lipomannan in *micrococci*. *Biochem. J.* **Volume 151**: 387-397.
117. **Powell, J.K., and K.D. Young.** 1991. Lysis of *Escherichia coli* by beta-lactams which bind penicillin-binding proteins 1a and 1b: inhibition by heat shock proteins. *J. Bacteriol.* **Volume 173**: 4021-4026.

118. **Prasad, S.C., Soldatenkov, V.A., Kuettel, M.R., Thraves, P.J., Zou, X., and A. Dritschilo.** 1999. Protein changes associated with ionizing radiation-induced apoptosis in human prostate epithelial tumour cells. *Electrophoresis*. **Volume 20:** 1065-1074.
119. **Rabilloud, T.** 1996. Solubilization of proteins for electrophoretic analysis. *Electrophoresis*. **Volume 17:** 813.
120. **Rashid, M.H., Mori, M., and J. Sekiguchi.** 1995. Glucosamidases of *Bacillus subtilis*: cloning, regulation, primary structure and biochemical characterization. *Microbiol.* **Volume 141:** 2391-2404.
121. **Recsei, P.A., Gruss, A.D., and R.P. Novick.** 1987. Cloning, sequence, and expression of the lysostaphin gene from *Staphylococcus simulans*. *Proc. Natl. Acad. Sci. USA*. **Volume 84:** 1127-1131.
122. **Rich, R. L., and D.G. Myszka.** Advantages in surface plasmon resonance biosensor analysis. *Curr. Opinion Biotechnol.* **Volume 11:** 54-61.
123. **Rodionov, D.G., and E.E. Ishiguro.** 1995. Direct correlation between overproduction of guanosine 3', 5'-bispyrophosphate (ppGpp) and penicillin tolerance in *Escherichia coli*. *J. Bacteriol.* **Volume 177:** 4224-4229.
124. **Rogers, H.J., Perkins, H.R., and J.B. Ward.** 1980. *Microbial cell walls and membranes*. London: Chapman and Hall.
125. **Romeis, T., Vollmer, W., and J.V. Holtje.** 1993. Characterization of three different lytic transglycosylases in *Escherichia coli*. *FEMS Microbiol. Lett.* **Volume 111:** 141-146.
126. **Schmid, R., Bernhardt, J., Antelmann, H., Volker, A., Mach, H., Volker, U., and M. Hecker** 1997. Identification of vegetative proteins for a 2-Dimensional index of *Bacillus subtilis*. *Microbio.* **Volume 143:** 991.
127. **Shockman, G.D., and R. Barrette.** 1983. Structure, function, and assembly of cell walls of gram-positive bacteria. *Annu. Rev. Microbiol.* **Volume 37:** 501-527.

128. **Shockman, G.D., Daneo-Moore, L., Kariyama, R., and O. Massidda.** 1996. Bacterial walls, Peptidoglycan Hydrolases, Autolysins, and Autolysis. *Microbial Drug Resistance. Volume 2:* 95-98.
129. **Shopsin, B., Mathema, B., Alcabes, P., Said-Salim, B., Lina, G., Matsuka, A., Martinez, J., and B.N. Kreiswirth.** 2003. Prevalence of *agr* specificity groups among *Staphylococcus aureus* strains colonizing children and their guardians. *J. Clinical Microbiol. Volume 41:* 456-459.
130. **Smith, T.J., and S.J. Foster.** 1995. Characterisation of the involvement of two compensatory autolysins in mother cell lysis during sporulation of *Bacillus subtilis* 168. *J. Bacteriol. Volume 177:* 3855-3862.
131. **Spellerberg, B., Rozdzinski, E., Martin, S., Weber-Heynemann, J., and R. Lütticken.** 2002. *rgf* Encodes a novel two-component signal transduction system of *Streptococcus agalactiae*. *Infect. and Immunity. Volume 70:* 2434-2240.
132. **Strating, H. and A.J. Clark.** 2001. Differentiation of Bacterial Autolysins by Zymogram Analysis. *Analyt. Biochem. Volume 291:* 149-154.
133. **Stoscheck, C.M.** 1990. Quantitation of Protein. *Methods in Enzym. Volume 182:* 50-69.
134. **Studer, R.E., and D. Karamata.** 1988. In Actor, P. (ed.) Cell wall proteins in *Bacillus subtilis*. Antibiotic inhibition of bacterial cell surface assembly and function. Washington, D.C: American Society for Microbiology. 146-150.
135. **Sugai, M., Akiyama, T., Komatsuzawa, H., Miyake, Y. and H. Suginaka.** 1990. Characterization of Sodium Dodecyl Sulfate-Stable *Staphylococcus aureus* Bacteriolytic enzymes by polyacrylamide gel electrophoresis. *J. Bacteriol. Volume 172:* 6494-6498.
136. **Sutchliffe, I.C., and N. Shaw.** 1991. Atypical lipoteichoic acids of gram-positive bacteria. *J. Bacteriol. Volume 173:* 7065-7069.

137. **Takahashi, T., Ikegami-Kawai, M., Okuda, R., and K. Suzuki.** 2003. A fluorimetric Morgan-Elson assay method for hyaluronidase activity. *Analyt. Biochem.* **Volume 322:** 257-263.
138. **Taylor, A., Das, B.C., and J. van Heijenoort.** 1975. Bacterial cell wall peptidoglycan fragments produced by phage lamda or Vi II endolysin and containing 1, 6-anhydro-N-acetylmuramic acid. *J. Biochem.* **Volume 53:** 47-54.
139. **Thiemermann, C.** 2002. Interactions between lipoteichoic acid and peptidoglycan from *Staphylococcus aureus*: a structural function analysis. *Microbes Infect.* **Volume 4:** 927-935.
140. **Thunnissen, A.M.W.H., Dijkstra, A.J., Rozeboom, K.H., Engel, H., Keck, W., and B.W. Dijkstra.** 1994. Doughnut-shaped structure of a bacterial muramidase revealed by X-ray crystallography. *Nature.* **Volume 367:** 750-753.
141. **Tomasz, A.** Building and breaking of bonds in the cell walls of bacteria – the role for autolysins, pg 3-12. In C. Nombela (ed.), *Microbial cell wall synthesis and autolysis.* Elsevier Science Publishers, Amsterdam, the Netherlands.
142. **Tomasz, A., Albino, A., and E. Zanati.** 1970. Multiple antibiotic resistance in a bacterium with suppressed autolytic system. *Nature.* **Volume 227:** 137-140.
143. **Tsui, H.C., Feng, G., and M.E. Winkler.** 1996. Transcription of the *mutL* repair, *miaA* tRNA modification, *hfq* pleiotrophic regulator, and *hflA* region protease genes of *Escherichia coli* K-12 from clustered E sigma 32-specific promoters during heat shock. *J. Bacteriol.* **Volume 178:** 5719-5731.
144. **Tuomanen, E., and A. Tomasz.** 1986. Induction of autolysis in non-growing *Escherichia coli*. *J. Bacteriol.* **Volume 167:** 1077-1080.
145. **Ursanus, A., and V. Holtje.** 1992. Purification of a membrane-bound lytic transglycosylases from *Escherichia coli*. *J. Bacteriol.* **Volume 176:** 338-343.

146. **van der Linden, M.P.G., De Haan, L., Hoeyer, M.A., and W. Keck.** 1992. Possible role of penicillin-binding protein 6 from *Escherichia coli* in the stabilization of stationary phase peptidoglycan. *J. Bacteriol.* **Volume 174:** 7572-7578.
147. **van Dreil, D., Wicken, A.J., Dickson, M.R., and K.W. Know.** 1973. Cellular location of the lipoteichoic acids of *Lactobacillus fermenti* NCTC 6991 and *Lactobacillus casei* NCTC 6375. *J. Ultrastruc. Res.* **Volume 43:** 483-497.
148. **van Heijenoort, J., Praque, C., Flouret, B., and Y. van Heijenoort.** 1975. Envelope-bound N-acetylmuramyl-L-alanine amidase of *Escherichia coli*. *Eur. J. Biochem.* **Volume 58:** 611-619.
149. **Vincent, S., Glauner, B., and L. Gutmann.** 1991. Lytic effect of two fluoroquinolones, ofloxacin and pefloxacin, on *Escherichia coli* W7 and its consequences on peptidoglycan composition. *Antimicrob. Agents Chemother.* **Volume 35:** 1391-1385.
150. **Wecke, J., Madela, K., and W. Fisher.** 1997. The absence of D-alanine from lipoteichoic acid and wall teichoic acid alters surface charge, enhances autolysis and increases susceptibility to methicillin in *Bacillus subtilis*. *Microbiology.* **Volume 143:** 2953-2960.
151. **Wicken, A.J., Evans, J.K., and K.W. Knox.** 1986. Critical micelle concentrations of lipoteichoic acids. *J. Bacteriol.* **Volume 166:** 72-77.
152. **Wilkins, J.C., Homer, K.A., and D. Beighton.** 2001. Altered protein expression of *Streptococcus oralis* cultured at low pH revealed by two-dimensional gel electrophoresis. *Appl. Environ. Microbiol.* **Volume 67:** 3396-3405.
153. **Winslow, D.L., Damme, J. and E. Dieckman.** 1983. Delayed bactericidal activity of beta-lactam antibiotics against *Listeria monocytogenes*: antagonism of chloramphenicol and rifampin. *Antimicrob. Agents Chemother.* **Volume 4:** 555-558.

154. **Yem, D.W., and H.C. Wu.** 1976. Purification and properties of β -N-acetylglucosaminidase from *Escherichia coli*. J. Bacteriol. **Volume 125**: 324-331.

155. **Young, F.E.** 1966. Autolytic enzyme association with the cell walls of *Bacillus subtilis*. J. Biol. Chem. **Volume 241**: 3462-3467.